

**Robert J. Sandberg. "Temperature."**

**Copyright 2000 CRC Press LLC. <<http://www.engnetbase.com>>.**

# Temperature Measurement

---

**Robert J. Stephenson**

*University of Cambridge*

**Armelle M. Moulin**

*University of Cambridge*

**Mark E. Welland**

*University of Cambridge*

**Jim Burns**

*Burns Engineering Inc.*

**Meyer Sapoff**

*MS Consultants*

**R. P. Reed**

*Proteun Services*

**Randy Frank**

*Motorola, Inc.*

**Jacob Fraden**

*Advanced Monitors Corporation*

**J.V. Nicholas**

*Industrial Research Limited*

**Franco Pavese**

*CNR Istituto di Metrologia  
"G. Colonnetti"*

**Jan Stasiek**

*Technical University of Gdansk*

**Tolestyn Madaj**

*Technical University of Gdansk*

**Jaroslawn Mikielewicz**

*Institute of Fluid Flow Machinery*

**Brian Culshaw**

*University of Strathclyde*

- 32.1 **Bimaterials Thermometers**  
Linear Bimaterial Strip • Industrial Applications • Advanced Applications • Defining Terms
- 32.2 **Resistive Thermometers**  
Introduction to Resistance Temperature Detectors • Resistance of Metals • Who Uses RTDs? Common Assemblies and Applications • Overview of Platinum RTDs • Temperature Coefficient of Resistance • RTD Construction • Calibration • Use of RTDs Today • The Future of RTD Technology • Defining Terms
- 32.3 **Thermistor Thermometers**  
Thermal Properties of NTC Thermistors • Electrical Properties of NTC Thermistors • Linearization and Signal Conditioning Techniques
- 32.4 **Thermocouple Thermometers**  
The Simplest Thermocouple • Simple Thermocouple Thermometry • Thermoelectric Effects • Realistic Thermocouple Circuits • Grounding, Shielding, and Noise • Thermal Coupling • Thermocouple Materials • The Functional Model of Thermoelectric Circuits • Inhomogeneity • Calibration • Thermocouple Failure and Validation • Environmental Compatibility • Data Acquisition • Signal Transmission • Sources of Thermocouple Application Information • Summary
- 32.5 **Semiconductor Junction Thermometers**  
The Transistor as a Temperature Sensor • Thermal Properties of Semiconductors: Defining Equations • Integrated Temperature Sensors • Other Applications of Semiconductor Sensing Techniques • Temperature Sensing in Power ICs for Fault Protection and Diagnostics • Reliability Implications of Temperature to Electronic Components • Semiconductor Temperature Sensor Packaging • Defining Terms
- 32.6 **Infrared Thermometers**  
Thermal Radiation: Physical Laws • Emissivity • Blackbody • Detectors for Thermal Radiation • Pyrometers • IR Thermometers • Components of IR Thermometers • Some Special Applications
- 32.7 **Pyroelectric Thermometers**  
Pyroelectric Effect • Pyroelectric Materials • Manufacturing Process • Pyroelectric Sensors • Applications

- 32.8 Liquid-in-Glass Thermometers  
General Description • Liquid Expansion • Time-Constant Effects • Thermal Capacity Effects • Separated Columns • Immersion Errors • Organic Liquids • Storage • High Accuracy • Defining Terms
- 32.9 Manometric Thermometers  
Vapor Pressure • Gas Thermometry
- 32.10 Temperature Indicators  
Melting and Shape/Size Changing Temperature Indicators • Color-Change Temperature Indicators
- 32.11 Fiber-Optic Thermometers  
Fiber Optic Temperature Sensors • Fiber Optic Point Temperature Measurement Systems • Distributed and Quasi-distributed Optical Fiber Temperature Measurement Systems • Applications for Optical Fiber Temperature Probes

## 32.1 Bimaterials Thermometers

---

*Robert J. Stephenson, Armelle M. Moulin, and Mark E. Welland*

The first known use of differential thermal expansion of metals in a mechanical device was that of the English clockmaker John Harrison in 1735. Harrison used two dissimilar metals in a clock escapement to account for the changes in temperature on board a ship. This first marine chronometer used a gridiron of two metals that altered the flywheel period of the clock through a simple displacement. This mechanical actuation, resulting from the different thermal expansivities of two metals in contact, is the basis for all bimetallic actuators used today.

The bimetallic effect is now used in numerous applications ranging from domestic appliances to compensation in satellites. The effects can be used in two ways: either as an actuator or as a temperature measuring system. A bimetallic actuator essentially consists of two metal strips fixed together. If the two metals have different expansivities, then as the temperature of the actuator changes, one element will expand more than the other, causing the device to bend out of the plane. This mechanical bending can then be used to actuate an electromechanical switch or be part of an electrical circuit itself, so that contact of the bimetallic device to an electrode causes a circuit to be made. Although in its simplest form a bimetallic actuator can be constructed from two flat pieces in metal, in practical terms a whole range of shapes are used to provide maximum actuation or maximum force during thermal cycling.

As a temperature measuring device, the bimetallic element, similar in design to that of the actuator above, can be used to determine the ambient temperature if the degree of bending can be measured. The advantage of such a system is that the amount of bending can be mechanically amplified to produce a large and hence easily measurable displacement.

The basic principle of a bimetallic actuator is shown in [Figure 32.1](#). Here, two metal strips of differing thermal expansion are bonded together. When the temperature of the assembly is changed, in the absence

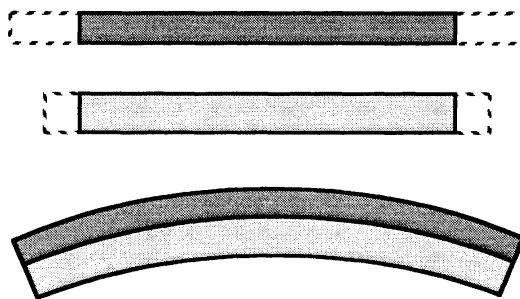


FIGURE 32.1 Linear bimetallic strip.

of external forces, the bimetallic actuator will take the shape of an arc. The total displacement of the actuator out of the plane of the metal strips is much greater than the individual expansions of the metallic elements. To maximize the bending of the actuator, metals or alloys with greatly differing coefficients of thermal expansion are normally selected. The metal having the largest thermal expansivity is known as the *active element*, while the metal having the smaller coefficient of expansion is known as the *passive element*. For maximum actuation, the passive element is often an iron–nickel alloy, Invar, having an almost zero thermal expansivity (actually between  $0.1$  and  $1 \times 10^{-6} \text{ K}^{-1}$ , depending upon the composition). The active element is then chosen to have maximum thermal expansivity given the constraints of operating environment and costs.

In addition to maximizing the actuation of the bimetallic element, other constraints such as electrical and thermal conductivity can be made. In such cases, a third metallic layer is introduced, consisting of either copper or nickel sandwiched between the active and passive elements so as to increase both the electrical and thermal conductivity of the actuator. This is especially important where the actuator is part of an electrical circuit and needs to pass current in addition to being a temperature sensor.

## Linear Bimaterial Strip

### Basic Equations

The analysis of the stress distribution and the deflection of an ideal bimetallic strip was first deduced by Timoshenko [1], who produced a simple derivation from the theory of elasticity. Figure 32.2 shows the internal forces and moments that induce bending in a bimetallic strip followed by the ideal stress distribution in the beam. This theory is derived for bimetallic strips, but is equally applicable to bimaterial strips.

The general equation for the curvature radius of a bimetallic strip uniformly heated from  $T_0$  to  $T$  in the absence of external forces is given by [1]:

$$\frac{1}{R} - \frac{1}{R_0} = \frac{6(1+m)^2(\alpha_2 - \alpha_1)(T - T_0)}{t \left[ 3(1+m)^2 + (1+mn)(m^2 + 1/mn) \right]} \quad (32.1)$$

- where  $1/R_0$  = Initial curvature of the strip at temperature  $T_0$   
 $\alpha_1$  and  $\alpha_2$  = Coefficients of expansion of the two elements: (1) low expansive material and (2) high expansive material  
 $n$  =  $E_1/E_2$ , with  $E_1$  and  $E_2$  their respective Young's moduli  
 $m$  =  $t_1/t_2$ , with  $t_1$  and  $t_2$  their respective thicknesses  
 $t$  =  $t_1 + t_2$  thickness of the strip

The width of the strip is taken as equal to unity.

Equation 32.1 applies for several strip configurations, including the simply supported strip and a strip clamped at one end (i.e., a cantilever). For a given configuration, the deflection of a strip can be determined by its relationship with curvature,  $1/R$ .

An example of a calculation of deflection is a bimetallic strip simply supported at its two ends. The initial curvature  $1/R_0$  is assumed to be zero. Figure 32.3 shows the geometrical relationship between the radius  $R$  of the strip and the deflection  $d$  at its mid-point and is given by:

$$(R - t_2)^2 = (R - d - t_2)^2 + \left(\frac{L}{2}\right)^2 \quad (32.2)$$

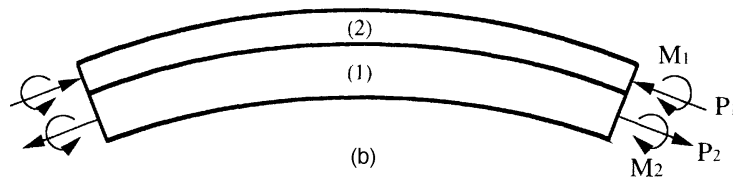
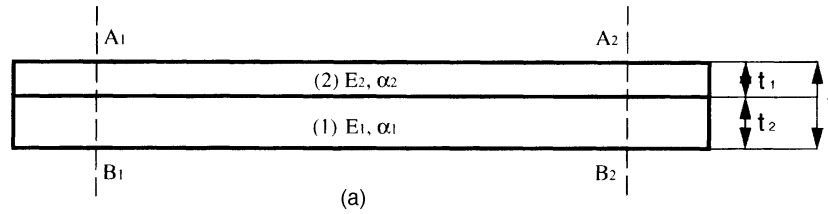


**FIGURE 32.2** Bending of bimetallic strip uniformly heated with  $\alpha_2 \geq \alpha_1$ . (a) Bimetallic strip.  $A_1B_1-A_2B_2$  is an element cut out from the strip. (b) Bending of the element  $A_1B_1-A_2B_2$  when uniformly heated. Assuming  $\alpha_2 > \alpha_1$ , the deflection is convex up. The total force acting over the section of (1) is an axial tensile force  $P_1$  and bending moment  $M_1$ , whereas over the section of (2) it is an axial compressive force  $P_2$  and bending moment  $M_2$ . (c) Sketch of the internal resulting stress distribution. (Left): normal stresses over the cross section of the strip. The maximum stress during heating is produced at the interface between the two components of the strip. This stress is due to both axial force and bending. (Right): shearing stresses at the ends of the strip.

Hence,

$$\frac{1}{R} = \frac{8d}{L^2 + 4d^2 + 8dt_2} \quad (32.3)$$

Making the assumption that the deflection and the thickness are less than 10% of the length of the strip (which is true in most practical cases) means the terms  $8dt_2$  and  $4d^2$  are therefore negligible and the expression reduces to:

$$d = \frac{L^2}{8R} \quad (32.4)$$

or

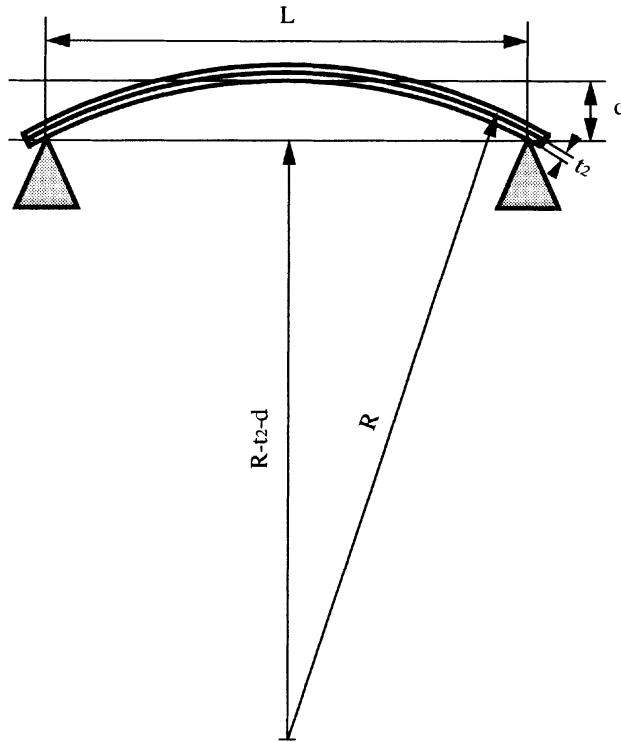


FIGURE 32.3 Bending of a strip simply supported at its ends.

$$d = L^2 \frac{3(1+m)^2}{4t \left[ 3(1+m)^2 + (1+mn)(m^2 + 1/mn) \right]} (\alpha_2 - \alpha_1)(T - T_0) \quad (32.5)$$

If a 100-mm strip is composed of two layers of the same thickness (0.5 mm) with the high-expansive layer being made of iron (from Table 32.1,  $E_2 = 211$  GPa and  $\alpha_2 = 12.1 \times 10^{-6} \text{ K}^{-1}$ ), the low-expansive layer made of Invar (from Table 32.1,  $E_1 = 140$  GPa and  $\alpha_1 = 1.7 \times 10^{-6} \text{ K}^{-1}$ ), and the temperature increases from 20°C to 120°C, then the theoretical bending at the middle of the strip will be 1.92 mm.

As a second example, consider the calculation of the deflection of the free end of a bimetallic cantilever strip as illustrated in Figure 32.4. In this case, the geometrical relation is:

$$(R+t_1)^2 = (R+t_1-d)^2 + L^2 \quad (32.6a)$$

or

$$\frac{1}{R} = \frac{2d}{L^2 + d^2 - 2dt_1} \quad (32.6b)$$

Making the same assumptions as before, that is,  $d^2 \ll L^2$  and  $dt_1 \ll L^2$ , then the deflection of the free end is given by:

$$d = \frac{L^2}{8R} \quad (32.7)$$

**TABLE 32.1** Properties for Selected Materials Used in Bimaterial Elements

Material	Density ( $\rho$ ) (kg m <sup>-3</sup> )	Young's Modulus ( $E$ ) (GPa)	Heat capacity ( $C$ ) (J kg <sup>-1</sup> K <sup>-1</sup> )	Thermal expansion (10 <sup>-6</sup> K <sup>-1</sup> )	Thermal conductivity (W m <sup>-1</sup> K <sup>-1</sup> )
Al	2700 <sup>c</sup> 2707 <sup>a</sup>	61–71 <sup>b</sup> 70.6 <sup>c</sup>	896 <sup>a</sup> 900 <sup>c</sup>	24 <sup>b</sup> 23.5 <sup>c</sup>	237 <sup>c</sup> 204 <sup>a</sup>
Cu	8954 <sup>a</sup> 8960 <sup>c</sup>	129.8 <sup>c</sup>	383.1 <sup>a</sup> 385 <sup>c</sup>	17.0 <sup>c</sup>	386 <sup>a</sup> 401 <sup>c</sup>
Cr	7100 <sup>c</sup>	279 <sup>c</sup>	518 <sup>c</sup>	6.5 <sup>c</sup>	94 <sup>c</sup>
Au	19300 <sup>b,c</sup>	78.5 <sup>b,c</sup>	129 <sup>b,c</sup>	14.1 <sup>b,c</sup>	318 <sup>b,c</sup>
Fe	7870 <sup>c</sup>	211.4 <sup>c</sup>	444 <sup>c</sup>	12.1 <sup>c</sup>	80.4 <sup>c</sup>
Ni	8906 <sup>a</sup> 8900 <sup>c</sup>	199.5 <sup>c</sup>	446 <sup>a</sup> 444 <sup>c</sup>	13.3 <sup>c</sup>	90 <sup>a</sup> 90.9 <sup>c</sup>
Ag	10524 <sup>a</sup> 10500 <sup>c</sup>	82.7 <sup>c</sup>	234.0 <sup>a</sup> 237 <sup>c</sup>	19.1 <sup>c</sup>	419 <sup>a</sup> 429 <sup>c</sup>
Sn	7304 <sup>a</sup> 7280 <sup>c</sup>	49.9 <sup>c</sup>	226.5 <sup>a</sup> 213 <sup>c</sup>	23.5 <sup>c</sup>	64 <sup>a</sup> 66.8 <sup>c</sup>
Ti	4500 <sup>c</sup>	120.2 <sup>c</sup>	523 <sup>c</sup>	8.9 <sup>c</sup>	21.9 <sup>c</sup>
W	19350 <sup>a</sup> 19300 <sup>c</sup>	411 <sup>c</sup>	134.4 <sup>a</sup> 133 <sup>c</sup>	4.5 <sup>c</sup>	163 <sup>a</sup> 173 <sup>c</sup>
Invar (Fe64/Ni36)	8000 <sup>c</sup>	140–150 <sup>c</sup>	—	1.7–2.0 <sup>c</sup>	13 <sup>c</sup>
Si	2340 <sup>c</sup>	113 <sup>c</sup>	703 <sup>c</sup>	4.7–7.6 <sup>c</sup>	80–150 <sup>c</sup>
<i>n</i> -Si	2328 <sup>b</sup>	130–190 <sup>b</sup>	700 <sup>b</sup>	2.6 <sup>b</sup>	150 <sup>b</sup>
<i>p</i> -Si	2300 <sup>b</sup>	150–170 <sup>b</sup>	770 <sup>b</sup>	—	30 <sup>b</sup>
Si <sub>3</sub> N <sub>4</sub>	3100 <sup>a</sup>	304 <sup>b</sup>	600–800 <sup>b</sup>	3.0 <sup>b</sup>	9–30 <sup>b</sup>
SiO <sub>2</sub>	2200 <sup>b</sup>	57–85 <sup>b</sup>	730 <sup>b</sup>	0.50 <sup>b</sup>	1.4 <sup>b</sup>

<sup>a</sup> From Reference [13], Table A1 at 20°C.

<sup>b</sup> From Reference [13], Table A2 at 300K.

<sup>c</sup> From Goodfellow catalog 1995/1996 [14].

and combining this with Equation 32.1 yields:

$$d = L^2 \frac{3(1+m)^2}{t \left[ 3(1+m)^2 + (1+mn)(m^2 + 1/mn) \right]} (\alpha_2 - \alpha_1)(T - T_0) \quad (32.8)$$

If an aluminum and silicon nitride bimaterial microcantilever as used for sensor research [2] is considered, then  $L = 200 \mu\text{m}$ ,  $t_1 = 0.6 \mu\text{m}$ ,  $t_2 = 0.05 \mu\text{m}$ ,  $E_1 = 300 \text{ GPa}$ ,  $E_2 = 70 \text{ GPa}$ ,  $\alpha_1 = 3 \times 10^{-6} \text{ K}^{-1}$ ,  $\alpha_2 = 24 \times 10^{-6} \text{ K}^{-1}$  (see Table 32.1). In this situation, a temperature difference of 1°C gives a theoretical deflection of the cantilever of 0.103  $\mu\text{m}$ .

### Terminology and Simplifications

For industrial purposes, bimetallic thermostatic strips and sheets follow a standard specification — ASTM [3] in the U.S. and DIN [4] in Europe. Important parameters involved in this specification are derived directly from the previous equations, in which simplifications are made based on common applications.

It can be seen that the magnitude of the ratio  $E_1/E_2 = n$  has no substantial effect on the curvature of the strip, and taking  $n = 1$  implies an error less than 3%. Assuming again that the initial curvature is zero, Equation 32.1 can be simplified to:

$$\frac{1}{R} = \frac{6m}{t(m+1)^2} (\alpha_2 - \alpha_1)(T - T_0) \quad (32.9)$$

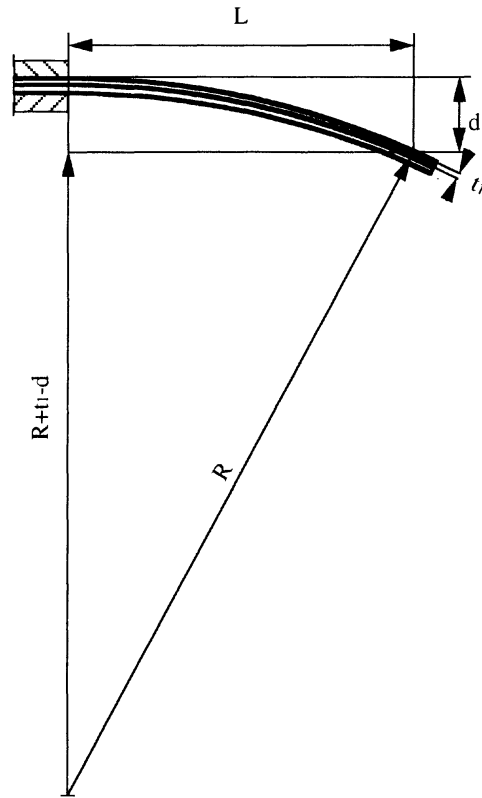


FIGURE 32.4 Bending of a strip fixed at one end.

In most industrial applications involving bimetallic elements, the thicknesses of the two component layers are taken to be equal ( $m = 1$ ), thus Equation 32.6 becomes:

$$\frac{1}{R} = \frac{3}{2} \frac{(\alpha_2 - \alpha_1)(T - T_0)}{t} \quad (32.10)$$

The constant  $\frac{3}{2}(\alpha_2 - \alpha_1)$  is known as **flexivity** in the U.S. and as **specific curvature** in Europe. Introducing the flexivity,  $k$ , and rearranging Equation 32.10 gives:

$$k = \frac{t}{R(T - T_0)} \quad (32.11)$$

Flexivity can be defined as “the change of curvature of a bimetal strip per unit of temperature change times thickness” [5]. The experimental determination of the flexivity for each bimetallic strip has to follow the test specifications ASTM B388 [3] and DIN 1715 [4]. The method consists of measuring the deflection of the midpoint of the strip when it is simply supported at its ends. Using Equation 32.4 derived above and combining with Equation 32.11 gives:

$$k = \frac{8dt}{(T - T_0)L^2} \quad (32.12)$$

**TABLE 32.2** Table of Selected Industrially Available ASTM Thermostatic Elements

Type (ASTM)	Flexivity $10^{-6}$ ( $^{\circ}\text{C}^{-1}$ )	Max. sensitivity temp. range ( $^{\circ}\text{C}$ )	Max. operating temp. ( $^{\circ}\text{C}$ )	Young's Modulus (GPa)
TM1	$27.0 \pm 5\%^a$	-18–149	538	17.2
	$26.3 \pm 5\%^b$			
TM2	$38.7 \pm 5\%^a$	-18–204	260	13.8
	$38.0 \pm 5\%^b$			
TM5	$11.3 \pm 6\%^a$	149–454	538	17.6
	$11.5 \pm 6\%^b$			
TM10	$23.6 \pm 6\%^a$	-18–149	482	17.9
	$22.9 \pm 6\%^b$			
TM15	$26.6 \pm 5.5\%^a$	-18–149	482	17.2
	$25.9 \pm 5.5\%^b$			
TM20	$25.0 \pm 5\%^a$	-18–149	482	17.2
	$25.0 \pm 5\%^b$			

<sup>a</sup> 10–93 $^{\circ}\text{C}$ . From ASTM Designation B 388 [15].

<sup>b</sup> 38–149 $^{\circ}\text{C}$ . From ASTM Designation B 388 [15].

Coming back to the second example of the calculation of the deflection (cantilever case), using Equation 32.10 and the same assumptions ( $m = n = 1$ ), Equation 32.7 becomes:

$$d = \frac{k L^2}{2 t} (T - T_0) \quad (32.13)$$

In Europe, the constant  $a = dt/(T - T_0)L^2$  (theoretically equal to  $k/2$ ) is called **specific deflection** and is measured following the DIN test specification from the bending of a cantilever strip. It can be noted that the experimental value differs from the theoretical value as it takes into account the effect of the external forces suppressing the cross-curvature where the strip is fastened (i.e., the theory assumes that the curvature is equal along the strip; whereas in reality, the fact that the strip is fastened implies that the radius is infinite at its fixed end).

Tables 32.2 and Table 32.4 present a selection of bimetallic elements following ASTM and DIN standards, respectively. Flexivity (or specific curvature), linear temperature range, maximum operating temperature, and specific deflection (DIN only) are given. The details of the chemical composition of these elements are specified in Tables 32.3 and Table 32.5.

## Industrial Applications

The mechanical thermostat finds a wide range of applications in temperature control in industrial processes and everyday life. This widespread use of thermostats is due to the discovery of Invar, a 36% nickel alloy that has a very low thermal expansion coefficient, and was so named because of its property of invariability [6].

There are two general classes of bimetallic elements based on their movement in response to temperature changes. Snap-action devices jump from one position to another at a specific temperature depending on their design and construction. There are numerous different shapes and sizes of snap-action elements and they are typically ON/OFF actuators. The other class of elements, creep elements, exhibit a gradual change in shape in response to a change in temperature and are employed in temperature gauges and other smooth movement applications. Continuous movement bimetallics will be considered first. A linear configuration was covered previously, so the discussion will focus on coiled bimetallic elements.

### Spiral and Helical Coil Configurations

For industrial or commercial measurements, a spiral or helical coil configuration is useful for actuating a pointer on a dial as the thermal deflection is linear within a given operating range. Linearity in this

**TABLE 32.3** Composition of Selected Industrially Available ASTM Thermostatic Elements Given in Table 32.2

	Element	TM1	TM2	TM5	TM10	TM15	TM20
High-expansive material chemical composition (% weight)	Nickel	22	10	25	22	22	18
	Chromium	3	72	8.5	3	3	11.5
	Manganese	—	18	—	—	—	—
	Copper	—	—	—	—	—	—
	Iron	75	—	66.5	75	75	70.5
	Aluminum	—	—	—	—	—	—
	Carbon	—	—	—	—	—	—
Intermediate nickel layer		No	No	No	Yes	Yes	No
Low-expansive material chemical composition (% weight)	Nickel	36	36	50	36	36	36
	Iron	64	64	50	64	64	64
	Cobalt	—	—	—	—	—	—
Component ratio (% of thickness)	High	50	53	50	34	47	50
	Intermediate	—	—	—	32	6	—
	Low	50	47	50	34	47	50

From ASTM Designation B 388 [15].

**TABLE 32.4** Table of Selected Industrially Available DIN Thermostatic Elements

Type (DIN)	Specific deflection ( $10^{-6} \text{ K}^{-1}$ )	Specific curvature ( $10^{-6} \text{ K}^{-1}$ ) $\pm$ 5%	Linear range ( $^{\circ}\text{C}$ )	Max. operating temperature ( $^{\circ}\text{C}$ )
TB0965	9.8	18.6	−20–425	450
TB1075	10.8	20.0	−20–200	550
TB1170A	11.7	22.0	−20–380	450
TB1577A	15.5	28.5	−20–200	450
TB20110	20.8	39.0	−20–200	350

Note: From DIN 1715 standard [4]. Specific deflection and curvature are for the range 20 $^{\circ}\text{C}$  to 130 $^{\circ}\text{C}$ .

**TABLE 32.5** Composition of Selected Industrially Available DIN Thermostatic Elements Given in Table 32.4

	Element	TB0965	TB1075	TB1170A	TB1577A	TB20110
High-expansive chemical composition (% mass)	Nickel	20	16	20	20	10-16
	Chromium	—	11	—	—	—
	Manganese	6	—	6	6	Remainder
	Copper	—	—	—	—	18-10
	Iron	Remainder	Remainder	Remainder	Remainder	0.5
	Carbon	—	—	—	—	—
Low-expansive chemical composition (% mass)	Nickel	46	20	42	36	36
	Iron	Remainder	Remainder	Remainder	Remainder	Remainder
	Cobalt	—	26	—	—	—
	Chromium	—	8	—	—	—

From DIN 1715 Standard [4].

case means that the deflection does not vary by more than 5% of the deflection, as calculated from the flexivity [4]. The basic bimaterial ideas from the previous section still apply, with some additional equations relating the movement of a bimetal coil to a change in temperature. As in the previous section, standard methods for testing the deflection rate of spiral and helical coils exist and can be found in [7]. The following equations have been taken from the Kanthal Thermostatic Bimetal Handbook [8], with some change in notation. The angular rotation of a bimetal coil is given by (see Figure 32.5):

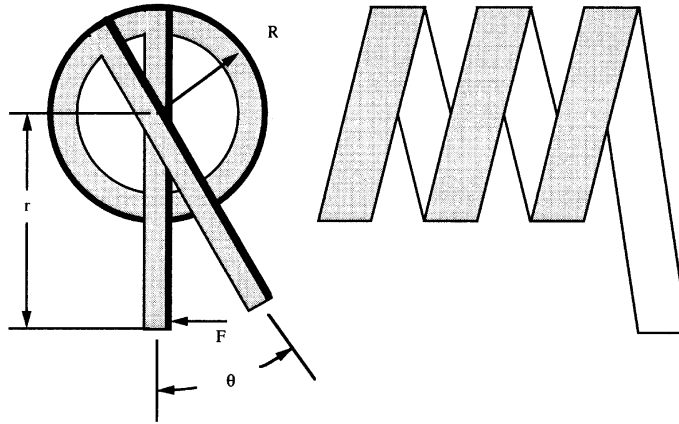


FIGURE 32.5 Helical coiled bimetal element.

$$\theta = \left( \frac{1}{R} - \frac{1}{R_0} \right) L \quad (32.14)$$

where  $L$  = length of the strip

$R_0$  and  $R$  = initial and final bending radii (assumed to be constant along the strip), respectively.

In terms of the specific deflection  $a$ , this can be written as:

$$\theta = \frac{2aL}{t} (T - T_0) \frac{360}{2\pi} \quad (32.15)$$

where  $t$  = thickness of the device

$T_0$  and  $T$  = initial and final temperatures, respectively.

An example would be a helical bimetal coil inside a steel tube with one end of the coil fixed to the end of the tube and the other connected to a pointer. The accuracy of a typical commercial product is 1% to 2% of full-scale deflection with an operating range of 0°C to 600°C [9].

If a change in temperature is required to both move a pointer and produce a driving force, then the angular rotation is reduced and is given by:

$$\theta = \left( \frac{2a(T - T_0)L}{t} - \frac{12(F - F_0)Lr}{wt^3E} \right) \frac{360}{2\pi} \quad (32.16)$$

where  $w$  = width of the element

$r$  = distance from the center of the coil to the point of applied force,  $F$

This can be rewritten as:

$$T - T_0 = \frac{\theta t}{2aL} \frac{2\pi}{360} + \frac{6(F - F_0)r}{wt^2Ea} \quad (32.17)$$

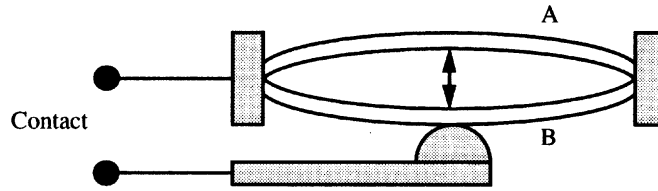


FIGURE 32.6 Snap-action bimetallic element.

where the first term represents the temperature associated with the angular rotation of the strip and the second term represents the temperature associated with the force generated by the strip. In general, the strip is designed so that the two are equal, as this leads to the minimum volume for the strip and consequently less weight and cost for the device.

Finally, if the coil is prevented from moving then the change in torque is given by

$$(F - F_0)r = \frac{1}{6} wt^2 Ea (T - T_0) \quad (32.18)$$

**Example:** Consider a bimetal element that measures a temperature change from 20°C to 100°C and moves a lever 50 mm away with a force of 1 N. A dial reading range of 180° is required.

Choosing thermostatic bimetal TM2 gives the largest deflection per degree temperature change and TM2 meets the operating temperature requirements. Both a force and a movement are involved, so use Equation 32.7. Choosing each term equal to half the temperature change gives the minimum volume for the strip as:

$$\frac{1}{2}(T - T_0) = \frac{\theta t}{2aL} \frac{2\pi}{360} = \frac{6(F - F_0)r}{wt^2 Ea} \quad (32.19)$$

Selecting a thickness of 1.0 mm and using a specific deflection of  $19 \times 10^{-6} \text{°C}^{-1}$  ( $a = k/2$  from Table 32.2) gives a width of 29 mm. Similarly, the length of the bimetal strip is obtained from the second term in the equality, giving  $L = 2.1$  m.

### Snap-Action Configurations

Snap-action bimetal elements are used in applications where an action is required at a threshold temperature. As such, they are not temperature measuring devices, but rather temperature-activated devices. The typical temperature change to activate a snap-action device is several degrees and is determined by the geometry of the device (Figure 32.6). When the element activates, a connection is generally made or broken and in doing so, a gap between the two contacts exists for a period of time. For a mechanical system, there is no problem; however, for an electrical system, the gap can result in a spark that can lead to premature aging and corrosion of the device. The amount and duration of spark is reduced by having the switch activate quickly, hence the use of snap-action devices.

Snap-action elements also incorporate a certain amount of hysteresis into the system, which is useful in applications that would otherwise result in an oscillation about the set-point. It should be noted, however, that special design of creep action bimetals can also lead to different ON/OFF points, such as in the reverse lap-welded bimetal [8].

### Sensitivity and Accuracy

Modern techniques are more useful where sensitivity and accuracy are concerned for making a temperature measurement; however, bimetals find application in commercial and industrial temperature control where an action is required without external connections. Evidently, geometry is important for bimetal

systems as the sensitivity is determined by the design, and a mechanical advantage can be used to yield a large movement per degree temperature change. A demonstration of sensitivity using a helical coil was made by Huston [10] that gave 6 in. (15.2 cm) deflection per degree in their measurement system — yielding a sensitivity of 0.01°F per 1/16 in. (0.0035°C mm<sup>-1</sup>). Huston also demonstrated a repeatable accuracy of 0.05°F (0.027°C) based on the use of a 0.1°F (0.056°C) accuracy calibration instrument.

The operating range for many bimetals is quite large; however, there is a range over which the sensitivity is a maximum. A bimetal element is generally chosen to operate in this range and specific details are provided by manufacturers in their product catalogs. Of particular note is that, despite extended thermal cycling, bimetal strips reliably return to the same position (i.e., show no hysteresis) at a given temperature and are very robust as long as they are not subjected to temperatures outside their specified operating range.

## Advanced Applications

Thermostatic valves are a ready and robust means of measuring temperature and controlling heating and cooling in industrial settings. The basic designs have been around for many years and are the mainstay of many commercial temperature-control systems. New applications of bimetals are being found in microactuators and microsensors.

Besides operating as temperature-measuring instruments, bimaterial devices can be used for a variety of applications where temperature is the controlling or triggering phenomenon, or indeed, other material properties are inferred from the temperature response. One such example is a nickel–silicon actuator developed by engineers at HP labs in Palo Alto, CA; the actuator operates by heating a thin nickel resistor on the silicon side of a bilayer device [11]. Both the silicon and nickel layers expand due to heating; however, the nickel layer expands more, thereby curling the device, which leads to the actuation of a tiny valve. The device can control gas flow rates from 0.1 to 600 standard cm<sup>3</sup> per minute with pressures ranging from 5 psi to 200 psi (34.5 kPa to 1379 kPa).

The use of micromachined thermal sensors compatible with modern silicon integrated circuit fabrication methods has recently received significant attention. One way of achieving highly sensitive thermal measurements is by using micromechanical bimetallic cantilevers and measuring the deflection as a result of thermal fluctuations. Rectangular or triangular cantilevers, typically 100 μm long made of silicon or silicon nitride, are coated with a thin high-expansive metallic layer (e.g., aluminum or gold). Precise measurement of the deflection of the end of the cantilever is achieved using an optical sensing arrangement commonly used in atomic force microscopes. The micromechanical nature of the cantilever-based sensor leads to significant advantages in the absolute sensitivity achievable. In this way, the device is capable of measuring temperature, heat, and power variations of 10<sup>-5</sup> K, 150 fJ, or 100 pW, respectively [2]. In addition to their use as thermal sensors, the bimetallic cantilever systems have been used to investigate physical phenomena where heat is produced by the sample. Examples include photothermal spectroscopy studies of amorphous silicon [2] and the observation of oscillations in the catalyzed reaction of hydrogen and oxygen on platinum [12]. Thus, bimaterial sensors are becoming an increasingly important area of development.

## Defining Terms

**Linear coefficient of thermal expansion:** The change in length of a material per degree change in temperature expressed as a fraction of the total length ( $\Delta L/L$ ).

**Flexivity:** The change in radius of curvature of a bimaterial per degree change in temperature times the width of the element (See Equation 32.11).

**Specific curvature:** The European term for flexivity.

**Specific deflection:** Theoretically equal to half the flexivity. Specific deflection is measured by mounting the test element as a cantilever — supported at one end and free to move at the other.

## References

1. S.P. Timoshenko, *The Collected Papers*, New York: McGraw-Hill, 1953.
2. J.R. Barnes, R.J. Stephenson, M.E. Welland, C. Gerber, and J.K. Gimzewski, Photothermal spectroscopy with femtojoule sensitivity using a micromechanical device. *Nature*, 372, 79-81, 1994.
3. ASTM Designation B 388.
4. DIN 1715. Part 1. Thermostat Metals. 1983.
5. ASTM Designation B 106.
6. M. Kutz, *Temperature Control*, New York: John Wiley & Sons, 1968.
7. ASTM Designation B 389.
8. *The Kanthal Thermostatic Bimetal Handbook*. Box 502. S-73401 Hallstammar, Sweden, 1987.
9. Bourdon Sedeme, F-41103 Vendome Cedex, France.
10. W.D. Huston, The accuracy and reliability of bimetallic temperature measuring elements, in C.M. Herzfeld and A.I. Dahl (eds.), *Temperature — Its Measurement and Control in Science and Industry*, New York: Reinhold, 1962.
11. L. O'Connor, A bimetallic silicon microvalve. *Mechanical Engineering*, 117(1), 1, 1995.
12. J.K. Gimzewski, C. Gerber, E. Meyer, and R. Schlittler, Observation of a chemical reaction using a micromechanical sensor. *Chem. Phys. Lett.* 217, 589-594, 1994.
13. G.C.M. Meijer and A.W. van Herwaarden, *Thermal Sensors*, Bristol, U.K.: Institute of Physics Publishing, 1994.
14. Goodfellow Cambridge Limited. Cambridge Science Park. U.K. CB4 4DJ.
15. American Society for Testing and Materials, *Annual Book of ASTM Standards*, Philadelphia, 1991.

## Further Information

V.C. Miles, *Thermostatic Control — Principles and Practice*, Liverpool: C. Tinling and Co., 1965.

## 32.2 Resistive Thermometers

---

*Jim Burns*

### Introduction to Resistance Temperature Detectors

One common way to measure temperature is by using Resistive Temperature Detectors (RTDs). These electrical temperature instruments provide highly accurate temperature readings: simple industrial RTDs used within a manufacturing process are accurate to  $\pm 0.1^\circ\text{C}$ , while Standard Platinum Resistance Thermometers (SPRTs) are accurate to  $\pm 0.0001^\circ\text{C}$ .

The electric resistance of certain metals changes in a known and predictable manner, depending on the rise or fall in temperature. As temperatures rise, the electric resistance of the metal increases. As temperatures drop, electric resistance decreases. RTDs use this characteristic as a basis for measuring temperature.

The sensitive portion of an RTD, called an element, is a coil of small-diameter, high-purity wire, usually constructed of platinum, copper, or nickel. This type of configuration is called a wire-wound element. With thin-film elements, a thin film of platinum is deposited onto a ceramic substrate.

Platinum is a common choice for RTD sensors because it is known for its long-term stability over time at high temperatures. Platinum is a better choice than copper or nickel because it is chemically inert, it withstands oxidation well, and works in a higher temperature range as well.

In operation, the measuring instrument applies a constant current through the RTD. As the temperature changes, the resistance changes and the corresponding change in voltage is measured. This measurement is then converted to thermal values by a computer. Curve-fitting equations are used to define

this resistance vs. temperature relationship. The RTD can then be used to determine any temperature from its measured resistance.

A typical measurement technique for industrial thermometers involves sending a constant current through the sensor (0.8 mA to 1.0 mA), and then measuring the voltage generated across the sensor using digital voltmeter techniques. The technique is simple and few error-correcting techniques are applied.

In a laboratory where measurement accuracies of 10 ppm or better are required, specialized measurement equipment is used. High-accuracy bridges and digital voltmeters with special error-correcting functions are used. Accuracies of high-end measurement equipment can reach 0.1 ppm (parts per million). These instruments have functions to compensate for errors such as thermoelectric voltages and element self-heating.

In addition to temperature, strain on and impurities in the wire also affect the sensor's resistance vs. temperature characteristics. The Matthiessen rule states that the resistivity ( $\rho$ ) of a metal conductor depends on temperature, impurities, and deformation.  $\rho$  is measured in ( $\Omega$  cm):

$$\rho(\text{total}) = \rho(\text{temperature}) + \rho(\text{impurities}) + \rho(\text{deformation}) \quad (32.20)$$

Proper design and careful material selection will minimize these effects so that resistivity will only vary with a change in temperature.

### Resistance of Metals

Whether an RTD's element is constructed of platinum, copper, or nickel, each type of metal has a different [sensitivity](#), [accuracy](#), and temperature range. Sensitivity is defined as the amount of resistance change of the sensor per degree of temperature change. [Figure 32.7](#) shows the sensitivity for the most common metals used to build RTDs.

Platinum, a noble metal, has the most stable resistance-to-temperature relationship over the largest temperature range  $-184.44^\circ\text{C}$  ( $-300^\circ\text{F}$ ) to  $648.88^\circ\text{C}$  ( $1200^\circ\text{F}$ ). Nickel elements have a limited temperature

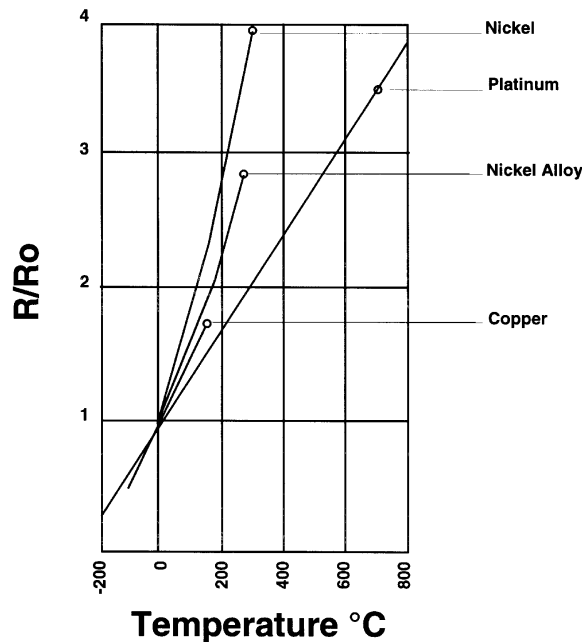


FIGURE 32.7 Of the common metals, nickel has the highest sensitivity.

**TABLE 32.6**

Probe	Basic application	Temperature	Cost	Probe style <sup>a</sup>	Handling
SPRT	Calibration of Secondary SPRT	−200 to 1000°C (−328 to 1832°F)	\$5000	I	Very fragile
Secondary SPRT	Lab use	−200 to 500°C (−328 to 932°F)	\$700	I, A	Fragile
Wirewound IPRT	Industrial field use	−200 to 648°C (−328 to 1200°F)	\$60–\$180	I, S, A	Rugged
Thin-film IPRT	Industrial field use	−50 to 260°C (−200 to 500°F)	\$40–\$140	I, S, A	Rugged

<sup>a</sup> I = immersion; A = air; S = surface.

range because the amount of change in resistance per degree of change in temperature becomes very nonlinear at temperatures above 300°C (572°F). Copper has a very linear resistance-to-temperature relationship. However, copper oxidizes at moderate temperatures and cannot be used above 150°C (302°F).

Platinum is the best metal for RTD elements for three reasons. It follows a very linear resistance-to-temperature relationship; it follows its resistance-to-temperature relationship in a highly repeatable manner over its temperature range; and it has the widest temperature range among the metals used to make RTDs. Platinum is not the most sensitive metal; however, it is the metal that offers the best long-term [stability](#).

The accuracy of an RTD is significantly better than that of a thermocouple within an RTD's normal temperature range of −184.44°C (−300°F) to 648.88°C (1200°F). RTDs are also known for high stability and repeatability. They can be removed from service and recalibrated for verifiable accuracy and checked for any possible drift.

## Who Uses RTDs? Common Assemblies and Applications

Different applications require different types of RTDs. A direct-immersion Platinum Resistance Thermometer (PRT) and a connection head can be used for low-velocity pipelines, tanks, or air temperature measurement. A spring-loaded PRT, thermowell, and connection head are often used in pipelines or storage tanks. An averaging temperature element senses and measures temperatures along its entire sheath, which can range from 1 to 20 m in length. A heavy-duty underwater temperature sensor is designed for complete submersion under rivers, cooling ponds, or sewers. These are just a few examples of RTD configurations and applications.

## Overview of Platinum RTDs

There are three main classes of Platinum Resistance Thermometers (PRTs): Standard Platinum Resistance Thermometers (SPRTs), Secondary Standard Platinum Resistance Thermometers (Secondary SPRTs), and Industrial Platinum Resistance Thermometers (IPRTs). [Table 32.6](#) presents information about each.

## Temperature Coefficient of Resistance

Each of the different metals used for sensing elements (platinum, nickel, copper) has a different amount of relative change in resistance per unit change in temperature. A measure of a resistance thermometer's sensitivity is its temperature coefficient of resistance. It is defined as the element's change in resistance per degree C change in temperature per ohm of sensor resistance over the range of 0°C to 100°C.

The [alpha](#) value is the average change in resistance per degree C per ohm resistance. The actual change in resistance per degree C per ohm is largest at −200°C and decreases steadily as the use temperatures increase.

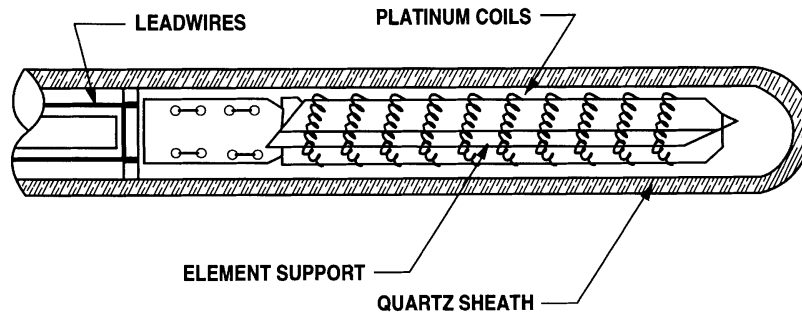


**FIGURE 32.8** The Standard Platinum Resistance Thermometer is fragile and used only in laboratory environments.

The units for the coefficient are  $\Omega/\Omega^{-1}/^{\circ}\text{C}^{-1}$ . This is called the alpha value and is commonly denoted by the Greek letter  $\alpha$ . The larger the temperature coefficient, the greater the change in resistance for a given change in temperature. Of the commonly used RTD metals, nickel has the highest temperature coefficient, 0.00672, while that of copper is 0.00427. The  $\alpha$  value of the sensor is calculated using the equation:

$$\alpha = \frac{R_{100} - R_0}{100^{\circ}\text{C} \times R_0} \quad (32.21)$$

where  $R_0$  = the resistance of the sensor at  $0^{\circ}\text{C}$

$R_{100}$  = the resistance of the sensor at  $100^{\circ}\text{C}$

Three primary temperature coefficients are specified for platinum:

1. ITS-90, the internationally accepted temperature scale, requires a minimum temperature coefficient of 0.003925 for SPRTs. This is achieved using high-purity wire (99.999% or better) wound in a strain-free configuration.
2. With reference-grade platinum wire used in industrial elements, the temperature coefficient is 0.003902.
3. IEC 751 [1] and ASTM 1137 [2] have standardized the temperature coefficient of 0.0038500 for platinum.

## RTD Construction

Standard Platinum Resistance Thermometers (SPRTs), the highest-accuracy platinum thermometers, are fragile and used in laboratory environments only (Figure 32.8). Fragile materials do not provide enough strength and vibration resistance for industrial environments. SPRTs feature high repeatability and low drift, but they cost more because of their materials and expensive production techniques.

SPRT elements are wound from large-diameter, high-purity platinum wire. Internal leadwires are usually made from platinum and internal supports from quartz or fused silica. SPRTs are used over a very wide range, from  $-200^{\circ}\text{C}$  ( $-328^{\circ}\text{F}$ ) to above  $1000^{\circ}\text{C}$  ( $1832^{\circ}\text{F}$ ). For SPRTs used to measure temperatures up to  $660^{\circ}\text{C}$  ( $1220^{\circ}\text{F}$ ), the ice point resistance is typically  $25.5 \Omega$ . For high-temperature thermometers, the ice point resistance is  $2.5 \Omega$  or  $0.25 \Omega$ . SPRT probes can be accurate to  $\pm 0.001^{\circ}\text{C}$  ( $0.0018^{\circ}\text{F}$ ) if properly used.

Secondary Standard Platinum Resistance Thermometers (Secondary SPRTs) are also intended for laboratory environments (Figure 32.9). They are constructed like the SPRT, but the materials are less expensive, typically reference-grade, high-purity platinum wire, metal sheaths, and ceramic insulators. Internal leadwires are usually a nickel-based alloy. The secondary grade sensors are limited in temperature

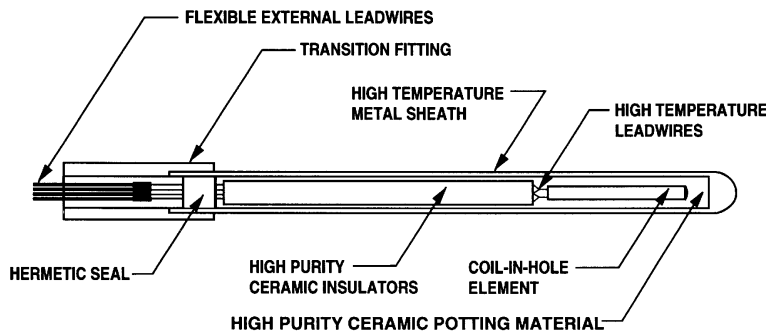


FIGURE 32.9 The Secondary Standard Platinum Resistance Thermometer is intended for laboratory environments.

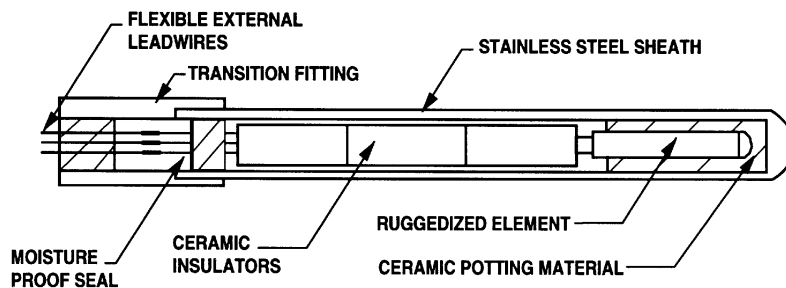


FIGURE 32.10 Industrial Platinum Resistance Thermometers are almost as durable as thermocouples.

range —  $-200^{\circ}\text{C}$  ( $-328^{\circ}\text{F}$ ) to  $500^{\circ}\text{C}$  ( $932^{\circ}\text{F}$ ) — and are accurate to  $\pm 0.03^{\circ}\text{C}$  ( $\pm 0.054^{\circ}\text{F}$ ) over their temperature range.

Secondary standard thermometers can withstand some handling, although they are still quite strain-free. Rough handling, vibration, and shock will cause a shift in calibration. The nominal resistance of the ice point is most often  $100\ \Omega$ . This simplifies calibration procedures when calibrating other  $100\text{-}\Omega$  RTDs. The temperature coefficient for secondary standards using reference-grade platinum wire is usually  $0.00392\ \Omega\ \Omega^{-1}\ ^{\circ}\text{C}^{-1}$  or higher.

Industrial Platinum Resistance Thermometers (IPRTs) are designed to withstand industrial environments and are almost as durable as thermocouples (Figure 32.10). IEC 751 [1] and ASTM 1137 [2] standards cover the requirements for industrial platinum resistance thermometers. The most common temperature range is  $-200^{\circ}\text{C}$  ( $-328^{\circ}\text{F}$ ) to  $500^{\circ}\text{C}$  ( $932^{\circ}\text{F}$ ). Standard models are interchangeable to an accuracy of  $\pm 0.25^{\circ}\text{C}$  ( $\pm 0.45^{\circ}\text{F}$ ) to  $\pm 2.5^{\circ}\text{C}$  ( $\pm 4.5^{\circ}\text{F}$ ) over their temperature range.

Several element designs are available for different applications. One common configuration is the wirewound element (Figure 32.11). This durable design was developed as a substitute for the fragile SPRT. The small platinum sensing wire (usually within  $7$  to  $50\ \mu\text{m}$  ( $0.0003$  in. to  $0.002$  in. diameter)) is non-inductively wound around a cylindrical ceramic mandrel, and usually covered with a thin layer of material that provides electrical insulation and mechanical protection. Because the sensing element wire is firmly supported, it cannot expand and contract as freely as the SPRT's relatively unsupported platinum wire. This type of element offers higher durability than SPRTs and secondary standards, and very good accuracy for most industrial applications.

In another wirewound design, the coil suspension, a coil of fine platinum wire is assembled into small holes in a cylindrical ceramic mandrel (Figure 32.12). The coils are supported by ceramic powder or cement, and sealed at both ends. When ceramic powder is loosely packed in the bores of the mandrel,

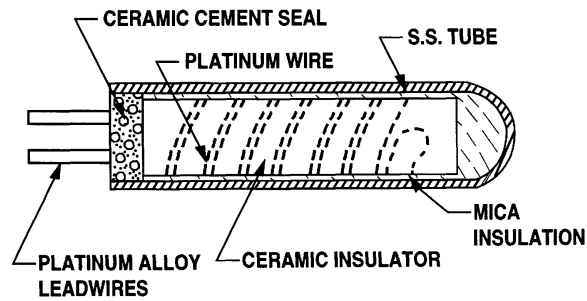


FIGURE 32.11 The wirewound RTD is noninductively wound around a cylindrical ceramic mandrel.

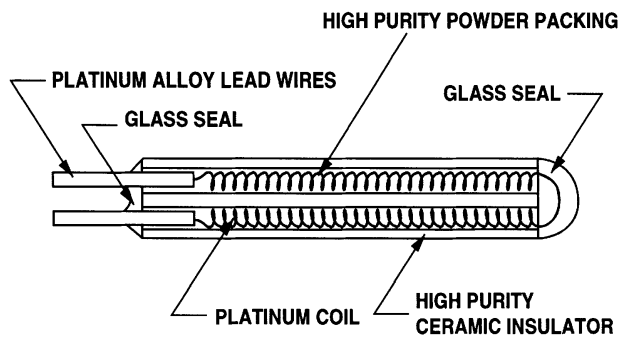


FIGURE 32.12 The coil suspension RTD has a coil of wire assembled into small holes.

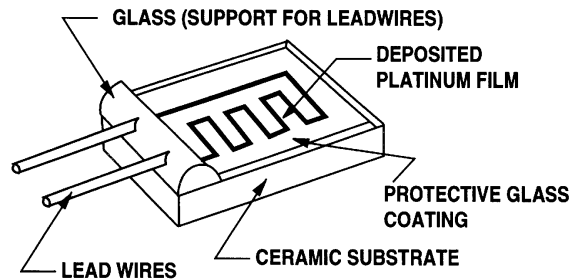


FIGURE 32.13 Thin-film elements have a thin film of platinum deposited onto a ceramic substrate.

the element can expand and contract freely. This reduces the effects of strain on the resistance characteristics, resulting in very high accuracy and stability for use in secondary temperature standards and docile industrial applications (with little or no vibration or shock). Recent improvements in ceramic materials give the sensing coil more stability — it will be capable of maintaining accuracies of  $0.03^{\circ}\text{C}$  after thousands of hours at temperatures of  $500^{\circ}\text{C}$ . These ceramic powders support the coils in the mandrel bores and hold them firmly in place with minimum strain.

Thin-film elements are extremely small, often less than 1.6 mm (1/16 in.) square (Figure 32.13). They are manufactured by similar techniques employed to make integrated circuits. First, a thin film of platinum is deposited onto a ceramic substrate. Some manufacturers use photolithography to etch the deposited platinum, leaving the element pattern on the ceramic substrate. Then, the element's surfaces are covered with glass material to protect the elements from humidity and contaminants.

The temperature range of thin film platinum elements is  $-50^{\circ}\text{C}$  ( $-58^{\circ}\text{F}$ ) to  $400^{\circ}\text{C}$  ( $752^{\circ}\text{F}$ ); accuracy is from  $0.5^{\circ}\text{C}$  ( $0.9^{\circ}\text{F}$ ) to  $2.0^{\circ}\text{C}$  ( $3.6^{\circ}\text{F}$ ). The most common thin-film element has a  $100\text{-}\Omega$  ice point resistance and a temperature coefficient of  $0.00385^{\circ}\text{C}$ .

Thin-film RTDs can be extremely durable if the small-diameter leadwires and the thin element are properly protected. The accuracy and stability might not be as good as some wirewound elements due to hysteresis, long-term stability errors, and self-heating errors.

### Self-heating Errors

The current that measures sensor resistance also heats the sensor. This is known as  $I^2R^*$  heating or Joule heating. Because of this effect, the sensor's indicated temperature is somewhat higher than the actual temperature. This inconsistency is commonly called self-heating error. Self-heating errors, which are dependent on the application, can range from negligible values to  $1^{\circ}\text{C}$ . The greatest heating errors occur because of poor heat transfer between the sensing element and application, or excessive current used in measuring resistance.

The following are methods for reducing the self-heating error.

1. Minimize the power dissipation in the sensor. There is a tradeoff between the signal level and the self-heating of the sensor. Typically, 1 mA of current is used as the sensing current.
2. Use a sensor with a low thermal resistance. The lower the thermal resistance of the sensor, the better the sensor can dissipate the  $I^2R$  power and the lower the temperature rise in the sensor. Small time constants indicate a sensor with a low thermal resistance.
3. Maximize thermal contact between the sensor and the application.

### Calibration

Testing programs are essential to verify the accuracy of PRTs. Some IPRTs are factory-calibrated to a temperature such as at the ice point, but PRT users might want to calibrate them at other temperatures, depending on their application.

The calibration results can be compared to prior calibrations from the same instrument. This will determine if it is necessary to repair or replace the instrument, or if calibration is required more often.

Since frequent repairs and recalibration are usually costly, purchasers and specifiers of PRTs might want to investigate various RTDs before installation by referring to ASTM Standard #E1137-95 [2], published by The American Society for Testing and Materials (ASTM).

*Frequency.* An RTD's stability depends on its working environment. High temperatures can cause drift and contamination of the platinum wire. The higher the temperature, the faster the drift occurs. Below  $400^{\circ}\text{C}$ , the high-temperature drift is not a significant problem, but temperatures reaching  $500^{\circ}\text{C}$  to  $600^{\circ}\text{C}$  are the most significant causes of drift — up to several degrees per year. Severe shock can damage a sensor instantly and cause failure. Shock, vibration, and rough handling will put strains in the platinum wire and change its characteristics, and ultimately damage the entire unit. If a sensor is not properly sealed, humidity can get into the sensor and cause some problems with the insulation resistance. Since the water in humidity is conductive, it will get between the lead wires and the sensing element, and basically shunt off the resistance of the element's wires. Under extreme operating conditions, a sensor should be calibrated on a monthly or bimonthly basis. If five or more calibrations are completed without a significant change, then the time between calibrations can be doubled; at least once a year is recommended, however.

*Techniques.* Two common calibration methods are the fixed point method and the comparison method.

*Fixed point calibration,* used for the highest accuracy calibrations, uses the triple point, freezing point or melting point of pure substances such as water, zinc, tin, and argon to generate a known and repeatable temperature (Figure 32.14). The fixed point cells are sealed to prevent contamination and to prevent atmospheric conditions from affecting the cell's temperature. These cells allow the user to reproduce actual conditions of the ITS-90 temperature scale.

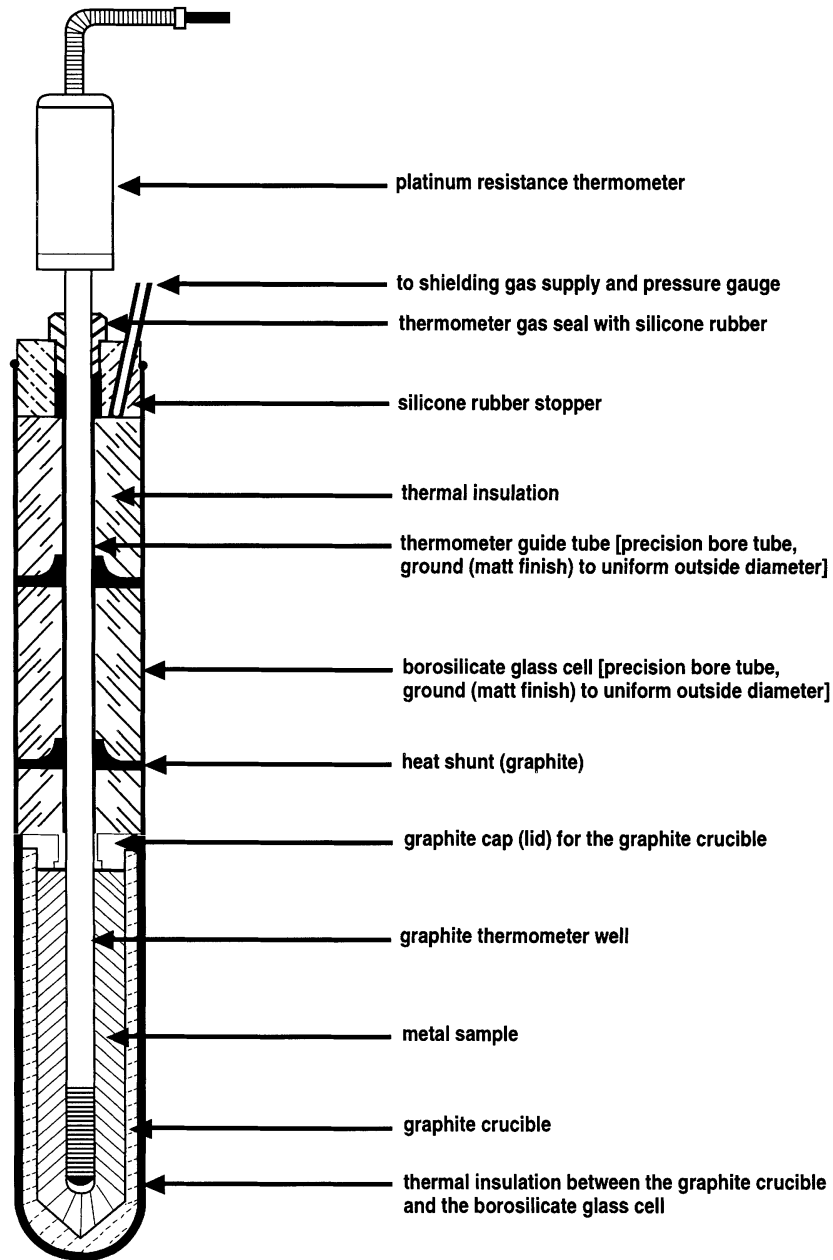


**FIGURE 32.14** Fixed point calibration uses the triple point, freezing point, or melting point of water, zinc, tin, and argon.

Fixed point calibrations provide extremely accurate calibrations (within  $\pm 0.001^{\circ}\text{C}$ ), but the cells are time-consuming to use and can only accommodate one sensor at a time. For this reason, they are not widely used in calibrating industrial sensors. Each fixed point cell has a unique procedure for achieving the fixed point.

A generalized procedure for fixed point calibration is as follows:

1. Prepare the cell. Different procedures exist for each fixed point.
2. Insert the thermometer to be calibrated.

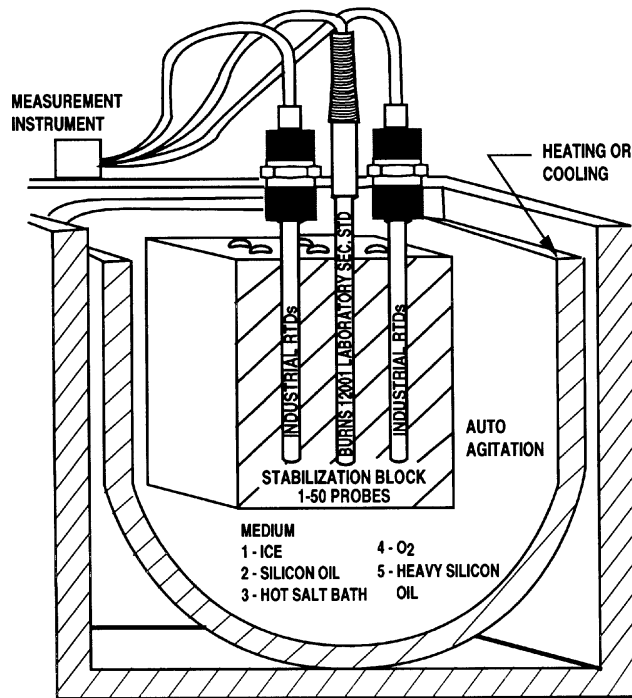


FIGURE 32.15 An isothermal bath permits calibration of industrial RTDs compared with a secondary standard.

3. Allow the system to stabilize. Stabilization times depend on thermometer/fixed point cells. Usually, 15 to 30 min is sufficient.
4. Measure the resistance of the thermometer. For the highest accuracy measurements, special resistance bridges are used. They have accuracies in the range of 10 ppm to 0.1 ppm.

A common fixed point calibration method for industrial-grade probes is the ice bath. The equipment is inexpensive, easy to use, and can accommodate several sensors at once. The ice point is designated as a secondary standard because its accuracy is  $\pm 0.005^{\circ}\text{C}$  ( $\pm 0.009^{\circ}\text{F}$ ), compared to  $\pm 0.001^{\circ}\text{C}$  ( $\pm 0.0018^{\circ}\text{F}$ ) for primary fixed points.

In *comparison calibrations*, commonly used with secondary SPRTs and industrial RTDs, the thermometers being calibrated are compared to calibrated thermometers by means of an isothermal bath whose temperature is uniformly stable (Figure 32.15). Unlike fixed point calibrations, comparisons can be made at any temperature between  $-100^{\circ}\text{C}$  ( $-148^{\circ}\text{F}$ ) and  $500^{\circ}\text{C}$  ( $932^{\circ}\text{F}$ ). This method might be more cost-effective since several sensors can be calibrated simultaneously with automated equipment.

These isothermal baths, electrically heated and well-stirred, use silicone oils as the medium for temperatures ranging from  $-100^{\circ}\text{C}$  ( $-148^{\circ}\text{F}$ ) to  $200^{\circ}\text{C}$  ( $392^{\circ}\text{F}$ ), and molten salts for temperatures above  $200^{\circ}\text{C}$  ( $392^{\circ}\text{F}$ ). At temperatures above  $500^{\circ}\text{C}$  ( $932^{\circ}\text{F}$ ), air furnaces or fluidized beds are used, but are significantly less uniformly stable.

The procedure for comparison calibration is as follows:

1. Insert the standard thermometer and thermometers being calibrated into the bath.
2. Allow the bath to stabilize.
3. Measure the resistance of the standard to determine the temperature of the bath.
4. Measure the resistance of each thermometer under calibration.

*Deriving the resistance vs. temperature relationship of a PRT.* After determining the PRT's resistance, the calibration coefficients can be determined. By plugging these values into an equation, temperature

**TABLE 32.7** Defining Fixed Points of the ITS-90

Material <sup>a</sup>	Equilibrium State <sup>b</sup>	Assigned value of temperature	
		$T_{90}$ (K)	$t_{90}$ (°C)
He	VP	3–5	–270.15 to –268.15
e-H <sub>2</sub>	TP	13.8033	–259.3467
e-H <sub>2</sub> (or He)	VP (or GT)	≈17	≈–256.16
e-H <sub>2</sub> (or He)	VP (or GT)	≈20.3	≈–252.85
Ne	TP	24.5561	–248.5939
O <sub>2</sub>	TP	54.3584	–218.7916
Ar	TP	83.8058	–189.3442
Hg	TP	234.3156	–38.8344
H <sub>2</sub> O	TP	273.16	0.01
Ga	MP	302.9146	29.7646
In	FP	429.7485	156.5985
Sn	FP	505.078	231.928
Zn	FP	692.677	419.527
Al	FP	933.473	660.323
Ag	FP	1234.93	961.78
Au	FP	1337.33	1064.18
Cu	FP	1357.77	1084.62

<sup>a</sup> e-H<sub>2</sub> indicates equilibrium hydrogen; that is, hydrogen with the equilibrium distribution of its *ortho* and *para* forms at the corresponding temperatures. Normal hydrogen at room temperature contains 25% *para* and 75% *ortho* hydrogen. The isotopic composition of all materials is that naturally occurring.

<sup>b</sup> VP indicates vapor pressure point or equation; GT indicates gas thermometer point; TP indicates triple point; FP indicates freezing point; MP indicates melting point.

from any measured resistance can be derived. The two most common curve-fitting techniques are the ITS-90 and Callendar–Van Dusen equations.

On January 1, 1990, the International Temperature Scale of 1990 (ITS-90) became the official international temperature scale [3]. ITS-90 extends upward from 0.65 K (–272.5°C or –458.5°F) and defines temperatures of 0.65 K (0.65°C above absolute zero) and up by fixed points (see Table 32.7).

Two reference functions are used to define the temperature coefficient for an ideal SPRT: one for temperatures below 0°C and the other for temperatures above 0°C. When a PRT is calibrated on the ITS-90, the coefficients determined in the calibration are used to describe a deviation function that represents the difference between the resistance of the standard PRT and the reference function at all temperatures within the range. Using the calibration coefficients and the deviation functions, the SPRT can be used to determine any temperature from its measured resistance. Because ITS-90 equations are complex, computer software is necessary for accurate calculations.

ITS-90 affects:

- Standards and temperature calibration laboratories
- Users of standard and secondary SPRTs with traceability to standards laboratories
- Users of temperature measurement and control systems within companies concerned with verifiable total quality management

The National Institute for Standards and Technology (NIST) has published Technical Note 1265, *Guidelines for Realizing the International Temperature Scale of 1990* [4]. Not all PRT users need to follow the complex equations and computer programs associated with ITS-90. As a rule of thumb: if the minimum required uncertainty of measurement is less than 0.1°C, one probably will want to use ITS-90. For uncertainty of measurements greater than 0.1°C, the effect of the change in scales is relatively small and one will not be affected.

Callendar–Van Dusen equations are interpolation equations that describe the temperature vs. resistance relationship of industrial PRTs. These simple-to-use second- and fourth-order equations can be programmed

easily into many electronic controllers. The equation for the temperature range of 0°C (32°F) to 850°C (1562°F) is:

$$R(t) = R_0 (1 + At + Bt^2) \quad (32.22)$$

For the temperature range -200°C (-392°F) to 0°C (32°F):

$$R(t) = R_0 [1 + At + Bt^2 + C(t-100)t^3] \quad (32.23)$$

where  $R(t)$  = Resistance of the PRT at temperature  $t$   
 $t$  = Temperature in °C  
 $R_0$  = Nominal resistance of the PRT at 0°C  
 $\alpha, \delta, \beta$  = Calibration coefficients

To determine the temperature from a measured resistance, a different set of equations and calibration coefficients is required. For temperatures greater than 0°C (measured resistances greater than the known ice point resistance of the PRT):

$$t(^{\circ}\text{C}) = \left[ (R_t - R_0) / (\alpha R_0) \right] + \delta \left[ (t/100) - 1 \right] (t/100) \quad (32.24)$$

For temperatures less than 0°C (measured resistances less than the known ice point resistance of the PRT):

$$t(^{\circ}\text{C}) = \left[ (R_t - R_0) / (\alpha R_0) \right] + \delta \left[ (t/100) - 1 \right] (t/100) + \beta \left[ (t/100) - 1 \right] (t/100)^3 \quad (32.25)$$

where  $t$  = Temperature to be calculated  
 $R(t)$  = Measured resistance at unknown temperature  
 $R_0$  = Resistance of the sensor at 0°C  
 $\alpha, \delta, \beta$  = Coefficients

To correctly determine the temperature from a given resistance with these equations, one must iterate the equations a minimum of five times. After each calculation, the new value of temperature ( $t$ ) is plugged back into the equations. The calculated temperature value will converge on its true value. After five iterations, the calculated temperature should be within  $\pm 0.001^{\circ}\text{C}$  of the true value.

For industrial sensors, an alternative method would be to use nonlinear least squares curve fits to produce the temperature/resistance relationship. However, these methods should not be used for secondary and primary level thermometers as they cannot sufficiently match the defined ITS-90 scale. Curve fitting errors of up to  $0.05^{\circ}\text{C}$  are possible.

## Usage of RTDs Today

Throughout the industry, usage of RTDs is increasing for many reasons. With the advent of the computer age, industries recognize the need for better temperature measurement, and an electrical signal to accompany advances in computerized process instrumentation. RTDs produce an electrical signal; and because of automatic control in industrial plants, it makes it simpler and easier to interface with process controllers. With the focus on reengineering, companies are searching for ways to improve processes. Improved temperature measurement and control is one good way to save energy, reduce material waste, reduce expenses and improve overall operating efficiencies.

Governmental regulations are another reason why RTDs are gaining popularity. In the pharmaceutical industry, the FDA [5] requires validation; among them the verification that temperature measurement is accurate. New regulations are currently being written for the food industry as well [6].

The growing worldwide acceptance of ISO 9000 standards has forced companies to calibrate their temperature measurement systems and instrumentation. In addition, the calibration must be documented, and must be traceable to a recognized national, legal standard.

RTDs are safer for the environment. With mercury thermometers, disposal of mercury is a problem. In many industries, the mere presence of mercury thermometers presents a risk.

### **Examples of Advanced Applications for Critical Temperature Measurement**

RTD technology allows for custom design in a wide range of applications and industries. In many of these cases, the RTD becomes an integral part of an advanced application when temperature is critical.

Power plants use RTD sensors to monitor fuel and coolant temperatures entering and exiting heat exchangers. Accurate temperature measurement is also critical for nuclear power plants to perform pressure leak tests on the containment vessel surrounding the reactor core.

Microprocessor manufacturers require precise temperature control throughout their clean room areas. Air temperature is critical to production; many temperature measurement points need to be accurate  $\pm 0.028^\circ\text{C}$  within ( $\pm 0.05^\circ\text{F}$ ). To achieve this, an RTD is calibrated with a temperature transmitter. This matched pair ensures the highest level of system accuracy and eliminates the interchangeability error of the RTD.

### **The Future of RTD Technology**

The future of RTD technology is driven by end-user needs and unsolved problems. For example, the need for high-temperature industrial RTDs exists for applications above  $600^\circ\text{C}$  ( $1200^\circ\text{F}$ ). In order to function at high temperatures, the RTD's platinum element must be protected from contamination. However, the sheath material can be a problem because, at high temperatures, it will react with the oxygen in the air and give off metal particles that can attach themselves to the platinum.

RTDs must be mechanically strong enough to survive higher temperatures as well. A high-temperature industrial RTD would require a thermally resistant sheath, perhaps Inconel 600. In addition, sensor components must be designed and manufactured to resist ultra-high temperatures. Some RTDs are specified to operate above  $600^\circ\text{C}$  ( $1200^\circ\text{F}$ ), but when tested, are not always reliable. Drift and nonrepeatability are problem areas that are in need of further attention.

Advances in RTD calibration provide significant improvements for temperature measurement and control. New measurement technologies combined with powerful computational techniques, have simplified the calibration process and made it more reliable.

Another current area of growth is in-house calibration and calibration baths. Governmental validation requirements and ISO-9000 standards are the driving forces in this area. Because third-party calibration services are expensive, companies want to be more productive and more cost-efficient. Wong [7] discusses the benefits of setting up an in-house calibration lab in addition to traceability concepts. Traceability refers to an unbroken chain of comparisons, linking the temperature measurement to a recognized national, legal standard. In the U.S., this national standard is maintained by the National Institute of Standards and Technology (NIST). All RTD manufacturers, laboratories, and calibration labs must adjust their standards to meet NIST standards.

### **Defining Terms**

**Accuracy:** The degree of agreement between an actual measurement and its reference standard.

**Alpha ( $\alpha$ ):** The temperature coefficient of resistance of a PRT over the range  $0^\circ\text{C}$  to  $100^\circ\text{C}$ . For example,  $\alpha$  for a standard platinum resistance thermometer (SPRT) is 0.003925.

**Calibrate:** To check, adjust or determine an RTD's accuracy by comparing it to a standard.

**DIN (Deutsche Industrial Norm):** A German organization that develops technical, scientific, and dimensional standards that are recognized worldwide.

**Error:** The difference between a correct value and the actual reading taken.

**Primary Standard (or Standard PRT):** A platinum resistance thermometer that meets the requirements for establishing calibrations according to the ITS-90. This highly accurate instrument is intended for laboratory environments and is accurate to 0.001°C.

**Reliability:** Used to designate precision for measurements made within a very restricted set of conditions.

**Repeatability:** The ability to give the same measurement under repeated, matching conditions.

**Stability:** The state of being resistant to change or deterioration.

**Sensitivity:** The amount of resistance change of the sensor per degree temperature change.

## References

1. IEC, Industrial platinum resistance thermometer sensors, IEC International Standard 751.1995-07, Genève, Suisse: Bureau Central de la Commission Electrotechnique Internationale, 1995.
2. ASTM Standards, Standard Specification for Industrial Platinum Resistance Thermometers, Standard E 1137-95, 1995.
3. H. Preston-Thomas, The International Temperature Scale of 1990 (ITS-90), *Metrologia*, 27(1), 3-10, 1990. For errata, see *ibid*, 27(2), 107, 1990.
4. NIST Technical Note 1265, Guidelines for Realizing the International Temperature Scale of 1990 (ITS-90), National Institute of Standards and Technology, 1990.
5. FDA validation for the pharmaceutical industry.
6. FDA validation for the food industry.
7. W. Wong, Traceability tops in-house calibration, *InTech*, 41(8), 27-29, 1994.

## 32.3 Thermistor Thermometers

---

### *Meyer Sapoff*

A thermistor is a thermally sensitive resistor whose primary function is to exhibit a change in electric resistance with a change in body temperature. Unlike a wirewound or metal film resistance temperature detector (RTD), a thermistor is a ceramic semiconductor. An RTD exhibits a comparatively low temperature coefficient of resistance on the order of 0.4 to 0.5% °C<sup>-1</sup>. Depending on the type of material system used, a thermistor can have either a large positive temperature coefficient of resistance (PTC device) or a large negative temperature coefficient of resistance (NTC device).

Two types of PTC thermistors are available. Silicon PTC thermistors rely on the bulk properties of doped silicon and exhibit resistance–temperature characteristics that are approximately linear. They have temperature coefficients of resistance of about 0.7 to 0.8% °C<sup>-1</sup>. The most common application of silicon PTC thermistors is compensation of silicon semiconductor devices and circuits [1]. The materials used for switching-type PTC thermistors are compounds of barium, lead, and strontium titanates. Figure 32.16 shows the resistance–temperature characteristic of a typical switching-type PTC thermistor [2]. At low temperatures, from below 0°C to  $R_{\min}$ , the resistance value is low, and  $R_T$  vs.  $T$  exhibits a small negative temperature coefficient of resistance on the order of  $-1\%$  °C<sup>-1</sup>. As the temperature increases, the temperature coefficient of resistance becomes positive and the resistance begins to rise. At a threshold or switching temperature, the rate of rise becomes very rapid and the PTC characteristic becomes very steep. Within its switching range, the temperature coefficient of resistance can be as high as 100% °C<sup>-1</sup> and the device exhibits a high resistance value. At temperatures above the switching range, the resistance reaches a maximum value beyond which the temperature coefficient becomes negative again. The switching temperature can be varied between 80°C and 240°C by altering the chemical composition of the ceramic. Typical applications for switching-type PTC thermistors are over-temperature protection, current limiting, and self-regulated heating. The temperature coefficient of resistance of a unit used as a heating element typically is about 25% °C<sup>-1</sup> at a switching temperature of 240°C [1, 2].

NTC thermistors consist of metal oxides such as the oxides of chromium, cobalt, copper, iron, manganese, nickel, and titanium. Such units exhibit a monotonic decrease in electric resistance with an

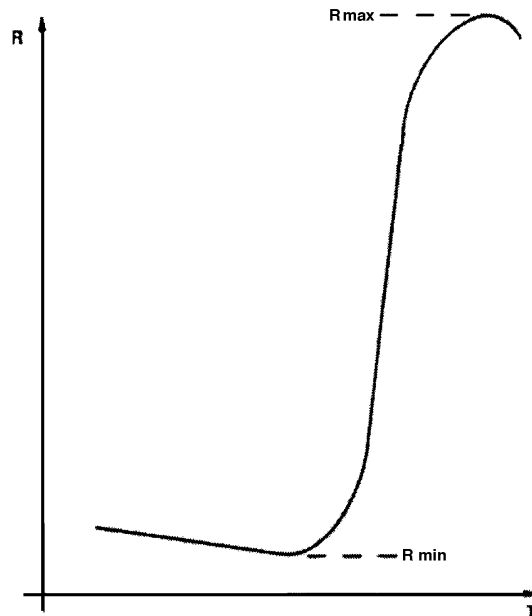


**FIGURE 32.16** Resistance–temperature characteristic of a typical switching-type PTC thermistor. At low temperatures, from below  $0^{\circ}\text{C}$  to  $R_{\min}$ , the resistance value is low and  $R_T$  vs.  $T$  exhibits a small negative temperature coefficient of resistance on the order of  $-1\% \text{ }^{\circ}\text{C}^{-1}$ . As the temperature increases, the temperature coefficient of resistance becomes positive and the resistance begins to rise. At a threshold or switching temperature, the rate of rise becomes very rapid and the PTC characteristic becomes very steep. Within its switching range, the device exhibits a high resistance value. At temperatures above the switching range, the resistance reaches a maximum value beyond which the temperature coefficient becomes negative again.

increase in temperature. The resistance–temperature characteristics of NTC thermistors are nonlinear and approximate the characteristics exhibited by intrinsic semiconductors for which the temperature dependence of resistance is due to the excitation of carriers across a single energy gap. As such, the logarithm of resistance of an NTC thermistor is approximately a linear function of its inverse absolute temperature. Below room temperature, the slope of the function decreases and the thermistor behaves more like an extrinsic semiconductor. The actual conduction mechanism is comparable to the “hopping” mechanism observed in ferrites and manganites that have a spinel crystal structure. Conduction occurs when charge carriers hop from one ionic site in the spinel lattice to an adjacent site. Such hopping can occur when ions of the same element, with valences differing by 1, are present on equivalent lattice sites.

Because of its nonlinear resistance–temperature characteristic, the temperature coefficient of resistance of an NTC thermistor changes with temperature. Depending on the material system used, the temperature coefficient at  $25^{\circ}\text{C}$  typically is in the range of  $-3$  to  $-5\% \text{ }^{\circ}\text{C}^{-1}$ . At  $-60^{\circ}\text{C}$ , it is in the range of  $-6.4$  to  $-11.3\% \text{ }^{\circ}\text{C}^{-1}$ ; and at  $100^{\circ}\text{C}$ , it varies between  $-2.1$  and  $-3.7\% \text{ }^{\circ}\text{C}^{-1}$ . The corresponding resistance ratios with respect to  $25^{\circ}\text{C}$ ,  $R_T/R_{25}$ , are 41 to 228 at  $-60^{\circ}\text{C}$  and 0.13 to 0.03 at  $100^{\circ}\text{C}$ . The slope of the  $\log R$  vs.  $1/T$  characteristic  $\beta$  is relatively constant. The material systems for which the above data are presented exhibit  $\beta$  values of 2930 to 5135 K over the range of 25 to  $125^{\circ}\text{C}$  [1].

Although the resistance–temperature characteristic of an NTC thermistor is nonlinear, it is possible to achieve good linearity of the conductance–temperature and resistance–temperature characteristics using thermistor–resistor networks. The use of a resistor in series with a thermistor results in a linear conductance network, such as a voltage divider. The current obtained in response to a voltage applied to the network is linear with temperature. Consequently, the output of the voltage divider (voltage across the resistor) is linear with temperature. The parallel combination of a resistor and thermistor is a linear resistance network. Techniques exist for optimizing the linearity of single thermistor networks [3, 4].

Such networks exhibit S-shaped curves for their voltage–temperature or resistance–temperature characteristics. For temperature spans of 20°C to 30°C, the maximum deviation is small between any point on the curve and the best straight-line approximation of the curve. As the span increases beyond 30°C, the maximum deviation from linearity increases rapidly from about 0.15°C for a 30°C span to 0.7°C for a 50°C span. Using a two-thermistor network, a maximum linearity deviation of 0.22°C can be obtained over a range of 0°C to 100°C, as compared with a 2°C deviation obtained with a single-thermistor network [5]. Applications for NTC thermistors include temperature measurement, control, and compensation.

When current flows through a thermistor, there is a self-heating effect caused by the power dissipated in it. The thermistor temperature rises until the rate of heat loss from the thermistor to its surrounding environment equals the power dissipated. For this condition of thermal equilibrium, the temperature rise is directly proportional to the power dissipated in the thermistor. The constant of proportionality  $\delta$  is the dissipation constant of the thermistor. By definition,  $\delta$  is the ratio — at a specified ambient temperature, mounting condition, and environment — of the change in power dissipation in a thermistor to the resultant body temperature change. Factors that affect the dissipation constant are the thermistor surface area, the thermal conductivity and relative rate of motion of the medium surrounding the thermistor, the heat loss due to free convection in a still medium, the heat transfer between the thermistor and its mount through the thermistor lead wires, and heat loss due to radiation (significant for gases at low pressure). Because the thermal conductivities of fluids vary with temperature and free convection depends on the temperature difference between the thermistor and its ambient,  $\delta$  is not a true constant. For gases in particular, the dissipation constant varies both with the thermistor body temperature and the amount of self-heating.

The thermal time constant  $\tau$  is the 63.2% response to a step-function change in the thermistor temperature when the power dissipated in the thermistor is negligible. The thermal time constant only has meaning when there is a single exponential response. In such a case, an elapsed time of  $\tau$  results in a 63.2% change between the initial and final steady-state temperatures, while an elapsed time of  $5\tau$  results in a 99.3% change. For a more complex structure, such as a thermistor encapsulated in a sensor housing, multiple exponentials can exist and one cannot predict that the 99% response will occur after an interval of five time constants. As with the dissipation constant, the thermal time constant is dependent on the rate of heat transfer between the thermistor and its environment. Consequently, all of the factors that increase the dissipation constant decrease the time constant.

The most common types of silicon PTC devices are the glass diode package having diameters of 1.8 mm to 2.5 mm and lengths of 3.8 mm to 7.5 mm, and the molded epoxy package with diameters of 3.6 mm to 6.0 mm and lengths of 10.4 mm to 15.0 mm. Such units have axial leads. Epoxy-coated chips and disks with radial leads also are available, with diameters of approximately 3 mm. Silicon PTC thermistors that comply with MIL-T-23648 have an operating temperature range of –55°C to 125°C. Commercial versions can be obtained with a range of –65°C to 150°C [6].

The most common configuration for switching-type PTC thermistors is the radial lead disk, with and without an insulating coating. Such units are available in diameters of 4 mm to 26 mm. The thickness dimension is in the range between 0.5 mm to 6.5 mm. They also are available as surface-mount devices, disks without leads, and in glass diode packages. Switching-type PTC disks have a storage temperature range of –25°C to 155°C and an operating range of 0°C to 55°C [1].

The emphasis of this text will be on NTC thermistors. Most thermistor applications use such devices. Two major categories of NTC thermistors exist. Bead-type thermistors have platinum alloy lead wires sintered into the body of the ceramic. Chip, disk, surface-mount, flake, and rod-type thermistors have metallized surface electrodes. The latter category includes glass diode packages in which dumet leads are compression-bonded to disks or chips.

Glass-coated beads include both adjacent and opposite lead configurations with diameters of 0.125 mm to 1.5 mm. Glass probes with diameters of 0.4 mm to 2.5 mm have lengths ranging from 1.5 mm to 6.35 mm. Probes with diameters of 1.5 mm to 2.5 mm have lengths of 3 mm to 12.7 mm, while larger probes with diameters of 2 mm to 2.5 mm have lengths of up to 50 mm. Glass rods typically are 6.3 mm long with diameters of 1.5 mm to 2.5 mm. A glass probe consists of a bare-bead-type thermistor sealed

at the tip of a solid glass rod and radial dumet leads. A glass rod, by comparison, has its bead sealed in the center of a solid glass rod and has axial dumet leads. The temperature range specified in MIL-T-23648 is  $-55^{\circ}\text{C}$  to  $200^{\circ}\text{C}$  for glass-coated beads and  $-55^{\circ}\text{C}$  to  $275^{\circ}\text{C}$  for glass probes and glass rods. Commercial versions of such glass-enclosed devices typically have a range of  $-80^{\circ}\text{C}$  to  $300^{\circ}\text{C}$ . Some units are rated for intermittent operation at  $600^{\circ}\text{C}$ , while special cryogenic devices are rated for operation in the range of  $-196^{\circ}\text{C}$  to  $25^{\circ}\text{C}$ .

Chip thermistors with radial leads are available with cross-sections of  $0.25\text{ mm} \times 0.25\text{ mm}$  to  $13\text{ mm} \times 13\text{ mm}$  and a thickness range of  $0.175\text{ mm}$  to  $1.5\text{ mm}$ . Disks having diameters of  $1\text{ mm}$  to  $25\text{ mm}$  are available in both radial and axial lead configurations, with a thickness range of  $0.25\text{ mm}$  to  $6.35\text{ mm}$ . Chips and disks also are available in glass diode packages with axial dumet leads. Surface-mount chips are available in sizes ranging from  $2\text{ mm}$  to  $3.2\text{ mm}$  long  $\times$   $1.1\text{ mm}$  to  $1.6\text{ mm}$  wide  $\times$   $0.36\text{ mm}$  to  $1.3\text{ mm}$  thick. Flake thermistors with both adjacent and opposite leads are available in a thickness range of  $0.025\text{ mm}$  to  $0.125\text{ mm}$ , with cross-sections of  $0.5\text{ mm} \times 0.5\text{ mm}$  to  $3\text{ mm} \times 3\text{ mm}$ . The temperature range specified for chips, disks, rods, and glass diode packages in MIL-T-23648 is  $-55^{\circ}\text{C}$  to  $125^{\circ}\text{C}$ . Commercial chips and disks are available with an operating temperature range of  $-80^{\circ}\text{C}$  to  $155^{\circ}\text{C}$  [1]. Rods are available for use over the range of  $-60^{\circ}\text{C}$  to  $150^{\circ}\text{C}$  [7], and glass diode packages are available with an operating range of  $-60^{\circ}\text{C}$  to  $300^{\circ}\text{C}$  [8].

## Thermal Properties of NTC Thermistors

The energy dissipated as heat in a thermistor connected to an electric circuit causes the thermistor body temperature to rise above the ambient temperature of its environment. At any instant, the applicable heat transfer equation is:

$$\frac{dH}{dt} = P = E_T I_T = \delta(T - T_a) + cm \frac{dT}{dt} \quad (32.26)$$

where  $dH/dt = P = E_T I_T$  = Rate of thermal energy or heat supplied to the thermistor

$\delta$  = Dissipation constant

$T_a$  = Ambient temperature

$\delta(T - T_a)$  = Rate of heat loss to the surrounding environment

$c$  and  $m$  = Respectively, specific heat and mass of the thermistor

$cm(dT/dt)$  = Rate of heat absorbed by the thermistor

The solution of Equation 32.26 when  $P$  is constant is:

$$T = T_a + \frac{P}{\delta} \left[ 1 - \exp\left(-\frac{\delta}{cm} t\right) \right] \quad (32.27)$$

The transient solution of Equation 32.27 is the basis for the current–time characteristic of a thermistor. When,  $t \gg cm/\delta$ , then  $dT/dt \rightarrow 0$ , and the steady state solution of Equation 32.27 becomes:

$$P = E_T I_T = \delta(T - T_a) \quad (32.28)$$

where  $E_T$  and  $I_T$  are the steady-state thermistor voltage and current, respectively. Equation 32.28 is the basis for the voltage–current characteristic of a thermistor.

By reducing the thermistor power to a value that results in negligible self-heating,  $P \rightarrow 0$ , Equation 32.26 becomes:

$$\frac{dT}{dt} = -\frac{\delta}{cm}(T - T_a) \quad (32.29)$$

**TABLE 32.8** Thermal Properties of Hermetically Sealed Beads and Probes

Style	Diameter (mm)		Dissipation constant (mW °C <sup>-1</sup> )		Time constant (s)	
	Still air	Still water	Still air	Still water	Still air	Water plunge
Glass-coated bead	0.13	0.045	0.45	0.12	0.45	0.005
Glass-coated bead	0.25	0.09	0.9	0.5	0.9	0.010
Glass-coated bead	0.36	0.10	0.98	1.0	0.98	0.015
Ruggedized bead	0.41	0.12	1.1	1.2	1.1	0.016
Glass probe	0.63	0.19	1.75	1.9	1.75	0.020
Glass-coated bead	0.89	0.35	3.8	4.5	3.8	0.10
Glass-coated bead	1.1	0.40	4.0	5.5	4.0	0.14
Ruggedized bead	1.4	0.51	4.3	7.0	4.3	0.20
Glass probe	1.5	0.72	4.4	12.0	4.4	0.30
Glass probe	2.16	0.90	4.5	16.0	4.5	0.40
Glass probe	2.5	1.0	4.5	22.0	4.5	0.65

From Reference [1].

**TABLE 32.9** Thermal Properties of Thermistors with Metallized Surface Electrodes

Style	Diameter (mm)	Dissipation constant (mW °C <sup>-1</sup> )	Time constant (s)
Chip or disk in glass diode package	2	2–3	7–8
Interchangeable epoxy coated chip or disk	2.4	1	10
Disk with radial or axial leads	2.5	3–4	8–15
Disk with radial or axial leads	5.1	4–8	13–50
Disk with radial or axial leads	7.6	7–9	35–85
Disk with radial or axial leads		10.28–11	28–150
Disk with radial or axial leads		12.75–16	50–175
Disk with radial or axial leads		19.615–20	90–300
Disk with radial or axial leads		25.424–40	110–230
Disk with radial or axial leads	1.3	25–3	16–20
Rod with radial or axial leads	1.8	4–10	35–90
Rod with radial or axial leads	4.4	8–24	80–125

From References [1, 6, 9, 10].

Equation 32.29 is a mathematical statement of Newton's law of cooling and has the solution:

$$T = T_a + (T_i - T_a) \exp\left(-\frac{t}{\tau}\right)$$

where  $T_i$  = Initial thermistor body temperature  
 $T_a$  = Ambient temperature  
 $\tau = cm/\delta$  = Thermal time constant

Table 32.8 gives dissipation and time constant data for glass-coated beads, glass probes, and glass rods. Table 32.9 lists similar data for chip, disk, and rod-type thermistors with metallized surface contacts. Data for the dissipation and time constants are for the thermistor suspended by its leads at 25°C using the procedure specified in MIL-T-23648A. The temperature increment used for computing the dissipation constant results from self-heating the thermistors to 75°C from an ambient of 25°C. The time constant data result from allowing the thermistors to cool from 75°C to an ambient of 25°C. The water-plunge time constant data result from rapidly immersing the thermistors from room temperature air into still water. The transit time was negligible. The air temperature was approximately 25°C and the water temperature was about 5°C. The diameters specified for epoxy-coated interchangeable units are maximum diameters. To illustrate the effect of the environment on the thermal properties of these units, the

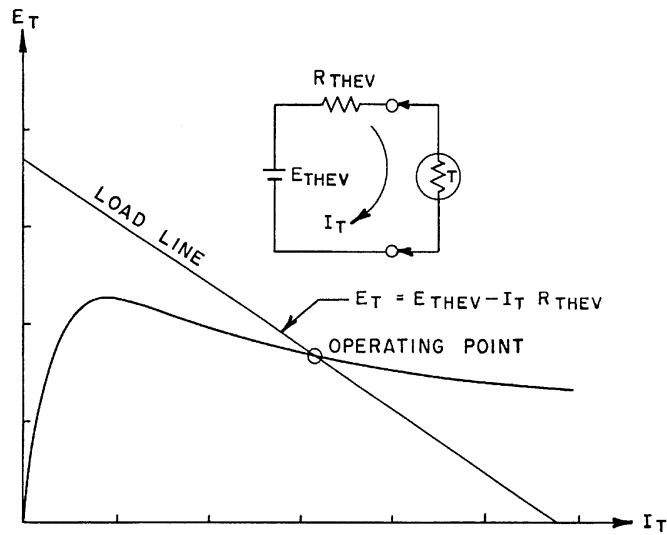


**FIGURE 32.17** Typical voltage–current characteristic of an NTC thermistor. Due to self-heating of the thermistor, the slope of the  $E_T$  vs.  $I_T$  curve decreases with increasing current. This continues until a maximum value of  $E_T$  is reached for which the slope is equal to zero. Beyond this value, the slope continues to decrease and the thermistor exhibits a negative resistance characteristic. The Thevenin equivalent circuit with respect to the thermistor terminals provides a straight-line relationship between  $E_T$  and  $I_T$  that can be plotted as a load line. The intersection of the load line with the  $E_T$  vs.  $I_T$  curve is the operating point.

dissipation and time constants are  $8 \text{ mW } ^\circ\text{C}^{-1}$  and  $1 \text{ s}$ , respectively, when tested in stirred oil, as compared with  $1 \text{ mW } ^\circ\text{C}^{-1}$  and  $10 \text{ s}$ , respectively, when tested in still air. The dissipation and time constants for disks depend on the disk thickness, lead wire diameter, quantity of solder used for lead attachment, distance between the thermistor body and its mount, and the thermistor material. The dissipation and time constants for rods depend on the rod length as well as the variables specified above for disks.

## Electrical Properties of NTC Thermistors

Thermistor applications depend on three fundamental electrical characteristics. These are the voltage–current characteristic, the current–time characteristic, and the resistance–temperature characteristic.

### Voltage–Current Characteristics

Figure 32.17 shows a typical voltage–current curve. At low currents, the power dissipated is small compared with the dissipation constant and the self-heating effect is negligible. Under these conditions, the resistance is constant, independent of the current, and the voltage is proportional to the current. Consequently, at low currents, the characteristic curve is tangent to a constant resistance line equal to the zero-power resistance of the thermistor. As the current increases, the effects of self-heating become more evident; the thermistor temperature rises, and its resistance begins to decrease. For each subsequent incremental increase in current, there is a corresponding decrease in resistance. Hence, the slope of the voltage–current characteristic decreases with increasing current. This continues until the current reaches a value at which the slope becomes zero. Beyond this point, at which the voltage exhibits its maximum value, the slope continues to decrease and the thermistor exhibits a negative resistance characteristic. The temperature, voltage, and current corresponding to the peak of the curve are:

$$T_p = \frac{\beta - \sqrt{\beta^2 - 4\beta T_a}}{2} \quad (32.30)$$

**TABLE 32.10** Applications Based on the Voltage–Current Characteristic of Thermistors

- 
1. Variation in dissipation constant (fixed load line on a family of curves)
    - Vacuum manometers
    - Anemometers, flowmeters, fluid velocity
    - Thermal conductivity analysis, gas detectors, gas chromatography
    - Liquid level measurement, control, and alarm
  2. Variation in circuit parameters (rotation and/or translation of load line on a fixed  $E$ – $I$  curve)
    - Oscillator amplitude and/or frequency regulation
    - Gain or level stabilization and equalization
    - Volume limiters
    - Voltage compression and expansion
    - Switching devices
  3. Variation in ambient temperature (fixed or variable load line on a family of curves)
    - Temperature control or alarm
  4. Microwave power measurement
    - Bolometers
- 

From References [1, 14].

$$E_p = \sqrt{R_p \delta (T_p - T_a)} \quad (32.31)$$

$$I_p = \sqrt{\delta (T_p - T_a) / R_p} \quad (32.32)$$

where  $T_p$  = Absolute temperature (in K) at which the peak occurs  
 $T_a$  = Absolute ambient temperature (in K)  
 $R_p$  = Thermistor resistance at  $T_p$

Applications based on the voltage–current characteristics involve changes in the operating point on a single curve or family of curves. Such changes result from changes in the environmental conditions or variations in circuit parameters. Figure 32.17 shows a graphical solution for obtaining the operating point. The curve represents a nonlinear relationship between the thermistor voltage and current. The Thevenin equivalent circuit with respect to the thermistor terminals provides the relationship given by Equation 32.33.

$$E_T = E_{\text{THEV}} - I_T R_{\text{THEV}} \quad (32.33)$$

where  $E_T$  and  $I_T$  are the thermistor voltage and current, respectively. The straight-line relationship of Equation 32.33 is the load line of the self-heated thermistor. Its intersection with the voltage–current characteristic is the operating point. Table 32.10 categorizes the more familiar applications into four groups distinguished by the form of thermistor excitation [1, 14].

### Current–Time Characteristics

The voltage–current characteristic discussed above deals with a self-heated thermistor operated under steady-state conditions. This condition, for which a decrease in thermistor resistance results from a current sufficiently high to cause self-heating, does not occur instantaneously. A transient condition exists in a thermistor circuit from the time at which power is first applied ( $t = 0$ ) until the time equilibrium occurs ( $t \gg \tau$ ). The relationship between the thermistor current and the time required to reach thermal equilibrium is the current–time characteristic. Generally, the excitation is a step function in voltage through a Thevenin equivalent source. Figure 32.18 shows the current–time characteristics for several

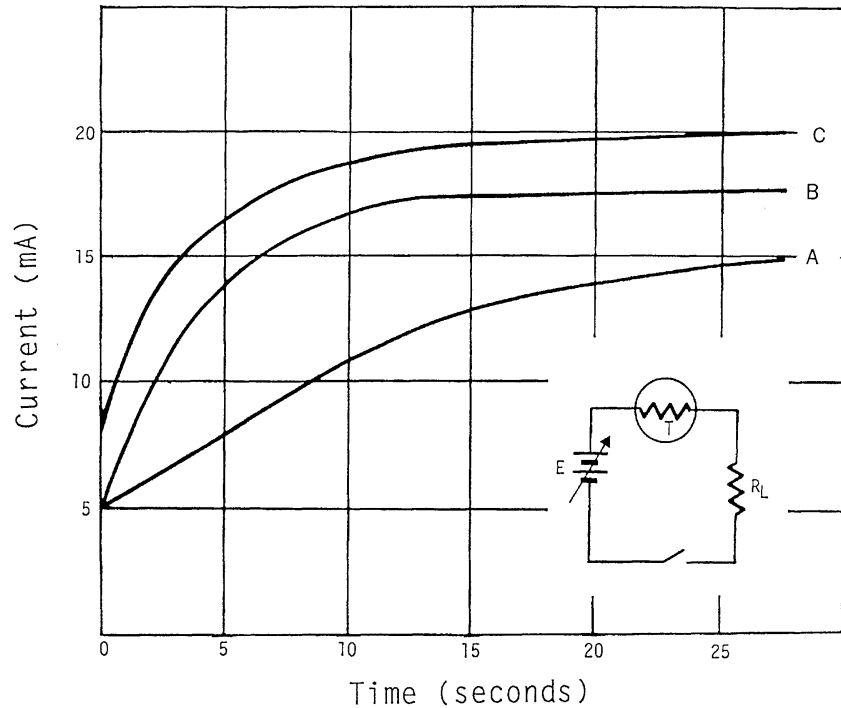


**FIGURE 32.18** Current–time characteristics of Thermometrics, Inc. epoxy-coated chip thermistors. Curves A and C are for a DC95F402 having a zero-power resistance at 25°C of 4 kΩ. Curve B is for a DC9F802 having a zero-power resistance at 25°C of 8 kΩ. The excitation is a step function in voltage through a Thevenin equivalent source. The source voltage and resistance values for curve A are 24 V and 1 kΩ, respectively. For curves B and C, the source voltage is 48 V and source resistance is 2 kΩ.

thermistor disks and voltage sources. For any given characteristic, the source voltage, source resistance, and thermistor zero-power resistance determine the initial current. The source voltage, source resistance, and voltage–current characteristic determine the final equilibrium value. The curve between the initial and final values depends on the circuit design parameters, as well as the dissipation constant and heat capacity of the thermistor. The proper choice of thermistor and circuit design results in a transient time range of a few milliseconds to several minutes.

Applications based on the current–time characteristic are time delay, surge suppression, filament protection, overload protection, and sequential switching.

### Resistance–Temperature Characteristics

The term zero-power resistance applies to thermistors operated with negligible self-heating. This characteristic describes the relationship between the zero-power resistance of a thermistor and its ambient temperature. Over small temperature spans, the approximately linear relationship between the logarithm of resistance and inverse absolute temperature is given by:

$$\ln R_T \cong A + \frac{\beta}{T} \quad (32.34)$$

where  $T$  = Absolute temperature (K)  
 $\beta$  = Material constant of the thermistor

If one lets  $R_T = R_{T_0}$  at a reference temperature  $T = T_0$  and solves for  $R_T$ , one obtains:

$$R_T \cong R_{T_0} \exp \left[ \frac{\beta(T_0 - T)}{TT_0} \right] \quad (32.35)$$

The temperature coefficient of resistance  $\alpha$  is defined as:

$$\alpha \equiv \frac{1}{R_T} \frac{dR_T}{dT} \quad (32.36)$$

Solving Equation 32.34 for  $\alpha$  yields:

$$\alpha = -\frac{\beta}{T^2} \quad (32.37)$$

In Equation 32.34, the deviation from linearity results in temperature errors of 0.01°C, 0.1°C, and 0.3°C for temperature spans of 10°C, 30°C, and 50°C, respectively, within the range of 0°C to 50°C. Using a polynomial for  $\ln R_T$  vs.  $1/T$  reduces the error considerably. The degree of the polynomial required depends on the temperature range and material system used. The use of a third-degree polynomial is adequate for most applications. Hence, more accurate expressions for the resistance–temperature characteristic are:

$$\ln R_T = A_0 + \frac{A_1}{T} + \frac{A_2}{T^2} + \frac{A_3}{T^3} \quad (32.38a)$$

$$\ln R_T = A_0 + \frac{A_1}{T} + \frac{A_2}{T^2} + \frac{A_3}{T^3} \quad (32.38b)$$

$$\frac{1}{T} = \alpha_0 + \alpha_1 \ln R_T + \alpha_2 (\ln R_T)^2 + \alpha_3 (\ln R_T)^3 \quad (32.39)$$

Steinhart and Hart proposed the use of Equation 32.39 for the oceanographic range of –2°C to 30°C [11]. Their analysis showed that no significant loss in accuracy occurred by eliminating the square term  $\alpha_2(\ln R_T)^2$ . Consequently, they proposed the use of Equation 32.40.

$$\frac{1}{T} = b_0 + b_1 \ln R_T + b_3 (\ln R_T)^3 \quad (32.40)$$

Mangum reported that the use of Equation 32.40 resulted in interpolation errors of approximately 0.001°C over the range of 0°C to 70°C [12].

The technical staff at Thermometrics, Inc. evaluated Equation 32.38 over the range of –80°C to 260°C using 17 different thermistor materials. The glass probes investigated encompassed a span of specific resistance values of 2 Ω cm to 300 kΩ cm and a resistance range at 25°C of 10 Ω to 2 MΩ. The results were presented at the *Sixth International Symposium on Temperature* and show that the interpolation errors do not exceed the total measurement uncertainties. For temperature spans of 100°C within the range of –80°C to 260°C, 150°C within the range of –60°C to 260°C, and 150°C to 200°C within the

**TABLE 32.11** Interpolation Errors for  $\ln R_T = C_0 + C_1/T + C_3/T^3$ 

Temperature range (°C)	Temperature span (°C)	Interpolation error (°C)
-80 to 0	50	0.002–0.01
0 to 200	50	0.001–0.003
-80 to 0	100	0.02–0.03
0 to 200	100	0.01
-60 to 90	150	0.1
0 to 150	150	0.045
50 to 200	150	0.015
0 to 200	200	0.08

range of 0°C to 260°C, the interpolation errors are 0.005°C to 0.01°C [13]. Lowering the temperature span to 50°C within the range of 0°C to 260°C reduces the interpolation error to 0.001°C to 0.003°C.

Sapoff and Siwek [14] evaluated the loss in accuracy introduced by eliminating the quadratic term in Equation 32.38. For this condition, Equation 32.38 reduces to Equation 32.41.

$$\ln R_T = C_0 + \frac{C_1}{T} + \frac{C_3}{T^3} \quad (32.41)$$

The interpolation errors introduced by Equations 32.40 and 32.41 depend on the material system, temperature range (nonlinearity increases at low temperatures), and the temperature span considered. Table 32.11 summarizes the errors associated with the use of Equation 32.41 for various temperature spans and ranges.

Equations 32.38 through 32.41 can be rewritten as:

$$R_T = \exp\left(A_0 + \frac{A_1}{T} + \frac{A_2}{T^2} + \frac{A_3}{T^3}\right) \quad (32.42)$$

$$T = \left[ a_0 + a_1 \ln R_T + a_2 (\ln R_T)^2 + a_3 (\ln R_T)^3 \right]^{-1} \quad (32.43)$$

$$T = \left[ b_0 + b_1 \ln R_T + b_3 (\ln R_T)^3 \right]^{-1} \quad (32.44)$$

$$R_T = \exp\left(C_0 + \frac{C_1}{T} + \frac{C_3}{T^3}\right) \quad (32.45)$$

The solutions for Equations 32.38, 32.39, 32.42, and 32.43 require four calibration points and the use of simultaneous equations. Similarly, the solutions for Equations 32.40, 32.41, 32.44, and 32.45 require three calibration points. The use of a polynomial regression analysis involving additional calibration points can minimize the effects of calibration uncertainties.

Applications that depend on the resistance–temperature characteristic are temperature measurement, control, and compensation. There also are applications for which the thermistor temperature depends on some other physical phenomenon. For example, an hypsometer is an instrument in which the temperature of a boiling liquid provides an indication of the liquid vapor pressure. Another example involves the use of thermistor-type cardiac catheters for thermodilution analysis. A saline or dextrose

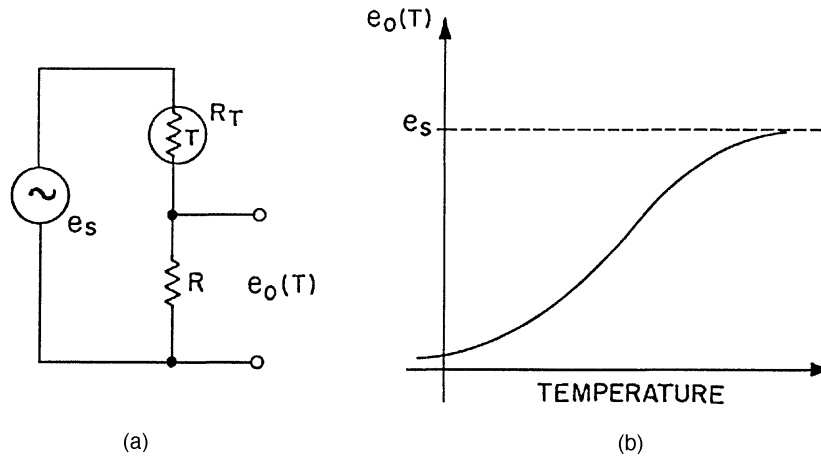


FIGURE 32.19 (a) Thermistor voltage divider. The resistor  $R$  represents the parallel combination of the load resistance and the fixed divider resistor. (b) The output,  $e_o$  vs.  $T$ , is an S-shaped curve that is linear over a portion of the temperature range.

solution of known volume and temperature is injected into the bloodstream through one of the catheter lumens. The mixing of the solution with the blood dilutes the solution and decreases the temperature of the blood as it flows downstream past a thermistor located at the surface of another lumen in the catheter. The cardiac output computed from the temperature–time response data measured by the thermistor provides an indication of the heart pump efficiency.

### Linearization and Signal Conditioning Techniques

The measured resistance and computed constants for Equations 32.43 and 32.44 can be used with a computer to determine temperature without the need for a linear network. This is useful for obtaining high accuracy over relatively wide temperature ranges. Most applications based on the resistance–temperature characteristics of thermistors, however, use some form of linearization or signal conditioning. The use of a constant current source and a linear resistance network provides a voltage output that is linear with temperature. By using the proper combination of current and resistance level, a digital voltmeter connected across the network provides a direct display of temperature. The use of a constant voltage source results in a linear conductance network with a current that is linear with temperature.

#### Linear Conductance Networks

Voltage dividers, ohmmeter circuits and Wheatstone bridge circuits are linear conductance networks. Consider the voltage divider circuit shown in Figure 32.19. Using the fixed resistor for the output eliminates the effect of the load resistance. For the purpose of analysis, the resistor denoted by  $R$  is the parallel combination of the load and fixed divider resistors. Another advantage is that the output voltage increases with temperature with this arrangement. The ratio of output voltage to input voltage is given by:

$$\frac{e_o}{e_s} = \frac{R}{R + R_T} = \frac{1}{1 + R_T/R} \quad (32.46)$$

- where  $e_o$  = Output voltage
- $e_s$  = Source voltage
- $R$  = Parallel combination of the load and fixed resistors
- $R_T$  = Thermistor resistance at a specified temperature  $T$

If one normalizes the thermistor resistance with respect to its value at a specified reference temperature  $T_0$ , then:

$$r_T = \frac{R_T}{R_{T_0}} \quad (32.47)$$

where  $R_{T_0}$  = Thermistor resistance at  $T_0$   
 $r_T$  = Resistance ratio

Thermistor manufacturers typically supply resistance ratio–temperature characteristics in their catalogs. Substituting Equation 32.47 in Equation 32.46 yields:

$$\frac{e_0}{e_s} = \frac{1}{1 + r_T R_{T_0}/R} \quad (32.48)$$

If the circuit constant  $\sigma = R_{T_0}/R$ , then Equation 32.48 becomes:

$$F(T) = \frac{e_0}{e_s} = \frac{1}{1 + r_T \sigma} \quad (32.49)$$

The output for the voltage divider of Figure 32.19a is the S-shaped curve shown in Figure 32.19b. The value of the circuit constant  $\sigma$  determines the temperature range for which good linearity exists between  $e_0$  and  $T$ . References [3, 4] include families of S-shaped curves over the range  $0.01 \leq \sigma \leq 20.0$  for the three basic material systems of MIL-T-23648. A good criterion for achieving optimum linearity is to equate the slopes of the function  $F(T)$  at the end-points of the specified temperature range  $T_L \leq \sigma \leq T_H$ . Specifying that  $dF(T_L)/dT = dF(T_H)/dT$  results in the following:

$$\sigma = \frac{X - Y}{Yr_{T_L} - Xr_{T_H}} \quad (32.50)$$

where  $X$  and  $Y$  are determined by the end-point conditions and the equation constants for  $\ln R_T$  vs.  $T$ . When Equation 32.41 is used,  $X$  and  $Y$  are given by:

$$X = T_H \sqrt{r_{T_L} \left( C_1 + 3 \frac{C_3}{T_H^2} \right)} \quad (32.51)$$

$$Y = T_L \sqrt{r_{T_H} \left( C_1 + 3 \frac{C_3}{T_L^2} \right)} \quad (32.52)$$

When Equation 32.38 is used,  $X$  and  $Y$  are given by:

$$X = T_H \sqrt{r_{T_L} \left( A_1 + 2 \frac{A_2}{T_L} + 3 \frac{A_3}{T_L^2} \right)} \quad (32.53)$$

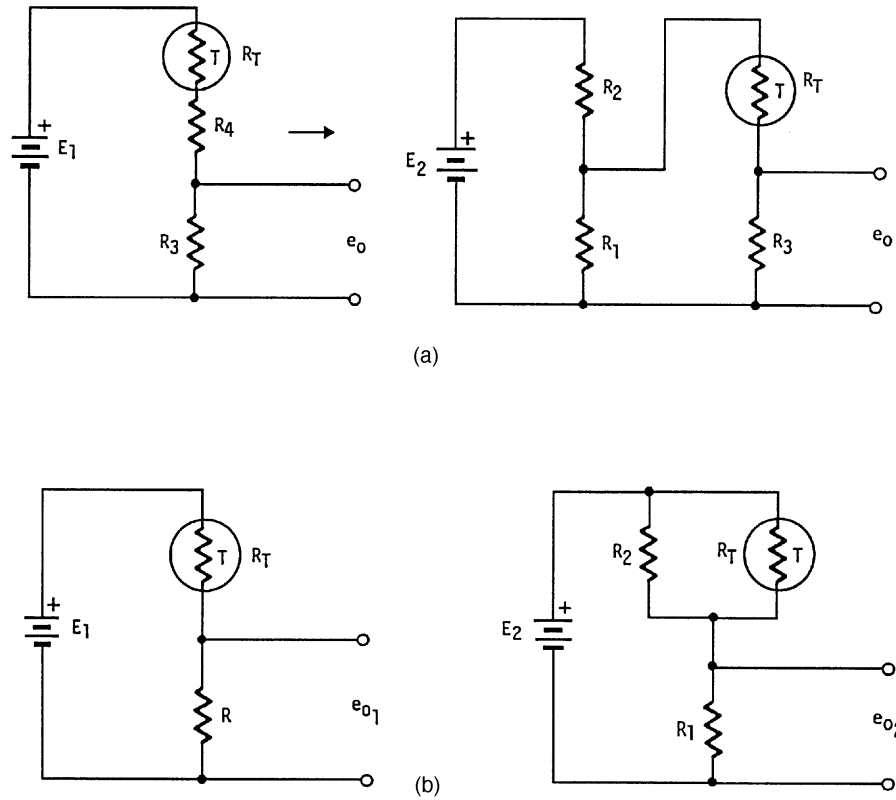


**FIGURE 32.20** Equivalent thermistor voltage divider circuits for converting a network with a nonstandard voltage source to a network that uses a standard voltage source. Only a portion of the output is available in (a). Ohmmeter-type thermometers use such circuits. The conversion circuit of (b) provides the full available output voltage in a series with a bias voltage. (b) is used with bridge circuit-type thermometers.

$$Y = T_L \sqrt{r_{TH} \left( A_1 + 2 \frac{A_2}{T_H} + 3 \frac{A_3}{T_H^2} \right)} \quad (32.54)$$

By allowing  $e_s$  and  $R$  to be the Thevenin equivalent voltage and resistance with respect to the thermistor terminals, respectively, the voltage divider analysis applies to any more complex circuit such as a Wheatstone bridge [3, 4].

Thermistor self-heating constraints typically result in nonstandard voltage sources for thermometer circuit designs. The modified divider circuits of Figure 32.20 provide equivalent circuits with standard voltage sources. Only a portion of the available output voltage appears across the output detector in Figure 32.20a. Ohmmeter-type thermometers use such circuits. The circuit of Figure 32.20a provides the full available output voltage. However, the conversion results in a bias voltage in series with the output. Bridge circuit-type thermometers use the circuit of Figure 32.20b. The conversion equations applicable to Figure 32.20a are:

$$K = \frac{R_1}{R_1 + R_2} = \frac{E_1}{E_2} = \frac{R_3}{R_2} \quad (32.55)$$

$$R = R_3 + R_4 = R_3 + \frac{R_1 R_2}{R_1 + R_2} \quad (32.56)$$

$$E_2 = \text{Desired source voltage} \quad (32.57)$$

$$R_2 = \frac{R_4}{K} \quad (32.58)$$

$$R_1 = \frac{R_2 R_4}{R_2 - R_4} \quad (32.59)$$

$$\left( \frac{R_3}{R_3 + R_4} \right) F(T) \quad (32.60)$$

The conversion equations applicable to Figure 32.20*b* are:

$$K = \frac{R_2}{R_1 + R_2} = \frac{E_1}{E_2} = \frac{R}{R_1} \quad (32.61)$$

$$R = \frac{R_1 R_2}{R_1 + R_2} \quad (32.62)$$

$$E_2 = \text{Desired source voltage} \quad (32.63)$$

$$R_1 = \frac{R}{K} \quad (32.64)$$

$$R_2 = \frac{R R_1}{R_1 - R} \quad (32.65)$$

$$e_{0_2} = (E_2 - E_1) + e_{0_1} \quad (32.66)$$

Reference [15] includes design examples that use these conversion equations.

#### Temperature Controllers.

Thermistor temperature controllers frequently use voltage divider and bridge circuits. The use of a thermistor in such a circuit results in much higher sensitivity than that obtainable with a thermocouple or RTD. The most sensitive standard thermocouples exhibit output voltage slopes of 50 to 55  $\mu\text{V } ^\circ\text{C}^{-1}$  in the range of 0°C to 300°C. Thermistor voltage dividers typically exhibit output slopes of about 8 to 10 mV  $^\circ\text{C}^{-1}$  per volt applied to the divider. Since the input to a thermistor voltage divider typically is in the range of 1 to 5 V, a thermistor provides about 200 to 1000 times the sensitivity of a thermocouple. The temperature coefficient of resistance of a thermistor is about 10 times that of an RTD. However, the temperature span about the control point of a thermistor controller is small compared with that available with a thermocouple or RTD.

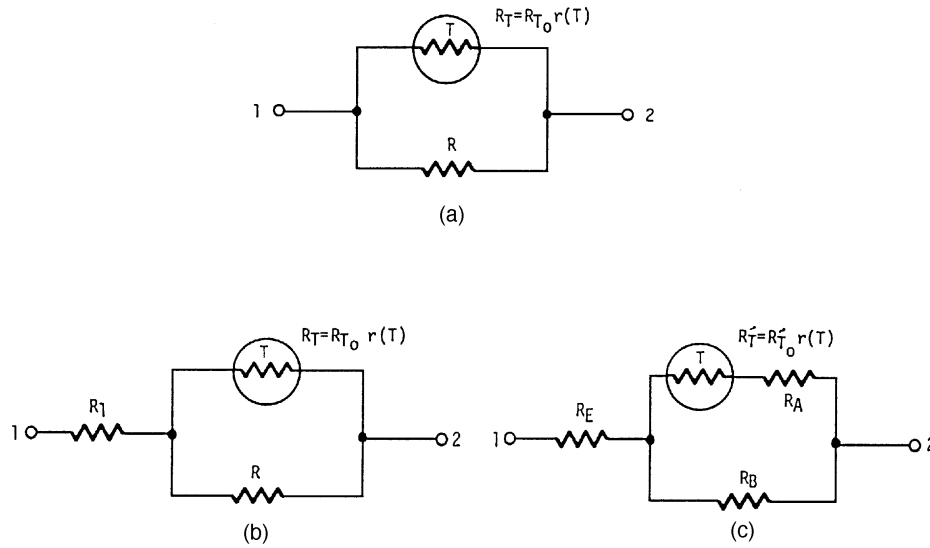


**FIGURE 32.21** Equivalent linear thermistor networks for converting a network with a nonstandard  $R_{T_0}$  to a network with a standard catalog value for  $R'_{T_0}$ . A requirement is that both thermistors have the same resistance ratio–temperature characteristic.

Reference [1] includes some typical low-cost thermistor temperature controllers. Thermistor temperature controllers are available from Hart Scientific, Inc. that provide control stabilities of better than  $0.001^\circ\text{C}$  [16].

### Linear Resistance Networks

A common technique for designing a thermometer circuit is to apply a constant-current source to a linear resistance network. This results in a voltage across the network that is linear with temperature. Temperature compensation for resistance changes that occur in coil windings, instruments, relays, motors, and generators also use such networks. For example, a copper coil has a positive temperature coefficient of resistance of approximately  $0.39\% \text{ }^\circ\text{C}^{-1}$ . The thermistor network has a negative temperature coefficient. The compensator is designed to provide a slope that is equal in magnitude, but opposite in sign to that of the copper coil. Hence, the  $\Omega$  vs.  $^\circ\text{C}$  slope of the compensator is equal to the  $\Omega/^\circ\text{C}$  change of the coil. This results in a current through the coil that is independent of temperature. Additional applications include compensation of drift in silicon strain gages, infrared detectors, and circuits that contain both passive and active components.

For the basic linear resistance network of [Figure 32.21a](#):

$$R_{12} = R_C = \frac{RR_T}{R + R_T} = R \left( 1 - \frac{1}{1 + R_T/R} \right) \quad (32.67)$$

Normalizing with respect to  $R$  and substituting  $r_T = R_T/R_{T_0}$  and  $R_{T_0}/R = \sigma$  in Equation 32.67 yields:

$$R_n = \frac{R_C}{R} = 1 - \frac{1}{1 + r_T \sigma} = 1 - F(T) \quad (32.68)$$

Consequently, the techniques used for optimizing the linearity of voltage dividers also apply to linear resistance networks. The use of the series resistor  $R_1$  in [Figure 32.21b](#), translates the curve to a higher resistance level and does not affect the  $\Omega/^\circ\text{C}$  output.

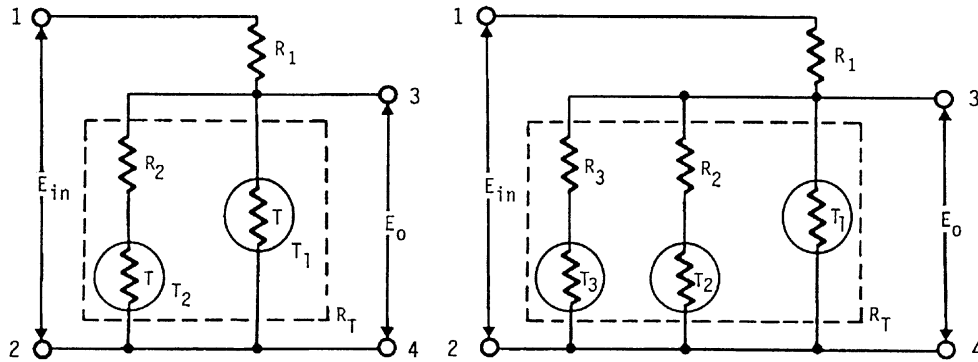


**FIGURE 32.22** Two-thermistor and three-thermistor linear voltage dividers that provide improved linearity. Placing the resistors  $R_1$  across the output terminals 3–4 converts the networks to linear resistance networks.

Frequently, the design of a compensator that provides the desired  $\Omega/^\circ\text{C}$  output results in a thermistor that has a nonstandard  $R_{T_0}$  value. The conversion circuit of Figure 32.21c permits the use of a standard  $R_{T_0}$  value. The conversion equations are as follows:

$$K_1 = \sqrt{\frac{R'_{T_0}}{R_{T_0}}} \quad (32.69)$$

$$R_E = R_1 - R(K_1 - 1) \quad (32.70)$$

$$R_A = RK_1(K_1 - 1) \quad (32.71)$$

$$R_B = RK_1 \quad (32.72)$$

where  $R_{T_0}$  is the nonstandard value and  $R'_{T_0}$  is the standard value. A requirement is that both thermistors have the same resistance–temperature characteristic. Setting  $R_1 = R(K_1 - 1)$  in Figure 32.21b results in  $R_E = 0$  for Figure 32.21c. Consequently, the conversion of Figure 32.21a to that of Figure 32.21c requires the use of the minimum insertion resistance  $R_1 = R(K_1 - 1)$ .

The network provides good linearity for small temperature spans of  $10^\circ\text{C}$  to  $30^\circ\text{C}$ . However, the error increases rapidly from about  $0.15^\circ\text{C}$  for a  $30^\circ\text{C}$  span to  $0.7^\circ\text{C}$  for a  $50^\circ\text{C}$  span ( $0^\circ\text{C}$  to  $50^\circ\text{C}$ ). The use of the two-thermistor network shown in Figure 32.22 results in a maximum linearity error of  $0.22^\circ\text{C}$  over the range of  $0^\circ\text{C}$  to  $100^\circ\text{C}$ , while the three-thermistor network shown reduces the error to  $0.04^\circ\text{C}$  for the same  $0^\circ\text{C}$  to  $100^\circ\text{C}$  range [5]. The networks shown in Figure 32.22 are linear voltage dividers. Placing the resistor  $R_1$  across the output terminals 3–4 converts these networks to linear resistance networks. Many manufacturers sell an interchangeable, three-wire, dual thermistor that is suitable for use in the two-thermistor circuit of Figure 32.2.

Interchangeable thermistors and the linearization techniques described above have been available for many years. In addition, the stability of NTC thermistors is better than that of thermocouples and frequently better than or equal to that of commercial RTDs [17]. However, the nonlinear resistance–temperature characteristics of thermistors continue to limit their use in industrial temperature measurement and control applications. The availability of low-cost microprocessors has eliminated this limitation. Such devices can use the equation constants of Equations 32.38 or 32.39 to compute and display temperature directly. They also can be used to compute lookup tables to provide interpolation uncertainties in the

range of 0.001°C to 0.01°C. There are instruments described in the literature that utilize such microprocessor chips [18, 19]. Thermometrics, Inc. sells a commercial instrument that reads the equation constants from a chip in the connector of each probe supplied for use with the instrument [1]. The use of thermistors for industrial applications will continue to increase as the cost of microprocessor chips continues to fall.

## References

1. Thermometrics, Inc., *Thermometrics NTC & PTC Thermistors*, Edison, NJ, 1993.
2. J. Fabien, Heating with PTC thermistors, *EDN Products Edition*, 41(12A), 10, 1996.
3. M. Sapoff and R. M. Oppenheim, The design of linear thermistor networks, *IEEE International Convention Record*, Part 8, 12, 1964.
4. M. Sapoff, Thermistors: Part 4, Optimum linearity techniques, *Measurements & Control*, 14(10), 1980.
5. C. D. Kimball and R. W. Harruff, Thermistor thermometry design for biological systems, *Temperature, Its Measurement and Control in Science and Industry*, Vol. 4, Pittsburgh, PA: Instrument Society of America, 1972, Part 2.
6. Ketema, Rodan Division, *Thermistor Product Guide*, Anaheim, CA, 1995.
7. Cesiwid Inc., *Alphalite® Bulk Ceramic NTC Thermistors*, Niagara Falls, NY, 1996.
8. Fenwal Electronics, Inc., *Standard Products Catalog*, Milford, MA, 1994.
9. Fenwal Electronics, Inc., *Thermistor Manual*, Milford, MA, 1974.
10. Victory Engineering Corporation, *Technical Corporation of Thermistors & Varistors*, Springfield, NJ, 1962.
11. J. S. Seinhart and S. R. Hart, Calibration curves for thermistors, *Deep Sea Research*, 15, 497, 1968.
12. B. W. Mangum, The triple point of succinonitrile and its use in the calibration of thermistor thermometers, *Rev. Sci. Instrum.*, 54(12), 1687, 1983.
13. M. Sapoff, W. R. Siwek, H. C. Johnson, J. Slepian, and S. Weber, The exactness of fit of resistance–temperature data of thermistors with third-degree polynomials, in J. F. Schooley (ed.), *Temperature, Its Measurement and Control in Science and Industry*, Vol. 5, New York, NY: American Institute of Physics, 1982, 875.
14. M. Sapoff and R. M. Oppenheim, Theory and application of self-heated thermistors, *Proc. IEEE*, 51, 1292, 1963.
15. M. Sapoff, Thermistors: Part 5, Applications, *Measurements & Control*, 14(12), 1980.
16. Hart Scientific, Inc., *Hart Scientific Calibration Equipment*, Pleasant Grove, UT, 1995.
17. W. R. Siwek, M. Sapoff, A. Goldberg, H. C. Johnson, M. Botting, R. Lonsdorf, and S. Weber, Stability of NTC thermistors, in J. F. Schooley (ed.), *Temperature, Its Measurement and Control in Science and Industry*, Vol. 6, New York, NY: American Institute of Physics, 1992, 497.
18. R. L. Berger, T. Clem, C. Gibson, W. Siwek, and M. Sapoff, A digitally linearized thermistor thermometer referenced to IPTS—26(13), 68, 1980.
19. W. R. Siwek, M. Sapoff, A. Goldberg, H. C. Johnson, M. Botting, R. Lonsdorf, and S. Weber, A precision temperature standard based on the exactness of fit of thermistor resistance–temperature data using third degree polynomials, in J. F. Schooley (ed.), *Temperature, Its Measurement and Control in Science and Industry*, Vol. 6, New York, NY: American Institute of Physics, 1992, 491.

## 32.4 Thermocouple Thermometers

---

*R. P. Reed*

### The Simplest Thermocouple

Despite an increasing variety of temperature sensors, the self-generating thermocouple remains the most generally used sensor for thermometry because of its versatility, simplicity, and ease of use. Any pair of

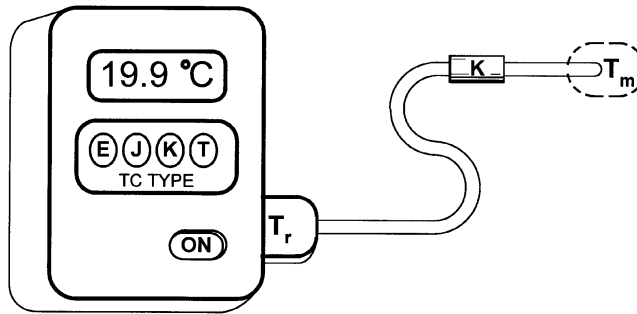


**FIGURE 32.24** The simple modern digital thermocouple thermometer. Modern digital electronics has made casual thermometry very easy, but has obscured the continuing need to have an authentic understanding of thermoelectric principles for accurate thermometry with more complicated circuits and more important measurements.

electrically conducting and thermoelectrically dissimilar materials coupled at an interface is a *thermocouple* [1]. The legs are *thermoelements*. The *Seebeck effect* produces a voltage in all such thermoelements where they are not at a uniform temperature. Any electric interface between dissimilar electric conductors is a *real thermoelectric junction*. A free end of a thermoelement is a *terminus*, not a junction. Couplings between *identical* thermoelements are *splices* or *joints*, not junctions.

It is the thermoelements that determine thermocouple *sensitivity* and calibration; but, it is the temperatures of the end-points of thermoelements (i.e., junction temperatures) that determine the *net* emf observed in thermometry. The Seebeck effect, which converts temperature to voltage, is used for thermoelectric thermometry but is also a primary low-frequency noise source in all low-level electronic circuits [2].

### Simple Thermocouple Thermometry

In the simplest applications, thermocouple thermometry now is as easy to use as is a multimeter to measure resistance. In fact, many present-day digital multimeters (in addition to voltage, current, and resistance) do provide a thermocouple temperature probe, and temperature measurement is just another button-selectable function. These thermocouple thermometers consist of an indicator that digitally displays the temperature of the tip of a plug-in thermocouple probe (Figure 32.24). The simpler of such versatile multimeters can be purchased for less than U.S.\$60 [3]. Interchangeable thermocouple probes of different standard thermocouple material types and specialized sensing tips of widely varying designs are adapted to measurement from surface temperatures to internal temperatures in foodstuffs [4].

With some probes, temperatures up to 1370°C can be indicated merely by (1) ensuring that the selected thermocouple types of the indicator and probe correspond, (2) pressing a power-on button, and (3) applying the probe tip at the point where temperature is to be measured. Promptly, and without calibration, the present temperature of the probe tip is digitally displayed selectably in °C or °F, usually to a resolution of 0.1°C or 1°C. Some specifications claim “accuracy” of 0.3% (4°C at 1370°C) of reading. Some even offer certified *calibration traceability* to NIST or other national standards laboratory.

Modern digital electronics has created the illusion that very accurate thermocouple thermometry is no different than other routine electrical measurements. It has encouraged the perception that arbitrarily fine accuracy can be always be accomplished by calibration and guaranteed by certification. The remarkable simplification of instruments that is now commonplace and an abundance of misleading tutorials obscure the real need for a sound understanding of principles of thermocouple circuits for anything other than inconsequential thermometry.

Manufacturers can shelter users from many problems inherent in thermocouple application. Unfortunately, there are many pitfalls from which the manufacturer cannot isolate the user by design or construction. In less simple applications, it is necessary for the user to avoid problems by carefully learning

and applying the true principles of thermoelectric circuits and thermocouple thermometry. Even the simplest indicators and probes can easily be misused and produce unrecognized substantial error.

Thermometry errors of only a few °C or even much less in energy, process, manufacturing, and research fields annually cost many millions of dollars in lost yield, fuel cost, performance bonuses, etc. Consequence of error can also be incurred as incorrect interpretation of data, failure of objective, equipment damage, personal injury, or even loss of life.

Unusual thermocouple circuits, installations, and special applications often produce *inconspicuous* error or else *peculiar* results that are very puzzling if an authentic model of thermoelectric circuits is not understood. This chapter section presents the factual principles of thermoelectric circuits that equip the user to easily apply thermocouples for reliable and critical thermometry, even in unusual circumstances with justified confidence. These principles are very simple, yet they justify study even by experienced thermocouple users as thermoelectric circuits are very often misrepresented or misunderstood in subtle ways that, although unrecognized, degrade measurement. The aim of the chapter section is to allow thermometry with all *practical* simplicity while avoiding possibly costly measurement errors.

## Thermoelectric Effects

The three thermoelectric phenomena are the Seebeck, Peltier, and Thomson effects [1, 2, 5-7]. Of these, *only* the Seebeck effect converts thermal energy to electric energy and results in the thermocouple voltage used in thermometry. The current-dependent Peltier and Thomson effects are insignificant in practical thermometry. Neither produces a voltage, contrary to common misconceptions. The Peltier and Thomson effects only transport heat by electric current and redistribute it around a circuit. Thermocouple thermometry is properly conducted by *open-circuit* measurement. The Seebeck emf occurs even without current where Peltier and Thomson effects *necessarily* vanish. Related *thermo-magneto-electric* effects are significant only in the presence of large magnetic fields and infrequently degrade applied thermoelectric thermometry [2, 5, 6].

### The Seebeck Effect

The Seebeck effect is the occurrence of a net source emf, the *absolute Seebeck emf*, between pairs of points in any individual electrically conducting material due to a difference of temperature between them [1, 2, 5, 7, 8]. The Seebeck emf occurs *without* dissimilar materials. It is *not* a junction phenomenon, nor is it related to Volta's contact potential.

### Absolute Seebeck Properties

The *absolute Seebeck coefficient* expresses the measurement sensitivity (volts per unit of temperature) of the Seebeck effect. It is defined over any *thermoelectrically homogeneous* region of a slender individual conducting material by:

$$\sigma(T) = \lim_{\Delta T \rightarrow 0} \Delta E / \Delta T = dE/dT, \text{ or} \quad (32.73)$$

$$dE = \sigma(T) dT \quad (32.74)$$

The Seebeck coefficient is a transport property of *all* electrically conducting materials. Equation 32.74 will be acknowledged later as the functional law that governs thermoelectric emf. From Equation 32.74,

$$\Delta E = \int_{T_1}^{T_2} \sigma(T) dT = E(T_2) - E(T_1) \quad (32.75)$$

where  $\Delta E$  is the increment of emf between a pair of points, separated by *any* distance, between which the temperature difference is  $\Delta T = (T_2 - T_1)$ .

From Equation 32.75, the net Seebeck effect for a particular material depends only on the temperatures at the two points and *not* on the values of temperature gradients between the two points. The Seebeck coefficient is a nonlinear function of temperature. It is not a constant. For accurate thermometry, the Seebeck coefficient must remain dependent on temperature alone.  $\sigma(T)$  cannot vary along a thermoelement, nor can it vary significantly during the time interval of use. Although vulnerable to such environmental effects, for accurate thermometry it must not depend during measurement on such environmental variables as strain, pressure, or magnetic field.

The coefficient,  $\sigma_M(T)$ , is an *absolute Seebeck coefficient* for an individual material  $M$  [1, 2, 7, 8]. A corresponding *source voltage* within a single material is an *absolute Seebeck emf*,  $E_M(T)$ . The absolute Seebeck emf does physically exist but it is not simply observable. The absolute Seebeck coefficient can be determined indirectly by measuring the *Thomson coefficient*,  $\tau$ , of the individual material and applying a Kelvin relationship,

$$\sigma = \int_0^{T_{\text{abs}}} \left( \tau / T_{\text{abs}} \right) dT \quad (32.76)$$

to deduce the thermodynamically related Seebeck coefficient [1, 2, 5, 7, 8].

### Relative Seebeck Properties

The difference between the Seebeck emfs of two thermoelements, of materials A and B, of a thermocouple with their shared junction at temperature,  $T_m$ , and both their termini at a *physical reference temperature*,  $T_r$ , is their *relative Seebeck emf*,  $E_{AB}(T)$ , expressed as:

$$E_{AB}(T_m, T_r) = E_A(T_m, T_r) - E_B(T_m, T_r) \quad (32.77)$$

The corresponding relative Seebeck coefficient for the pair is:

$$\sigma_{AB}(T_m, T_r) = \sigma_A(T_m, T_r) - \sigma_B(T_m, T_r) \quad (32.78)$$

It is this relative Seebeck coefficient that has been called by the anachronistic and inept term “thermopower” [1]. It is these *relative voltage* or coefficient values that are directly observable and usually used in thermometry. These relative properties, defined for convenience in the *series* circuits of thermometry, have no general meaning for electrically paralleled thermoelements [2]. These are the relative values that are presented in the familiar tables of thermocouple emf vs. measuring junction temperature,  $T_m$ , referred to as a *designated reference temperature*  $T_0 = T_r$  [1, 4, 9-12]. For convenience,  $T_0$  is usually taken as 0°C, but the value is arbitrary.

### Realistic Thermocouple Circuits

The thermocouple is often represented as only a pair of dissimilar thermoelements joined by two junctions in a closed circuit. One junction, at temperature  $T_m$ , is the *measuring junction*; the other, at temperature  $T_r$ , is the *reference junction*. The net Seebeck emf is proportional to the temperature difference between the two junctions and to a relative coefficient for the paired materials.

The Seebeck phenomenon has wrongly been characterized as the occurrence of current in the closed loop. The true nature of the Seebeck phenomenon is the occurrence of a *source emf* that, for accurate thermometry, must be measured in open-circuit mode that suppresses current. In practical thermometry, no realistic thermocouple circuit has only two dissimilar materials. Some have many and several of these can be expected to contribute some Seebeck emf. The most common thermometry circuits have two separate reference junctions, not one. Valid, but uncommon, circuits can simultaneously have more than one reference temperature [1].

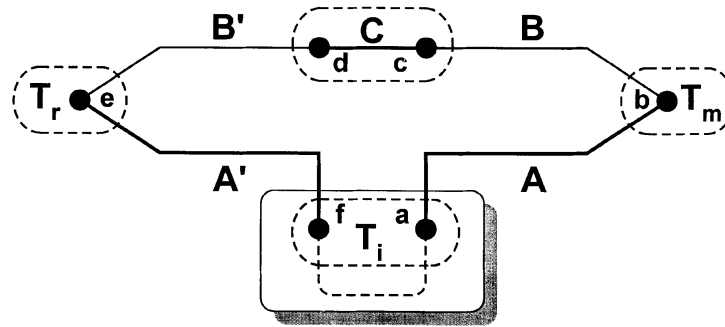


**FIGURE 32.25** The basic thermocouple circuit with a *single* temperature reference junction, **e**. The Seebeck voltage measured in open-circuit mode at terminals **a** and **f** is proportional to the temperature difference between thermocouple *measuring junction* **b** and the necessary temperature *reference junction* **e**. For convenience,  $T_r$  is usually made to be  $0^\circ\text{C}$ . For thermometry, the zones at temperatures  $T_r$  and  $T_i$  must be isothermal.

### Reference Temperature

The *physical* reference temperature,  $T_r$ , can be different from the *designated* reference temperature,  $T_0$ , of the characterizing relation. If  $T_r$  is not identical to  $T_0$ , then, to use standard scaling functions, the observed thermocouple emf must be corrected for the temperature difference by adding an emf equivalent to  $E_{AB}(T_r) - E_{AB}(T_0)$  to the observed thermocouple emf [1, 7, 9-12]. This is often accomplished by separately monitoring  $T_r$  and applying a correction, either numerically or electrically, using a fixed  $E_{AB}(T)$  relation that only *approximates* that of the actual thermocouple and the standardized characteristic over a limited range in the vicinity of  $T_0$  and  $T_r$ . The error due to the slight discrepancy between the approximation and the actual  $E_{AB}(T)$  is small if the two temperatures are similar.

Special thermocouple extension leads are used in most applied thermometry. Many industrial principal thermocouples are inflexibly metal sheathed [1, 4, 10-12]. Others have bare thermoelements separated by bead insulators. Often, these kinds of assemblies are housed in protective wells, have measuring junctions of complex construction, or are distant from the monitoring instrument. Short “pigtailed” and extension leads can be of larger wire size, lower resistance, greater flexibility, and very different rugged cable construction than the principal thermocouple (Figure 32.24). All thermoelements must be very well electrically isolated except at measuring and reference junctions. Most modern thermometry is conducted with variants of two basic circuits.

#### Circuit with Single Reference Junction.

Figure 32.25 shows a thermometry circuit now used mostly in calibration laboratories. This form is convenient when a *fixed point temperature reference* such as an ice point bath or water triple point cell is used to impose the known *physical* reference temperature,  $T_r$  [1, 7, 9-12]. The circuit of the thermocouple indicator between **a** and **f** inconspicuously includes many incidental materials and complex circuitry within the instrument. It is necessary that  $T_i = T_a = T_f$ . Unless instrument temperatures are constant throughout measurement, any nonisothermal portion of the circuit within the instrument can contribute Seebeck emf as noise. This emf can be correctly offset *only* if it is constant.

Often, in circuits like Figure 32.25, the measuring junction, **b** of the principal thermocouple, and reference junction, **e**, are provided by *separately* acquired thermocouples **a-b-c** and **d-e-f**. The two might have significantly different calibrations although they are nominally of the same thermocouple material type. With  $T_m$  at  $40^\circ\text{C}$  and  $T_0$  at  $0^\circ\text{C}$  the reference, thermocouple **d-e-f** contributes about half the Seebeck emf.

This commonplace circuit has at least four distinct thermoelement materials — A, A', B, and B' — each of which must be homogeneous. Also, they can be joined, as between **c** and **d**, by an intermediate uncalibrated linking material, C (unless  $T_c = T_d$ , material C contributes unwanted Seebeck emf). If B

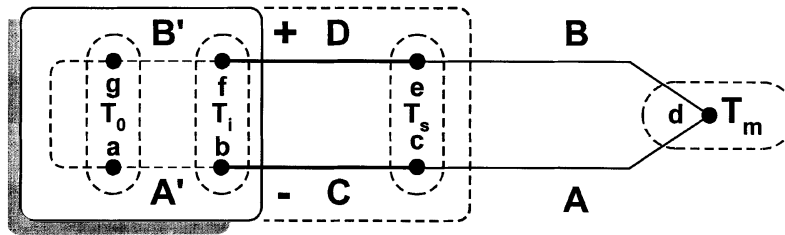


**FIGURE 32.26** The basic thermocouple circuit with *dual* temperature reference junctions. The principal thermocouple is the AB pair. Pair CD is the extension lead. The Seebeck voltage measured in open-circuit mode between terminals **b** and **f** is proportional to the temperature difference between thermocouple *measuring junction* **d** and the necessary temperature *reference junctions*. Depending on the type of extension leads, the reference junctions might be either **c** and **e**, or else **b** and **f**. For thermometry, the zones at temperatures  $T_s$  and  $T_i$  must be isothermal.

and  $B'$  are not *identical* in Seebeck characteristics, then **c** (and/or **d**) are *real* junctions. If so, it is also necessary that  $T_i = T_c = T_d$ . The termini **a** and **f**, when connected to a monitor, also become real junctions. They must be controlled so that both stay at the same temperature.

In Figure 32.25, for thermometry the physical reference temperature is intended to be  $T_r = T_c$ . However, monitoring instruments that internally compensate for reference junction temperature presume (*incorrectly for this circuit*) that  $T_r = T_a = T_f$ . Therefore, the *single-reference circuit* of Figure 32.25 cannot be used directly with thermocouple instruments that automatically apply reference junction temperature compensation.

#### Circuits with Dual Reference Junctions.

In the simple “black box” thermocouple thermometer (Figure 32.24), as well as in most applied thermoelectric thermometry, the most common circuit is that of Figure 32.26. This circuit is now the most commonly used in modern thermocouple thermometry. The thermocouple **c-d-e** with thermoelements joined at the measuring junction, **d**, is the *principal thermocouple*. This circuit might have only the principal thermocouple with a plug and jack at the indicator input. More often, as in Figure 32.24, the relatively inflexible principal thermocouple probe also has flexible *extension leads*, pair **C-D**, which can reside unseen within the indicator. Dashed pair  $A'-B'$  schematically represents internal reference junction temperature compensation.

Circuits like Figure 32.26 have two separate *reference junctions* that must be held at the same *known* temperature. Net Seebeck terminal voltage is measured between **b** and **f**. When thermocouple leads **C** and **D** are connected to the monitor, the input terminals, **b-f**, might be intended to be reference junctions. If so, their reference temperature is accurately monitored and emf reference correction corresponding to the difference between  $T_r$  and  $T_0$  is applied. Accurate thermocouple measurements cannot be made with ordinary voltmeters in which the temperatures of **b** and **f** are not deliberately controlled to be equal and known.

#### Extension Leads

Paired thermoelements **C** and **D** are thermoelectric *extension leads*. Extension leads are of three kinds: (1) *neutral*, (2) *matching*, and (3) *compensating*. All types are readily available; some are proprietary. Which of the junctions in Figure 32.26 must be reference junctions varies with the type of extension. Depending on the extension type, materials **A**, **B**, **C**, and **D** might, intentionally, all be of very different materials.

#### Neutral Extension Leads.

In the simplest application of Figure 32.26, legs **C** and **D** are thermoelectrically homogeneous and are carefully matched to have the same Seebeck coefficient ( $\sigma_C = \sigma_D$ ). Such pairs are *neutral extension leads*. Provided that  $T_c = T_e$  and  $T_b = T_f$ , they contribute no *net* Seebeck emf, so the like pair function effectively serve only as “passive” leads. Therefore, the leads could be made of any electrically conducting material. Such extension leads should be made of solid unplated copper, for which the Seebeck coefficient is small and uniform.

Neutral extension leads require that junctions **c** and **e** be the reference junctions at temperature  $T_r = T_s$ . *Thermocouple monitors that provide reference junction temperature compensation at input terminals **b** and **f** cannot be used with neutral extension leads.*

The reference temperature can be controlled on both junctions by a fixed point physical temperature reference such as an ice bath external to the voltage monitor [1, 9-12]. Ice baths, very carefully made and maintained, can routinely approximate 0°C to within 0.1°C to 0.2°C [9, 11]. Carelessly applied and maintained, they can deviate from the “icepoint temperature” by up to 4°C [10]. Peltier thermoelectric refrigeration is also used. More often, in thermometry, that reference temperature is not physically imposed. Instead, the actual temperature of the reference junctions is accurately measured and electrical compensation is applied (schematically by A'-B') for the difference between  $T_r$  and  $T_0$ . The particular value of the temperature at **b** and **f** does not matter if  $T_b = T_f$  is compensated.

#### Complementary Extension Leads.

Two kinds of complementary extension leads are allowed to contribute to the circuit Seebeck emf: *matched* and *compensating* extensions. The legs *C* and *D* are thermoelectric extension leads that are usually uncalibrated, and possibly are of broader or even unknown tolerance. It is expected that  $T_s$  and  $T_i$  are similar so that the uncalibrated contribution is small and the error is negligible. For very accurate thermometry, this assumption might not be justified.

Complementary extension leads can be used directly with thermocouple indicators that internally compensate the reference junction temperature for the difference between the physical reference junction temperature,  $T_r$ , and the designated reference temperature,  $T_0$ . For both matched and compensating complementary extensions, the reference temperature is  $T_r = T_i$  over the isothermal reference zone around the terminals **b** and **f**.

#### Matching Extension Leads.

*Matching leads* have  $\sigma_C = \sigma_A$  and also  $\sigma_D = \sigma_B$ . It is essential that  $T_b = T_e$ , but it is not essential (although it is desirable) that  $T_c = T_e$ . Near room temperature, thermoelements are intended to have  $\sigma_{CD}$ , as a pair, be nearly the same as  $\sigma_{AB}$  for the temperature span near  $T_r$ . Error due to slightly mismatched and unproven calibration of the extension is minimized if  $T_s \cong T_i$ . Matched extensions are used with base metal thermocouples, not with refractory or precious metal thermocouples.

#### Compensating Extension Leads.

The third variation of the circuit in Figure 32.26 is often used for economy and convenience with expensive precious and refractory metal principal thermocouples that are intended for use at very high temperatures and in special environments [1, 7, 9-12]. Usually, only a portion of the principal thermocouple need be exposed to the adverse environment. Extension leads *C* and *D* need only survive a more benign environment. Therefore, they can be made of a less expensive or more conveniently handled material, use lower temperature insulation, be more flexible and of lower resistance, add bulky shielding and mechanical protection, and extend a great distance to a recording facility.

*Compensating leads* have  $\sigma_{CD}$  of the extension *C-D*, only as a pair, match  $\sigma_{AB}$  of the *A-B* pair. It is not necessary that material *A* be like *C*, nor that *C* and *D* be alike. A practical circuit can have four very dissimilar materials. However, to allow this, it is essential that  $T_c = T_e$ . Therefore, this circuit with compensating leads is more vulnerable to error from improperly matched temperatures of incidental junctions than with matching extension leads. The reference junction temperature is  $T_r = T_b = T_f$ , and only this temperature must be independently known. Reference junction compensation is the same as for the matching leads.

## Modular Signal Conditioning Components

The myriad of diverse and capable thermocouple indicators and recorders now commercially available, ranging from simple and very inexpensive to sophisticated and versatile yet reasonably priced, makes it unnecessary for most applied thermometry to assemble special signal conditioning circuits. Some, seeking economy of hardware, have built custom systems. Too often, these have not achieved accurate measurement

and have proved to be very costly because the critical distinctions between thermoelectric circuits and ordinary electric circuits were not appreciated. For special situations where thermocouples are incorporated into special measurement or operational components or systems, several manufacturers now offer modular and integrated circuit components that simplify special application and do protect the unaware from some pitfalls [13].

#### Thermocouple Signal Conditioning on a Chip.

As thermocouple signals are low level, it is sometimes desired to amplify them for improved resolution, recording, or control. It might be desirable to incorporate thermocouple sensing as a functional component in other instrumentation packages. There are now several miniature and inexpensive integrated circuit modules for thermocouples that provide reference junction compensation, linearization, isolation, open input indication, amplification, and set point control. Properly applied, these make the integration of thermocouple sensing into other devices, such as computer data acquisition boards, very simple [13].

When a user applies modular components such as these, it is particularly important to understand and to apply the authentic thermoelectric circuit model and principles introduced in the section "The Functional Model of Thermoelectric Circuits." Some precautions normally provided in commercial thermocouple monitors must be provided by the user.

#### Reference Temperature Sensors.

Thermocouples are self-generating. For casual approximate temperature and differential temperature measurement, they require neither excitation nor reference temperature. For accurate thermometry, unless a known reference temperature is physically imposed, an accurate measurement of the reference junction temperature by independent means is necessary. This sensing is usually by powered resistance temperature detectors, thermistors, transistors, or integrated circuit sensors [1, 4].

#### Reference Temperature Compensators.

Proper reference compensation requires (1) the establishment of an isothermal temperature zone that includes the terminals of the thermocouples, (2) sensing of the temperature of this zone, and (3) application of a complementary physical or numerical voltage to the thermocouple terminal voltage before scaling the total voltage to temperature.

An analog method includes the resistive zone temperature sensor in a bridge that nonlinearly modulates a supplied voltage according to an approximated nonlinear curve of the  $E(T)$  characteristic of the thermocouple. This method is adapted to compensation of only a single thermocouple type. An alternate method numerically converts the sensed reference temperature to the appropriate compensating voltage value. The numerical approach allows applying a separate compensating voltage to each individual thermocouple and for different standard types. In principle, for accuracy, a numerical compensating voltage could be programmed by the user to conform to the specific calibration of the individual thermocouple, whether or not of standardized type.

Reference temperature compensators are internal to the more advanced thermocouple monitors. In advanced units, eight to ten thermocouple inputs are grouped on a separately removable isothermal terminal assembly so they can be removed for reference sensor calibration or for replacement. Like thermocouples, reference sensors occasionally drift, causing significant temperature error. For most thermocouple types, a  $1^\circ$  error in temperature reference produces a similar error in the measured temperature. A variety of external battery- or line-powered, single- or multichannel reference junction compensating units are also commercially available [4, 14].

## Grounding, Shielding, and Noise

The technically well-founded principles of noise control for electric circuits apply also to thermoelectric circuits [15, 16]. There are, however, some additional considerations that are necessary for thermocouple circuits. Some noise control problems stem from the nature of thermoelectricity; others from commercial thermocouple design practices.

## Noise Problems Peculiar to Thermocouples

Temperature control of all deliberate and incidental junctions and components, and the distributed nature of Seebeck source emf, cannot be ignored with impunity in thermocouple application. The unavoidable requirements of such control are best visualized using methods such as given later in “The Functional Model of Thermoelectric Circuits.” Incidental circuit components such as balancing or swamping resistors, feedthrus, splices, and terminal strips, not intended to contribute Seebeck emf, must deliberately be maintained *isothermal*. Shields, unavoidably nonisothermal, made electrically common with the thermocouple must be explicitly recognized as latent sources of random dc noise which contributes Seebeck emf if not properly connected.

### Electromagnetic (EM) Noise

In thermocouple probes of mineral-insulated metal-sheathed (MIMS) construction, ceramic-bead-insulated thermocouples, and in some paired insulated thermocouple wires, the paired thermoelements are not twisted and are well separated. Lengthy and larger diameter thermocouple probes present a significant circuit loop area to couple magnetic noise fields. Even if probes are entirely metal-sheathed, the standardized sheaths are very thin and of low magnetic permeability. They are scarcely effective for electromagnetic (EM) shielding. These features prevent the use of some classic techniques for the rejection of EM noise [15, 16]. To reduce troublesome EM noise, the principal thermocouple probe should be of the smallest practical diameter, and of minimum length. In instances where the EM source is localized and identified, the orientation of the probe relative to the source can be arranged to minimize EM coupling. For rejection of EM noise, extension leads should always be of twisted-pair construction, with a pitch small enough to reject high-frequency noise [15].

### Electrostatic (ES) Noise

Electrostatic noise is more easily reduced. Shields of low resistance, though thin, can be effective if properly connected [15, 16]. Plated copper braid is commonly used and is effective for noise of moderate frequency. Continuous shields, such as the MIMS sheaths and aluminized mylar film, are effective for low-frequency ES noise and are more effective than braid shields for very-high-frequency noise. Electrostatic shields must be continuous (without gaps and holes as in braid) for maximum effectiveness. Optimum benefits from shielding require use with thermocouple monitors that provide three-wire input and multiplexers that, individually for each thermocouple, switch both the signal pair and their separate shield lead.

### Grounding

Shielding for ES noise and pair twisting for EM noise are important for reduction of high-frequency noise. A secondary overall shield, isolated from inner shields and separately grounded, can improve the rejection of EM noise. Appropriate circuit grounding is also particularly important for both high-frequency EM and ES control, but it is even more significant for low-frequency and dc noise, which are often more consequential in thermocouple measurements. Appropriate grounding is complicated where intimate thermal contact of the measuring junction with an earth-grounded conducting test subject is needed for rapid transient thermometry or for accuracy in the presence of static temperature gradients.

Figure 32.27 illustrates appropriate grounding for several of many possible situations. Low-level thermocouple circuits should be grounded only at a single electric reference point. Because the measuring junction is not a localized site of source emf, the point of grounding must be carefully considered. Grounding should never be at any point of the thermocouple circuit other than measuring or reference junctions. Electric contact, and particularly shunting or shorting, on a thermoelement at any point between measuring and reference junctions usually introduces spurious Seebeck emf from incidental unrecognized thermoelements.

Allowable grounding might be dictated by the internal design of monitors and data loggers. Each instrument design addresses noise control in a distinctive way. Simple and inexpensive line-powered thermocouple thermometers might have only single-ended inputs with the negative lead internally

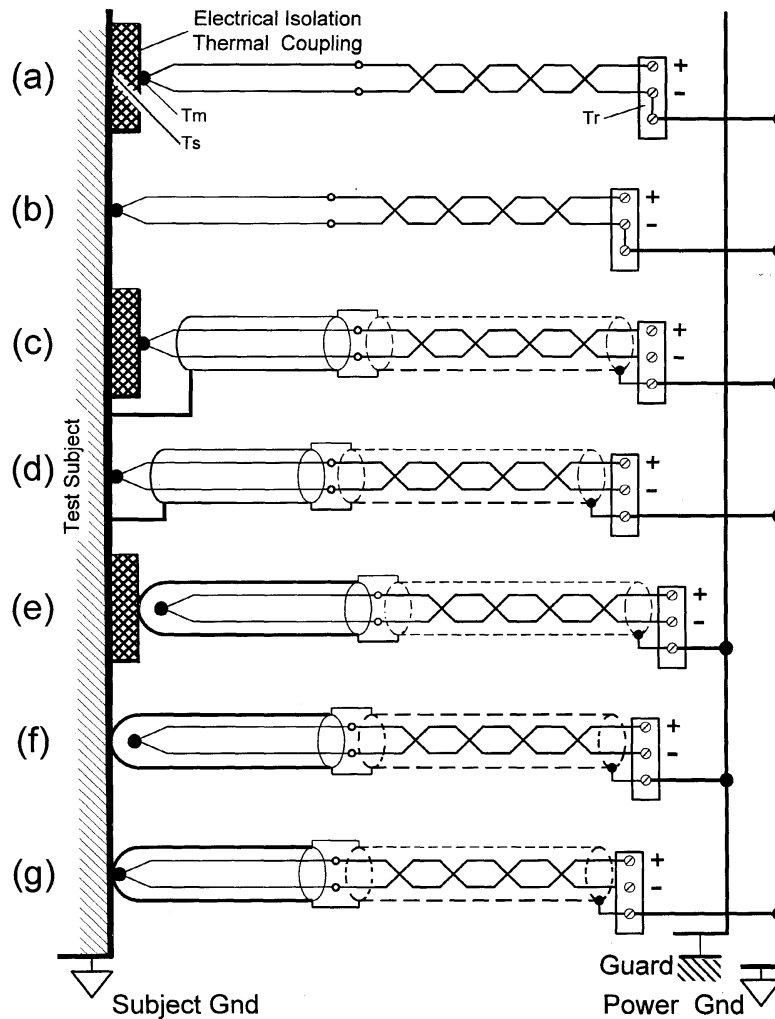
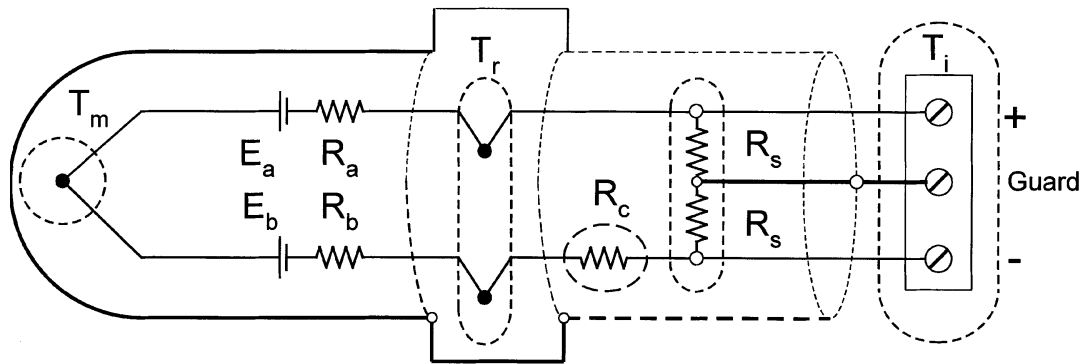


FIGURE 32.27 Preferred grounding and shielding for several thermometry situations. Electromagnetic (EM) and electrostatic (ES) noise must be controlled by different means. The design of the thermocouple monitoring instrument may dictate the grounding and shielding scheme that can be used.

connected to the power ground. This forces the sensor grounding to also refer to power ground. A grounded-junction arrangement might also be required for fast transient thermometry. In use, initially isolated thermocouples can short to the protective sheath or test subject. Although this does change the grounding configuration, resulting errors due to other effects usually are then predominant.

### Balanced Thermocouple Circuits

The more sophisticated multichannel data acquisition systems specialized to thermocouple thermometry usually have high-resistance balanced inputs for high common-mode signal rejection. Some differential input amplifiers require significant input resistance for stability. Most have an internal chassis that provides a common signal reference guard surface that is well-isolated from power ground. In a few designs, the guard is electrically driven to a particular reference point. Because many variations are used, it is prudent to study and follow the specific grounding instructions recommended in the user's manual for the instrument. Most accommodate alternative grounding arrangements.



**FIGURE 32.28** A circuit arrangement for balanced input recorders to improve common-mode noise rejection. The thermoelement balancing resistor,  $R_c = |R_a - R_b|$ , and the matched pair of high-resistance input resistors  $R_s$  must be held isothermal.

In sheathed thermocouple probes of standard MIMS dimensions, the thermoelements are of the same cross-section, parallel and well spaced, and located within the cylindrical sheath symmetrically [10]. Noise tends to be coupled equally to the paired thermoelements in common mode. However, lengthy or fine gage thermocouples have legs of high resistance compared to copper circuits. The ratio between the resistances of the dissimilar legs can be up to 25:1. Noise introduced in common mode adversely tends to convert to normal mode.

In addition, unlike most voltage sources, the Seebeck emf is not localized to the measuring junction (a material interface). The emf can arise anywhere along the thermoelements. In transient thermometry, it first occurs adjacent to, and then spreads away from the measuring junction. In the more commonplace *static* thermometry, the site of source emf is usually distant from the measuring junction.

Most specialized thermocouple recorders provide reference temperature compensation. They do not allow convenient user access to the circuit beyond the reference junctions. This restricts the noise control methods available to the user. For externally referenced thermocouples, some effective simple circuit modifications are possible. Figure 32.28 shows the addition of three resistors that, used with monitors of balanced input, improve noise rejection. Isothermal balancing resistor,  $R_c = |R_a - R_b|$  is added in series with the thermoelement of lower resistance. Making the resistance of the two circuit branches equal reduces the undesired conversion of noise from common mode to normal mode. The matched pair of shunting resistors,  $R_s$ , presents a significant definite minimum source resistance to the amplifier input for stability and symmetrically couples the signals and sheath to the common reference point. The resistors must be large enough,  $R_s \geq 1000 (R_a + R_b)$ , to avoid significant shunting resistive attenuation of the thermocouple source Seebeck emf. With great care to maintain these resistors strictly isothermal, the balancing and shunt resistors could be placed just at the input terminals *external* to the instrument-provided reference junction temperature compensation.

### Filtering

For low-frequency thermometry, to complement the user-provided passive rejection of EM and ES noise by proper grounding and shielding, internal filtering provided by data acquisition monitor manufacturers can effectively reject high-frequency noise. Filtering before recording is preferred. This control can be performed by conventional filters; but for quasi-static thermocouple measurements, other very effective techniques such as “double-slope integration” are provided in some designs. These techniques effectively average the signal over several measured samples. The noise reduction and stability under real-life conditions is remarkable. Routine resolution and stability to  $0.1 \mu\text{V}$  variation over a period of days is achieved by many modern thermocouple data loggers. However, this noise rejection method restricts the sampling speed so that samples can be limited to intervals no shorter than 10 ms to 20 ms that are unsuited to very fast transient thermometry.

## Thermal Coupling

Accurate thermometry obviously requires that the temperature of thermocouple measuring junctions closely agree with the temperatures to be measured. In static measurements at thermal equilibrium, this is often easy to accomplish. In fast transient measurements, it can be very difficult.

### Static Thermometry

Thermocouple thermometry of steady-state or slowly varying temperatures requires close thermal coupling of the measuring junctions to the point of measurement. This agreement of temperatures naturally occurs by equilibration if the point of measurement can be chosen to be well within a region that stays at uniform temperature during measurement. Even in such nearly static thermometry, the thermoelements should be as small as practical to reduce any conduction of heat along the thermocouple that could affect the temperature being measured.

In typical situations, however, the vicinity of the measuring point is not isothermal and, even at steady state, static temperature gradients can cause the measuring junction to be at a significantly different temperature from the subject [18]. This source of error is more severe for surface, liquid, and gas measurements than for internal solid measurements, and is aggravated for the measurement of subjects of low thermal mass. Efficient thermal coupling of the thermocouple to the subject, as in Figure 32.27, is essential.

Noise or safety might require electrical isolation of the thermocouple. Commonplace electrical insulating materials are poor thermal conductors. There are now special greases, coatings, and thin sheet materials available designed to provide high electrical isolation, yet good thermal contact [17]. Where needed, they can improve accuracy by efficient thermal coupling.

### Transient Thermometry

Monitoring very rapid variations of temperature is most effectively accomplished by thermocouples because of the low sensing mass and small size of measuring junction that they allow. Fast thermal response requires the use of special thermoelement configurations in the vicinity of the measuring junction, special circuitry, special thermocouple monitoring instruments, and characterizing methods [16, 18]. Some suppliers offer very thin (10  $\mu\text{m}$  thick) foil and fine wire thermocouples that are especially well adapted to such measurement [19, 20].

A thermocouple alone has no characteristic response time. The Seebeck effect occurs at electronic speed. The thermocouple source emf always promptly corresponds to the temperatures of all junctions in the circuit. However, the transient temperature response of a thermocouple installation is very much slower, and is primarily governed by the thermal interaction of the thermocouple components adjacent to the junctions and the adjacent mass of the test subject [18, 22, 23]. That slow conductive heat transfer is retarded many-fold by even a thin film of air, vacuum, or an insulating solid layer. In fast transient thermometry, the electrical parameters of the thermocouple and associated circuitry and dynamic response of the recording system can further degrade response time.

Intimate thermal coupling by special materials required for static measurement in a thermal gradient is even more critical to transient than to static thermometry [17]. Even the special coupling materials slow response. They should be as thin as feasible. For very fast thermometry, such coupling might not be tolerable. It may be necessary to place the bare measuring junction in direct electric contact with the subject (Figure 32.27).

### Intrinsic Thermocouples.

Where the subject of thermometry is an electric conductor, it is possible to electrically fuse the two thermoelements separately to the test subject. This is an “intrinsic” thermocouple junction arrangement. Fine wires or thin foils spot-welded to the subject allow the fastest possible electrothermal response and reduce the influence of the thermocouple on the temperature being measured.

Observe two special precautions in the use of intrinsic junctions. First, the two thermoelements should be fused to the subject side-by-side, close together (not one over the other.) With intrinsic junctions, the

bridging segment of the subject becomes a part of the series thermoelectric circuit. (There are two intrinsic junctions coupled by the intermediate subject material.) This produces the fastest response; but in very fast transients, the temperatures of the two junctions can very briefly be slightly different and thus introduce a momentary error, as the unknown Seebeck coefficient of the bridging subject material is different from that of one or both of the principal thermoelements [21].

Second, for transient thermometry, the fine thermoelements leading to the intrinsic junctions should be as short and fine as feasible to reduce their thermal loading; however, this results in a relatively high electric lead resistance. A strain-relieved transition from the fine filaments to more substantial low-resistance compensating lead wires should be made near the measuring junction to enhance electric response. The electrical effect of capacitive coupling of the circuit on electric transient response must also be minimized.

#### Numerical Correction.

All feasible physical techniques to achieve fast transient temperature response when applied might not be sufficient for a very fast measurement. An inadequate transient response can be further enhanced by numerical analysis [21]. Two additional steps must be taken.

First, an *authentic* experimental or *correctly* modeled transient response characterization of the overall thermal-electrical thermometry system must be made. The usual simplistic first-order representations of *in situ* thermocouple response might be inadequate [21–23].

Second, this authentic characterization must be applied by mathematical *deconvolution* to better estimate the true temperature history of data indicated by a system that had inadequate physical transient response [16, 19]. Critical and reliable improvements of effective response time by factors of four or more are often possible. If uncorrected, indicated transient peak temperatures can be in error by a much greater percentage than the error that results from static thermocouple calibration error. *No general uncertainty can be assigned to a transient measurement without such response characterization.*

## Thermocouple Materials

### Thermocouple Standardization

Many materials are in regular use as thermocouples for thermometry. Some pairs are *standardized*; some are not. The distinction is a matter of formal consensus group approval by balanced standards committees of experienced users, producers, and standards laboratory staff [10, 24]. The most extensive application data is available for standardized thermocouples. In the U.S., eight materials presently are letter-designated (Types *B*, *E*, *J*, *K*, *N*, *R*, *S*, and *T*) [9–12, 24]. Some properties of these are summarized in [Table 32.12](#). The standardized  $E(T)$  characteristics of these are now *defined exactly* by polynomial functions of high degree rather than by tabulated values [1, 9, 10]. Thermoelements should be used as selectively paired for thermocouples by the producer, as randomly paired thermoelements of the same type from the same or different manufacturers are not assured to conform to the standard pair values or tolerances [1, 9–12].

The properties of a few other popular pairs, such as precious metal and tungsten refractory alloys, have also been committee-proposed, but letter designations and color codes have not been formally assigned [10]. Infrequently, other popular materials are considered for standardization. Limited Seebeck and application information is available for a multitude of nonstandard materials [25, 26].

### Low Temperature Thermometry

Most thermometry is at elevated temperatures. Thermocouple measurement of temperatures below the ice point requires special consideration. Cryogenic thermometry has been very loosely defined as measurement below 280 K (7°C) [1]. More restrictively, the defined cryogenic range has been limited to below 90 K (–183°C, the boiling point temperature of liquid oxygen at 1 atm) [1]. The former range broadly overlaps the measure of atmospheric temperatures (down to –50°C) below the ice point that, along with higher ambient temperatures, often are measured by a single thermocouple system. The latter definition favors characterizing as cryogenic only the extremely low-temperature regime over which thermometry involves distinctive severe problems and different techniques.

**TABLE 32.12** Characteristics of U.S. Letter-Designated Thermocouples

Type	Common name	Color code	M.P. (°C)	Recommended range, (°C) <sup>d</sup>	emf at 400°C, (mV)	Uncertainty, +/- Special tolerance Normal tolerance	ρ (μΩ-cm)
B	—	Brown <sup>a</sup>	1810	870 to 1700	0.787	0.25%	34.4
BX	—	Gray <sup>a</sup>	—	—	—	0.50%	—
BP	Pt30Rh	Gray	1910	—	—	—	18.6
BN	Pt6Rh	Red	1810	—	—	—	15.8
E	—	Brown <sup>a</sup>	1270	-200 to 870	28.946	1.0°C or 0.40%	127
EX	—	Purple <sup>a</sup>	—	—	—	1.7°C or 0.50%	—
EP	Chromel <sup>b</sup>	Purple	1430	—	—	—	80
EN	Constantan	Red	1270	—	—	—	46
J	—	Brown <sup>a</sup>	1270	0 to 760	21.848	1.1°C or 0.40%	56
JX	—	White <sup>a</sup>	—	—	—	2.2°C or 0.75%	—
JP	Iron	White	1536	—	—	—	10
JN	Constantan	Red	1270	—	—	—	46
K	—	Brown <sup>a</sup>	1400	-200 to 1260	16.397	1.1°C or 0.40%	112
KX	—	Yellow <sup>a</sup>	—	—	—	2.2°C or 0.75%	—
KP	Chromel	Yellow	1430	—	—	—	80
KN	Alumel <sup>b</sup>	Red	1400	—	—	—	31
N	—	Brown <sup>a</sup>	—	0 to 1260	12.974	1.1°C or 0.40%	—
NX	—	Orange <sup>a</sup>	—	—	—	2.2°C or 0.75%	—
NP	Nisil	Orange	—	—	—	—	—
NN	Nicrosil	Red	—	—	—	—	—
R	—	Brown <sup>a</sup>	1769	0 to 1480	3.408	0.6°C or 0.10%	29
RX	—	Green <sup>a</sup>	—	—	—	1.5°C or 0.25%	—
RP	Pt13Rh	Green	1840	—	—	—	19
RN	Pt	Red	1769	—	—	—	10
S	—	Brown <sup>a</sup>	1769	0 to 1480	3.259	0.6°C or 0.10%	30
SX	—	Green <sup>a</sup>	—	—	—	1.5°C or 0.25%	—
SP	Pt10Rh	Green	1830	—	—	—	20
SN	Pt	Red	1769	—	—	—	10
T	—	Brown <sup>a</sup>	1083	-200 to 370	20.810	0.5°C or 0.40%	48
TX	—	Blue <sup>a</sup>	—	—	—	1.0°C or 0.75%	—
TP	Copper	Blue	1083	—	—	—	2
TN	Constantan	Red	1270	—	—	—	46

From References [1, 4, 9, 10]

<sup>a</sup> Overall jacket color.

<sup>b</sup> Chromel and Alumel are trademarks of Hoskins Mfg. Co.

<sup>c</sup> Initial tolerances are for material as manufactured and used within recommended temperature range, Table 32.15, protected in a benign environment.

<sup>d</sup> Recommended temperature range is a guideline for service in compatible environments and for short durations.

The Seebeck coefficient of all conductors is insignificant at 0 K and common materials progressively decrease in thermoelectric sensitivity below the ice point. A few natural superconductor metal elements experience an abrupt drop in Seebeck coefficient to zero at a characteristic superconducting threshold that is below 10 K for most unalloyed metal superconductors [27]. Special alloys have recently been developed to raise the superconducting threshold to about 120 K — well above the formal cryogenic

range. Superconducting transitions complicate thermoelectric thermometry at the lowest cryogenic temperatures [7, 8].

Standard Seebeck characteristics are defined for Types *E*, *J*, *K*, *N*, and *T* down to  $-270^{\circ}\text{C}$ . The characteristics for Types *R* and *S* extend only down to  $-50^{\circ}\text{C}$ , and Type *B* is not characterized below  $0^{\circ}\text{C}$ . The standard polynomials that define the Seebeck properties of letter-designated thermocouples and the production tolerances for commercial materials are different for temperatures below and above the ice point. Materials manufactured for thermometry at elevated temperatures might conform less well to the standard cryogenic characteristics than alloys of the same type especially furnished for such use [1]. This quality issue should be discussed with the thermocouple supplier. Special alloys are available for cryogenic thermometry.

For the lower cryogenic range, of the letter-designated thermocouple materials, Type *E* is preferred for use down to  $-233^{\circ}\text{C}$  (40 K) because of its higher relative Seebeck coefficient [1]. The less-sensitive Type *K* and Type *T* are also used in this range. Below 40 K, special alloy combinations, such as Type *KP* vs. Au/0.07 Fe, are recommended. Special thermoelectric relations apply to these materials in the cryogenic range [1].

As Peltier heating at junctions and Thomson heating along thermoelements are current-dependent thermoelectric effects, neither is a significant problem if thermometry is properly conducted by open-circuit measurement. There is no significant thermocouple self-heating as with resistance thermometers. Some thermoelement alloys experience grain growth and incur serious inhomogeneity under prolonged exposure to deep cryogenic temperatures. More sensitively at cryogenic temperatures than at elevated temperatures, the Seebeck coefficient of most thermocouple alloys is very strongly dependent on magnetic field. Strong magnetic fields are often involved in cryogenic experiments, so thermo-magneto-electric effects become significant in studies of superconductivity [2, 27].

### Sensitivity

The need for large thermocouple output has been drastically reduced by the enhanced sensitivity, stability, and noise suppression of modern solid-state digital thermocouple indicators. These instruments can routinely indicate temperature to  $0.1^{\circ}\text{C}$  resolution and stability for all letter-designated types. The standard pairs differ significantly in their sensitivity (Table 32.12). The sensitivity of the Type *E* thermocouple is 10 times that of the Type *B* thermocouple at  $1000^{\circ}\text{C}$ . Because the Type *B* thermocouple has extremely small sensitivity around room temperature, it is intended for use only with the measuring junction above  $870^{\circ}\text{C}$ . The most sensitive standardized thermocouple, Type *E*, has a maximum Seebeck coefficient of  $81\ \mu\text{V }^{\circ}\text{C}^{-1}$  and, referenced to  $0^{\circ}\text{C}$ , has a maximum Seebeck emf of 76 mV. While initial tolerances for both normal- and special-grade material have been standardized, the difference between *commercial* and *premium* grades is small and, in use, special-grade materials can degrade to exceed the initial tolerances of the normal-grade material.

### Letter Designations

The U.S. ANSI standard letter designations and color codes for eight particular thermocouple types (*B*, *E*, *J*, *K*, *N*, *R*, *S*, and *T*) were first established by the ISA in Standard MC-96.1 [28]. The same conventions are followed by Standards of the ASTM and ANSI [10, 24]. A first suffix to the type letter designator, *P* or *N*, as in types *KP* or *KN*, designates the positive or negative thermoelement of a thermocouple pair. A final “*X*” suffix designates an extension wire material, as in *KPX* for a positive type *K* extension thermoelement. For non-standardized material pairs, producers and vendors often apply their own unofficial letter designations, color codes, and trade names. These *commercial* identifiers of individual manufacturers have no universal meaning.

### Color Codes

Intended to ease identification, the standards of many nations have assigned color codes to the different letter-designated thermocouples and to thermoelements and extensions. As the individual thermoelements determine both polarity and sensitivity, it is very important to properly identify each leg. Color codes now used in the U.S. are shown in Table 32.12.

**TABLE 32.13** International Thermocouple Color Codes

Type	U.S.	IEC	England	China	France	Germany	Japan	Russia
B	Brown	—	—	—	—	—	—	— B
BX	Gray	—	—	—	—	Gray	Gray	— BX
BP	Gray	—	—	—	—	Red	Red	— BP
BN	Red	—	—	—	—	Gray	Gray	— BN
E	Brown	—	—	—	—	—	—	— E
EX	Purple	Purple	Brown	—	Purple	Black	Purple	— EX
EP	Purple	Purple	Brown	Red	Yellow	Red	Red	Purple or black EP
EN	Red	White	Blue	Brown	Purple	Black	White	Yellow or orange EN
J	Brown	—	Red	—	—	—	—	— J
JX	Black	Black	Black	—	Black	Blue	Yellow	— JX
JP	White	Black	Yellow	Red	Yellow	Red	Red	White JP
JN	Red	White	Blue	Purple	Black	Blue	White	Yellow or orange JN
K	Brown	—	—	—	—	—	—	— K
KX	Yellow	Green	Red	—	Yellow	Green	Blue	— KX
KP	Yellow	Green	Brown	Red	Yellow	Red	Red	Red KP
KN	Red	White	Blue	Blue	Purple	Green	White	Brown KN
N	Brown	—	—	—	—	—	—	— N
NX	Orange	—	—	—	—	—	—	— NX
NP	Orange	—	—	—	—	—	—	— NP
NN	Red	—	—	—	—	—	—	— NN
R	Brown	—	—	—	—	—	—	— R
RX	Black	Orange	Green	—	Green	White	Black	— RX
RP	Black	Orange	White	Red	Yellow	Red	Red	— RP
RN	Red	White	Blue	Green	Green	White	White	— RN
S	Brown	—	—	—	—	—	—	— S
SX	Black	Orange	Green	—	Green	White	Black	— SX
SP	Black	Orange	White	Red	Yellow	Red	Red	Red or pink SP
SN	Red	White	Blue	Green	Green	White	White	Green SN
T	Brown	—	—	—	—	—	—	— T
TX	Blue	Brown	Blue	—	Blue	Brown	Brown	— TX
TP	Blue	Brown	White	Red	Yellow	Red	Red	Red or pink TP
TN	Red	White	Blue	White	Blue	Brown	White	Brown TN
Std.	ANSI	IEC	BS	NMI	NFC42	DIN	JIS	
No.	MC96.1	584-3	1843		42-323	43714	1620	

From References [1, 4, 9, 10].

U.S.-standardized color codes have remained uniform for several decades; thus color code confusion of material types in the U.S. is mostly due to user carelessness. The present globally discordant color codes can cause costly misinterpretation in multinational use, particularly outside the U.S. where neighboring countries and trading partners have unlike or multiple color codes. Clearly, a single universal international color code accepted by all nations would be beneficial. Such an international color code is embodied in standard *IEC 584* that is being considered by several nations [28].

Unlike the standardized Seebeck characteristics that are fairly uniform worldwide, the uncoordinated color codes of different national standards are very inconsistent. The unfortunate Babel of national color codes that existed in 1998 is displayed in [Table 32.13](#) [1, 4].

Unfortunately, and uniquely, in present U.S. thermocouple standards, the *negative* thermoelement is always *red*, contrary to customary U.S. electrical and instrument practices. This is also contrary to the historic national thermocouple color codes of China, Germany, and Japan, in which *red* designates the *positive* thermoelement. In English standards, the *negative leg* of all types is *blue*.

In France, the *positive* thermoelement is always coded *yellow*. However, a *yellow positive* leg in the U.S. standard designates Type *KP* material. The wire leads of some U.S. electric blasting caps use yellow insulated wire with a parallel red tracer that has been confused with Type *KX* thermocouple extension wire. In England, yellow denotes Type *JP* material. The *white positive* and *black negative* of the present U.S. ANSI color code for Type *J* are *transposed* in international standard IEC 584.

Despite the clear desirability for a uniform color code, there remains a huge quantity of material of different color codes in stock and in use worldwide. For any nation that switches to any new color standard, there would be, immediately and over an unavoidably lengthy transition period following acceptance, the new color-coded thermocouple material intermixed with the multitude of inconsistent legacy color codes. The immediate possibility for confusion of material type would greatly increase rather than decrease. Also, even the present color codes can become indistinct on long-installed material, colors can fade, and/or colors may have been incorrectly applied in manufacture.

### Identifying Thermoelements

The color codes apply directly to extension lead wires and effectively to the principal thermocouple wire. Many principal thermoelements and thermocouples are not color coded. A user might not correctly recall the color code. The prudent user will, before use, *confirm* material type identification independent of the color code. *Definite* type identification must be by a combination of methods. Any single identification method can be indefinite, and no method is adaptable to all materials or circumstances.

Visual Identification.

*TP* thermoelements are of copper and thus are distinguished by their distinctive reddish color. *JP* thermoelements are iron and have a distinctive matte gray cast. Other base metal alloys and platinum and its alloys, if bare, all have a very similar bright silvery appearance unless, if bared from compressed mineral insulation, fabrication has effected a roughened gray matte surface appearance.

Magnetic Identification.

Type *JP* (iron) is strongly magnetic. Type *KN* (Alumel) is slightly magnetic. All other standard thermoelement materials are nonmagnetic. *JP* and *KN* thermoelements can be distinguished from the others by testing the attraction to them of a small magnet.

Resistive Identification.

Resistivities of thermoelements are given in Table 32.12. Although assembled thermocouples have a measuring junction that cannot generally be removed for testing, a bare junction can be directly accessible or it can be electrically accessible at a probe tip for resistance measurement of each leg if the junction is of the type made common at the measuring junction to a conductive sheath. Thermocouple assemblies or cable usually have paired thermoelements of the same length and cross-section. The resistance of each leg distinguishes the material if the wire size and length are known. In these instances, *with both ends of the cable at the same temperature*, the resistance of each thermoelement can be directly measured. The ratio between positive and negative leg resistances can aid type confirmation. For assembled thermocouples with inaccessible measuring junctions, only the loop resistance can be measured and compared with calculated loop resistances.

Thermoelectric Identification.

Less conveniently, a pair can be identified by the output for a known temperature of measuring junction and reference junction. *Complementary extension cables* can be thermally identified by temporarily forming a junction between a pair at one end. Identification can be definite using a less precise procedure than necessary for formal calibration. For identification, both reference and measuring junction temperatures must be independently known or measured. The approximate temperature of the reference junction can be determined by momentarily shorting the input directly at the indicator input terminals of an instrument that provides reference compensation. Because the thermocouple material might not correspond to the compensation applied, the temperature must be determined separately.

The temperature applied to the measuring junction for identification must be at least 200°C because uncertainty of the thermocouple calibration and of the imposed temperature makes unreliable the emf

distinction of thermocouple pairs, such as *E* from *J*, and *K* from *N* or *T* using either ice or boiling water baths. Very similar Types *R* and *S* can be reliably distinguished only at much higher temperatures or by formal calibration.

## The Functional Model of Thermoelectric Circuits

For simplicity, the relation between junction temperatures required for accurate measurement was merely asserted in the section on “Practical Thermocouple Circuits,” without any physical explanation. Some subtle problems of realistic thermoelectric circuits are difficult to visualize without an explicit circuit model. A simple, practical, and general-purpose model of thermoelectric circuits now explains why those temperature structures are appropriate. More significantly, it makes clear the consequences of deviation from these temperatures. It illuminates the common problems of calibration and inhomogeneity. It explains why the commonplace misconception that the Seebeck emf is localized to junctions can lead to serious error in general thermocouple circuits.

Real thermocouple circuits involve several materials and incidental real junctions, often many more than in Figures 32.24 or 32.25. The incidental uncontrolled materials of feedthrus, terminals, splices, etc. might not be recognized as source elements, yet they can, unnoticed, contribute significant unwanted Seebeck emf to the measurement. Therefore, for practical thermocouple thermometry, it is essential to understand and use a descriptive circuit model that is simple to apply and that forces the attention to locations of potential error so that problems can be avoided.

One such authentic model, the *Functional Model of Thermoelectric Circuits* [1, 2, 5, 7, 29–31], combines (1) a basic thermoelectric circuit element, (2) a single fundamental law that describes the sensitivity of that element, (3) a set of practical corollaries from that law that illuminate its practical implications, and (4) a graphic tool for circuit visualization to simplify analysis. This very simple but nontraditional model is crafted for practical thermometry and is worth studying.

### The Basic Thermoelectric Circuit Element

Any thermoelectrically homogeneous nonisothermal segment of arbitrary length of material *M* within any thermoelement is a *Seebeck cell*. Each such segment across which a net temperature difference exists (Figure 32.29) is a *non-ideal voltage source* with internal resistance  $R(T)$ . The Seebeck *source emf* must be observed in an “open-circuit” (null current) mode for the most accurate thermometry. Any  $iR$  voltage

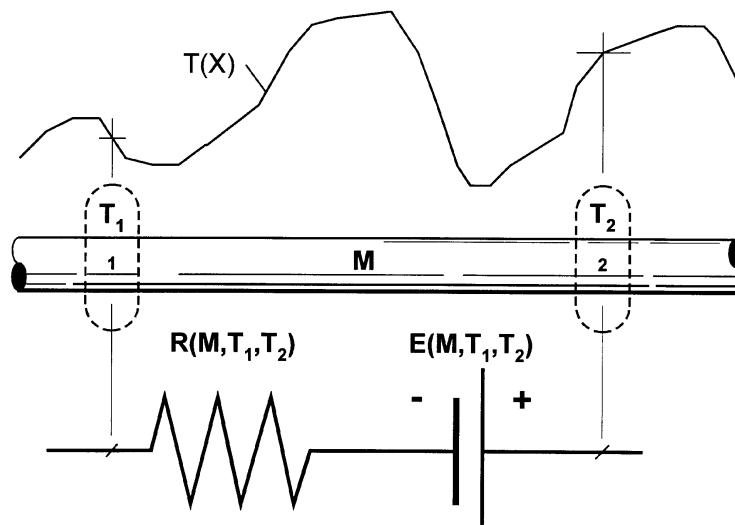


**FIGURE 32.29** The Seebeck emf cell. Every homogeneous, nonisothermal, electrically conducting material is a source of Seebeck emf. The basic cell, a nonideal voltage source with internal resistance, contributes a Seebeck emf that depends only on the material *M* and the temperatures at the segment end-points 1 and 2.

drop due to current allowed by a low input resistance of the voltage monitor reduces the Seebeck source emf to a lower terminal Seebeck voltage. For thermometry, that voltage difference causes a temperature error unless corrected.

In *static* thermometry, as in calibration and in typical process measurement, the measuring junction and a substantial length of the adjacent thermoelements are immersed in a stationary and somewhat isothermal zone so that most of the Seebeck emf occurs well apart from the measuring junction in thermoelements where they cross remote temperature transition regions. In *transient* thermometry, the zone of principal temperature difference initially is adjacent to the measuring junction so that the emf arises across a region of spreading extent adjacent to, but not in, the measuring junction (a material interface).

### The Law of Seebeck emf

Equation 32.74,  $dE = \sigma(T)dT$ , is the functional law that governs the emf of the Seebeck cell and, thus, the net voltage of the most complex thermoelectric circuits. It is the *Law of Seebeck emf*. Every thermoelectric aspect of circuit behavior follows from only this simple relation. Physical details of the process that leads to the Seebeck effect are very complex [5, 6]. Nevertheless, this one simple law is entirely consistent with all physical theory and is experimentally confirmed. If this simple relationship *does* apply to the basic Seebeck cell then accurate thermometry is possible. If it does not, then accurate and reliable thermoelectric thermometry is *not* possible.

The source emf of an individual cell of material M, from Equation 32.75, is:

$$\Delta E_M(T) = E_M(T_2) - E_M(T_1) \quad (32.79)$$

and, for *thermally paired* segments of materials A and B that happen *at any instant* to share a pair of end-point temperatures, *regardless of their residence or proximity in a circuit*,

$$\Delta E_{AB}(T) = E_{AB}(T_2) - E_{AB}(T_1) \quad (32.80)$$

They need not be directly joined at a junction (nor, indeed, be electrically joined). The values of  $E_{AB}(T)$  are obtained directly from the standard thermocouple polynomial defining equations, simpler representations of those equations, tables, or graphs [1, 9–12]. Absolute Seebeck properties for many materials are also available, but are less commonly reported [1, 5, 7, 8]. As is evident from this model, absolute properties could always be used in thermoelectric analysis. They *must* be used in some realistic circumstances where the conventional relative properties are meaningless or where the relative properties are not known.

Either the absolute Seebeck coefficient, the temperature increment across the segment, or both of them, can be either positive or negative. Therefore, the polarity of a cell within a circuit depends both on the material and, unlike the electrochemical emf cell, on the *momentary* sense of temperature difference across the segment. *Polarity, and even function, changes with temperature distribution.*

### Corollaries from the Seebeck Law

From the single Law of Seebeck emf (Equation 32.74), five particularly instructive practical corollaries that aid thermoelectric circuit analysis have been recognized. These are the corollaries of: (1) functional roles, (2) functional determinacy, (3) temperature determinacy, (4) emf determinacy, and (5) Seebeck emf [1, 2, 7, 29–31]. These are stated in [Table 32.14](#), abbreviated from [29]. These revealing corollaries relate more directly to practical thermometry than do the three familiar thermocouple “laws” [32] that actually are only oblique alternative corollaries to the sole physical law (Equation 32.74).

### The T/X Visualization Sketch

The practical significance of the fundamental law and its corollaries for realistic thermoelectric circuits is revealed by a simple graphic sketch ([Figure 32.30](#)). The *T/X sketch* is used for visualization and numerical analysis only. It is *not* drawn to scale. It is *not* used for graphic solution. It illuminates essential

**TABLE 32.14** Corollaries from the Law of Seebeck emf

In any circuit of electrically conducting materials that have an absolute Seebeck coefficient  $\sigma(T)$ , that are each *thermoelectrically homogeneous*, and which follow the Seebeck Law,  $dE(T) = \sigma(T)dT$ :

**1. The Corollary of Functional Roles**

- There are three thermoelectric functional roles: *junctions*, “*conductors*,” and *Seebeck emf sources*:
- *Real thermoelectric junctions* are interfaces that ohmically couple dissimilar materials,
  - “*Conductors*” are segments that, *in effect*, individually or in combination, contribute no *net* Seebeck emf, and
  - *All other segments* are sources of Seebeck emf.

**2. The Corollary of Functional Determinacy**

Instantaneous thermoelectric roles around a circuit *cannot* be predetermined by physical construction, material choice, or circuit arrangement alone; they are governed by temperature distribution.

**3. The Corollary of Temperature Determinacy**

In a circuit with multiple junctions, the temperature of a single junction can be determined from the net Seebeck emf only if the temperatures of all other real junctions are defined.

**4. The Corollary of emf Determinacy**

Seebeck emf is produced *only* by thermoelements, but the net Seebeck emf is governed by the temperatures only of *real junctions*.

**5. The Corollary of Seebeck emf**

The Seebeck emf of any segment of material M with end-point temperatures  $T_1$  at segment endpoint  $X_1$  and  $T_2$  at segment endpoint  $X_2$  is independent of *temperature distribution*, *temperature gradient*, or *cross-section* as it is determined by:

$$E_M(T) = \int_{T_1(X_1)}^{T_2(X_2)} \sigma_M(T) dT = E_M(T_2(X_2)) - E_M(T_1(X_1))$$

From References [1, 7, 29, 30].

facts that are not obvious from a conventional electrical schematic or  $E(T)$  plot. The  $T/X$  sketch shows the temperatures of *all* real junctions in the sequence in which they occur around the circuit. Real junctions are indicated by closed circles. Junctions are joined by thermoelements. The sketch is not drawn to scale, so slopes do not represent temperature gradients.

The  $T/X$  sketch reveals that segments that span a temperature interval always occur in pairs — but significantly only in *series* circuits. It is this fact that allows the convenient use of relative Seebeck properties. This conventional simplification does *not* apply to circuits with paralleled branches [2]. The  $T/X$  sketch, applied to the thermocouple circuit of Figure 32.26, depicts the significant circuit elements (the junctions and thermoelements) in a way that focuses on their unavoidable thermoelectric *functions* (*Corollary 1*). Figure 32.30 shows a circuit temperature distribution with junction temperatures  $T_b \neq T_c$ , that were shown (intentionally improperly different) to illustrate a principle and the benefit of the sketch.

**Temperatures of Incidental Junctions.**

The *reference junction* temperatures must independently be accurately known for measurement. The unknown temperature of the *measuring junction* is to be deduced from the Seebeck voltage. The specific temperatures of all incidental real junctions of a circuit are rarely known accurately in practice. For use in the  $T/X$  sketch, *the actual values need not be accurately known*. Nevertheless, if the *relative* values of all incidental junctions are not properly controlled, as described in the section “Practical Thermocouple Circuits,” and if some essential junction temperatures are not known well enough to draw the sketch, then *accurate* thermometry cannot be ensured! *The revealing  $T/X$  sketch requires no more information than is essential for the physical measurement.*

In the estimate of measurement consequences and to visualize how junction temperatures must be controlled in circuits of many materials, it is sufficient to assume, for qualitative analysis, plausible *relative*

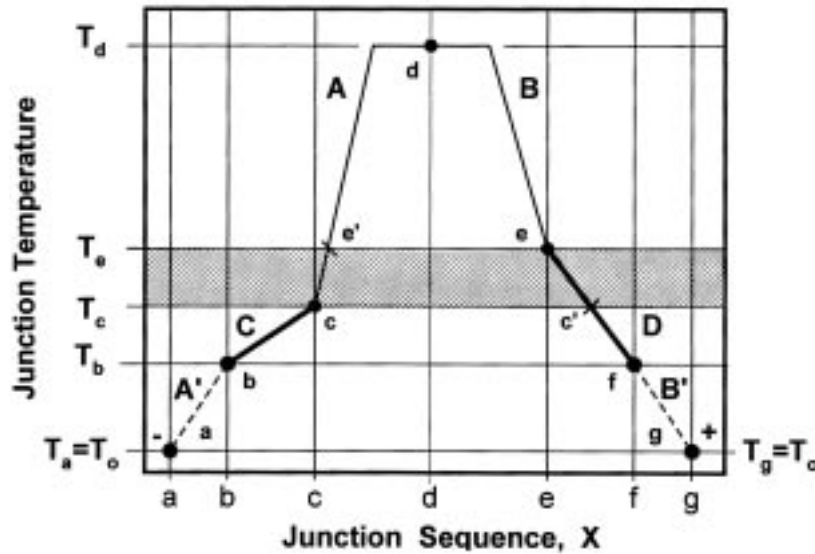


**FIGURE 32.30** The  $T/X$  sketch for thermoelectric circuit visualization. The temperature of the reference junction(s) and the relation between (not necessarily the specific values of) the temperatures of *all* incidental real junctions in a circuit must be known for accurate thermometry, just as for the use of the  $T/X$  sketch. The simple sketch is an aid in recognizing temperatures of incidental junctions that must be controlled to the same temperature. It also makes clear which thermoelements are *thermally paired*, even if not directly joined in the series circuit.

temperature levels and their consequences. The sketch is most often used for visualizing consequences by inspection [1, 2, 29–31]. Nevertheless, it also can aid in quantitative analysis of error for *plausible* temperature distributions.

#### Virtual Junctions and Thermoelements.

On the  $T/X$  sketch, isotherms through *real* junctions intersect some thermoelements. It is useful for analysis to view these intercepts (e.g.,  $c'$  and  $e'$ ), each marked by a *tic*, as *virtual junctions*. For inspection and analysis, they conveniently delineate the arbitrary temperature end-points of segments. Also, on the diagram, virtual thermoelements, **b-c** and **f-g** are indicated by dashed lines. These segments represent the imaginary thermoelectric source of complementary emf that must be supplied to extend the physical reference temperature,  $T_r$ , to the designated reference temperature value,  $T_0$ . The virtual thermoelements represent the reference junction compensation.

The  $T/X$  sketch aids in assigning segment bounding temperatures and thus a polarity and an emf to each thermoelement in the circuit. The circuit is traversed on the sketch from one instrument terminal, conveniently the negative, to the other terminal. Then, if the absolute Seebeck coefficient of a thermoelement is positive, the emf contribution of the segment adds emf if the temperature increases in proceeding across the segment from the negative toward the positive instrument terminal, etc. For inspection and analysis, it is efficient to consider segments as thermally paired over a temperature zone bounded by isotherms.

#### Examples.

On the  $T/X$  sketch, consider the absolute Seebeck emfs supplied by the four thermoelements of Figure 32.26. As connected in this series circuit, proceeding from negative to positive terminals, the net Seebeck emf of the physical circuit between terminals  $b$  and  $f$  is:

$$E_{\text{net}} = E_C + E_A + E_B + E_D \quad (32.81)$$

where

$$\begin{aligned}
E_C &= E_C \Big|_{T_b}^{T_c} \\
E_A &= E_A \Big|_{T_c}^{T_d} \\
E_B &= E_B \Big|_{T_d}^{T_e} \\
E_D &= E_D \Big|_{T_e}^{T_f}
\end{aligned} \tag{32.82}$$

Recall that these individual Seebeck emfs *do* physically exist in the thermoelements whether or not they are connected by junctions as a circuit. It is the temperature dependence of both the magnitude and the momentary polarity of emf that distinguishes thermoelectric from ordinary electric circuit analysis (Corollary 5).

Note that emf from thermoelement *A* can be rewritten as:

$$E_A \Big|_{T_c}^{T_d} = E_A \Big|_{T_c}^{T_{e'}} + E_A \Big|_{T_{e'}}^{T_d} \tag{32.83}$$

This arbitrarily breaks thermoelement *A* into two segments joined at *virtual* junction *e'*. Thermoelement *D* can be segmented as well. Now, across the shaded temperature zone between  $T_c$  and  $T_e$ , there are improperly thermally paired segments *c-e'* and *c'-e*. The net emf from these thermally paired segments is:

$$E_{\text{net}} \Big|_{T_c}^{T_e} = E_A \Big|_{T_c}^{T_{e'}} - E_D \Big|_{T_c}^{T_e} \tag{32.84}$$

From Equation 32.75, recognize that this is the *relative* Seebeck emf for the *unintended* *A-D* pair over that arbitrary temperature zone even though they are not directly joined in the circuit. That improper pairing of segments clearly is avoided only if  $T_c = T_e$ , whatever the temperature. In the instance that Figure 32.26 represents a principal thermocouple *A-B* with matching extension leads *C-D*, materials *A* and *C* are alike and *B* and *D* are alike. If the legs of extension leads *C-D* each exactly match the corresponding legs of thermocouple *AB*, then

$$E_{CD} \Big|_{T_c}^{T_e} = E_{AB} \Big|_{T_c}^{T_e} \tag{32.85}$$

and (*for matching extension leads only*) the accidental pairing is benign.

Otherwise, with *compensating extension leads* ( $\sigma_A = \sigma_C$  and  $\sigma_B = \sigma_D$ ), error occurs even if  $\sigma_{CD}$  closely matches  $\sigma_{AB}$  as a pair but not individually. In the instance of *neutral extension leads* where *C* and *D* are alike, the net emf from the pair is *null* over the zone from  $T_b$  to  $T_c$ . In this instance, the physical reference junction is recognized as necessarily  $T_r = T_c = T_e$ , rather than  $T_r = T_b = T_f$ .

If  $T_c$  and  $T_e$  were interchanged, the error would be of different magnitude, not merely of opposite sign, simply because of the temperature distribution (Corollary 2). The unknown temperature of only one junction can be determined; the others, including incidental junctions, must be defined by value or, indirectly, as being isothermal (Corollary 4).

Note that such relative contributions (the null net contribution from two opposed like segments or the inappropriate thermal mispairing between *B* and *D*) are immediately evident simply *by inspection* of the informal *T/X* sketch without tedious algebra. These critical facts of thermoelectric circuits are not evident from the usual electrical schematic or from  $E(T)$  plots.

Most real circuits include several incidental uncalibrated materials such as connectors, terminals, splices, feedthrus, short pigtailed, or extension leads that each have their own (usually indefinite) Seebeck

properties. In some circuits, some thermoelements might accidentally be paralleled. It is important to include them in the sketch to recognize the unnoticed potential error that could be contributed by such circuit elements if they are not held isothermal. Also, multiple extension circuit elements might be improperly connected with crossed polarity. The specific voltage or temperature consequence of these situations is easily calculated for any plausible temperature distribution. The  $T/X$  plot was designed specifically to aid in circuit visualization to avoid these very common practical problems and to easily assess their possible impact.

## Inhomogeneity

### The Nature of Inhomogeneity

A slender thermoelement is inhomogeneous if  $\sigma_M(T)$  varies along its length. The environment during application can introduce irregular inhomogeneity in one or both thermoelements of a pair. The effect is as if one or more additional dissimilar materials had been added to the circuit.

### The Significance of Inhomogeneity

Adequate thermoelectric homogeneity is the most critical assumption of thermocouple application. It usually is presumed; rarely is it confirmed. Inhomogeneity is a real but phantom problem. Inhomogeneity often remains undetected even while producing substantial error. It rarely is discovered by even the most careful conventional calibration [1, 7, 11, 29–31, 33, 34]. In physical thermometry, thermocouple *drift* is *invariably* a symptom of progressing *inhomogeneity*. Such change is progressive, often insidious, and usually is misinterpreted [34].

Rather than envisioned correctly as localized degradation of Seebeck coefficient, *drift* is often viewed improperly as a uniform “black-box” decalibration of the thermocouple rather than progressing inhomogeneity. For this reason, it is a far more commonplace problem than recognized by most experienced users. It can occur in use, in fabrication, or in calibration because of mechanical strain, thermal phase change, surface contamination, chemical interaction between materials, evaporation or migration of alloy constituents, transmutation under radiation, and a variety of other realistic causes.

Inhomogeneity error in thermocouples, as manufactured, is intended to be covered by standard tolerances [1, 9, 10, 28]. Troublesome inhomogeneity is most common in used and abused thermocouples, but can sometimes occur in new thermocouples that have been individually calibrated to high temperature. It can occur within and through apparently impervious protective metal sheaths or thermal wells and between bead insulators.

The example, Figure 32.30, illustrated the effect of improperly controlled junction temperatures that resulted in the subtle introduction of relative Seebeck emf from an unintended thermal pairing of segments of homogeneous thermoelements. The analogous *inhomogeneity* problem, best visualized with the  $T/X$  sketch, arises when a portion of one or both thermoelements locally changes in Seebeck coefficient over some nonisothermal span of the thermocouple. In effect, this introduces *phantom* dissimilar segments of indefinite graduated property and unrecognized location [35]. This most often occurs over a lengthy region near the measuring junction where the thermoelements are exposed to damaging environments in an oven or process.

The *maximum possible* error of inhomogeneity is determined by the location and magnitude of greatest deviation from normal of the Seebeck coefficient. The *actual* error depends on the momentary distribution of temperature during use. In thermometry and in calibration, the *likely* error introduced by inhomogeneity is moderated. While present only within an isothermal region, inhomogeneities introduce *no* error. Under unfavorable temperature distributions, inhomogeneity error can be extreme and results in peculiar puzzling responses [34]. Changes of relative Seebeck coefficient by more than 60% over 25-cm spans have been observed in individually calibrated, certified, premium-grade fine wire Type R MIMS thermocouples entirely enclosed within intact platinum sheaths and exposed to temperature within the tabulated temperature range [18].

## Testing for Inhomogeneity

Many authentic sensitive and accurate tests for thermoelectric inhomogeneity have been developed, and their practical need has been demonstrated; however, they are rarely used [33]. All true inhomogeneity tests require moving an abrupt *step* of temperature progressively along thermoelements.

The commonplace application of a *very narrow symmetric* temperature pattern is the antithesis of an inhomogeneity test. It is *not* a test for inhomogeneity. Its popular use has misled many to discount inhomogeneity as a real and significant problem in accurate thermoelectric thermometry.

Valid tests range from simple methods of low resolution to advanced methods that can accurately resolve inhomogeneity with spatial resolution of a few millimeters [21, 33]. Regrettably, as inhomogeneity errors usually are not recognized, inhomogeneity is not authentically tested in commercial practice nor by calibration laboratories. Nevertheless, invalid though certified NIST-traceable certification to great *precision* is possible on a thermocouple that can be accurately measured to be *severely* inhomogeneous and of indefinite uncertainty [29–31, 33, 34].

## Calibration

The measurement uncertainty of most kinds of sensors can be reduced by *individual* calibration. Initial calibration, periodic recalibration of unused thermocouples, and even of degraded *individual* thermocouples, although commonplace, is often less beneficial (or even harmful) and more costly. Such ill-advised thermocouple calibration has been mandated by some “quality assurance” programs.

Surveys reveal a trend for customers to demand progressively higher accuracy of thermometry [36]. In some applications, a 1°F (0.56°C) error now is deemed too large, and 0.1°F tolerance may be specified independent of temperature level. (Compare with tolerances in Table 32.12.) There are a few industrial applications that truly require such accuracy. More often, the specification merely presumes that such accuracy in thermocouple thermometry is routinely attainable merely by calibration. Calibration is an opiate of quality assurance. The illusion of accuracy provided by NIST-traceable certified calibration and purported *in situ* calibration is counterproductive if it is not authentic.

Consideration of the details of thermocouple calibration suggests why authentic accuracy at the 0.1°C level is unlikely in industrial thermoelectric thermometry. The approach to achieving authentic calibration of thermocouple system accuracy (*ignoring* thermal coupling and transient response errors) is illustrated in Figure 32.31. Figure 32.31(a) represents the thermocouple system to be calibrated. Calibration for thermoelectric thermometry must distinguish three system components: (1) the thermocouple circuit, (2) the reference junction temperature compensator, and (3) the monitoring instrument. Each separately affects temperature uncertainty.

## The Principal Thermocouple

Calibration of principal thermocouples is performed by immersing the vicinity of the measuring junction in the isothermal region of a bath or oven [37]. Several compact dry-well calibrators available are convenient for calibration at the job site [38]. Fixed-point cells, liquid baths, and fluidized solid beds can be more accurate and are widely used in the calibration laboratory [39]. Sufficient depth of immersion into an isothermal calibration zone, usually at least 10 to 20 times the probe diameter, ensures that conduction of heat along the thermocouple from the environment does not affect the junction temperature.

The appropriate concern for the effect of longitudinal heat conduction on measuring junction temperature has led to the misperception that it is the *junction* that is being calibrated [30]. Clearly, thermocouple calibration is *not* of the measuring junction; it *is* of unidentified segments of thermoelements, remote from the measuring junction, only where they enter the isothermal calibration zone through a temperature transition.

Segments of service-induced inhomogeneity that seriously degrade measurement accuracy are often placed, during unsuccessful attempted recalibration, within the isothermal region where they contribute no Seebeck emf, so inhomogeneity is not discovered. The act of calibration at temperatures above 400°C can actually induce inhomogeneity and degrade accuracy [9, 10]. Not even costly “NIST-traceable”

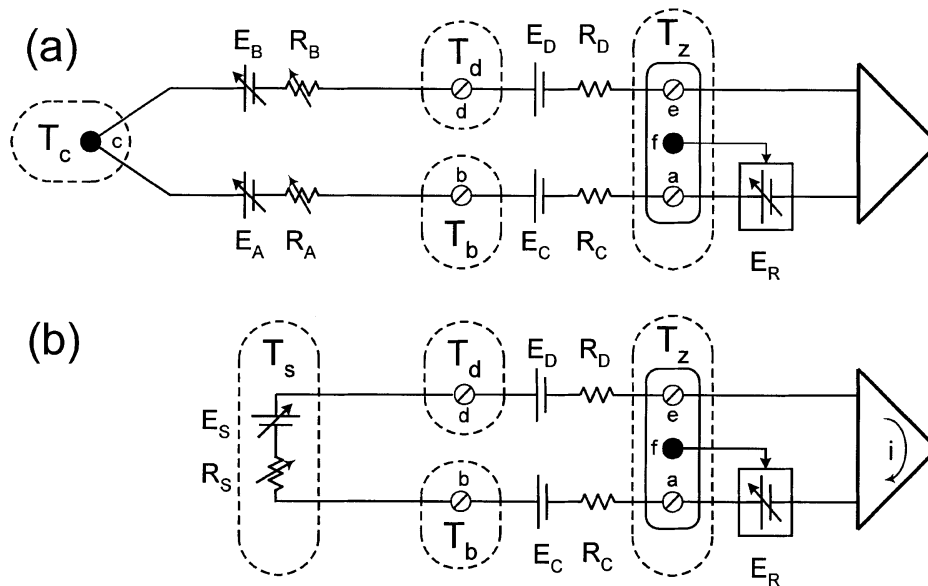


**FIGURE 32.31** Contributions of Seebeck and compensating emf in system calibration: (a) the circuit to be calibrated or simulated, (b) a general calibration simulation of a system that includes internal reference junction temperature compensation.

calibration and certification by competent calibration laboratories, without specific assurance of homogeneity, are a guarantee of accuracy at *any* level.

*Commercial Tolerances.* Standardized tolerances for new thermocouple materials are established by the formal consensus judgment of many experienced producers, users, and calibration standards laboratories staff [10, 24, 28]. The tolerances include not only deviation from the overall Seebeck properties, but also cover inevitable uncertainty from inhomogeneity and irregular deviations from the smoothed standardized characteristic over small spans of temperature. They apply to material as delivered and not exposed to excessive temperature. The conservative tolerances for standard letter-designated thermocouple types as delivered are usually reliable until the thermocouples are exposed too long to excessive temperatures or adverse environments. Recalibration of used thermocouples without separate assurance of homogeneity can be misleading [31].

To address calibration problems presented by undiscovered inhomogeneity, two practices are common. For inexpensive base metal thermocouples, it is presumed that unused thermocouples are homogeneous and uniform within standardized tolerances. The typical Seebeck property of a production batch is characterized by the manufacturer or user by calibrating one or more expended surrogate samples. These are discarded after calibration. Their first-cycle calibration is taken as representative of other thermocouples of the same batch. Used principal thermocouples that have experienced drift are discarded.

A commonplace second approach is recalibration. This is usually in response to drift observed in service. Drift signals progressing inhomogeneity. Apart from an authentic inhomogeneity prescreening, recalibration is not recommended. Even widely promoted *in situ* recalibration of degraded thermocouples is ineffective if temperature distribution will vary in use [31].

Platinum-based thermocouple wire can be annealed full length by electrically heating in air [9–12]. Such annealed thermoelements can be presumed to be free of reversible strain-induced inhomogeneity and, thus, accurate recalibration might be justified. However, annealing cannot reverse decalibration from the migration, absorption, or evaporation of alloy constituents or other chemical contamination; therefore, recalibration, even of used precious metal thermocouples, should be performed only where the likelihood of homogeneity is factually based. Unlike base metal thermoelements, precious metal

thermoelement materials often can be reconditioned. Also, precious metals have a significant material salvage value if recycled.

### Extension Leads

Compensating extension leads, although Seebeck sources, usually are not calibrated. It is commonly assumed that they will be exposed to only a small fraction of the temperature span that is being measured and, if so, will contribute insignificantly to error. Extension insulations are rated for continuous use to maximum temperatures between 105°C and 540°C [43]. Seebeck characteristics might not be well approximated over this range [1, 10]. The possible contribution from extensions can be very large. The plausible error is easily estimated using the model in “The Functional Model of Thermoelectric Circuits.” The more usual consequential errors due to extension leads result from failure to correctly control the temperatures of incidental splice junctions, as described in “Practical Thermocouple Circuits.”

### Reference Temperature Compensation

Modern thermocouple indicators usually provide internal reference junction temperature compensation. A few make compensation a selectable alternative. The accuracy of reference junction compensation, Figure 32.31(a), depends on the accuracy of the sensor(s), **f**, used to monitor reference junction temperature of isothermal terminations, but also on the conformity of the scaling algorithm or analog circuitry to the characteristic of the individual thermocouple. The zone sensor determines the compensating voltage,  $E_r$ . Some monitors have replaceable isothermal terminal blocks that include the zone temperature sensor. Most monitor designs unfortunately do not allow separate thermal calibration of the reference temperature sensor. Simply shorting the indicator input terminals, **b-d**, should produce a temperature indication near, and usually slightly above, ambient temperature. Specifications claim reference uncertainty on the order of 0.1°C to 0.5°C and error contributions usually *are* small but *infrequently* they have been *very* large and insidiously progressive up to *many* times the standard thermocouple tolerances [35].

### Monitoring Instruments

The accuracy of conversion of the Seebeck voltage at terminals **b-d** to deduce the temperature  $T_c$  requires calibration of the monitoring instrument. Both the accuracy of voltage measurement and of linearization are sources of uncertainty. The scaling accuracy is based on an approximation of the defining  $E(T)$ , and *not* on the individual thermocouple characteristic.

Instrument designs are varied. The general principles of *authentic* calibration required to approach 0.1°C uncertainty for a thermocouple indicator that provides internal reference temperature compensation are illustrated with the circuit of Figure 32.31(b). A thermocouple simulator/calibrator supplies a well-known voltage  $E_s$  that corresponds, for the standard thermocouple type, to a desired temperature calibration point. The simulator must remain in thermal equilibrium during calibration, with irrelevant Seebeck voltage properly nulled.

If the input resistance of the indicator is *very large*, resistance matching of the simulator to the thermocouple is not required. If the indicator has a *low* input resistance or it internally produces current **i** when its terminals **b-d** are shorted, then a temperature error proportional to the indicator current and the loop resistance will be experienced. For accuracy with such indicators, the simulator  $R_s$  must also mimic the source resistance of the individual thermocouple ( $R_A + R_B$ ). However, that thermocouple loop resistance may vary considerably in application as it depends on the temperature distribution around the thermocouple over a broad range of temperatures.

The input terminals of the indicator are **b** and **d**. For accurate calibration, it is essential that  $T_b = T_d = T_z$ . Some indicators and reference temperature compensators connect the isothermal zone block to the terminals with compensating thermocouple leads. For these, if  $T_b \neq T_d \neq T_z$ , an indefinite error results that cannot be overcome by calibration.

The simulator voltage must imitate the behavior of only the thermocouple, **b-c-d**. The voltage it must provide depends on whether or not the indicator supplies internal reference temperature compensation. If  $T_b = T_d = T_z$ , the proper total Seebeck voltage is  $E_{AB}|_{T_b=0^\circ\text{C}}^{T_c} = E_{AB}|_{T_z}^{T_c} + E_{AB}|_{0^\circ\text{C}}^{T_z}$ . If the indicator *does not* apply

reference temperature compensation,  $E_R$ , then the simulator must provide  $E_s = E_{AB|0^\circ\text{C}}^T$ . If the indicator *does* apply  $E_R$ , then the simulator must supply *only*  $E_s = E_{AB|T_z}^T$ .

This requires that the internal  $T_z$  of the indicator be accurately known by the simulator. Some simulators allow setting a *presumed*  $T_z$  in calibration. Those that do not *cannot* be used directly without error for calibration of the commonplace reference temperature compensating indicators. Many convenient thermocouple instrument calibrators allow setting the desired calibration by temperature rather than by voltage for standardized thermocouple types. This convenience introduces an additional nonlinear scaling and only approximate conformity to the standard characteristic.

## Thermocouple Failure and Validation

A thermocouple measurement has *failed* when its indications are beyond uncertainty limits required for a measurement. Thermocouples sometimes fail “open” as junctions separate or thermoelements corrode, yield, or melt. Explicit “open circuit” indication is a promoted feature of many modern thermocouple indicators. This popular indication is useful, but is not an adequate indicator of thermocouple integrity.

The more common but less apparent circuit failures are by inobvious shunting, shorting, or progressing inhomogeneity of thermoelements. These are not detected by the “open circuit” indication. The continual indication of a *plausible* temperature is not proof of *authentic* temperature measurement.

A deliberate or accidental electrical shunting or direct short between thermoelements at ambient temperature local to an electronic compensating reference junction should result in an indication near *ambient* temperature, not  $0^\circ\text{C}$ . A thermocouple failure resulting from direct shorting between thermoelements at some distance from the intended measuring or reference junctions can go undetected because it occurs in a temperature region that is very different from the reference temperature and where a valid or plausible temperature measurement can continue to be made *but at an irrelevant and unexpected and unrecognized location* [35]. In some situations, as in predictably hostile environments, such failure of some thermocouples in service is anticipated. Where the failure is because of thermocouple circuit damage, it may not be evident immediately (or ever) without special circuit diagnostics. For such critical situations, special thermoelectric circuits and monitoring methods have been developed to assess the continued circuit integrity, although not the accuracy, of thermometry [35].

## Environmental Compatibility

A primary consideration in thermocouple selection is compatibility of the thermoelements with their protective enclosures and of both thermoelements with the environment of measurement. Thermoelements must be protected from corrosive environments and electrically conductive fluid or solid shunts. Plastic, ceramic, or fiber insulators, metallic sheaths, and thermowells are intended to serve this function but may fail in service [1, 9–12, 25]. The compressed granular insulation of mineral-insulated, metal-sheathed thermocouples, if exposed, rapidly absorbs moisture that can seriously degrade resistive isolation [1, 10–12]. When cut, ends of MIMS thermocouple sheaths must be quickly resealed to avoid moisture absorption. Fiber and bead insulators are easily contaminated and can degrade accuracy [1, 10].

## Temperature Exposure

The *unavoidable* environmental variables in thermometry are *temperature* and *duration*. Although thermoelements may not be visibly affected by an environment, the Seebeck coefficient might be substantially degraded. Even if only a very thin surface layer of a thermoelement is modified, the Seebeck coefficient could be changed. The properties can be degraded by use for a long period of time, at extreme temperatures, and in adverse environments [1, 9–12]. For these reasons, application should be limited to within the suggested temperature limits (Table 32.15). Calibration should be performed quickly, allowing time only for equilibration, and only to the maximum temperature of intended use. Degradation, observed in use as *instability* or *drift*, is necessarily a symptom of progressing *inhomogeneity* [30, 31].

Sustained excessive temperature alone can quickly degrade a thermoelement. Melting points define the absolute upper temperature range of thermocouple use. However, below this definite value, there are

**TABLE 32.15** Temperature Upper Limits For Different Wire Diameters

Dia., mm	0.025	0.127	0.254	0.406	0.813	1.600	3.175	
Dia., in.	0.001	0.005	0.010	0.016	0.032	0.063	0.125	
Dia., AWG	50	35	30	26	20	14	8	
Type	Temperature limit, °C							Type
E	290	325	370	400	510	775	855	E
J	230	275	305	350	460	600	750	J
K, N	690	730	790	840	950	1095	1250	K, N
T	90	110	150	185	270	370	375	T

*Note:* Recommended limits are guidelines for continual use of bead-insulated thermocouples in closed-end protection tubes in compatible environments. Mineral insulated metal-sheathed thermocouples can have slightly higher limits and tolerate longer exposure.

From References [1, 9, 13].

**TABLE 32.16** Environmental Tolerance of Letter Designated Thermocouples

Type	Environment							
	Oxygen rich	Oxygen poor	Reducing	Vacuum	Humid	Below 0°C	Sulfur traces	Neutron radiation
B	Good	Good	Poor	Fair	Good	Poor	Poor	Fair
E	Good	Poor	Poor	Poor	Good	Good	Poor	Poor
J	Fair	Good	Good	Good	Poor	Poor	Fair	Poor
K	Good	Poor	Poor	Poor	Good	Fair	Poor	Good
N	Good	Fair	Poor	Poor	Good	Good	Fair	Good
R,S	Good	Good	Poor	Poor	Good	Fair	Poor	Poor
T	Fair	Fair	Good	Good	Good	Good	Fair	Poor

From References [1, 4, 9, 10, 43].

indefinite application limits at which stability might be substantially reduced [1, 9–12]. Standard thermocouple tables extend only to the greatest temperature of *recommended* use for benign protected environments, short durations, and for wire materials of 3 mm or greater diameter [1, 9, 10]. Significantly reduced temperature limits apply for materials of smaller cross-section, Table 32.14 [1]. The thermocouples of smaller cross-section degrade more quickly. The standard tolerances apply only to material as manufactured.

### Chemical Environment

There are broad guidelines for environmental compatibility. These recommendations are conditional and critically depend on many specifics of exposure. A concise summary of environmental compatibility characteristics is given in Table 32.16. The references should be consulted for detailed compatibility information [1, 4, 9, 22, 23]. Many thermocouple catalogs include tables of *usually* tolerable chemical environments for thermoelements or thermowell materials [19, 20]. Service experience in working with customers in a wide variety of process environments sometimes enables manufacturers to advise users on special problems of compatibility. Often, suitability in a particular service can be assured only by trial.

### Metallurgical Change

Alloyed thermoelements can locally change composition by evaporation of constituents when exposed to vacuum. Alloy constituents evaporated from a sheath or from one thermoelement can deposit and coat adjacent thermoelements even through insulators [1, 9–12, 24, 30, 31]. Alloy components can migrate from one thermoelement to the other through the measuring junction. Traces of contaminants can penetrate through pinholes and hairline cracks and can actually diffuse through intact protective

sheaths and affect apparently isolated thermoelements. Minute trace impurities in sheaths or insulating materials can interact with thermoelements. Appropriate MIMS construction and material selection usually extends life and increases temperature limits, but damage can occur even within apparently fully sheathed assemblies [34]. Excessive strain can locally substantially modify the Seebeck coefficient of one or both thermoelements resulting in inhomogeneity. Very localized strain, as introduced by sharp bends, usually has little effect on practical thermometry.

## Data Acquisition

### Thermocouple Indicators

The instrument designer can shelter the user from many troublesome details that complicated measurement for thermocouple pioneers. Microvolt-level signal resolution, high input resistance, stability, noise reduction, nonlinear scaling, and reference temperature compensation are now routinely provided to allow the user to focus on the measurement rather than on details of its indication or recording.

Some thermocouple indicators are hand-held and accommodate only a single thermocouple and only of a single type. A few provide dual thermocouple inputs and allow direct differential temperature measurement for which reference junction compensation *must not* be directly applied. Other bench-top units accommodate several thermocouple inputs of the same or of intermixed thermocouple and other sensor types.

Claimed instrument accuracy could mislead the casual reader. Although many instruments are supplied complete with a thermocouple probe, some accuracy specifications describe only the accuracy of input terminal voltage measurement. The actual instrument accuracy should be determined by electrical calibration (see “Calibration” section). Occasionally, the error of the indicating instrument becomes substantially greater than specified due to drift of reference compensation, offset, or gain. The additional uncertainty of thermocouple calibration, Table 32.13, and the often larger discrepancy between measuring junction temperature and the actual temperature of the object being measured, cannot be included because the latter are governed by details of heat transfer and transient thermal response.

### Thermocouple Transmitters

A less familiar form of thermocouple signal conditioning, the *thermocouple transmitter*, is commonplace in process industries [4, 39]. Most two-wire thermocouple transmitters (not an RF wireless transmitter) are single-channel devices that perform reference junction compensation, linearizing, and isolation, and transmit the conditioned information to a remote monitoring site [1]. The transmitter converts the temperature-scaled Seebeck emf to an analogous signal for wire transmission over long lines to a remote recording or monitoring location. Such inexpensive and compact single-sensor signal conditioners are available specialized to most process variables. Thermocouple transmitters are well suited for monitoring slowly changing temperatures at monitoring sites distant from the measuring junction. Many are electrically isolated for safety. Some are adapted for use with the DIN rail mounting system. A transmitter can be installed near each thermocouple. Some are small enough to install in the connection head of a thermowell.

The transmitted signal can take either current-modulating or voltage-modulating form following ISA standards. The current-style transmitter temperature modulates, in proportion to temperature, a dc current supplied from the monitoring site. The signal ranges between 4 mA and 20 mA. The current-style transmitter conveys information over great distances without the voltage loss attendant to long-line voltage transmission. Some of the voltage-style transmitters modulate a supplied voltage over the span from 1 Vdc to 5 Vdc. Offset and scaling for some are adjusted at the transmitter. Some transmitters now have a local digital readout, and the scaling and offset can be remotely adjusted [4, 39].

### Recording

Some multichannel thermocouple data recorders are now battery powered for stand-alone use and small enough to be hand held [41]. Some simpler recorders now cost less than U.S.\$200. More sophisticated

units accommodate multiple thermocouples of the same or intermixed type. Larger digital data loggers with multiplexers that sequentially sample the output from individual thermocouples can accommodate up to several hundred inputs and can record a mix of both thermocouple and other signals at sample intervals programmable from a few milliseconds to hours or days. Desirable three-wire switching between thermocouples is commonplace.

Personal computers now accommodate inexpensive internal digital data acquisition boards that can convert the computer to a high-resolution temperature recording system. Laptop computers can accept special palm-sized PCMCIA plug-in cards for multiple thermocouple input. Digital computer based data acquisition systems with software specialized for data acquisition, analysis, and presentation, allow the user to apply special reference temperature compensation, customized linearization of thermocouple scaling functions for either standard or individual calibrations and of special thermocouple types. Computer-based thermocouple systems with suitable commercial data acquisition and other software, provide for experiment design, prediction, data acquisition, information management, analysis, reporting, archiving, and communication within a single compact fieldable laptop computer [42].

## Signal Transmission

The length of the principal thermocouple should be as short as feasible. The thermoelements should be continuous between measuring junction and reference junctions for best accuracy, but lengthy extension cables can be used if necessary (see “Practical Thermocouple Circuits” section). In field experiments and in process monitoring, recording might be separated from the measuring junction by hundreds of meters. There are several satisfactory possibilities for signal transmission over great distances.

### Extension Cable

Matching and compensating thermoelectric extension cables (see “Practical Thermocouple Circuits” section) are available in a wide variety of constructions and insulations [4, 43]. An extension cable, as a transmission line, can be a single twisted thermoelectric pair or a multipair cable designed for suppression of both electrostatic and electromagnetic noise and for environmental protection. While inexpensive unshielded insulated extension wire is available, in the common situation where electric noise is likely, each extension should be an insulated, individually shielded, and twisted pair. Where several extension pairs from a cluster of nearby thermocouples extend to a remote recorder, multipair thermoelectric cable is available that adds an overall electrostatic shield, mechanical strengthening reinforcement, and a robust environmental overjacket to protect from mechanical damage and chemical intrusion in harsh process environments [4, 42].

Such elaborate thermoelectric extension is more expensive than copper instrumentation cable; thus, alternative transmission systems should be considered. The proper use of twisted pair copper instrumentation cable as neutral extension leads, extending from external reference junction temperature compensation, can be sufficient and less costly than thermoelectric extensions.

Higher quality twisted-shielded-pair instrumentation cable can also improve signal fidelity in transient thermometry. For such neutral extension leads, insulated solid *unplated* copper instrumentation pair only should be used because nonuniform plating thickness can result in irregularly distributed inhomogeneity and cause Seebeck emf noise. Conventional *coaxial* instrumentation cable should never be used as lengthy neutral thermoelectric extension leads because the outer braid and center conductors have very different Seebeck coefficients. If not at uniform temperature, the cable can be a significant source of Seebeck noise emf.

Thermoelectric extensions and “pigtailed” assemblies should be checked full-length for hidden junctions between slightly mismatched spliced thermoelements and for deliberate, but hidden, pair splices incorrectly made in crossed polarity [10]. Pass a narrow heat source along the full length of the cable, while monitoring for local jumps of output local to such unintended junctions, using a thermocouple indicator. This test is very effective to pinpoint hidden junctions. It does not test for inhomogeneity [10, 30].

Optic fiber cable with electro-optic transmitters can be used for electric noise-free cable transmission over a long distance between signal conditioning that is local to the thermocouple and to a remote recorder or monitor.

### **Wireless Transmission**

In several situations, copper wire transmission is less effective, more expensive, or less convenient than wireless methods. Several low-cost wireless (not thermocouple transmitter) data acquisition systems are now adapted to combine thermocouple data acquisition and remote signal transmission [44]. *Radio modems* communicate data from a measuring location to recording sites as much as 5 km away. Most provide spread spectrum transmission that does not require a communications license. Wireless data transmission can be particularly economical where the distance between the measuring junction and recorder is great, when many thermocouples must be recorded, when little setup time is available for field cabling, and where the measuring setup must be moved occasionally. Some systems combine data logging and radio communication in a single unit. Others require the use of a thermocouple transmitter, a data logger, and the radio modem to form a system.

## **Sources of Thermocouple Application Information**

### **Technical Papers**

The most concentrated and broadest sources of refereed technical papers addressing thermocouple thermometry are the serial proceedings of a decennial international symposium on temperature [25]. The six volumes to date are a rich and reliable source of application data. Proceedings of annual symposia of the ISA and NCSL also have a few papers describing current developments in thermometry. Reference [26] has thermoelectric data on the widest variety of common and nonstandard materials. Current papers devoted specifically, not incidentally, to thermocouples are infrequent and are distributed broadly across trade magazines and journals of professional societies. Essential details of thermocouple thermometry are more often (poorly) described only incidentally in reports of experimental studies. Some manufacturers publish subscription technical journals specializing in thermometry [45].

One measurement journal frequently publishes articles on applied thermometry and, annually in the June issue, publishes an extensive directory of manufacturers of thermocouple materials and related instrumentation [46]. The directory includes, for several dozen listed manufacturers, concise descriptions of selected products and current prices.

### **Books, Reports, and Standards**

A very detailed and authoritative NIST monograph is the primary source for Seebeck properties and physical characteristics of letter-designated thermocouples [9]. Standards of the ASTM and ISA adopt the values and complement the NIST report [10, 24]. U.S. standards are reviewed and updated at intervals of 5 years or less. The ASTM also publishes interim tables of Seebeck emf for a few popular materials that have not been standardized [10]. Many standards are collected in a single, annually revised volume specializing in thermometry [10]. The hardcopy thermocouple tables from these volumes are now available as functional computer programs that calculate  $E(T)$  and  $T(E)$  of the NIST 175 document over ranges, at intervals, and in units selected by the user [46].

A comprehensive thermocouple application manual is published by the ASTM [1]. Many commercial publishers issue new reference and textbooks addressing measurement. Most of these include a brief obligatory section or chapter describing the bare elements of thermocouple thermometry. A few devote an entire volume to thermometry. There are many deeper scientific treatments of thermoelectricity, mostly in the historic literature [1, 11, 12].

Many national and international consensus standards organizations publish thermoelectric test methods and material characterizations [10, 21, 25]. Standards are instructive as well as being formalizations of procedures and materials. ASTM Standards and indexes to them are now available in computer CD-ROM file format. Some standards now are available on the World Wide Web or by FAX. Societies

with committees that specialize in thermoelectric standards now have Internet Web sites (such as <http://www.isa.org> and [astm.org](http://www.astm.org)) that provide information about available standards and solicit on-line technical questions from users.

### **Workshops**

Annually, there are several excellent workshops of a few hours or days duration devoted to measurement, thermometry, and even thermocouples. Professional societies such as the ISA, in association with special symposia or annual meetings, present special tutorial workshops. Some are offered without fee by manufacturers. Other measurement courses are offered by independent measurement specialists. Announcements of these workshops are published in the technical and trade journals.

### **Trade Literature**

Abundant, free, commercial catalog literature, handbooks, and Web site advertising describe thermocouple hardware and data acquisition products. Some manufacturers publish elaborate catalogs of thermocouple-related hardware, software, and books [4]. Most include tutorial material. A few include technical reprints, discussion of principles and practices, and present extensive tables of thermoelectric characteristics and physical properties of thermocouple materials. Demonstration programs and product information are available from manufacturers on CD-ROM and on the Internet. There are several trade journals that relate to measurement, explore current issues and developments, and are distributed free to qualified recipients.

### **Caveat**

The reader is cautioned that the extensive current and historic literature of thermoelectric thermometry, tutorial articles (*even this one*), standards, specifications, and advice from “experts,” all must be studied very critically with an authentic thermoelectric model in mind. At every level of sophistication, from the promotional to the most esteemed esoteric and sophisticated mathematical and physical thermoelectric theory, innocently propagated misconceptions concerning the thermoelectric effects are very commonplace.

### **Summary**

The Seebeck effect can be used to measure temperature with finer spatial and time resolution, over a broader temperature range, in more diverse geometries, and at lower cost than most other electric temperature sensors. The unique versatility of the thermocouple ensures that it will continue as the thermometry means of choice for many applications despite competition from an increasing variety and abundance of alternative special-purpose thermometers. However, the misleading seeming simplicity of the idealized thermocouple and the convenience and apparent accuracy afforded by modern signal conditioning instruments can be misleading. Correct application is simple.

Properly used within its limitations, the thermocouple is capable of accurate reliable thermometry. Improperly understood, the thermocouple is subject to misapplication and inconspicuous, but very significant, error. This precautionary overview described pitfalls and their avoidance in thermocouple practice. This can provide the receptive reader with an authentic basis for the knowledgeable use of even the most complex series and generalized thermoelectric circuits in circuit design, diverse applications, particularly in thermometry. The simple Functional Model presented here (and perhaps requiring some study) was deliberately crafted to aid the user in clearly distinguishing the authentic information from the misleading, and to aid in evaluating the designs and specifications of manufacturers of thermoelectric products.

### **References**

1. R. M. Park (ed.), *Manual on the Use of Thermocouples in Temperature Measurement*, MNL 12, 4th ed., Philadelphia, PA, American Society for Testing and Materials, 1993.
2. R. P. Reed, Thermal effects in industrial electronics circuits, in J. D. Irwin (ed.), *CRC Industrial Electronics Handbook*, Boca Raton, FL, CRC Press, 1996, 57–70.

3. *Catalog*, TRANSCAT/EIL, Rochester, NY, 1998.
4. *Catalog*, *The Temperature Handbook*, Issue 29, Omega Engineering, Inc., Stamford, CT, 1995.
5. D. D. Pollock, *Physics of Engineering Materials*, Englewood Cliffs, NJ, Prentice-Hall, 1990.
6. D. M. Rowe (ed.), *CRC Handbook of Thermoelectrics*, Boca Raton, FL, CRC Press, 1995.
7. R. P. Reed, Principles of thermoelectric thermometry, in R. M. Park (ed.), *Manual on the Use of Thermocouples in Temperature Measurement*, MNL 12, 4th ed., Philadelphia, PA, American Society for Testing and Materials, 1993, chap. 2, 4–42.
8. R. P. Reed, Absolute Seebeck thermoelectric characteristics — principles, significance, and applications, in J. F. Schooley (ed.), *Temperature, Its Measurement and Control in Science and Industry*, Vol. 6, Part 1, New York, American Institute of Physics, 1992, 503-508.
9. G. W. Burns, M. G. Scroger, G. F. Strouse, M. C. Croarkin, and W. F. Guthrie, *Temperature-Electromotive Force Reference Functions and Tables for the Letter-Designated Thermocouple Types Based on the ITS-90*, NIST, Monograph 175, Washington, D.C., Department of Commerce, 1993.
10. *Annual Book of ASTM Standards, Temperature Measurement*, 14.03, Philadelphia, PA, American Society for Testing and Materials, 1998.
11. J. V. Nicholas and D. R. White, *Traceable Temperatures — An Introduction to Temperature Measurement and Calibration*, New York, John Wiley & Sons, 1994.
12. T. W. Kerlin and R. L. Shepard, *Industrial Temperature Measurement*, Philadelphia, PA, Instrument Society of America, 1982.
13. *Catalog*, Analog Devices, Inc., Norwood, MA.
14. *Catalog*, *Equipment for Temperature Measurement and Control Systems*, Hades Manufacturing Corp., Farmingdale, NY.
15. R. Morrison, *Noise and Other Interfering Signals*, New York, John Wiley & Sons, 1992.
16. H. W. Markenstein, Proper shielding reduces EMI, *Electron. Packaging & Production*, 37, 72-78, 1997.
17. *Catalog*, Thermagon, Inc., Cleveland, OH.
18. N. R. Keltner and J. V. Beck, Surface temperature measurement errors, *J. Heat Transfer*, 105, 312-318, 1983.
19. *Catalog*, RdF Corporation, Hudson, NH.
20. *Catalog*, *Temperature Measurement Handbook*, Vol. IX, NANMAC Corporation, Framingham, MA.
21. R. P. Reed, Convolution & deconvolution in measurement and control, professional course, *Measurements & Control*, (178-188), 1997, 1998.
22. H. M. Hashemian, K. M. Peterson, D. W. Mitchell, M. Hashemian, and D. D. Beverly, In situ response time testing of thermocouples, *ISA Trans.*, 29, 1986.
23. R. P. Reed, The transient response of embedded thin film temperature sensors, *Temperature, Its Measurement and Control in Science and Industry*, Vol. 4, Part 3, New York, Instrument Society of America, 1972.
24. *Standard, Temperature Measurement Thermocouples*, ISA/ANSI Standard MC96.1-1982, Research Triangle Park, NC, ISA International Society for Measurement and Control, 1982. (Standard withdrawn 1993).
25. *Temperature, Its Measurement and Control in Science and Industry*, Vols. 2–6 (Serial), New York, American Institute of Physics, 1942–1992.
26. P. A. Kinzie, *Thermocouple Temperature Measurement*, New York, Wiley-Interscience, 1973.
27. H. L. Anderson (ed.), *Physics Vade Mecum*, New York, American Institute of Physics, 1981.
28. *Standard, Norme Internationale/International Standard*, IEC 584, Parts 1–3, Thermocouples, International Electrotechnical Commission, Geneva, Switzerland, 1995.
29. R. P. Reed, Thermoelectric thermometry: A functional model, in J. F. Schooley (ed.), *Temperature, Its Measurement and Control in Science and Industry*, vol. 5, Part 2, New York, American Institute of Physics, 1982, 915-922.
30. R. P. Reed, Ya can't calibrate a thermocouple junction! *Measurements & Control*, Part 1. *Why not?*, 178, 137–145; Part 2. *So What?*, 179, 93–100, 1996.

31. R. P. Reed, Thermocouples: calibration, traceability, instability, and inhomogeneity, *Isotech J. Thermometry*, 7(2), 91-114, 1996.
32. W. F. Roeser, Thermoelectric thermometry, *J. Appl. Phys.*, 11, 213-232, 1940.
33. R. P. Reed, Thermoelectric inhomogeneity testing. Part I: Principles; Part II: Advanced methods, in J. F. Schooley (ed.), *Temperature, Its Measurement and Control in Science and Industry*, Vol. 6, Part 1, New York, American Institute of Physics, 1992, 519-530.
34. W. Rosch, A. Fripp, W. Debnun, S. Sorokach, and R. Simchick, Damage of fine diameter platinum sheathed Type R thermocouples at temperatures between 950 and 1100°C, in J. F. Schooley (ed.), *Temperature, Its Measurement and Control in Science and Industry*, Vol. 6, Part 1, New York, American Institute of Physics, 1992, 569-574.
35. R. P. Reed, Validation diagnostics for defective thermocouple circuits, in J. F. Schooley (ed.), *Temperature, Its Measurement and Control in Science and Industry*, 5, Part 2, New York, American Institute of Physics, 1982, 915-922.
36. *Survey, Measurement Needs Tracking Study — 1997*, Keithley Instruments, Cleveland, OH, 1997.
37. J. P. Tavener, Temperature calibration, *Measurements and Control*, Sept., 160-164, 1986.
38. T. B. Fisher, Selecting a dry well calibrator, *Measurements and Control*, (185), 105, 1997.
39. *Catalog, Reference Manual for Temperature Products and Services*, 1st ed., Isothermal Technology Ltd., Merseyside, England, 1997.
40. *Catalog*, Moore Industries, Sepulveda, CA, 1997.
41. *Catalog*, DCC Corporation, Pennsauken, NJ, 1997.
42. *Catalog, Instrumentation Reference and Catalogue*, National Instruments, Austin, TX, 1997.
43. *Catalog, Temperature Sensors, Wire and Cable*, Watlow Gordon, Richmond, IL, 1997.
44. *Catalog*, ENCOM Radio Services, Calgary, Alberta, Canada.
45. *Isotech Journal of Thermometry*, ISSN 0968-347X, Isothermal Technology, Ltd., Merseyside, England.
46. *Measurements and Control* magazine, ISSN 0148-0057, Measurements & Data Corporation, Pittsburgh, PA.
47. R. P. Reed, A comparison of programs that convert thermocouple properties to the 1990 international temperature and voltage scales, *Measurements and Control*, 30(177), 105-109, 1996.

\* *Note*: Mention of *representative* products is to introduce the reader to the variety of available thermocouple-related hardware and is not an endorsement.

## 32.5 Semiconductor Junction Thermometers

---

*Randy Frank*

Temperature sensors can be easily produced with semiconductor processing technology by using the temperature characteristics of the *pn junction*. The batch processing and well-defined manufacturing processes associated with semiconductor technology can provide low cost and consistent quality temperature sensors. The temperature sensitivity of the *pn junction* is part of the transistor's defining equations and is quite predictable over the typical semiconductor operating range of  $-55^{\circ}\text{C}$  to  $+150^{\circ}\text{C}$ .

Most semiconductor junction temperature sensors use a diode-connected bipolar transistor (short-circuited collector-base junction) [1]. A constant current passed through the base-emitter junction produces a junction voltage between the base and emitter ( $V_{be}$ ) that is a linear function of the absolute temperature (Figure 32.32). The overall forward voltage drop has a temperature coefficient of approximately  $2\text{ mV }^{\circ}\text{C}^{-1}$ .

When compared to a thermocouple or a resistive temperature device (RTD), the temperature coefficient of a semiconductor sensor is larger but still quite small. Also, the semiconductor sensor's forward voltage has an offset that varies significantly from unit to unit. However, the semiconductor junction voltage vs. temperature is much more linear than that of a thermocouple or RTD. In addition to the

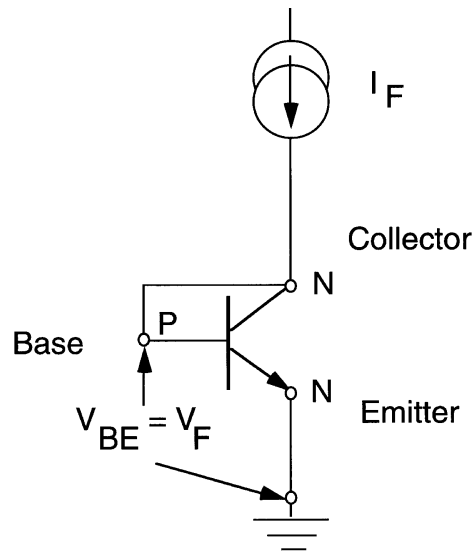


**FIGURE 32.32** Bipolar transistor configured as a temperature sensor. The base of the transistor is shorted to the collector. A constant current flowing in the remaining *pn* (base to emitter) junction produces a forward voltage drop  $V_F$  proportional to temperature.

temperature-sensing element, circuitry is easily integrated to produce a monolithic temperature sensor with an output that can be easily interfaced to a microcontroller and to provide features that are useful in specific applications. For example, by using an *embedded temperature sensor* with additional circuitry, protection features can be added to integrated circuits (ICs). A temperature sensor becomes an embedded item in a semiconductor product when it has a secondary or supplemental purpose instead of the primary function.

### The Transistor as a Temperature Sensor

A common semiconductor product for temperature sensing is a small-signal transistor such as a 2N2222 or a 2N3904. By selecting a narrow portion of the overall distribution of the  $V_{be}$  for these devices, a temperature sensor with a lower variation in characteristics can be obtained. The lower variation can provide a part-for-part replacement when a tolerance of only a few percent is acceptable. This device (formerly offered as an MTS102 but no longer in production) demonstrates the performance characteristics of the transistor used as a temperature sensor [2].

As shown in [Figure 32.33](#) [2], a silicon temperature sensor has a nominal output of 730 mV at  $-40^\circ\text{C}$  and an output of 300 mV at  $150^\circ\text{C}$ . The narrowly specified  $V_{be}$  ranges between 580 mV and 620 mV at  $25^\circ\text{C}$ . The linearity error, or variation from a straight line, of this device is shown in [Figure 32.34](#) [2]. The total accuracy is within  $\pm 3.0$  mV including nonlinearity which is typically within  $\pm 1^\circ\text{C}$  in the range of  $-40^\circ\text{C}$  to  $150^\circ\text{C}$ . These readings are made with a constant (collector) current of 0.1 mA, passing through the device to minimize the effect of self-heating of the junction. When the constant current applied is larger than 0.1 mA, the effect of self-heating in the device must be taken into account. The variation of the  $V_{be}$  with current is shown in [Figure 32.35](#) [2].

### Thermal Properties of Semiconductors: Defining Equations

A constant forward current supplied through an ideal silicon *pn* junction produces a forward voltage drop,  $V_F$  [3, 4]:

$$V_F = V_{be} = \left( \frac{kT}{q} \right) \ln \left( \frac{I_F}{I_S} \right) \quad (32.86)$$

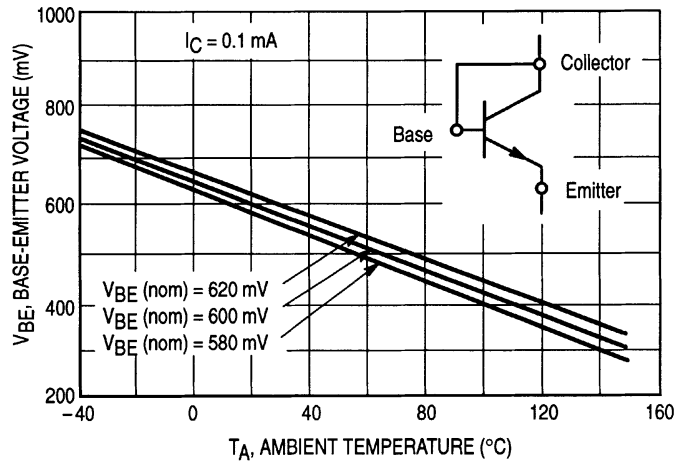


FIGURE 32.33 Base-emitter voltage vs. ambient temperature for a silicon temperature sensor.

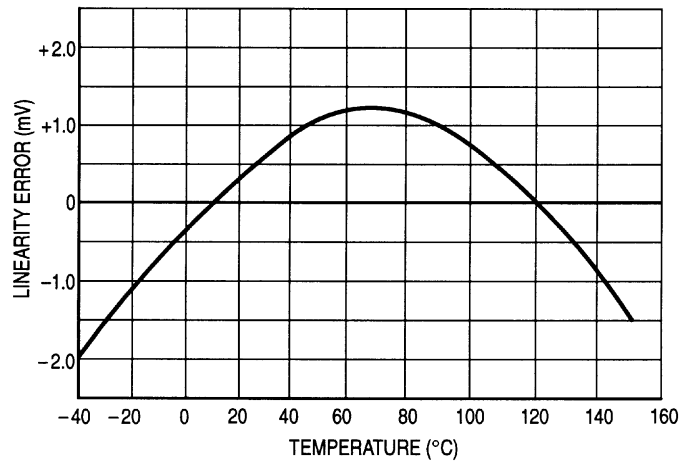


FIGURE 32.34 Linearity error (in mV) vs. temperature for a silicon temperature sensor.

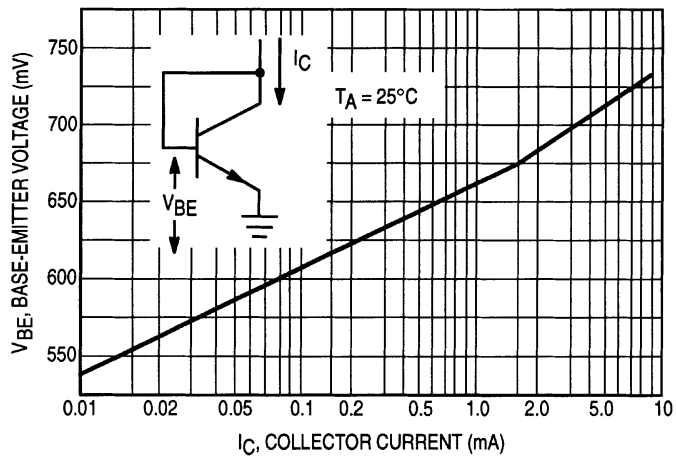


FIGURE 32.35 Base-emitter voltage vs. collector-emitter current.

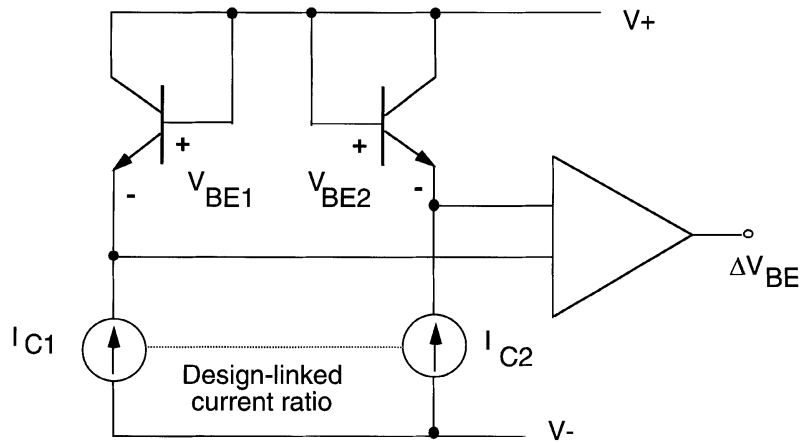


FIGURE 32.36 Differential pair formed by two *pn* junctions. The transistors are diode connected to form a temperature sensor independent of variations in source current.

where  $k$  = Boltzmann's constant ( $1.38 \times 10^{-23}$  J K<sup>-1</sup>)  
 $T$  = Temperature (K)  
 $q$  = Charge of electron ( $1.6 \times 10^{-19}$  C)  
 $I_F$  = Forward current (A)  
 $I_S$  = Junction's reverse saturation current (A)

For constant  $I_S$ , the **junction voltage** ( $V_{be}$ ) would be directly proportional to absolute temperature. Unfortunately,  $I_S$  is temperature dependent and varies with the cube of absolute temperature. As a result,  $V_F$  has an overall temperature coefficient of approximately  $-2\text{mV } ^\circ\text{C}^{-1}$ .

To reduce the temperature variation, a **band gap reference** is formed based on two adjacent and essentially identical-behavior transistors with proportional emitter area designed in an integrated circuit process. The two base-emitter junctions are biased with different current densities ( $I/A$ ), but the ratio of current densities is essentially constant over the operating temperature range ( $-55^\circ\text{C}$  to  $+150^\circ\text{C}$ ). The following equation shows how the differential voltage ( $\Delta V_{be}$ ) is related to the current ( $I$ ) and emitter area ( $A$ ) of the respective transistors:

$$V_{be1} - V_{be2} = \Delta V_{be} = \left( \frac{kT}{q} \right) \ln \left( \frac{I_1/A_1}{I_2/A_2} \right) \quad (32.87)$$

The differential voltage appearing at the output can be amplified as shown in Figure 32.36 and used as a direct indication of absolute temperature. Additional circuitry can eliminate the offset voltage at  $0^\circ\text{C}$  and provide an output in degrees Celsius or degrees Fahrenheit.

The ability to obtain temperature sensing using semiconductor processing techniques has two significant consequences: (1) semiconductor processing and integrated circuit design can be used to improve the temperature sensor's performance for specific applications, and (2) temperature sensors can be integrated within other integrated circuits to obtain additional features. The next two sections explain these approaches.

## Integrated Temperature Sensors

Once a temperature sensor can be manufactured using semiconductor processing techniques, a number of shortcomings of the sensor can be corrected by additional circuitry integrated into the sensor or by using circuit techniques external to the sensor. The linearity improvement, addition of precision voltage references, precision voltage amplifiers, and digital output for direct interface to a microcontroller (MCU)

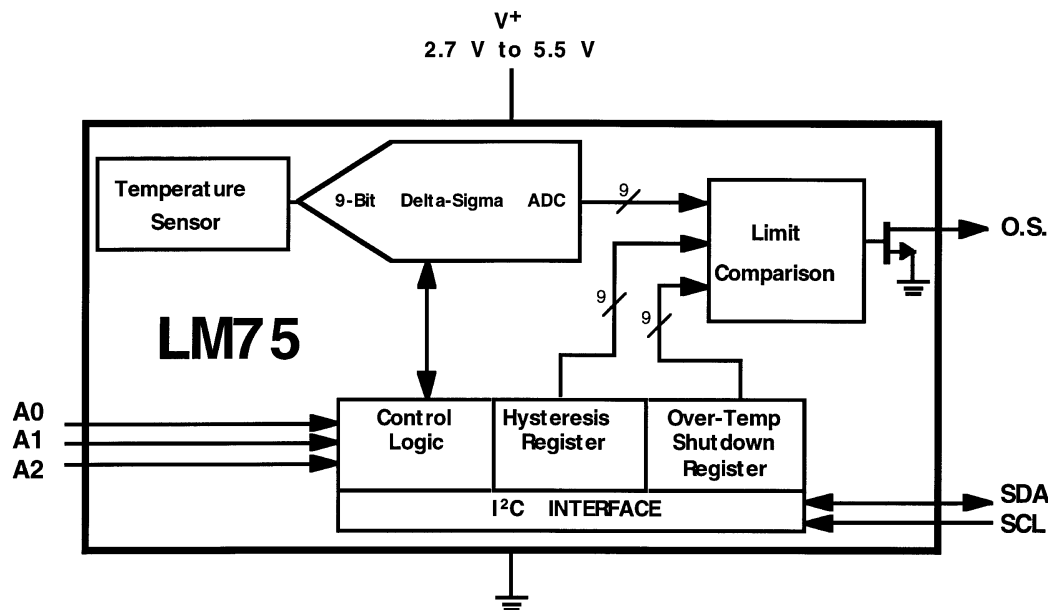


FIGURE 32.37 Block diagram of a monolithic digital-output temperature sensor. (Courtesy National Semiconductor Corp.)

are among the enhancements possible. Furthermore, resistance-measuring circuitry (i.e., RTD sensors) or cold junction compensation (i.e., thermocouple sensors) are not required. Three integrated circuits and one external circuit example are discussed.

### Integrated Digital Temperature Sensor

A *monolithic* (one piece of silicon) semiconductor junction temperature sensor (LM75 from National Semiconductor) that incorporates several features, including a digital output, is shown in Figure 32.37 [3]. The analog signal of the temperature sensor is converted to digital format by an on-board sigma–delta converter [3]. Digital communication is provided directly to a host microcontroller through a serial two-wire interface. The sensor has a software-programmable setpoint that can be used to terminate the operation of the controller or implementing protection [5]. To avoid false triggering, a user-programmable number of comparisons (up to six successive over-temperature occurrences) can be implemented.

Eight different sensors can be operated on the bus. Resolution is  $\pm 1/2^\circ\text{C}$  and the accuracy is  $\pm 2\%$  from  $-25^\circ\text{C}$  to  $+100^\circ\text{C}$ . The sensor consumes  $250\ \mu\text{A}$  during operation and only  $10\ \mu\text{A}$  in sleep mode.

### Analog Output Integrated Temperature Sensor

Another approach to integrated temperature sensing is shown in Figure 32.38 [4]. The TMP-1 resistor-programmable temperature controller features a  $5\text{-mV } ^\circ\text{C}^{-1}$  output high and low set points and over- and under-temperature output. A low-drift voltage reference is also included in the  $70\ \text{mil} \times 78\ \text{mil}$  ( $2.76\ \text{mm} \times 3.07\ \text{mm}$ ) design. Figure 32.39 shows a photomicrograph of the silicon die. The TMP-1 is specified for operation between  $-55^\circ\text{C}$  and  $+125^\circ\text{C}$ , with  $\pm 1^\circ\text{C}$  accuracy over the entire range.

### Digital Output Temperature Sensor

A direct-to-digital temperature sensor has been designed for multi-drop temperature sensing applications [6]. A unique serial number is etched onto each device. The 64-bit read-only memory (ROM) identifies the temperature of a particular sensor in a measurement system, with several sensors providing readings from different locations. The signal can be transmitted for distances up to 300 m.

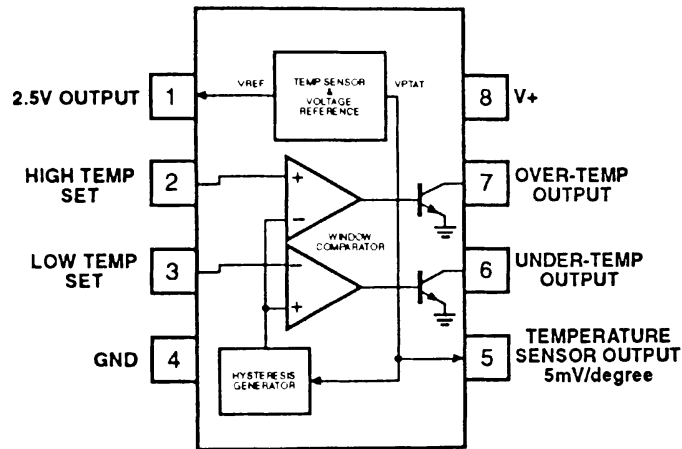


FIGURE 32.38 Block diagram and pinout of TMP-1 monolithic, programmable temperature controller. (Courtesy of Analog Devices, Inc.)

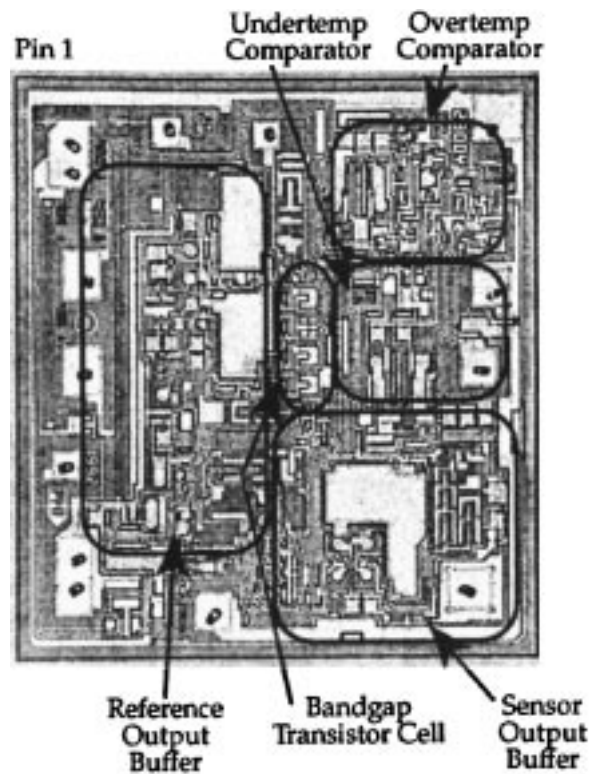
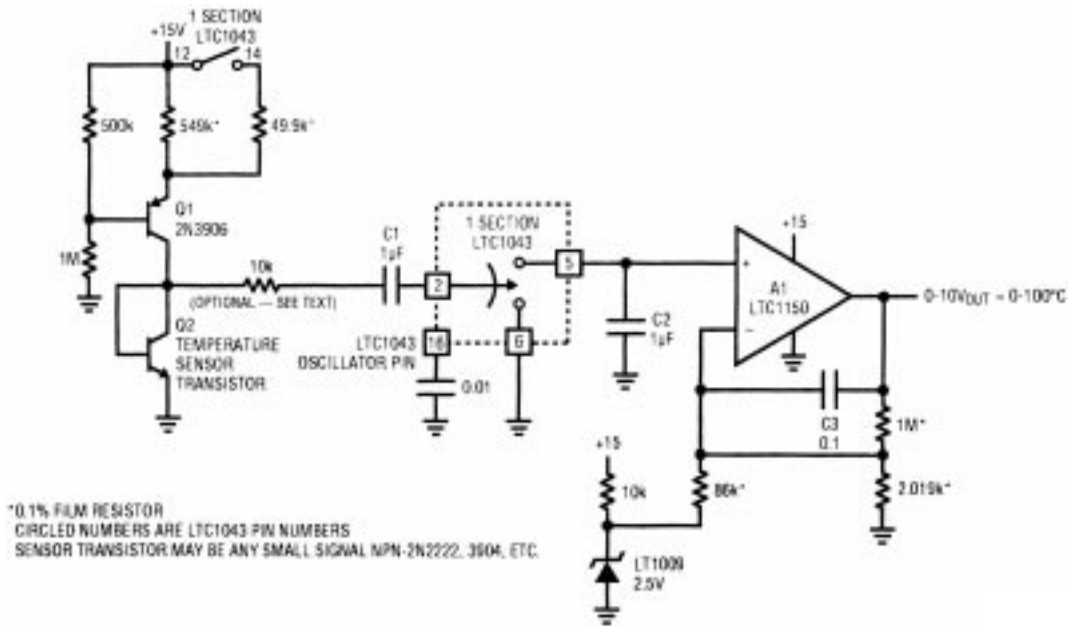


FIGURE 32.39 Detail of TMP-1 die. Note the relative size of the bandgap transistor cell to the other circuitry included in the monolithic device. (Courtesy of Analog Devices, Inc.)

The temperature sensor operates from  $-55^{\circ}\text{C}$  to  $125^{\circ}\text{C}$  with the power supplied from the data line. The measurement is resolved in  $0.5^{\circ}\text{C}$  increments as a 9-bit digital value, with the conversion occurring within 200 ms. User-definable alarm settings are included in the device.



**FIGURE 32.40** External circuitry provides  $\Delta V_{be}$ -based thermometer that does not require calibration. (Courtesy of Linear Technologies Corporation.)

### External Circuitry Eliminates Calibration

External circuitry can be designed to utilize the inherent sensing capability of low-cost transistors without incurring the additional cost of integrated circuitry or the need to calibrate each device. The circuit shown in [Figure 32.40](#) uses an integrated circuit (LTC1043 from Linear Technology Corporation) to provide a 0 V to 10 V output from 0°C to 100°C, with an accuracy of  $\pm 1^\circ\text{C}$  using any common small signal transistor as the temperature sensor [7]. The circuitry establishes a  $\Delta V_{be}$  vs. current relationship that is constant regardless of the  $V_{be}$  diode's absolute value. Substituting different transistors from multiple sources showed a variation of less than  $0.4^\circ\text{C}$ .

### Other Applications of Semiconductor Sensing Techniques

Several semiconductor parameters vary linearly over the operating temperature range. Power MOSFETs used to switch high levels of current (typically several amperes) at voltages that can exceed 500 V provide an example of these characteristics. As shown in [Figure 32.41](#) [8], the gate threshold voltage of a power MOSFET changes from 1.17 to 0.65 times its  $25^\circ\text{C}$  value when the temperature increases from  $-40^\circ\text{C}$  to  $150^\circ\text{C}$ . Also, the breakdown voltage of the power MOSFET varies from 0.9 to 1.18 times its value at  $25^\circ\text{C}$  over the same temperature range ([Figure 32.42](#)) [8]. These relationships are frequently used to determine the junction temperature of a semiconductor component in actual circuit operation during the design phase (see "Reliability Implications"). External package level temperature measurements can be many degrees lower than the junction temperature, especially during rapid, high-energy switching events. The actual junction temperature and the resulting effect on semiconductor parameters must be taken into account for the proper application of semiconductor devices.

Polysilicon diodes (and resistors) that are isolated from the power MOSFET can be produced as part of the semiconductor manufacturing process with minor process modifications. The diodes can be used as temperature sensing elements in an actual application [9]. The thermal sensing that is performed by the polysilicon elements is a significant improvement over power device temperature sensing that is performed by an external temperature sensing element. By sensing with polysilicon diodes, the sensor can be located close to the center of the power device near the source bond pads where the current

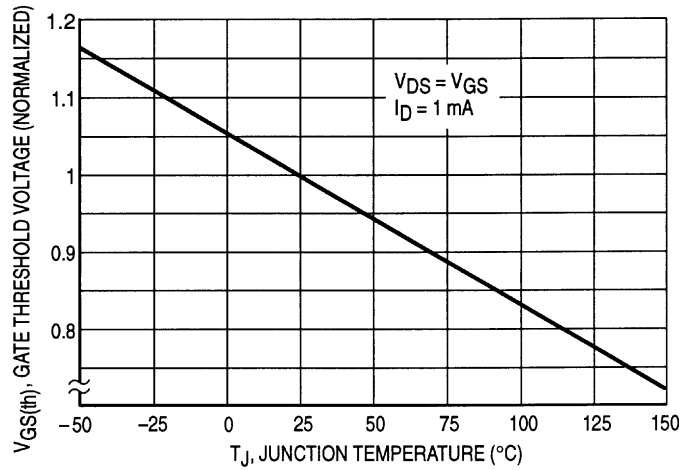


FIGURE 32.41 Power MOSFET's gate threshold variation vs. temperature.

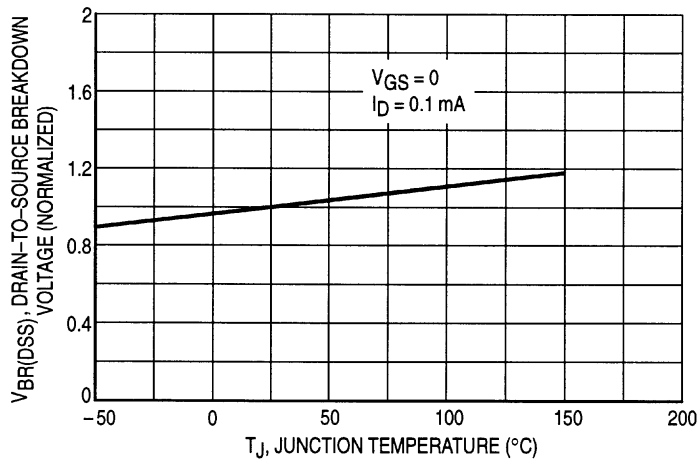
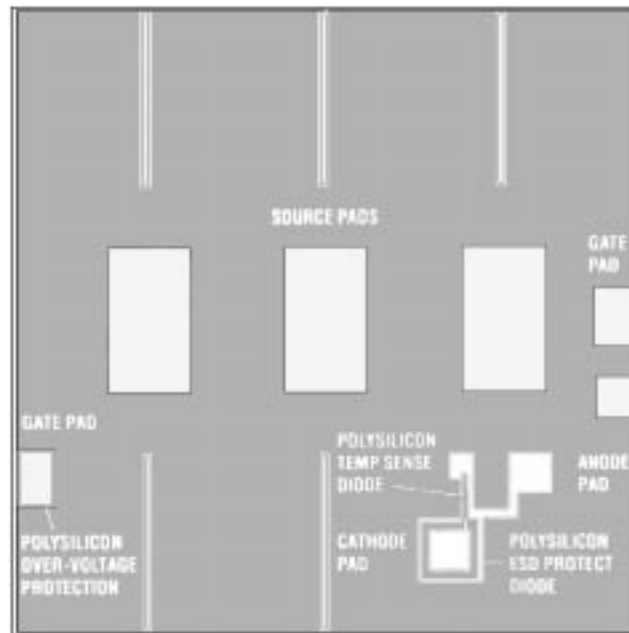


FIGURE 32.42 Power MOSFET's breakdown voltage variation vs. temperature.

density is the highest and, consequently, the highest die temperature occurs. The thermal conductivity of the oxide that separates the polysilicon diodes from the power device is 2 orders of magnitude less than that of silicon. However, because the layer is thin, the polysilicon element offers an accurate indication of the actual peak junction temperature.

A power FET that incorporates temperature sensing diodes is shown in Figure 32.43 [9]. By monitoring the output voltage when a constant current is passed through the integrated polysilicon diode(s), an accurate indication of the maximum die temperature is obtained. A number of diodes are actually provided in the design. A single diode in this design has a temperature coefficient of  $1.90 \text{ mV } ^\circ\text{C}^{-1}$ . Two or more can be placed in series if a larger output is desired. For greater accuracy, the diodes can be trimmed during wafer-level testing by blowing fusible links made from polysilicon. The response time of the diodes is less than  $100 \mu\text{s}$ , which has allowed the device to withstand a direct connection across an automobile battery with external circuitry providing shutdown prior to device failure. The sensing capability also allows the output device to provide an indication (with additional external circuitry) if the heatsinking is not proper when the unit is installed in a module or if a change occurs in the application that would ultimately cause a failure.



**FIGURE 32.43** Photomicrograph of temperature sensor integrated in power MOSFET. Note the relative size of the temperature sensor compared to the total area of the power MOSFET and the source pads which allow attachment of 15 mil (0.60 mm) aluminum wire. (Courtesy of Motorola, Inc.)

## Temperature Sensing in Power ICs for Fault Protection and Diagnostics

Sensing for fault conditions, such as a short-circuit, is an integral part of many smart power (or power) ICs. The ability to obtain temperature sensors in the semiconductor process provides protection and diagnostics as part of the features of these devices. The primary function of the power IC is to provide a microcontroller-to-load interface for a variety of loads. In multiple output devices, sensing the junction temperature of each device allows the status of each device to be provided to the microcontroller (MCU), and, if necessary, the MCU can shut down a particular unit that has a fault condition.

A *smart power IC* can have multiple power drivers integrated on a single monolithic piece of silicon [10]. Each of these drivers can have a temperature sensor integrated to determine the proper operating status and shut off only a specific driver if a fault occurs. Figure 32.44 shows an eight-output driver that independently shuts down the output of a particular driver if its temperature is excessive (i.e., between 155°C and 185°C) [10].

The octal serial switch (OSS) adds independent thermal sensing through over-temperature detection circuitry to the protection features. Faults can be detected for each output device, and individual shut-down can be implemented. In a multiple output power IC, it is highly desirable to shut down only the device that is experiencing a fault condition and not all of the devices that are integrated on the power IC. With outputs in various physical locations on the chip, it is difficult to predict the thermal gradients that could occur in a fault situation. Local temperature sensing at each output, instead of a single global temperature sensor, is required.

As shown in Figure 32.45, the eight outputs of the device with individual temperature sensors can be independently shut down when the thermal limit of 170°C is exceeded [10]. All of the outputs were connected to a 16-V supply at a room temperature ambient. A total current of almost 30 A initially flowed through the device. Note that each device turns off independently. The hottest device turns off first. Variations can result from differences in current level and thermal resistance. As each device turns off, the total power dissipation in the chip decreases and the devices that are still on can dissipate heat more effectively.

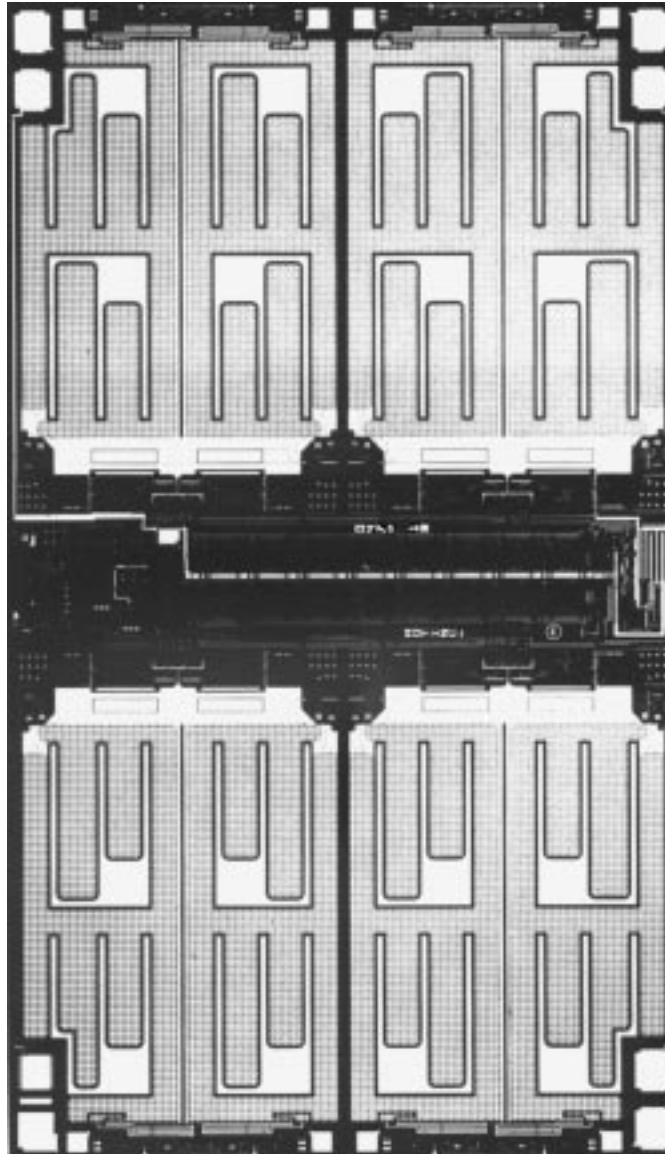


**FIGURE 32.44** Photomicrograph of eight-output power IC. Note that the area of the eight output devices (two located at each corner of the die) are considerably larger than the circuitry in the center, and top and bottom that provides the temperature sensing, signal conditioning, and other control features. (Courtesy of Motorola, Inc.)

Connecting directly to the battery is a hard short that could have been detected by current limit circuitry. However, a soft short is below the current limit, but exceeds the power-dissipating capability of the chip, and can be an extremely difficult condition to detect. Soft shorts require over-temperature sensing to protect the IC from destructive temperature levels.

The over-temperature condition sensed by the power IC could mean that the device turns itself off to prevent failure in one case; and in another situation, a fault signal provides a warning to the MCU but no action is taken, depending on the fault circuit design. The remaining portion of the system is allowed to function normally. With the fault conditions supplied to the MCU, an orderly system shutdown can be implemented. Integrated temperature sensing is essential to provide this type of protection in a multiple-output power IC.

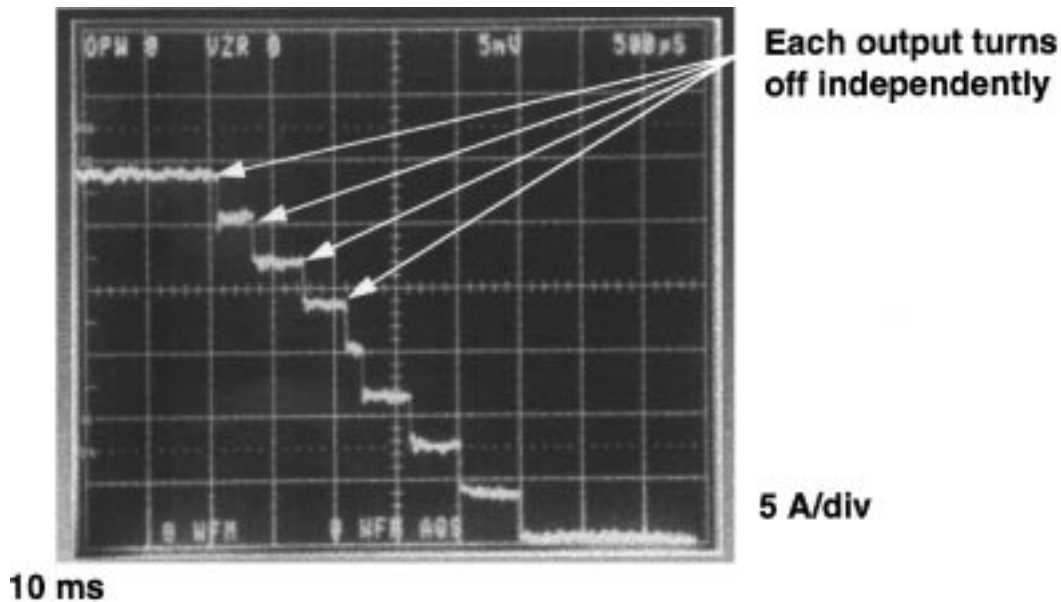


FIGURE 32.45 Independent thermal shutdown of an 8-output power IC. (Courtesy of Motorola, Inc.)

## Reliability Implications of Temperature to Electronic Components

The effect of temperature on electronic components and their successful application in electronic systems is one of the issues that must be addressed during the design of the system. Temperature affects the performance and expected life of semiconductor components. Mechanical stress created by different coefficients of thermal expansion can cause failures in thermal cycling tests (air-to-air) or during thermal shock (water-to-water) transitions.

The typical failure rate for semiconductor component can be expressed by the Arrhenius equation [9]:

$$\lambda = A e^{-\phi/KT} \quad (32.88)$$

where  $\lambda$  = Failure rate

$A$  = Constant

$\phi$  = Activation energy (eV)

$K$  = Boltzmann's constant ( $8.62 \times 10^{-5}$  eV  $K^{-1}$ )

$T$  = Junction temperature (K)

The failure rate of semiconductor components is typically stated to double for every 10 to 15°C increase in operating (i.e., junction) temperature. However, increased testing and design improvements have minimized the failures due to specific failure mechanisms.

One of the temperature-related parameters that must be taken into account during the design phase of a power switch is the transient thermal response, which is designated as  $r(t) R_{\theta_{JC}}$ , where  $r(t)$  represents the normalized transient thermal resistance. The value of  $r(t)$  is determined from the semiconductor manufacturer's data sheet using duty cycle and pulse duration used in the application. This reduced level of the thermal resistance (see "Junction Temperature Measurement"), based on the transistor operating in a switching mode and being off for a period of time, approaches the dc level within a second. Excessive temperatures can be generated quickly and must be detected within milliseconds to prevent failure.

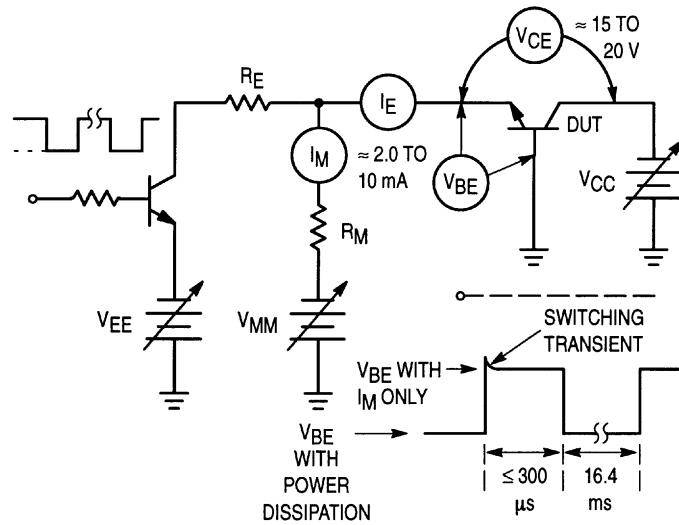


**FIGURE 32.46** Example of steady-state thermal resistance test circuit for a bipolar power transistor. Power is applied for 16.4 ms and interrupted for  $\leq 300 \mu\text{s}$  to measure the  $V_{\text{BE}}$ .

### Junction Temperature Measurement

In a semiconductor, the change in temperature is directly related to the power dissipated through the [thermal resistance](#). The steady-state dc thermal resistance junction-to-case,  $R_{\theta_{\text{JC}}}$ , is defined as the temperature rise per unit power above an external reference point (typically the case). The relationship is shown in Equation 32.89 [8].

$$R_{\theta_{\text{JC}}} = \Delta T / P_{\text{D}} \quad (32.89)$$

where  $\Delta T$  = Junction temperature minus the case temperature ( $^{\circ}\text{C}$ )

$P_{\text{D}}$  = Power dissipated in the junction (W)

The semiconductor device or silicon die is typically enclosed in a package that prevents a direct measurement of the junction temperature. The junction temperature is measured indirectly by measuring the case temperature,  $T_{\text{C}}$ ; the heatsink temperature,  $T_{\text{S}}$ ; for those higher-power applications that require a heatsink; the ambient temperature,  $T_{\text{A}}$ ; and a temperature-sensitive electrical parameter of the device.

The first step of the process requires calibrating the temperature-sensitive parameter. Using a bipolar power transistor as an example, the base-emitter forward voltage is measured and recorded with a low calibration current ( $I_{\text{M}}$ ) flowing through the device that is low enough to avoid [self-heating](#) (typically between 2 mA and 10 mA) and yet sufficiently high to be in the linear range of the forward voltage curve. The procedure is performed at room and elevated temperatures, typically  $100^{\circ}\text{C}$ .

After calibration, a power switching fixture (such as [Figure 32.46](#)) is used to alternately apply and interrupt the power to the device [8]. The on portion is long (typically several milliseconds) and the off portion is short (only a few  $100 \mu\text{s}$ ), so the temperature of the case is stabilized and junction cooling is minimal. The transistor is operated in its active region and the power dissipation is varied by adjusting the  $I_{\text{E}}$  and/or  $V_{\text{CE}}$  until the junction is at the calibration temperature. This point is known by measuring  $V_{\text{BE}}$  during the time that  $I_{\text{M}}$  is the only current flowing.

When the  $V_{\text{BE}}$  value equals the value on the calibration curve, the junction temperature is at the calibration temperature. Measurements of  $V_{\text{BE}}$ ,  $T_{\text{C}}$ , and  $I_{\text{E}}$  allow the thermal resistance for the device to

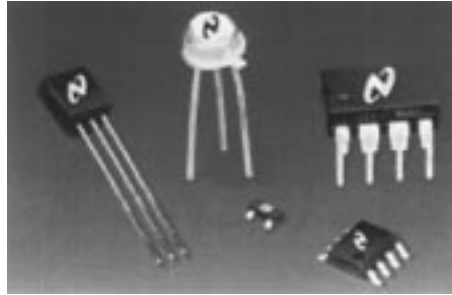


**FIGURE 32.47** Plastic TO-92, TO-99 metal can, 8-lead DIP, 8-lead SOIC, and TinyPak™ SOT-23 plastic packages. (Courtesy National Semiconductor Corp.)

be calculated using Equation 32.89. Since  $R_{\theta_{JC}}$  is a constant, subsequent measurements of  $T_C$ ,  $V_{CE}$ , and  $I_E$  under different operating conditions can be used to calculate the junction temperature to keep the device within its safe operating range in the actual application. For devices with different electrical characteristics, such as the power MOSFETs discussed earlier, other parameters that have a linear relationship to temperature are used for calibration and measurement.

## Semiconductor Temperature Sensor Packaging

Temperature sensors that are manufactured using semiconductor technology are typically packaged in packages common to the semiconductor industry. These include metal can (TO-99), ceramic, and more commonly available plastic (SOT-23, 8-lead DIP, TO-92, 8-lead SOIC, etc.) packages. These packages are designed for circuit board solder attachment that can be either through-hole or surface-mount technology. As a result, package form factors can be considerably different from packages for temperature sensors manufactured using other technologies. Figure 32.47 shows examples of five available silicon temperature sensor packages.

## Defining Terms

**Bandgap reference:** Forward-biased emitter junction characteristics of adjacent transistors used to provide an output voltage with zero temperature coefficient.

**Die:** An unpackaged semiconductor chip separated from the wafer.

**Embedded sensor:** A sensor included within an integrated circuit.

**Integrated circuit:** A multiplicity of transistors, as well as diodes, resistors, capacitors, etc., on the same silicon die.

**Junction:** The interface at which the conductivity type of a material changes from  $p$  type to  $n$  type.

**Junction voltage:** The voltage drop across a forward-biased  $pn$  interface in a transistor ( $V_{be}$ ) or diode.

**Junction temperature:** The temperature of the  $pn$  interface in a transistor or diode.

**Monolithic (integrated circuit):** Constructed from a single piece of silicon.

**Power IC or smart power IC:** Hybrid or monolithic (semiconductor) device that is capable of being conduction-cooled, performs signal conditioning, and includes a power control function such as fault management and/or diagnostics.

**Self-heating:** Temperature rise within a (semiconductor) device caused by current flowing in the device.

**Soft short:** An excessive load condition that causes excessive temperature but is below the current limit of a device.

**Thermal resistance:** The steady-state dc thermal resistance junction-to-case,  $R_{\theta_{JC}}$ , is the temperature rise per unit power above an external reference point (typically the case).

**TinyPak:** A trademark of National Semiconductor Corp.

## References

1. J. Carr, *Sensors and Circuits*, Englewood Cliffs, NJ, PTR Prentice-Hall, 1993.
2. *Pressure Sensor Device Data DL200/D Rev. 1*, Phoenix, AZ, Motorola, 1994.
3. K. Lacanette, "Silicon Temperature Sensors: Theory and Applications," *Measurements and Control*, pp. 120-126, April 1996.
4. R. Wegner and H. Hulsemann, "New Family of Monolithic Temperature Sensor and Controller Circuits Present Challenges In Maintaining Temperature Measurement Accuracy," *Proceedings of Sensors Expo West*, Anaheim, CA, Feb. 8-10, 1994.
5. W. Schweber, "Temperature sensors fill different needs," *EDN*, p. 20, 3/14/96.
6. "Digital Thermometer IC simplifies distributed sensing," *Electronic Products*, p. 56, 12/95.
7. J. Williams, "High Performance Signal Conditioning for Transducers," *Proceedings of Sensors Expo West*, San Jose, CA, March 2-4, 1993.
8. *TMOS Power MOSFET Transistor Data DL135/D Rev. 4*, Phoenix, AZ, Motorola Semiconductor.
9. R. K. Jurgen (ed.), *Automotive Electronics Handbook*, New York, McGraw-Hill, 1994.
10. R. Frank, *Understanding Smart Sensors*, Boston, MA, Artech House, 1995.

## 32.6 Infrared Thermometers

---

*Jacob Fraden*

### Thermal Radiation: Physical Laws

In any material object, every atom and every molecule exist in perpetual motion. When an atom moves, it collides with other atoms and transfers to them part of its kinetic energy, thus losing some of its own energy in this perpetual bouncing. On the other hand, an atom having a smaller kinetic energy, after a collision gains some energy. Afterward, the material body consisting of such agitated atoms reaches the energetic equilibrium where all atoms, while not vibrating with exactly the same intensity, still can be described by an average kinetic energy. Such an average kinetic energy of agitated particles is represented by the *absolute temperature*, which is measured in degrees kelvin. In other words, what is commonly called temperature, is a measure of the atomic motion.

According to the laws of electrodynamics, a moving electric charge (all atoms are made of electric charges) is associated with a variable electric field. The field, in turn, produces an alternating magnetic field. And again, when the magnetic field changes, it results in a coupled with it variable electric field, and so on. Thus, a moving particle becomes a source of electromagnetic field that propagates outwardly with the speed of light and is called *thermal radiation*. This radiation is governed by the laws of optics — it can be reflected, filtered, focused, etc. Also, it can be used to measure the object's temperature.

Electromagnetic waves originating from mechanical movement of particles can be characterized by their intensities and wavelengths. Both of these characteristics relate to temperature; that is, the hotter the object, the shorter the wavelength. Very hot objects radiate electromagnetic energy in the visible portion of the spectrum — wavelengths between 0.4  $\mu\text{m}$  (blue) and 0.7  $\mu\text{m}$  (red). For example, a filament in an incandescent lamp is so hot that it radiates bright visible light. If such a lamp is controlled by a dimmer, the light intensity can be reduced by turning the knob and observing that the dimmed light becomes more yellowish, reddish, and finally disappears. Near the end of the dimmer control, the filament is still quite hot, yet one cannot see it because it emanates light in the invisible infrared spectral range — wavelengths greater than 0.8  $\mu\text{m}$ . Cooler objects radiate light in the near-, mid-, and far-infrared spectral ranges, which one cannot see. For example, electromagnetic radiation emanating from human skin primarily is situated at wavelengths between 5  $\mu\text{m}$  and 15  $\mu\text{m}$  — in the mid- and far-infrared ranges and is not visible to human eyes; otherwise, we all would glow in the dark (sick people with fever would look even brighter). If one imagines that all atomic vibration stopped for some mysterious reason, no electromagnetic

radiation would be emanated. Such an imaginable but impossible event is characterized by infinitely cold temperature, which is called *absolute zero*.

Because temperature is a measure of the average atomic kinetic energy, it is logical to assume that one can determine the object's temperature by measuring the intensity of the emanated electromagnetic radiation or its spectral characteristics. This presumption is the basis for noncontact temperature measurements that are known by various names, depending on the application: infrared thermometry, optical pyrometry, radiation thermometry, etc. *Pyrometry* is derived from the Greek word *pyr*, which means fire, and thus is more appropriate for measuring hot temperatures. For lower temperatures, *infrared thermometry* is used interchangeably with term *radiation thermometry*.

### Planck's Law

A relationship between the magnitude of radiation at a particular wavelength  $\lambda$  and absolute temperature  $T$  is rather complex and is governed by Planck's law, which was discovered in 1901. It establishes radiant flux density  $W_\lambda$  as power of electromagnetic radiation per unit of wavelength:

$$W_\lambda = \frac{\epsilon(\lambda)C_1}{\pi\lambda^5 \left( e^{C_2/\lambda T} - 1 \right)} \quad (32.90)$$

where  $\epsilon(\lambda)$  = Emissivity of an object

$C_1 = 3.74 \times 10^{-12} \text{ Wcm}^2$  and  $C_2 = 1.44 \text{ cmK}$  are Constants

$e$  = Base of natural logarithms

Spectral densities for different temperatures are shown in [Figure 32.48](#).

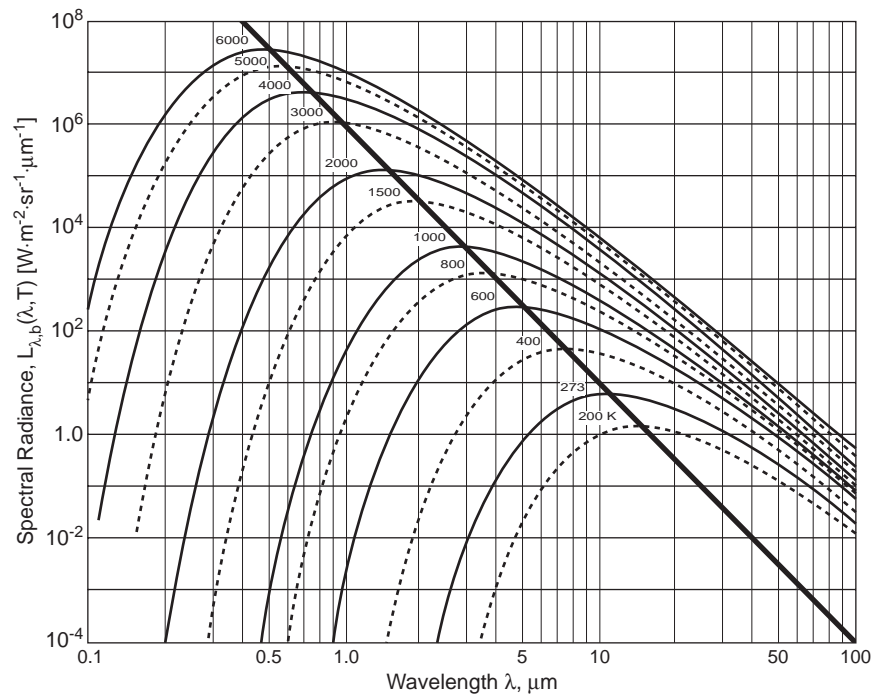


**FIGURE 32.48** Spectral densities calculated within a solid angle of 1 steradian for blackbody source ( $\epsilon = 1$ ) radiation toward infinitely cold space (at absolute zero).

### Wien's Law

Equation 32.90 does not lend itself to a simple mathematical analysis and thus is approximated by a simplified version, which is known as Wien's law:

$$W_{\lambda} = \frac{C_1}{\pi} \epsilon(\lambda) \lambda^{-5} e^{-\frac{C_2}{\lambda T}} \quad (32.91)$$

Because temperature is a statistical representation of an average kinetic energy, it determines the highest probability for the particles to vibrate with a specific frequency and to have a specific wavelength. This most probable wavelength follows from Wien's law by equating to zero a first derivative of Equation 32.91. The result of the calculation is a wavelength near which most of the radiant power is concentrated when light is emanated toward infinitely cold space at absolute zero:

$$\lambda_m = \frac{2898}{T} \quad (32.92)$$

where  $\lambda_m$  is in  $\mu\text{m}$  and  $T$  in kelvin. Wien's law states that the higher the temperature, the shorter the wavelength. This formula also defines the midpoint of spectral response of a pyrometer or infrared thermometer.

### Stefan-Boltzmann Law

Theoretically, a thermal radiation bandwidth is infinitely wide. Yet, most of the emanated power is situated within quite a limited bandwidth. Also, one must account for the filtering properties of the real world windows used in instruments. In order to determine the total radiated power limited within a particular bandwidth, Equation 32.90 or 32.91 must be integrated within the limits from  $\lambda_1$  to  $\lambda_2$ :

$$\Phi_{\text{bo}} = \frac{1}{\pi} \int_{\lambda_1}^{\lambda_2} \frac{\epsilon(\lambda) C_1 \lambda^{-5}}{e^{C_2/\lambda T} - 1} \quad (32.93)$$

This integral can be resolved only numerically or by approximation. For a narrow bandwidth ( $\lambda_1$  and  $\lambda_2$  are close to one another), the solution can be approximated by:

$$\Phi_{\text{bo}} = kT^x \quad (32.94)$$

where  $k$  is constant and  $x \approx (12/\lambda_2)(1200/T)$ . For example, in the visible portion of spectrum at  $\lambda_2 \approx 0.7 \mu\text{m}$  and for temperatures near 2000 K, the approximation is a 10<sup>th</sup>-order parabola. An approximation for a very broad bandwidth ( $\lambda_2 \rightarrow \infty$  or practically, when the range between  $\lambda_1$  and  $\lambda_2$  embrace well over 50% of the total radiated power) is a 4<sup>th</sup>-order parabola, which is known as the *Stefan-Boltzmann law*:

$$\Phi_{\text{bo}} = A\epsilon\sigma T^4 \quad (32.95)$$

where  $\sigma = 5.67 \times 10^{-8} \text{ W/m}^2\text{K}^4$  (Stefan-Boltzmann constant), and  $\epsilon$  is assumed to be wavelength independent. It is seen that with an increase in temperature, the intensity of electromagnetic radiation  $\Phi_{\text{bo}}$  grows very fast due to the 4<sup>th</sup> power of  $T$ .

### Kirchhoff's Law

While wavelengths of the radiated light are temperature dependent, the magnitude of radiation also is a function of the surface property. That property is called *emissivity*,  $\epsilon$ . Emissivity is measured on a scale

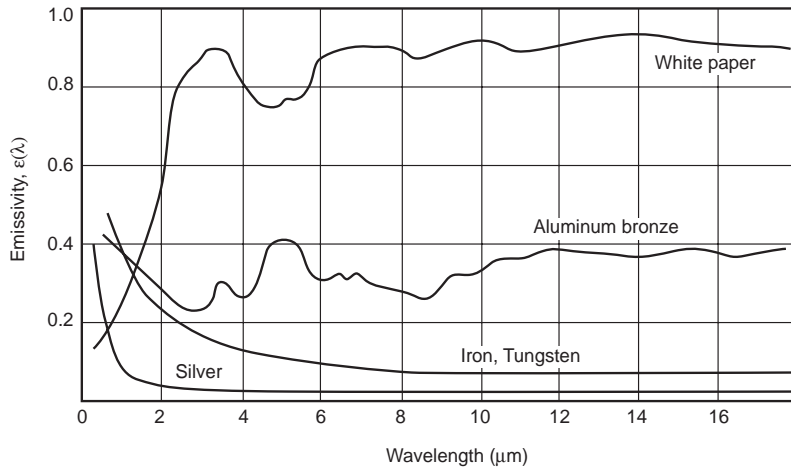


FIGURE 32.49 Wavelength dependence of emissivities.

from 0 to 1. It is a ratio of electromagnetic flux that is emanated from a surface to the flux that would be emanated from the ideal emitter having the same temperature. *Reflectivity*,  $\rho$ , and *transparency*,  $\gamma$ , also on a scale from 0 to 1, show what portion of incident light is reflected and passed through, respectively. There is a fundamental equation that connects these three characteristics:

$$\epsilon + \gamma + \rho = 1 \quad (32.96)$$

Equation (32.96) indicates that any one of the three properties of the material can be changed only at the expense of the others. As a result, for an opaque object ( $\gamma = 0$ ), reflectivity  $\rho$  and emissivity  $\epsilon$  are connected by a simple relationship:  $\rho = 1 - \epsilon$ , which, for example, makes a mirror a good reflector but a poor emitter.

## Emissivity

The emissivity of a material is a function of its dielectric constant and, subsequently, refractive index  $n$ . It should be noted, however, that emissivity is generally wavelength dependent (Figure 32.49). For example, a white sheet of paper is very much reflective in the visible spectral range and emits no visible light. In the far-infrared spectral range, its reflectivity is low and emissivity is high (about 0.92), thus making paper a good emitter of thermal radiation. However, for many practical purposes in infrared thermometry, emissivity can be considered constant.

For nonpolarized far-infrared light in normal direction, emissivity can be expressed by the equation:

$$\epsilon = \frac{4n}{(n+1)^2} \quad (32.97)$$

As a rule, emissivities of dielectrics are high and of metals are low. Due to the high emissivity of dielectrics, they lend themselves to easy and accurate noncontact temperature measurement. On the other hand, such measurements from nonoxidized metals are difficult, due to small amounts of emanated infrared flux. Table 32.17 gives typical emissivities of some opaque materials in a temperature range between 0°C and 100°C.

**TABLE 32.17** Typical Emissivities of Different Materials (from 0 to 100°C)

Material	Emissivity	Material	Emissivity
Blackbody (ideal)	1.00	Green leaves	0.88
Cavity radiator	0.99–1.00	Ice	0.96
Aluminum (anodized)	0.70	Iron or steel (rusted)	0.70
Aluminum (oxidized)	0.11	Nickel (oxidized)	0.40
Aluminum (polished)	0.05	Nickel (unoxidized)	0.04
Aluminum (rough surface)	0.06–0.07	Nichrome (80Ni-20Cr) (oxidized)	0.97
Asbestos	0.96	Nichrome (80Ni-20Cr) (polished)	0.87
Brass (dull tarnished)	0.61	Oil	0.80
Brass (polished)	0.05	Silicon	0.64
Brick	0.90	Silicone rubber	0.94
Bronze (polished)	0.10	Silver (polished)	0.02
Carbon-filled latex paint	0.96	Skin (human)	0.93–0.96
Carbon lamp black	0.96	Snow	0.85
Chromium (polished)	0.10	Soil	0.90
Copper (oxidized)	0.6–0.7	Stainless steel (buffed)	0.20
Copper (polished)	0.02	Steel (flat rough surface)	0.95–0.98
Cotton cloth	0.80	Steel (ground)	0.56
Epoxy resin	0.95	Tin plate	0.10
Glass	0.95	Water	0.96
Gold	0.02	White paper	0.92
Gold-black	0.98–0.99	Wood	0.93
Graphite	0.7–0.8	Zinc (polished)	0.04

Unlike most solid bodies, gases in many cases are transparent to thermal radiation. When they absorb and emit radiation, they usually do so only in certain narrow spectral bands. Some gases, such as N<sub>2</sub>, O<sub>2</sub>, and others of nonpolar symmetrical molecular structure, are essentially transparent at low temperatures, while CO<sub>2</sub>, H<sub>2</sub>O, and various hydrocarbon gases radiate and absorb to an appreciable extent. When infrared light enters a layer of gas, its absorption has an exponential decay profile, governed by *Beer's law*:

$$\frac{\Phi_x}{\Phi_0} = e^{-\alpha_\lambda x} \quad (32.98)$$

where  $\Phi_0$  = Incident thermal flux  
 $\Phi_x$  = Flux at thickness x  
 $\alpha_\lambda$  = Spectral coefficient of absorption

The above ratio is called a monochromatic transmissivity  $\gamma_\lambda$  at a specific wavelength  $\lambda$ . If gas is nonreflecting, then its emissivity is defined as:

$$\epsilon_\lambda = 1 - \gamma_\lambda = 1 - e^{-\alpha_\lambda x} \quad (32.99)$$

It should be emphasized that since gases absorb only in narrow bands, emissivity and transmissivity (transparency) must be specified separately for any particular wavelength. For example, water vapor is highly absorptive at wavelengths of 1.4, 1.8, and 2.7  $\mu\text{m}$ , and is very transparent at 1.6, 2.2, and 4  $\mu\text{m}$ .

All non-metals are very good diffusive emitters of thermal radiation with a remarkably constant emissivity defined by Equation 32.97 within a solid angle of about  $\pm 70^\circ$ . Beyond that angle, emissivity begins to decrease rapidly to zero with the angle approaching  $90^\circ$ . Near  $90^\circ$ , emissivity is very low. A typical calculated graph of the directional emissivity of non-metals into air is shown in [Figure 32.50A](#). It should be emphasized that the above considerations are applicable only to wavelengths in the far

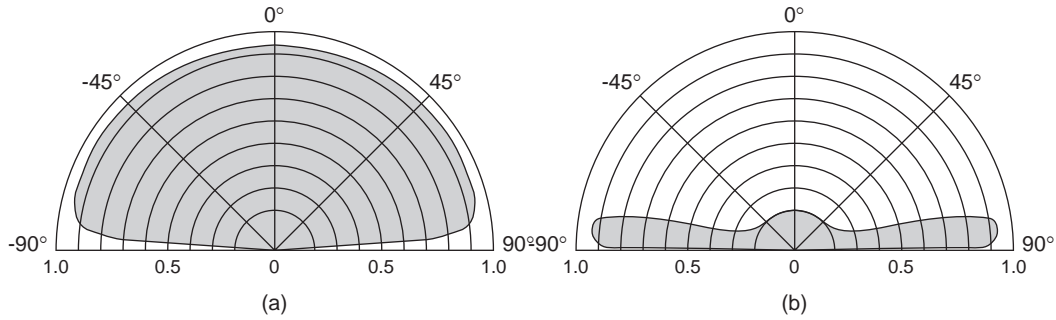


FIGURE 32.50 Spatial emissivities for non-metal (A) and a polished metal (B).

infrared spectral range and are not true for visible light, since emissivity of thermal radiation is a result of electromagnetic effects that occur at an appreciable depth.

Metals behave quite differently. Their emissivities greatly depend on surface finish. Generally, polished metals are poor emitters within the solid angle of  $\pm 70^\circ$ , while their emissivity increases at larger angles (Figure 32.50B). Oxidized metals start behaving more and more like dielectrics with increasing thickness of oxides.

## Blackbody

By definition, the highest possible emissivity is unity. It is attributed to the so-called blackbody — an ideal emitter of electromagnetic radiation. If the object is opaque ( $\gamma = 0$ ) and nonreflective ( $\rho = 0$ ) according to Equation 32.96, it becomes an ideal emitter and absorber of electromagnetic radiation. The name blackbody implies its appearance at normal room temperatures — indeed, it does look black because it is not transparent and not reflective at any wavelength. In reality, a blackbody does not exist, and any object with a nonunity emissivity often is called a *graybody*. A practical blackbody ( $\epsilon$  is about 0.99 or higher) is an essential tool for calibrating and verifying the accuracy of infrared thermometers.

## Cavity Effect

To make a practical blackbody, a cavity effect is put to work. The effect appears when electromagnetic radiation is measured from a cavity of an object. For this purpose, a cavity means an opening in a concave void of a generally irregular shape whose inner wall temperature is uniform over an entire surface. The emissivity of a cavity opening dramatically increases, approaching unity at any wavelength, as compared with a flat surface. The cavity effect is especially pronounced when its inner walls have relatively high emissivity. Consider a non-metal cavity. All non-metals are diffuse emitters. Also, they are diffuse reflectors. It is assumed that the temperature and surface emissivity of the cavity are homogeneous over an entire area. The ideal emitter (blackbody) would emanate from area  $a$ , the infrared photon flux  $\Phi_0 = \sigma T_b^4$ . However, the object has the actual emissivity  $\epsilon_b$  and, as a result, the flux radiated from that area is smaller:  $\Phi_r = \epsilon_b \Phi_0$  (Figure 32.51). Flux emitted by other parts of the object toward area  $a$  is also equal to  $\Phi_r$  (because the object is thermally homogeneous, one can disregard the spatial distribution of flux). A substantial portion of that incident flux  $\Phi_r$  is absorbed by the surface of area  $a$ , while a smaller part is diffusely reflected:

$$\Phi_p = \rho \Phi_r = (1 - \epsilon_b) \epsilon_b \Phi_0 \quad (32.100)$$

and the combined radiated and reflected flux from area  $a$  is:

$$\Phi = \Phi_r + \Phi_p = \epsilon_b \Phi_0 + (1 - \epsilon_b) \epsilon_b \Phi_0 = (2 - \epsilon_b) \epsilon_b \Phi_0. \quad (32.101)$$

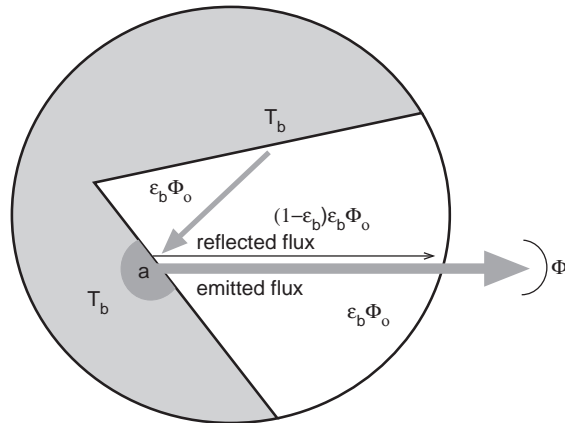


FIGURE 32.51 Cavity effect enhances emissivity. Note that  $\epsilon_c > \epsilon_b$ .

As a result, for a single reflection, the *effective emissivity* can be expressed as:

$$\epsilon_c = \frac{\Phi}{\Phi_0} = (2 - \epsilon_b)\epsilon_b \quad (32.102)$$

It follows from the above that due to a single reflection, a perceived (effective) emissivity of a cavity at its opening (aperture) is equal to the surface emissivity magnified by a factor of  $(2 - \epsilon_b)$ . Of course, there may be more than one reflection of radiation before it exits the cavity. In other words, the incident on area  $a$  flux could already be a result of a combined effect from the reflectance and emittance at other parts of the cavity's surface. For a cavity effect to work, the effective emissivity must be attributed only to the cavity opening (aperture) from which radiation escapes. If a sensor is inserted into the cavity facing its wall directly, the cavity effect could disappear and the emissivity would be close to that of a wall surface.

### Practical Blackbodies

A practical blackbody can be fabricated in several ways. Copper is the best choice for the cavity body material, thanks to its high thermal conductivity, which helps to equalize temperatures of the cavity walls. As an example, Figure 32.52 shows two practical blackbodies. One is a solid-state blackbody having

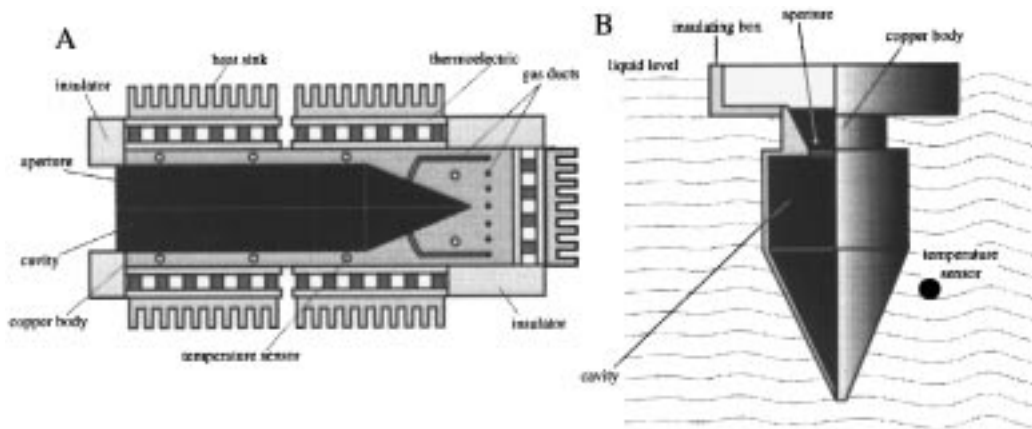


FIGURE 32.52 (A): Solid-state blackbody with thermoelectric elements. (B): Immersed blackbody.

thermoelectric elements (heat pumps) that provide either heating or cooling to the cavity body. The embedded temperature sensors are connected to the control circuit (not shown). The function of the multiple temperature sensors is to monitor thermal distribution over the length of the cavity. The inner shape of the cavity is partly conical to increase the number of reflections, and the entire surface is treated to provide it with as high emissivity as possible, typically over 0.9. This type of a blackbody has a relatively wide aperture that potentially can act as an entry for undesirable ambient air. The air can disturb the thermal uniformity inside the cavity, resulting in excessively high uncertainty of the radiated flux. To reduce this problem, the cavity is filled with dry air or nitrogen, which is continuously pumped in through the gas ducts. Before entering the cavity, the gas passes through the narrow channels inside the cavity and acquires the temperature of the blackbody.

Another example is an immersed blackbody. The cavity is fabricated of copper or aluminum and has relatively thin walls (a few millimeters). The entire cavity body is immersed into a stirred liquid bath, the temperature of which is precisely controlled by heating/cooling devices. The liquid assures uniform temperature distribution around the cavity with a typical thermal instability on the order of  $\pm 0.02^\circ\text{C}$ . The inner surface of the cavity is coated with high-emissivity paint. The aperture of the cavity is relatively small. The ratio of the inner surface of the cavity to the aperture area should be at least 100, and preferably close to 1000.

## Detectors for Thermal Radiation

### Classification

Generally speaking, there are two types of sensors (detectors) known for their capabilities to respond to thermal radiation within the spectral range from the near-infrared to far-infrared; that is, from approximately  $0.8\ \mu\text{m}$  to  $40\ \mu\text{m}$ . The first type is quantum detectors; and the second type is thermal detectors. The latter, in turn, can be subdivided into passive (PIR) and active (AFIR) detectors.

### Quantum Detectors

Quantum detectors (photovoltaic and photoconductive devices) rely on the interaction of individual photons with a crystalline lattice of semiconductor materials. Their operations are based on the photoeffect that was discovered by Einstein, and brought him the Nobel Prize. In 1905, he made a remarkable assumption about the nature of light: that at least under certain circumstances, its energy was concentrated into localized bundles, later named photons. The energy of a single photon is given by:

$$E = h\nu, \quad (32.103)$$

where  $\nu$  = frequency of light

$h = 6.63 \times 10^{-34}\ \text{J} \times \text{s}$  (or  $4.13 \times 10^{-15}\ \text{eV s}$ ) = Planck's constant, derived on the basis of the wave theory of light

When a photon strikes the surface of a conductor, it can result in the generation of a free electron.

The periodic lattice of crystalline materials establishes allowed energy bands for electrons that exist within that solid. The energy of any electron within the pure material must be confined to one of these energy bands, which can be separated by gaps or ranges of forbidden energies.

In insulators and semiconductors, the electron must first cross the energy bandgap in order to reach the conduction band and the conductivity is therefore many orders of magnitude lower. For insulators, the bandgap is usually 5 eV or more; whereas, for semiconductors, the gap is considerably less.

When a photon of frequency  $\nu_1$  strikes a semiconductive crystal, its energy will be high enough to separate the electron from its site in the valence band and push it through the bandgap into a conduction band at a higher energy level. In that band, the electron is free to serve as a current carrier. The deficiency of an electron in the valence band creates a hole that also serves as a current carrier. This is manifested

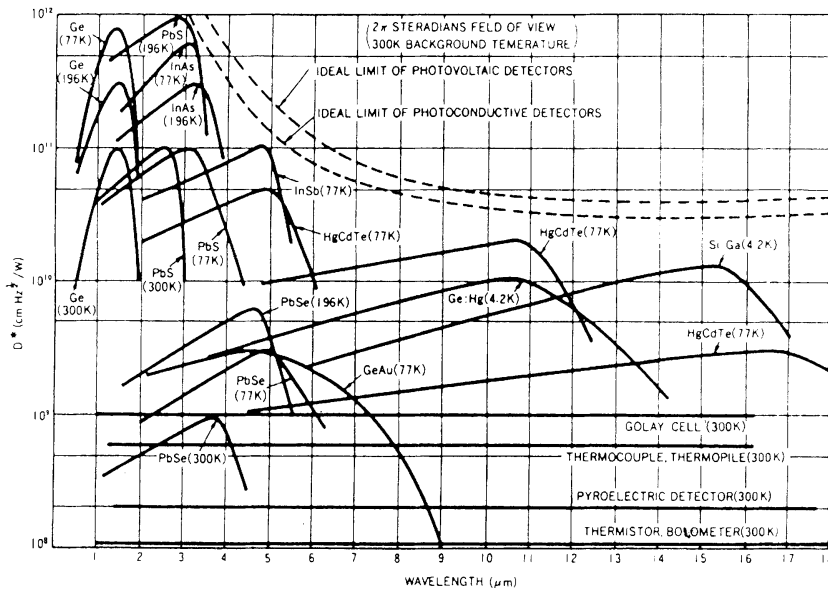


FIGURE 32.53 Operating ranges for some infrared detectors.

in the reduction of specific resistivity of the material. The energy gap serves as a photon energy threshold, below which the material is not light sensitive.

For measurements of objects emanating photons in the range of 2 eV or greater, quantum detectors having room temperature are generally used. For the smaller energies (longer wavelengths), narrower bandgap semiconductors are required. However, even if a quantum detector has a sufficiently small energy bandgap, at room temperature, its own intrinsic noise is much greater than a photoconductive signal. Noise level is temperature dependent; therefore, when detecting long-wavelength photons, a signal-to-noise ratio can become so small that accurate measurement becomes impossible. This is the reason why, for the operation in the near- and far-infrared spectral ranges, a detector not only should have a sufficiently narrow energy gap, but its temperature must be lowered to the level where intrinsic noise is reduced to an acceptable level. Depending on the required sensitivity and operating wavelength, the following crystals are typically used for the cryogenically cooled sensors (Figure 32.53): lead sulfide (PbS), indium arsenide (InAs), germanium (Ge), lead selenide (PbSe), and mercury-cadmium-telluride (HgCdTe).

The sensor cooling allows responses to longer wavelengths and increases sensitivity. However, response speeds of PbS and PbSe become slower with cooling. Methods of cooling include dewar cooling using dry ice, liquid nitrogen, liquid helium, or thermoelectric coolers operating on the Peltier effect.

### Thermal Detectors

Another class of infrared radiation detectors is called *thermal detectors*. Contrary to quantum detectors that respond to individual photons, thermal detectors respond to heat resulting from absorption of thermal radiation by the surface of a sensing element. The heat raises the temperature of the surface, and this temperature increase becomes a measure of the net thermal radiation.

The Stefan-Boltzmann law (Equation 32.95) specifies radiant power (flux) which would emanate from a surface of temperature,  $T$ , toward an infinitely cold space (at absolute zero). When thermal radiation is detected by a thermal sensor, the opposite radiation from the sensor toward the object must also be taken in account. A thermal sensor is capable of responding only to a net thermal flux, i.e., flux from the object minus flux from itself. The surface of the sensor that faces the object has emissivity  $\epsilon_s$  (and,

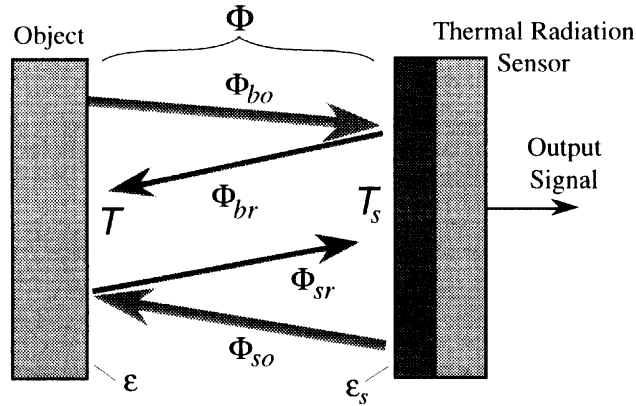


FIGURE 32.54 Heat exchange between the object and thermal radiation detector.

subsequently reflectivity  $\rho_s = 1 - \epsilon_s$ ). Because the sensor is only partly absorptive, the entire flux,  $\Phi_{bo}$ , is not absorbed and utilized. A part of it,  $\Phi_{ba}$ , is absorbed by the sensor, while another part,  $\Phi_{br}$ , is reflected (Figure 32.54) back toward to object (here, it is assumed that there is 100% coupling between the object and the sensor and there are no other objects in the sensor's field of view). The reflected flux is proportional to the sensor's coefficient of reflectivity:

$$\Phi_{br} = -\rho_s \Phi_{bo} = -A\epsilon(1 - \epsilon_s)\sigma T^4 \quad (32.104)$$

A negative sign indicates an opposite direction with respect to flux  $\Phi_{bo}$ . As a result, the net flux originated from the object is:

$$\Phi_b = \Phi_{bo} + \Phi_{br} = A\epsilon\epsilon_s\sigma T^4 \quad (32.105)$$

Depending on its temperature  $T_s$ , the sensor's surface radiates its own net thermal flux toward the object in a similar way:

$$\Phi_s = -A\epsilon\epsilon_s\sigma T_s^4 \quad (32.106)$$

Two fluxes propagate in the opposite directions and are combined into a final net flux existing between two surfaces:

$$\Phi = \Phi_b + \Phi_s = A\epsilon\epsilon_s\sigma(T^4 - T_s^4) \quad (32.107)$$

This is a mathematical model of a net thermal flux that is converted by a thermal sensor into the output signal. It establishes a connection between thermal power,  $\Phi$ , absorbed by the sensor, and the absolute temperatures of the object and the sensor. It should be noted that since the net radiation exists between the two bodies, the spectral density will have the maximum not described by Equation 32.92; but depending on the temperature gradient, it will be somewhat shifted toward the shorter wavelengths.

Dynamically, the temperature  $T_s$  of a thermal element in a sensor, in general terms, can be described by the first-order differential equation:

$$cm \frac{dT_s}{dt} = P - P_L - \Phi \quad (32.108)$$

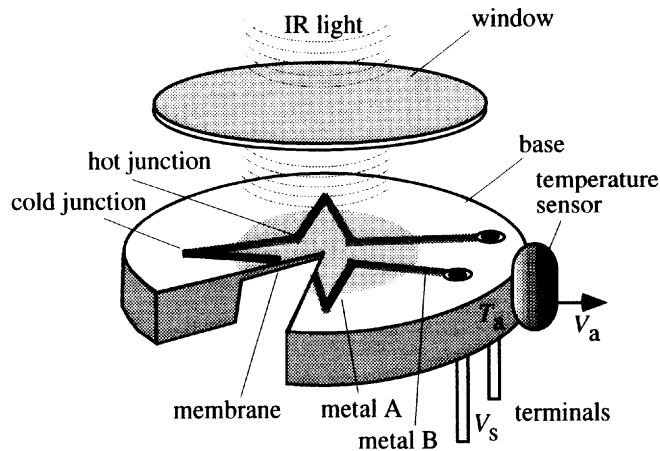


**FIGURE 32.55** Thermopile sensor. “Hot” junctions are deposited on a membrane and “cold” junctions on the supporting ring.

where  $P$  is the power supplied to the element from a power supply or an excitation circuit (only in AFIR sensors; see below);  $P_L$  is a nonradiative thermal loss attributed to thermal conduction and convection;  $m$  and  $c$  are the sensor’s mass and specific heat, respectively; and  $\Phi = \Phi_n + \Phi_b$  is the net radiative thermal flux. We select a positive sign for power  $P$  when it is directed toward the element.

In the PIR detector (thermopiles, pyroelectric, and bolometers), no external power is supplied ( $P = 0$ ); hence, the speed response depends only on the sensor’s thermal capacity and heat loss, and is a first-order function that is characterized by a thermal time constant  $\tau_T$ .

#### Thermopile Sensors.

Thermopiles belong to a class of PIR detectors. Their operating principle is the same as that of thermocouples. In effect, a thermopile can be defined as serially connected thermocouples. Originally, it was invented by Joule to increase the output signal of a thermoelectric sensor; he connected several thermocouples in series and thermally joined together their hot junctions. Presently, thermopiles have a different configuration. Their prime application is detection of thermal radiation.

A cut-out view of a thermopile sensor is shown in [Figure 32.55](#). The sensor consists of a base having a relatively large thermal mass, which is the place where the “cold” junctions are positioned. The base can be thermally coupled with a reference temperature sensor or attached to a thermostat having a known temperature. The base supports a thin membrane whose thermal capacity and thermal conductivity are small. The membrane is the surface where the “hot” junctions are positioned.

The best performance of a thermopile is characterized by high sensitivity and low noise, which can be achieved by the junction materials having high thermoelectric coefficient, low thermal conductivity, and low volume resistivity. Besides, the junction pairs should have thermoelectric coefficients of opposite signs. This dictates the selection of materials. Unfortunately, most of metals having low resistivity (i.e., gold, copper, silver) have only very poor thermoelectric coefficients. The higher resistivity metals (especially bismuth and antimony) possess high thermoelectric coefficients and they are the prime selection for designing thermopiles. By doping these materials with Se and Te, the thermoelectric coefficient has been improved up to  $230 \mu\text{V K}^{-1}$  [1].

Methods of construction of metal junction thermopiles can differ to some extent, but all incorporate vacuum deposition techniques and evaporation masks to apply the thermoelectric materials, such as bismuth and antimony on thin substrates (membranes). The number of junctions varies from 20 to several hundreds. The “hot” junctions are often blackened (e.g., with goldblack or organic paint) to improve their absorptivity of the infrared radiation. A thermopile is a dc device with an output voltage that follows its “hot” junction temperature quite well. It can be modeled as a thermal flux-controlled

voltage source that is connected in series with a fixed resistor. The output voltage  $V_s$  is nearly proportional to the incident radiation.

An efficient thermopile sensor can be designed using a semiconductor rather than double-metal junctions [2]. The thermoelectric coefficients for crystalline and polycrystalline silicon are very large and the volume resistivity is relatively low. The advantage of using silicon is in the possibility of employing standard IC processes. The resistivity and the thermoelectric coefficients can be adjusted by the doping concentration. However, the resistivity increases much faster, and the doping concentration must be carefully optimized for the high sensitivity–low noise ratios. Semiconductor thermopile sensors are produced with a micromachining technology by EG&G Heimann Optoelectronics GmbH (Wiesbaden, Germany) and Honeywell (Minneapolis, MN).

#### Pyroelectrics.

Pyroelectric sensors (see Chapter 6) belong to a class of PIR detectors. A typical pyroelectric sensor is housed in a metal TO-5 or TO-39 for better shielding and is protected from the environment by a silicon or any other appropriate window. The inner space of the can is often filled with dry air or nitrogen. Usually, two sensing elements are oppositely, serially or in parallel, connected for better compensation of rapid thermal changes and mechanical stresses resulting from acoustic noise and vibrations [3].

#### Bolometers.

Bolometers are miniature RTDs or thermistors, which are mainly used for measuring rms values of electromagnetic signals over a very broad spectral range from microwaves to near-infrared. An external bias power is applied to convert resistance changes to voltage changes. For the infrared thermometers, the bolometers are often fabricated in the form of thin films having relatively large area. The operating principle of a bolometer is based on a fundamental relationship between the absorbed electromagnetic signal and dissipated power [3].

The sensitivity of the bolometer to the incoming electromagnetic radiation can be defined as [4]:

$$\beta = \frac{1}{2} \epsilon \alpha_0 \sqrt{\frac{R_0 Z_T \Delta T}{(1 + \alpha_0 \Delta T) [1 + (\omega \tau)^2]}} \quad (32.109)$$

where  $\alpha = (dR/dT)/R =$  TCR (temperature coefficient of resistance) of the bolometer

$\epsilon$	= Surface emissivity
$Z_T$	= Bolometer thermal resistance, which depends on its design and the supporting structure
$\tau$	= Thermal time constant, which depends on $Z_T$ and the bolometer's thermal capacity
$\omega$	= Angular frequency
$\Delta T$	= Bolometer's temperature increase

Bolometers are relatively slow sensors and are used primarily when no fast response is required. For thermal imaging, bolometers are available as two-dimensional arrays of about 80,000 sensors [5].

#### Active Far-Infrared Sensors.

In the active far-infrared (AFIR) sensor, a process of measuring thermal radiation flux is different from previously described passive (PIR) detectors. Contrary to a PIR sensing element — the temperature of which depends on both the ambient and the object's temperatures — the AFIR sensor's surface is actively controlled by a special circuit to have a defined temperature  $T_s$  that, in most applications, is maintained constant during an entire measurement process [6]. To control the sensor's surface temperature, electric power  $P$  is provided by a control (or excitation) circuit (Figure 32.56). To regulate  $T_s$ , the circuit measures the element's surface temperature and compares it with an internal reference.

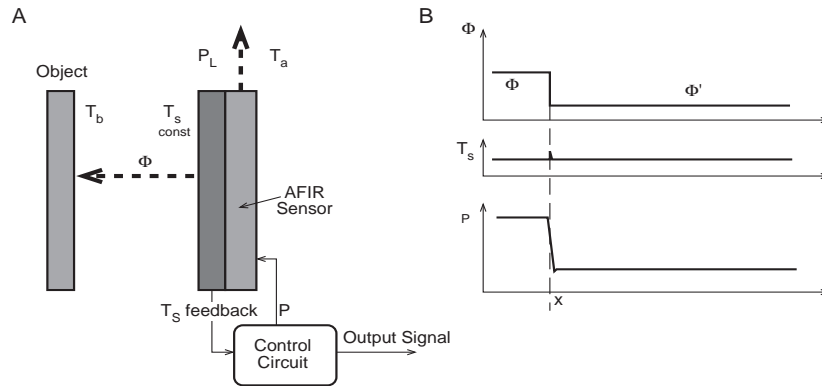


**FIGURE 32.56** (A) AFIR element radiates thermal flux  $\Phi_{\eta}$  toward its housing and absorbs flux  $\Phi_b$  from the object. (B) Timing diagrams for radiative flux, surface temperature, and supplied power.

Obviously, the incoming power maintains  $T_s$  higher than ambient, practically by just several tenths of a degree Celsius. Since the element's temperature is above ambient, the sensing element loses thermal energy toward its surroundings, rather than passively absorbing it, as in a PIR detector. Part of the heat loss is in the form of a thermal conduction; part is a thermal convection; and the other part is thermal radiation. The third part is the one that must be measured. Of course, the radiative flux is governed by the fundamental Stefan–Boltzmann law for two surfaces (Equation 32.99).

Some of the radiation power goes out of the element to the sensor's housing, while the other is coming from the object (or goes to the object). What is essential is that the net thermal flow (conductive + convective + radiative) must always come out of the sensor; that is, it must have a negative sign.

In the AFIR element, after a warm-up period, the control circuit forces the element's surface temperature  $T_s$  to stay constant; thus,

$$\frac{dT_s}{dt} = 0 \quad (32.110)$$

and Equation 32.108 becomes algebraic:

$$P = P_L + \Phi \quad (32.111)$$

It follows from the above that, under idealized conditions, its response does not depend on thermal mass and is not a function of time, meaning that practical AFIR sensors are quite fast. If the control circuit is highly efficient, since  $P_L$  is constant at given ambient conditions, the electronically supplied power  $P$  should track changes in the radiated flux  $\Phi$  with high fidelity. Nonradiative loss  $P_L$  is a function of ambient temperature  $T_a$  and a loss factor  $\alpha_s$ :

$$P_L = \alpha_s (T_s - T_a) \quad (32.112)$$

To generate heat in the AFIR sensor, it may be provided with a heating element having electrical resistance  $R$ . During the operation, electric power dissipated by the heating element is a function of voltage  $V$  across that resistance

$$P = V^2 / R \quad (32.113)$$

Substituting Equations 32.107, 32.112, and 32.113 into Equation 32.111, and assuming that  $T = T_b$  and  $T_s > T_a$ , after simple manipulations, the object's temperature can be presented as function of voltage  $V$  across the heating element:

$$T_b = \sqrt{T_s^4 - \frac{1}{A\sigma\epsilon_s\epsilon_b} \left( \frac{V^2}{R} - \alpha_s \Delta T \right)} \quad (32.114)$$

where  $\Delta T$  is the constant temperature increase above ambient. Coefficient  $\alpha_s$  has a meaning of thermal conductivity from the AFIR detector to the environment (housing).

One way to fabricate an AFIR element is to use a discrete thermistor having a relatively large surface area (3 mm<sup>2</sup> to 10 mm<sup>2</sup>) and operating in a self-heating mode. Electric current passing through the thermistor results in a self-heating effect that elevates the thermistor's temperature above ambient. In effect, the thermistor operates as both the heater and a temperature sensor.

Contrary to a PIR detector, an AFIR sensor is active and can generate a signal only when it works in orchestra with a control circuit. A control circuit must include the following essential components: a reference to preset a controlled temperature, an error amplifier, and a driver stage for the heater. In addition, it may include an RC network for correcting a loop response function and for stabilizing its operation; otherwise, an entire system could be prone to oscillations [7].

It can be noted that an AFIR sensor, along with its control circuit, is a direct converter of thermal radiative power into electric voltage and a quite efficient one. Its typical responsivity is in the range of 3000 V W<sup>-1</sup>, which is much higher as compared with a thermopile, whose typical responsivity is in the range of 100 V W<sup>-1</sup>. More detailed description of an AFIR sensor can be found in [3, 6].

## Pyrometers

### Disappearing Filament Pyrometer

Additional names for the disappearing filament pyrometer include: *optical pyrometer* and *monochromatic-brightness radiation thermometer*. This type of pyrometer is considered the most accurate radiation thermometer for temperatures over 700°C. This limitation is a result of human-eye sensitivity within a specific wavelength. The operating principle of this thermometer is based on Planck's law (Equation 32.90 and Figure 32.48) which states that intensity and color of the surface changes with temperature. The idea behind the design is to balance a radiation from an object having a known temperature against unknown temperature from a target. The pyrometer has a lens through which the operator views the target (Figure 32.57A). An image of a tungsten filament is superimposed on the image of the target. The filament

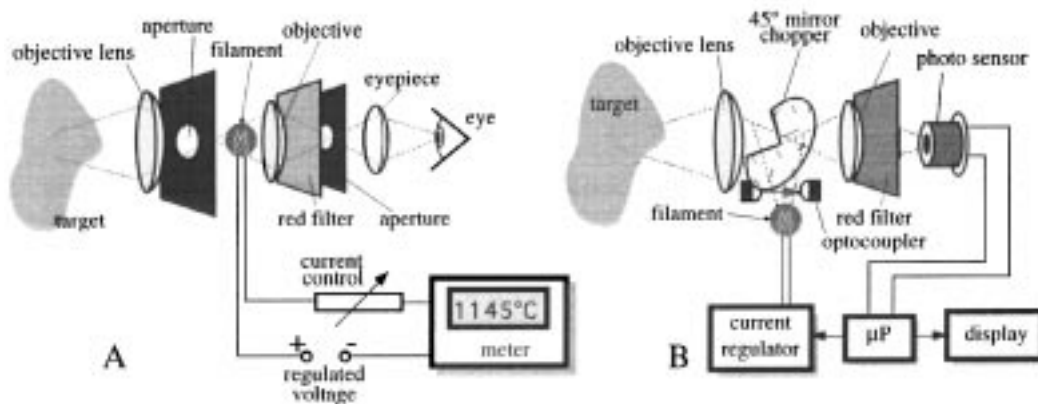


FIGURE 32.57 Disappearing filament optical pyrometer: (A): Manual, and (B): automatic versions.

is warmed up by electric current to glow. During the calibration, the relationship between the current and the filament temperature was established by measuring brightness of a blackbody of known temperature. The operator views the target through the eyepiece and manually adjusts the heating current to the level when an image of the glowing filament visible in the foreground disappears — that is, when both the target and the filament have the same brightness and color. A color component complicates the measurement somewhat; so to remove this difficulty, a narrow-band red filter ( $\lambda_f = 0.65 \mu\text{m}$ ) is inserted in front of an eyepiece. Therefore, the operator has to balance only the brightness of an image visible in red color. Another advantage of the filter is that the emissivity  $\epsilon_{\text{bf}}$  of the target needs to be known only at  $\lambda_f$ . The error in temperature measurement is given by [8]:

$$\frac{dT_b}{T_b} = -\frac{\lambda_f T_b}{C_2} \frac{d\epsilon_{\text{bf}}}{\epsilon_{\text{bf}}} \quad (32.115)$$

Thus, for a target at  $T_b = 1000 \text{ K}$ , a 10% uncertainty in knowing emissivity of the target at the filter's wavelength results in only  $\pm 0.45\%$  ( $\pm 4.5 \text{ K}$ ) uncertainty in measured temperature.

The instrument can be further improved by removing an operator from the measurement loop. [Figure 32.57B](#) shows an automatic version of the pyrometer where a rotating mirror tilted by  $45^\circ$  has a removed sector that allows the light from a target to pass through to the photosensor. Such a mirror serves as a chopper, which alternately sends light to a photosensor, either from a target or from the filament. The microprocessor ( $\mu\text{P}$ ) adjusts current through the filament to bring the optical contrast to zero. The optocoupler provides a synchronization between the chopper and the microprocessor.

### Two-color Pyrometer

Since emissivities of many materials are not known, measurement of a surface temperature can become impractical, unless the emissivity is excluded from the calculation. This can be accomplished by use of a radiometric technique: the so called “two-color radiation thermometer” or *ratio thermometer*. In such a thermometer, the radiation is detected at two separate wavelengths  $\lambda_x$  and  $\lambda_y$  for which emissivities of the surface can be considered nearly the same. The coefficients of transmission of the optical system at each wavelength respectively are  $\gamma_x$  and  $\gamma_y$ , then the ratio of two equations (2) calculated for two wavelengths is:

$$\phi = \frac{W_x}{W_y} = \frac{\gamma_x \epsilon(\lambda_x) \frac{C_1}{\pi} \epsilon(\lambda_x) \lambda_x^{-5} e^{-\frac{C_2}{\lambda_x T}}}{\gamma_y \epsilon(\lambda_y) \frac{C_1}{\pi} \epsilon(\lambda_y) \lambda_y^{-5} e^{-\frac{C_2}{\lambda_y T}}} \quad (32.116)$$

Because the emissivities  $\epsilon(\lambda_x) \approx \epsilon(\lambda_y)$ , after manipulations, Equation 32.116 can be rewritten for the displayed temperature  $T_c$ , where  $\phi$  represents the ratio of the thermal radiation sensor outputs at two wavelengths:

$$T_c \approx C_2 \left( \frac{1}{\lambda_y} - \frac{1}{\lambda_x} \right) \left( \ln \phi \frac{\gamma_y \lambda_x^5}{\gamma_x \lambda_y^5} \right)^{-1} \quad (32.117)$$

It is seen that the equation for calculating temperature does not depend on the emissivity of the surface. Equation 32.117 is the basis for calculating temperature by taking the ratio of the sensor outputs at two different wavelengths. [Figure 32.58](#) shows a block diagram of an IR thermometer where an optical modulator is designed in the form of a disk with two filters.

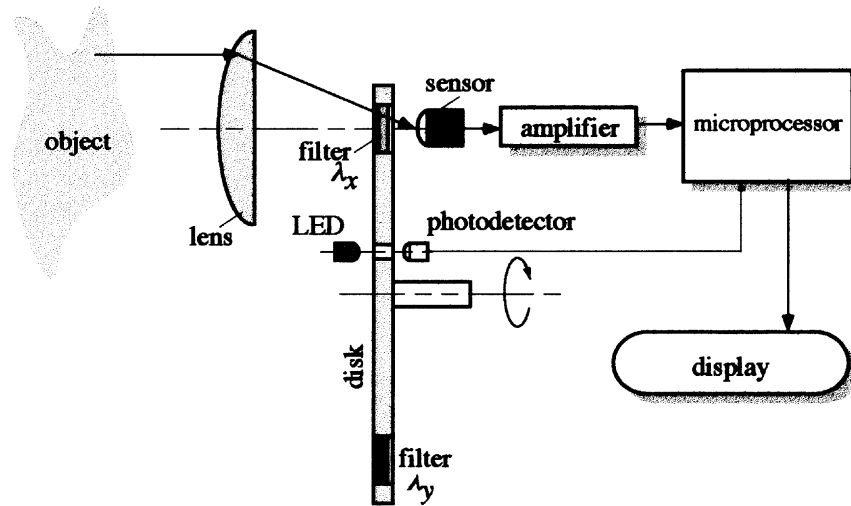


FIGURE 32.58 Two-color, non-contact thermometer. LED and photodetector are for synchronizing the disk rotation with the sensor response.

## IR Thermometers

### Operating Principle

Infrared (IR) Thermometer with PIR Sensors.

The operating principle of a noncontact infrared (IR) thermometer is based on the fundamental Stefan-Boltzmann law (Equation 32.118). For the purposes of calculating the object's temperature, when using the PIR sensor (thermopile, bolometer, or pyroelectric), the equation can be manipulated as:

$$T_c = \sqrt[4]{T_s^4 + \frac{\Phi}{A\sigma\epsilon\epsilon_s}} \quad (32.118)$$

where  $T_c$  is the calculated object's temperature in kelvin. Hence, to calculate the temperature of an object, one should first determine the magnitude of net thermal radiation flux  $\Phi$  and the sensor's surface temperature  $T_s$ . The other parts of Equation 32.118 are considered as constants and must be determined during the calibration of the instrument from a blackbody. Emissivity of the object  $\epsilon$  also must be known before the calculation. In practice, it is sometimes difficult to determine the exact temperature  $T_s$  of the sensor's surface, due to changing ambient conditions, drifts, handling of the instrument, etc. In such cases, the IR thermometer can be supplied with a reference target. Then, the calculation can still be done with the use of Equation 32.118; however, the value of  $\Phi$  will have a meaning of a flux differential between the object and the reference target, and the value of  $T_s$  will represent the reference target temperature.

IR Thermometer with AFIR Sensor.

The object's temperature can be calculated from Equation 32.118; but first the sensing element surface temperature should be determined by measuring the temperature of the sensor's housing:  $T_s = T_a + \Delta T$ , where  $\Delta T$  is the constant. In addition, the value of  $V$  must be measured. The AFIR sensor allows for continuous monitoring of temperature in a manner similar to thermopile sensors. Its prime advantage is simplicity and low cost.

### Continuous Monitoring of Temperature

Depending on the type of thermal radiation sensor employed, a non-contact infrared thermometer for continuous monitoring can incorporate different components. Thus, if a sensor with a dc response is

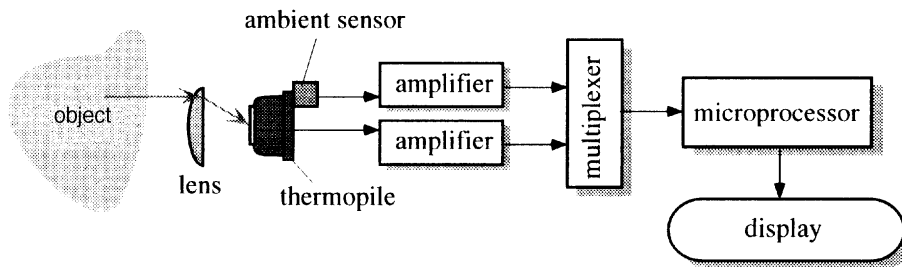


FIGURE 32.59 Infrared thermometer with a dc type of thermal radiation sensor.

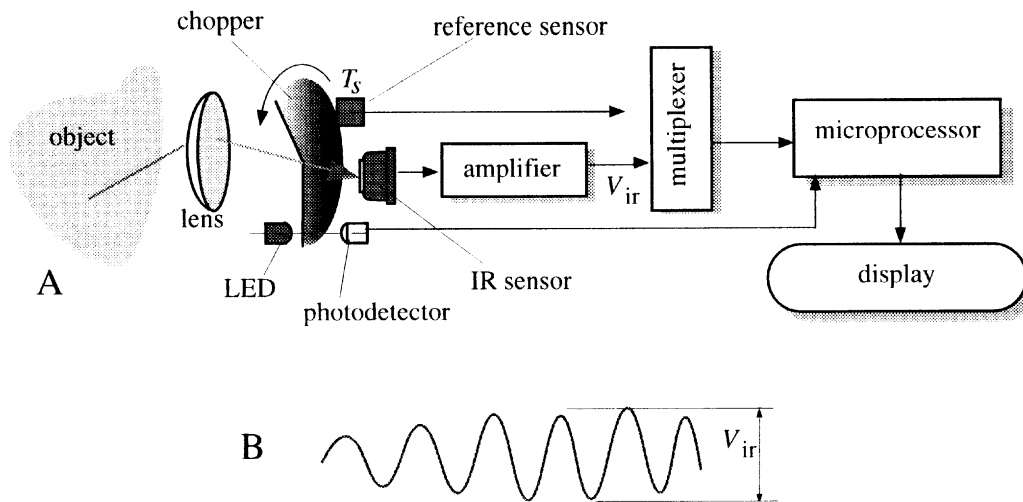


FIGURE 32.60 Infrared thermometer with a chopper.

used, the circuit might look like the one shown in [Figure 32.59](#). It has the following essential components: the optical system (the lens), the IR sensor (a thermopile in this example), the reference (ambient) sensor, and a conventional data acquisition circuit. The dc-type sensors are the thermopiles, bolometers, and AFIR. When the AFIR sensor is used, it should be supplied with an additional control circuit, as described above.

In the case when an ac-type of IR sensor is used (pyroelectric), the thermometer needs a chopper that breaks the IR radiation into series pulses, usually with a 50% duty cycle ([Figure 32.60](#)). The output of an amplifier is an alternate signal that has a magnitude dependent on both the chopping rate and the net IR radiation. The rotation of the chopper is synchronized with the data processing by the microprocessor by means of an optocoupler (LED and photodetector). It should be noted that the chopper not only converts the IR flux into an ac signal, but it also serves as a reference target, as described above. Use of a reference target can significantly improve IR thermometer accuracy; thus, the chopper is often employed, even with the dc-type sensors, although it is not essential for operation. Naturally, the chopper's surface emissivity will be high and known.

### Intermittent Monitoring of Temperature

Obviously, any infrared thermometer capable of continuous monitoring of temperature can be made operational in the intermittent mode. In other words, the continuous temperature can be processed to extract a single value of temperature that might be of interest to the user. For example, it may be a maximum, a minimum, or an averaged over time temperature; yet it is possible to design a low-cost IR thermometer that takes only a "snapshot" of the temperature at any specific moment. Such a thermometer

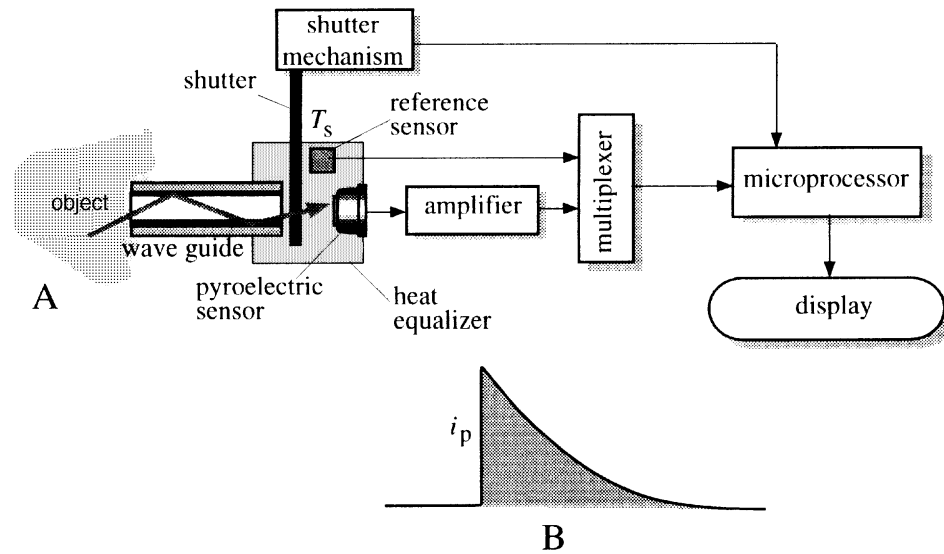


**FIGURE 32.61** (A): Infrared thermometer with a pyroelectric sensor. Note that a waveguide is used as part of an optical system. (B) Output current from a pyroelectric sensor.

can be designed with a pyroelectric sensor that produces electric charge virtually instantaneously upon receiving the IR radiation. Figure 32.61A shows a block diagram of such a thermometer. A mechanical or electromechanical shutter is positioned in front of the pyroelectric sensor. The shutter surface serves as a reference target. When the shutter is closed, the sensor produces no output. Immediately upon shutter actuation, the pyroelectric current flows from the sensor into an amplifier that contains a charge-to-voltage converter. The sensor's current response has a shape close to the exponential function (Figure 32.61B). The magnitude of the spike is nearly proportional to the IR flux at the moment of the shutter opening. The pyroelectric thermometer is widely used for medical purposes and is dubbed the "instant thermometer."

### Response Speed

All infrared thermometers are relatively fast; their typical response time is on the order of a second. Along with the non-contact way of taking temperature, this makes these devices very convenient whenever fast tracking of temperature is essential. However, an IR thermometer, while being very fast, still can require a relatively long warm-up time, and may not be accurate whenever it is moved from one environment to another without having enough time to adapt itself to new ambient temperature. The reason for this is that the reference and IR sensors (or the IR sensor and the shutter or chopper) must be in thermal equilibrium with one another; otherwise, the calculated temperature is erroneous.

## Components of IR Thermometers

### Optical Choppers and Shutters

The shutters or choppers must possess the following properties: (1) they should have high surface emissivity that does not change with time; (2) the opening and closing speed must be high; (3) the thermal conductivity between the front and back sides of the blade should be as small as possible; (4) the blade should be in good thermal contact with the reference sensor; and (5) while operating, the blade should not wear off or produce microscopic particles of dust that could contaminate the optical components of the IR thermometer.

For operation in the visible and near-infrared portions of the spectrum, when measured temperatures are over 800 K, the shutter can be fabricated as a solid-state device without the use of moving components

**TABLE 32.18** Materials Useful for Infrared Windows and Lenses

Material	$n$	$\rho$	Wavelength ( $\mu\text{m}$ )	Note
AMTIR-1 ( $\text{Ge}_{33}\text{As}_{12}\text{Se}_{55}$ )	2.6	0.330	1	Amorphous glass
	2.5	0.310	10	
AMTIR-3 ( $\text{Ge}_{28}\text{Sb}_{12}\text{Se}_{60}$ )	2.6	0.330	10	Amorphous glass
	$\text{As}_2\text{S}_3$	2.4	0.3290	
CdTe	2.67	0.342	10.6	
Diamond	2.42	0.292	0.54	Best IR material
Fused silica ( $\text{SiO}_2$ )	1.46	0.067	3.5	Near-IR range
GaAs	3.13	0.420	10.6	
Germanium	4.00	0.529	12.0	Windows and lenses
Irtran 2 ( $\text{ZnS}$ )	2.25	0.258	4.3	
KRS-6	2.1	0.224	24	Toxic
Polyethylene	1.54	0.087	8.0	Low-cost IR windows; lenses
Quartz	1.54	0.088		Near-IR range
Sapphire ( $\text{Al}_2\text{O}_3$ )	1.59	0.100	5.58	Chemically resistant. Near- and mid-IR ranges
Silicon	3.42	0.462	5.0	Windows in IR sensors
ZnSe	2.4	0.290	10.6	IR windows; brittle

Note:  $n$  is the refractive index and  $\rho$  is the coefficient of reflection from two surfaces in air.

(e.g., employing liquid crystals). However, for longer wavelengths, only the mechanical blades are useful. Special attention should be paid with regard to the prevention of reflection by the shutter or chopper of any spurious thermal radiation that originates from within the IR thermometer housing.

### Filters and Lenses

The IR filters and lenses serve two purposes: they selectively pass specific wavelengths to the sensing components, and they protect the interior of the instrument from undesirable contamination by outside pollutants. In addition, lenses — due to their refractive properties — divert light rays into specific direction [3]. In IR thermometry, the selection of filters and lenses is limited to a relatively short list. Table 32.18 lists some materials that are transparent in the infrared range. Note that most of these materials have a relatively high refractive index, which means that they have high surface reflectivity loss. For example, silicon (the cheapest material for the IR windows) reflects over 46% of incoming radiation which along with the absorptive loss, amounts to an even higher value of combined loss. To a certain degree, this problem can be solved by applying special antireflective (AR) coatings on both surfaces of the window or lens. These coatings are geared to specific wavelengths; thus, for a broad bandwidth, a multilayer coating may need to be deposited by a sputtering process.

Another problem with IR refractive materials is the relatively high absorption of light. This becomes a serious limitation for the lenses, as they need to be produced with appreciable thickness. The solution is to select materials with low absorption in the spectral range of interest. Examples are zinc selenide ( $\text{ZnSe}$ ) and AMTIR. Another solution is the use of polyethylene Fresnel lenses, which are much thinner and less expensive [3]. Any window or lens that is absorptive will also emanate thermal radiation according to its own temperature. Hence, to minimize this effect on the overall accuracy of an IR thermometer, the refractive devices should be kept at the same temperature as the IR sensor, the shutter (chopper), and the reference sensor.

### Waveguides

Waveguides are optical components intended for channeling IR radiation from one point to another. Usually, they are used when an IR sensor cannot be positioned close to the source of thermal radiation, yet must have a wide field of view. These components employ light reflection and are not focusing, even if they are designed with refractive materials. If focusing is required, the waveguides can be combined with lenses and curved or tilted mirrors. A waveguide has relatively wide entry and exit angles. A typical application is in a medical IR thermometer, where the waveguide is inserted into an ear canal (Figure 32.61).

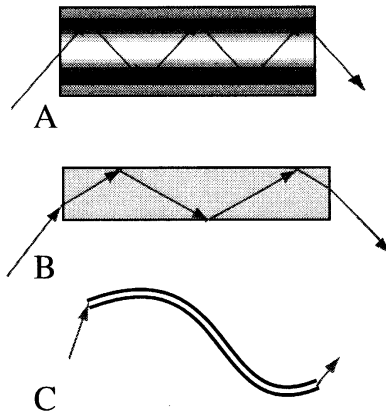


FIGURE 32.62 Light inside the barrel (A), rod (B) and fiber-optic (C) propagates on a zigzag path.

There are three types of waveguides: hollow tubes (barrels), optical fibers, and rods [3, 9, 10]. The latter two are made of IR-transparent materials, such as ZnSe or AMTIR, and use the angle of total internal reflection to propagate light inside in a zigzag pattern (Figure 32.62). The barrels are hollow tubes, polished and gold-plated on the inner surface.

### Error Sources in IR Thermometry

Any error in detection of either radiated flux ( $\Phi$ ) or reference temperature ( $T_a$ ) will result in inaccuracy in the displayed temperature. According to Equation 32.118, the emissivities of both the sensor ( $\epsilon_s$ ) and the object ( $\epsilon$ ) must be known for the accurate detection of thermal flux. Emissivity of the sensor usually remains constant and is taken care of during the calibration. However, uncertainty in the value of emissivity of the object can result in significant uncertainty in temperatures measured by non-contact infrared thermometers (Figure 32.63).

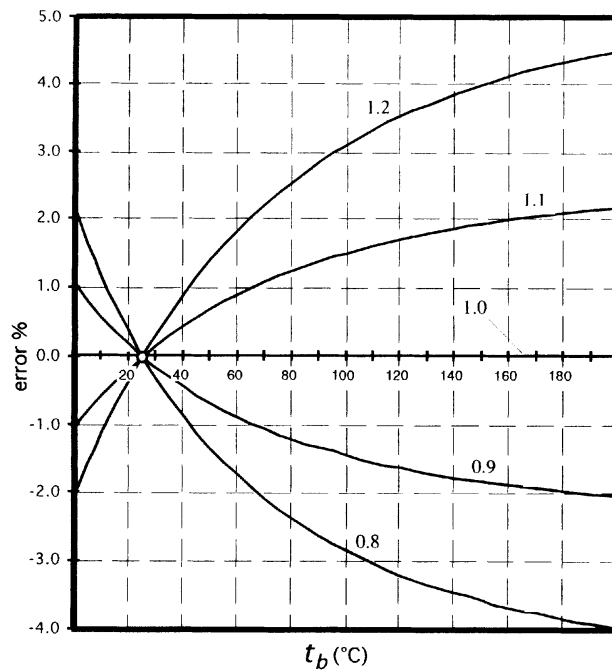


FIGURE 32.63 Error in temperature measurement resulted from uncertainty in the value of object's emissivity.

Another source of an error is spurious heat sources, which can emanate their thermal radiation either directly into the optical system of an IR thermometer, or by means of reflection from the measured surface [11]. Since no surface is an ideal emitter (absorber), its reflectivity may have significant value. For example, an opaque object with emissivity 0.9 has reflectivity of 0.1 (Equation 32.54); thus, about 10% of the radiation from a hot object in the vicinity of a measured surface is reflected and can greatly disturb the measurement.

Since emissivities of metals are quite small and one never can be sure about their actual values, it is advisable, whenever practical, to coat a portion of a metal surface with a dielectric material, such as metal oxide or organic paint having known emissivity. Alternatively, temperatures should not be taken from a flat surface, but rather from a hole or cavity that inside has a nonmetallic surface.

Another source of error is the thermal instability of the thermal sensing element. For example, in a thermopile or pyroelectric sensor, upon exposure to thermal radiation, the element's temperature might increase above ambient by just a few millidegrees. Hence, if for some reason, the element's temperature varies by the same amount, the output signal becomes indistinguishable from that produced by the thermal flux. To minimize these errors, the infrared sensors are encapsulated into metal bodies having high thermal capacity and poor coupling to the environment (high thermal resistance), which helps to stabilize the temperature of the sensor. Another powerful technique is to fabricate the IR sensor in a dual form; that is, with two identical sensing elements. One element is subjected to an IR signal, while the other is shielded from it. The signals from the elements are subtracted, thus canceling the drifts that affect both elements [3].

## Some Special Applications

### Semiconductor Materials

Temperature measurement of semiconductor material during processing, such as growth of epitaxial films in vacuum chambers, always has been a difficult problem. Various process controls require accurate temperature monitoring, often without physical contact with the substrates. As a rule, heating of a substrate is provided by resistive heaters. The substrates are often loaded into the chambers through various locks and rotated during processing. Therefore, it is very difficult to attach a contact sensor, such as a thermocouple, to the wafer. And, even if one does so, the thermal gradient between the sensor and the substrate may be so large that one should never trust the result. The attractive alternative is optical pyrometry; however, this presents another set of difficulties. The major problem is that semiconductors are substantially transparent in the spectral region where thermal radiation would be emanated. In other words, the emissivity of a semiconductor is negligibly small and the amount of thermal radiation from a semiconductor is also not only small, but due to wafer transparency, the radiation from the underlying devices (e.g., heater) will go through to the IR thermometer.

One relatively simple method is to coat a small portion of the semiconductor with a material having high emissivity in the IR spectral range. Then, the thermal radiation can be measured from that patch. An example of such a material is nichrome (see Table 32.17).

An attractive method of temperature monitoring, when no emissive patch can be deposited, is the use of temperature dependence of bandgaps of common semiconductors. The bandgap is determined from the threshold wavelength at which the radiation from the heaters behind the substrate is transmitted through the substrate [12]. Another method is based on the temperature dependence of diffuse reflection of a semiconductor. In effect, this method is similar to the former; however, it relies on reflection, rather than on transmission of the semiconductor. An external lamp is used for the measurement of a threshold wavelength from a front polished and backside textured substrate [13]. The temperature measurement arrangement is shown in [Figure 32.64](#) where the diffused light is detected by cryogenically cooled quantum detector. The monochromator has resolution of 3 nm and scans through the threshold area at a rate of 100 nm/s.

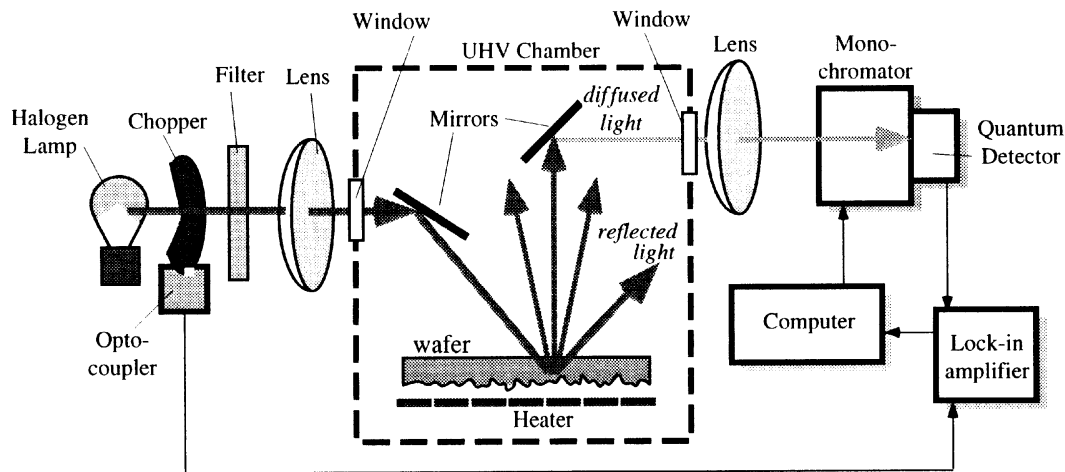


FIGURE 32.64 Diffused-light thermometer for measuring temperature of GaAs wafers. (After [12].)

### Medical Applications

Medical infrared thermometry has two distinct types of measurements: *body* temperature measurement and *skin* surface temperature measurement. Skin temperature measurements have specific applications in determining surface temperature of a human body. That temperature greatly depends on both the skin blood perfusion and environmental conditions. Therefore, skin temperature cannot be independently correlated with the internal body temperature.

Now, it is customary to measure the internal body temperature by placing the probe of an IR thermometer into the ear canal aiming it at a tympanic membrane [14]. The tympanic membrane has temperature close to that of blood. As a rule, the probe is designed with a gold-plated waveguide (Figure 32.61) which is protected either by a semiconductor or polymer window. Because a medical IR thermometer is used in direct contact with patient tissues, it is imperative to protect the probe from becoming a carrier of soiling compounds and a transmitter of infection from one patient to another (cross-contamination) or even from re-infecting the same patient (recontamination). Thus, a probe of a medical IR thermometer is protected by a special probe cover made of a polymer film (polyethylene, polypropylene, etc.) which is transparent in the spectrum range of thermal radiation. In effect, the probe cover becomes a part of the optical system. This demands that covers be produced with very tight tolerances so that they will not significantly affect transmission of IR signal.

### References

1. A. Völklein, A. Wiegand, and V. Baier, *Sensors and Actuators A*, 29, pp: 87-91, 1991.
2. J. Schieferdecker, R. Quad, E. Holzenkämpfer, and M. Schulze, Infrared thermopile sensors with high sensitivity and very low temperature coefficient. *Sensors and Actuators A*, 46-47, 422-427, 1995.
3. J. Fraden, *Handbook of Modern Sensors*. 2nd ed., Woodbury, NY: AIP Press, 1996.
4. J-S. Shie and P.K. Weng, Fabrication of micro-bolometer on silicon substrate by anisotropic etching technique. *Transducers'91, Int. Conf. Solid-state Sensors and Actuators*. 627-630, 1991.
5. R.A. Wood, Uncooled thermal imaging with silicon focal plane arrays. *Proc. SPIE 2020, Infrared Technology XIX*, pp: 329-36, 1993.
6. J. Fraden, Active far infrared detectors. In *Temperature, Its Measurement and Control in Science and Industry*. Vol. 6, Part 2, New York: American Institute of Physics, 1992, 831-836.

7. C.J. Mastrangelo and R.S. Muller, Design and performance of constant-temperature circuits for microbridge-sensor applications. *Transducers'91. Int. Conf. Solid-state Sensors and Actuators*. 471-474, 1991.
8. E. O. Doebelin, *Measurement Systems. Application and Design*, 4th ed., New York: McGraw-Hill Co., 1990.
9. A. R. Seacord and G. E. Plambeck. *Fiber optic ear thermometer*. U.S. Patent No. 5,167,235.
10. J. Fraden, *Optical system for an infrared thermometer*. U.S. Patent No. 5,368,038.
11. D.R. White and J.V. Nicholas, Emissivity and reflection error sources in radiation thermometry, in *Temperature, Its Measurement and Control in Science and Industry*. Vol. 6, Part 2, New York: American Institute of Physics, 1992, 917-922.
12. E.S. Hellman et al., *J. Crystal Growth*, 81, 38, 1986.
13. M.K. Weilmeyer et al., A new optical temperature measurement technique for semiconductor substrates in molecular beam epitaxy. *Can. J. Phys.*, 69, 422-426, 1991.
14. J. Fraden, Medical infrared thermometry (review of modern techniques), in *Temperature, Its Measurement and Control in Science and Industry*. Vol. 6, Part 2, New York: American Institute of Physics, 1992, 825-830.

## 32.7 Pyroelectric Thermometers

---

*Jacob Fraden*

### Pyroelectric Effect

The pyroelectric materials are crystalline substances capable of generating an electric charge in response to heat flow [1]. The pyroelectric effect is very closely related to the piezoelectric effect. The materials belong to a class of ferroelectrics. The name was given in association with ferromagnetics and is rather misleading because most such materials have nothing to do with iron.

A crystal is considered to be pyroelectric if it exhibits a spontaneous temperature-dependent polarization. Of the 32 crystal classes, 21 are noncentrosymmetric and 10 of these exhibit pyroelectric properties. Besides pyroelectric properties, all these materials exhibit some degree of piezoelectric properties as well — they generate an electric charge in response to mechanical stress.

Pyroelectricity was observed for the first time in tourmaline crystals in the 18th century (some claim that the Greeks noticed it 23 centuries ago). Later, in the 19th century, Rochelle salt was used to make pyroelectric sensors. A large variety of materials became available after 1915: KDP ( $\text{KH}_2\text{PO}_4$ ), ADP ( $\text{NH}_4\text{H}_2\text{PO}_4$ ),  $\text{BaTiO}_3$ , and a composite of  $\text{PbTiO}_3$  and  $\text{PbZrO}_3$  known as PZT. Presently, more than 1000 materials with reversible polarization are known. They are called ferroelectric crystals. Most important among them are triglycine sulfate (TGS) and lithium tantalate ( $\text{LiTaO}_3$ ).

A pyroelectric material can be considered a composition of a large number of minute crystallites, where each behaves as a small electric dipole. All these dipoles are randomly oriented, however, along a preferred direction. Above a certain temperature, known as the Curie point, the crystallites have no dipole moment.

When temperature of a pyroelectric material changes, the material becomes polarized. In other words, an electric charge appears on its surface. It should be clearly understood that the polarization occurs not as a function of temperature, but only as function of a *change in temperature* of the material. There are several mechanisms by which changes in temperature will result in pyroelectricity. Temperature changes can cause shortening or elongation of individual dipoles. It can also affect the randomness of the dipole orientations due to thermal agitation. These phenomena are called *primary pyroelectricity*. There is also *secondary pyroelectricity*, which, in a simplified way, can be described as a result of the piezoelectric effect; that is, a development of strain in the material due to thermal expansion.

The dipole moment,  $M$ , of the bulk pyroelectric sensor is:

$$M = \mu A h \quad (32.119)$$

**TABLE 32.19** Physical Properties of Pyroelectric Materials

Material	Curie temperature °C	Thermal conductivity W mK <sup>-1</sup>	Relative permittivity $\epsilon_r$	Pyroelectric charge coeff. C (m <sup>2</sup> K) <sup>-1</sup>	Pyroelectric voltage coeff. V (mK) <sup>-1</sup>	Coupling $k_p^2$ (%)
Single Crystals						
TGS	49	0.4	30	$3.5 \times 10^{-4}$	$1.3 \times 10^6$	7.5
LiTaO <sub>3</sub>	618	4.2	45	$2.0 \times 10^{-4}$	$0.5 \times 10^6$	1.0
Ceramics						
BaTiO <sub>3</sub>	120	3.0	1000	$4.0 \times 10^{-4}$	$0.05 \times 10^6$	0.2
PZT	340	1.2	1600	$4.2 \times 10^{-4}$	$0.03 \times 10^6$	0.14
Polymers						
PVDF polycrystalline layers	205	0.13	12	$0.4 \times 10^{-4}$	$0.40 \times 10^6$	0.2
PbTiO <sub>3</sub>	470	2 (monocrystal)	200	$2.3 \times 10^{-4}$	$0.13 \times 10^6$	0.39

*Note:* The above figures may vary depending on manufacturing technologies. From Reference [2].

where  $\mu$  = Dipole moment per unit volume  
 $A$  = Sensor's area  
 $h$  = Thickness

The charge,  $Q_a$ , which can be picked up by the electrodes, develops the dipole moment across the material:

$$M_0 = Q_a h \quad (32.120)$$

$M$  must be equal to  $M_0$ , so that:

$$Q_a = \mu A \quad (32.121)$$

As the temperature varies, the dipole moment also changes, resulting in an induced charge.

Thermal absorption can be related to a dipole change, so that  $\mu$  must be considered a function of both temperature,  $T_a$ , and an incremental thermal energy,  $\Delta W$ , absorbed by the material:

$$\Delta Q_a = A\mu(T_a, \Delta W) \quad (32.122)$$

The above equation shows the magnitude of electric charge resulting from absorption of thermal energy. To pick up the charge, the pyroelectric materials are fabricated in the shapes of a flat capacitor with two electrodes on opposite sides and the pyroelectric material serving as a dielectric.

## Pyroelectric Materials

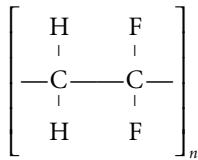
To select the most appropriate pyroelectric material, energy conversion efficiency should be considered. It is, indeed, the function of the pyroelectric sensor to convert thermal energy into electrical. "How effective is the sensor?" — is a key question in the design practice. A measure of efficiency is:  $k_p^2$  which is called the pyroelectric coupling coefficient [2, 3]. It shows the factor by which the pyroelectric efficiency is lower than the Carnot limiting value  $\Delta T/T_a$ . Numerical values for  $k_p^2$  are shown in [Table 32.19](#).

Table 32.19 shows that triglycine sulfate (TGS) crystals are the most efficient pyroelectric converters. However, for a long time they were quite impractical for use in sensors because of a low Curie temperature. If the sensor's temperature is elevated above that level, it permanently loses its polarization. In fact, TGS sensors proved to be unstable even below the Curie temperature, with the signal being lost quite spontaneously [4]. It was discovered that doping of TGS crystals with L-alanine (LATGS process patented by

Philips) during its growth stabilizes the material below the Curie temperature. The Curie temperature was raised to 60°C, which allows its use at the upper operating temperature of 55°C, which is sufficient for many applications.

Other materials, such as lithium tantalate and pyroelectric ceramics, are also used to produce pyroelectric sensors. Polymer films (KYNAR from AMP Inc.) have become increasingly popular for a variety of applications. During recent years, deposition of pyroelectric thin films has been intensively researched. Especially promising is the use of lead titanate (PbTiO<sub>3</sub>), which is a ferroelectric ceramic having both a high pyroelectric coefficient and a high Curie temperature of about 490°C. This material can be easily deposited on silicon substrates by the so called sol-gel spin casting deposition method [5].

In 1969, Kawai discovered strong piezoelectricity in the plastic materials, polyvinyl fluoride (PVF) and polyvinylidene fluoride (PVDF) [6]. These materials also possess substantial pyroelectric properties. PVDF is a semicrystalline polymer with an approximate degree of crystallinity of 50% [7]. Like other semicrystalline polymers, PVDF consists of a lamellar structure mixed with amorphous regions. The chemical structure contains the repeat unit of doubly fluorinated ethene CF<sub>2</sub>-CH<sub>2</sub>:



The molecular weight of PVDF is about 10<sup>5</sup>, which corresponds to about 2000 repeat units. The film is quite transparent in the visible and near-IR regions, and is absorptive in the far-infrared portion of the electromagnetic spectrum. The polymer melts at about 170°C. Its density is about 1780 kg m<sup>-3</sup>. PVDF is mechanically durable and flexible. In piezoelectric applications, it is usually drawn, uniaxially or biaxially, to several times its length. Elastic constants, for example, Young modulus, depend on this draw ratio. Thus, if the PVDF film was drawn at 140°C to the ratio of 4:1, the modulus value is 2.1 GPa; while for the draw ratio of 6.8:1, it was 4.1 GPa. Resistivity of the film also depends on the stretch ratio. For example, at low stretch, it is about 6.3 × 10<sup>15</sup> Ω cm, while for the stretch ratio 7:1 it is 2 × 10<sup>16</sup> Ω cm.

Since silicon does not possess pyroelectric properties, such properties can be added on by depositing crystalline layers of pyroelectric materials. The three most popular materials are zinc oxide (ZnO), aluminum nitride (AlN), and the so-called solid solution system of lead-zirconite-titanium oxides Pb(Zr,Ti)O<sub>3</sub> known as PZT ceramic, which is basically the same material used for fabrication of discrete piezoelectric and pyroelectric sensors. One of the advantages of using zinc oxide is the ease of chemical etching. The zinc oxide thin films are usually deposited on silicon by employing sputtering technology. Note, however, that silicon has a large coefficient of thermal conductivity. That is, its thermal time constant is very small (see below), so the pyroelectric sensors made with silicon substrates possess low sensitivity yet are capable of fast response.

## Manufacturing Process

Manufacturing of ceramic PZT elements begins with high-purity metal oxides (lead oxide, zirconium oxide, titanium oxide, etc.) in the form of fine powders having various colors. The powders are milled to a specific fineness, and mixed thoroughly in chemically correct proportions. In a process called “calcining,” the mixtures are then exposed to an elevated temperature, allowing the ingredients to react to form a powder, each grain of which has a chemical composition close to the desired final composition. At this stage, however, the grain does not yet have the desired crystalline structure.

The next step is to mix the calcined powder with solid and/or liquid organic binders (intended to burn out during firing) and mechanically form the mixture into a “cake” that closely approximates a shape of the final sensing element. To form the “cakes” of desired shapes, several methods can be used. Among them are pressing (under force of a hydraulic-powered piston), casting (pouring viscous liquid

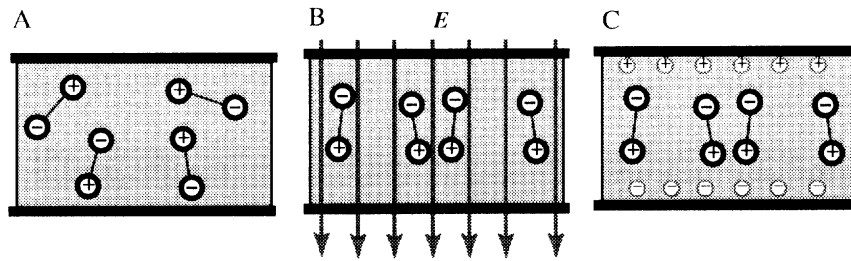


**FIGURE 32.65** Poling of a pyroelectric crystal in a strong electric field. The sensor must be stored and operated below the Curie temperature.

into molds and allowing to dry), extrusion (pressing the mixture through a die, or a pair of rolls to form thin sheets), and tape casting (pulling viscous liquid onto a smooth moving belt).

After the “cakes” have been formed, they are placed into a kiln and exposed to a very carefully controlled temperature profile. After burning out of organic binders, the material shrinks by about 15%. The “cakes” are heated to a red glow and maintained at that state for some time, which is called the “soak time,” during which the final chemical reaction occurs. The crystalline structure is formed when the material is cooled down. Depending on the material, the entire firing may take 24 h.

When the material is cold, contact electrodes are applied to its surface. This can be done by several methods. The most common are: fired-on silver (a silk-screening of silver-glass mixture and refiring), electroless plating (a chemical deposition in a special bath), and sputtering (an exposure to metal vapor in partial vacuum).

Crystallinities (crystal cells) in the material can be considered electric dipoles. In some materials, like quartz, these cells are naturally oriented along the crystal axes, thus giving the material sensitivity to stress. In other materials, the dipoles are randomly oriented and the materials need to be “poled” to possess piezoelectric properties. To give a crystalline material pyroelectric properties, several poling techniques can be used. The most popular poling process is thermal poling, which includes the following steps:

1. A crystalline material (ceramic or polymer film) that has randomly oriented dipoles (Figure 32.65A) is warmed to slightly below its Curie temperature. In some cases (for a PVDF film), the material is stressed. High temperature results in stronger agitation of dipoles and permits one to more easily orient them in a desirable direction.
2. The material is placed in strong electric field,  $E$ , (Figure 32.65B) where dipoles align along the field lines. The alignment is not total. Many dipoles deviate from the field direction quite strongly; however, statistically predominant orientation of the dipoles is maintained.
3. The material is cooled down while the electric field across its thickness is maintained.
4. The electric field is removed and the poling process is complete. As long as the poled material is maintained below the Curie temperature, its polarization remains permanent. The dipoles stay “frozen” in the direction that was given to them by the electric field at high temperature (Figure 32.65C). The above method is used to manufacture ceramic and plastic pyroelectric materials.

Another method, called a corona discharge poling, can be used to produce polymer piezo/pyroelectric films. The film is subjected to a corona discharge from an electrode at several million volts per centimeter of film thickness for 40 s to 50 s [8, 9]. Corona polarization is uncomplicated to perform and can be easily applied before electric breakdown occurs, making this process useful at room temperature.

The final operation in preparing the sensing element is shaping and finishing. This includes cutting, machining, and grinding. After the piezo (pyro) element is prepared, it is installed into a sensor’s housing, where its electrodes are bonded to electrical terminals and other electronic components.

After poling, the crystal remains permanently polarized; however, it remains electrically charged for a relatively short time. There is a sufficient amount of free carriers that move in the electric field setup

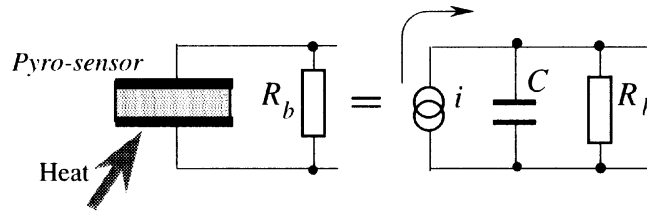


FIGURE 32.66 Pyroelectric sensor and its equivalent circuit.

inside the bulk material and there are plenty of charged ions in the surrounding air. The charge carriers move toward the poled dipoles and neutralize their charges (Figure 32.65C). Hence, after a while, the poled piezoelectric material becomes electrically discharged as long as it remains under steady-state conditions. When temperature changes and thermally induced stress develops, the balanced state is degraded and the pyroelectric material develops an electric charge. If the stress is maintained for a while, the charges again will be neutralized by the internal leakage. Thus, a pyroelectric material is responsive only to a changing temperature rather than to a steady level of it. In other words, a pyroelectric sensor is an ac device, rather than a dc device. Sometimes, it is called a *dynamic* sensor, which reflects the nature of its response.

### Pyroelectric Sensors

To make sensors, the pyroelectric materials are used in the form of thin slices or films with electrodes deposited on the opposite sides to collect the thermally induced charges (Figure 32.66). The pyroelectric detector is essentially a capacitor that can be charged by an influx of heat. The detector does not require any external electrical bias (excitation signal). It needs only an appropriate electronic interface circuit to measure the charge. Contrary to thermoelectrics (thermocouples), which produce a steady voltage when two dissimilar metal junctions are held at steady but different temperatures, pyroelectrics generate charge in response to a change in temperature. Since a change in temperature essentially requires propagation of heat, a pyroelectric device is a heat flow detector rather than a heat detector. Figure 32.66 shows a pyroelectric detector (pyro-sensor) connected to a resistor  $R_b$  that represents either the internal leakage resistance or a combined input resistance of the interface circuit connected to the sensor. The equivalent electrical circuit of the sensor is shown on the right. It consists of three components: (1) the current source generating a heat induced current,  $i$ , (remember that a current is a movement of electric charges), (2) the sensor's capacitance,  $C$ , and (3) the leakage resistance,  $R_b$ . Since the leakage resistance is very high and often unpredictable, an additional bias resistor is often connected in parallel with the pyroelectric material. The value of that resistor is much smaller than the leakage resistance, yet its typical value is still on the order of  $10^{10} \Omega$  (10 G $\Omega$ ).

The output signal from the pyroelectric sensor can be taken in the form of either charge (current) or voltage, depending on the application. Being a capacitor, the pyroelectric device is discharged when connected to a resistor,  $R_b$  (Figure 32.66). Electric current through the resistor and voltage across the resistor represent the heat flow-induced charge. It can be characterized by two pyroelectric coefficients [2]:

$$P_Q = \frac{dP_s}{dT} \quad \text{Pyroelectric charge coefficient} \quad (32.123)$$

$$P_V = \frac{dE}{dT} \quad \text{Pyroelectric voltage coefficient}$$

where  $P_s$  = Spontaneous polarization (which is the other way to say “electric charge”)

$E$  = Electric field strength

$T$  = Temperature in K

Both coefficients are related by way of the electric permittivity,  $\epsilon_r$ , and dielectric constant,  $\epsilon_0$ :

$$\frac{P_Q}{P_V} = \frac{dP_s}{dE} = \epsilon_r \epsilon_0 \quad (32.124)$$

The polarization is temperature dependent and, as a result, both pyroelectric coefficients in Equation 32.123 are also functions of temperature.

If a pyroelectric material is exposed to a heat source, its temperature rises by  $\Delta T$ , and the corresponding charge and voltage changes can be described by the following equations.

$$\Delta Q = P_Q A \Delta T \quad (32.125)$$

$$\Delta V = P_V h \Delta T \quad (32.126)$$

Remembering that the sensor's capacitance can be defined as:

$$C_e = \frac{\Delta Q}{\Delta V} = \epsilon_r \epsilon_0 \frac{A}{h} \quad (32.127)$$

then, from Equations 32.124, 32.126, and 32.127, it follows that:

$$\Delta V = P_Q \frac{A}{C_e} \Delta T = P_Q \frac{\epsilon_r \epsilon_0}{h} \Delta T \quad (32.128)$$

It is seen that the peak output voltage is proportional to the sensor's temperature rise and pyroelectric charge coefficient and inversely proportional to its thickness.

Figure 32.67 shows a pyroelectric sensor whose temperature,  $T_0$ , is homogeneous over its volume. Being electrically polarized, the dipoles are oriented (poled) in such a manner as to make one side of the material positive and the opposite side negative. However, under steady-state conditions, free charge carriers (electrons and holes) neutralize the polarized charge and the capacitance between the electrodes does not appear to be charged. That is, the sensor generates zero charge. Now, assume that heat is applied to the bottom side of the sensor. Heat can enter the sensor in a form of thermal radiation that is absorbed by the bottom electrode and propagates toward the pyroelectric material via the mechanism of thermal conduction. The bottom electrode can be given a heat-absorbing coating, such as goldblack or organic paint. As a result of heat absorption, the bottom side becomes warmer (the new temperature is  $T_1$ ), which causes the bottom side of the material to expand. The expansion leads to flexing of the sensor, which, in turn, produces stress and a change in dipole orientation. Being piezoelectric, stressed material generates electric charges of opposite polarities across the electrodes. Hence, one can regard secondary pyroelectricity as a sequence of events: a thermal radiation — a heat absorption — a thermally induced stress — an electric charge.

The temperature of the sensor  $T_s$  is a function of time. That function is dependent on the sensing element: its density, specific heat, and thickness. If the input thermal flux has the shape of a step function of time, for the sensor freely mounted in air, the output current can be approximated by an exponential function, so that:

$$i = i_0 e^{-t/\tau_T} \quad (32.129)$$

where  $i_0$  = Peak current

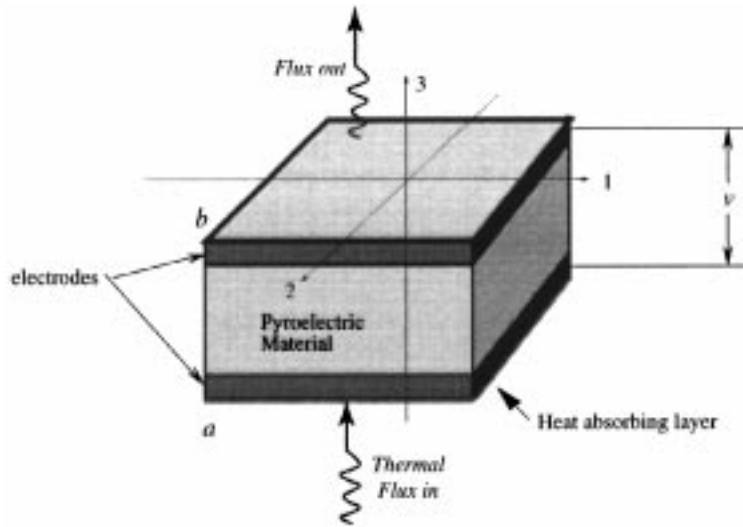


FIGURE 32.67 Pyroelectric sensor has two electrodes at the opposite sides of the crystalline material. Thermal radiation is applied along axis 3.

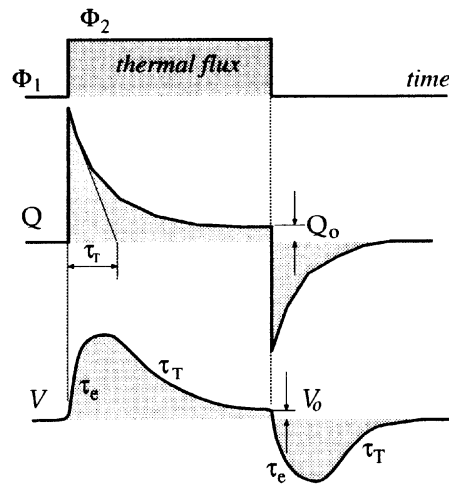


FIGURE 32.68 Response of a pyroelectric sensor to a thermal step function. The magnitudes of charge  $Q_0$  and voltage  $v_0$  are exaggerated for clarity.

Figure 32.68 shows timing diagrams for a pyroelectric sensor when it is exposed to a step function of heat. It is seen that the electric charge reaches its peak value almost instantaneously, and then decays with a *thermal time constant*,  $\tau_T$ . This time constant is a product of the sensor's thermal capacitance,  $C$ , and thermal resistance,  $r$ , which defines a thermal loss from the sensing element to its surroundings:

$$\tau_T = Cr = cAhr \quad (32.130)$$

where  $c$  = Specific heat of the sensing element.

The thermal resistance  $r$  is a function of all thermal losses to the surroundings through convection, conduction, and thermal radiation. For low-frequency applications, it is desirable to use sensors with  $\tau_T$  as large as practical; while for the high-speed applications (e.g., to measure the power of laser pulses), a

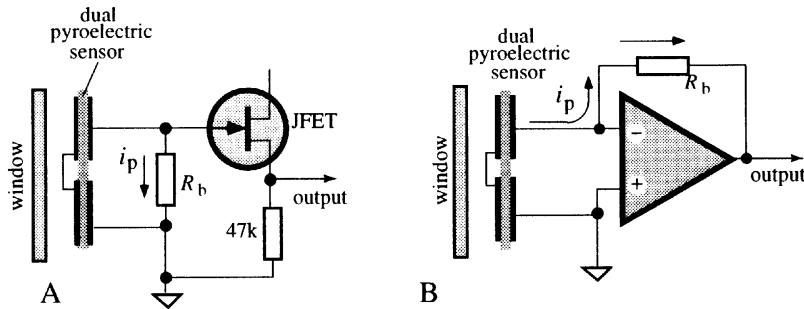


FIGURE 32.69 Interface circuits for pyroelectric sensors operating in voltage (A) and current (B) modes.

thermal time constant should be dramatically reduced. For that purpose, the pyroelectric material can be laminated with a heat sink: a piece of aluminum or copper.

When a heat flow exists inside the pyroelectric crystal, there is an outflow of heat from the opposite side of the crystal, as shown in Figure 32.67. Thermal energy enters the pyroelectric material from side *a*. Since the other side *b* of the sensor faces a cooler environment, part of the thermal energy leaves the sensor and is lost to its surroundings. Because the sides *a* and *b* face objects of different temperatures (one is the temperature of a target and the other is the temperature of the environment), a continuous heat flow exists through the pyroelectric material. As a result, in Figure 32.68, charge *Q* and voltage *V* do not completely return to zero, no matter how much time has elapsed. Electric current generated by the pyroelectric sensor has the same shape as the thermal current through its material. An accurate measurement can demonstrate that as long as the heat continues to flow, the pyroelectric sensor will generate a constant voltage  $V_0$  whose magnitude is proportional to the heat flow.

## Applications

The pyroelectric sensors are useful whenever changing thermal radiation or heat flow need to be measured. Examples are motion detectors for the security systems and light control switches [1], instant medical infrared thermometers, and laser power meters. Depending on the application, a pyroelectric sensor can be used either in *current* or in *voltage* mode. The voltage mode (Figure 32.69A) uses a voltage follower with a very high input resistance. Hence, JFET and CMOS input stages are essential. As a rule, in the voltage mode sensor, the follower is incorporated inside the same package along with the element and bias resistor. Advantages of the voltage mode are simplicity and lower noise. The disadvantages are slower speed response due to high capacitance of the sensor (typically on the order of 30 pF) and other influences of the sensor capacitance on the quality of output voltage. The output voltage of the follower is shown in Figure 32.68 (*V*). It is seen that it rises slowly with electric time constant  $\tau_e$  and decays with thermal time constant  $\tau_T$ .

The current mode uses an electronic circuit having a “virtual ground” as its input (Figure 32.69B). An advantage of this circuit is that the output signal is independent of the sensor’s capacitance and, as a result, is much faster. The signal reaches its peak value relatively fast and decays with thermal time constant  $\tau_T$ . The output voltage  $V_0$  has the same shape of charge *Q* in Figure 32.68. The disadvantages of the circuit are higher noise (due to wider bandwidth) and higher cost.

Note that Figure 32.69 shows dual pyroelectric sensors, where two sensing elements are formed on the same crystalline plate by depositing two pairs of electrodes. The electrodes are connected in a serial-opposite manner. If both sensors are exposed to the same magnitude of far-infrared radiation, they will produce nearly identical polarizations and, due to the opposite connection, the voltage applied to the input of the transistor or the current passing through resistor  $R_b$  will be nullified. This feature allows for cancellation of undesirable common-mode input signals in order to improve stability and reduce noise. Signals that arrive only to one of the elements will not be canceled.

## References

1. J. Fraden, *Handbook of Modern Sensors*, 2nd ed., Woodbury, NY: AIP Press, 1997.
2. H. Meixner, G. Mader, and P. Kleinschmidt, Infrared sensors based on the pyroelectric polymer polyvinylidene fluoride (PVDF), *Siemens Forsch. Entwickl. Ber.*, 15(3), 105-114, 1986.
3. P. Kleinschmidt, Piezo- und pyroelektrische Effekte. Heywang, W., ed., in *Sensorik*, Kap. 6: New York: Springer, 1984.
4. Semiconductor Sensors, *Data Handbook*, Philips Export B.V, 1988.
5. C. Ye, T. Tamagawa, and D.L. Polla, Pyroelectric PbTiO<sub>3</sub> thin films for microsensor applications, *Transducers'91. Int. Conf. Solid-State Sensors and Actuators*. 904-907, 1991.
6. H. Kawai, The piezoelectricity of poly(vinylidene fluoride), *Jap. J. Appl. Phys.*, 8, 975-976, 1969.
7. A. Okada, Some electrical and optical properties of ferroelectric lead-zirconite-lead-titanate thin films, *J. Appl. Phys.*, N. 48, 2905, 1977.
8. P.F. Radice, *Corona Discharge poling process*, U.S. Patent No. 4,365,283; 1982.
9. P.D. Southgate, *Appl. Phys. Lett.*, 28, 250, 1976.

## 32.8 Liquid-In-Glass Thermometers

---

*J.V. Nicholas*

The earliest form of thermometer, known as a thermoscope, was a liquid-in-glass thermometer that was open to the atmosphere and thus responded to pressure. By sealing a thermoscope so that it responded only to temperature, the modern form of a liquid-in-glass thermometer resulted. As a temperature sensor, its use dominated temperature measurement for at least 200 years. Liquid-in-glass thermometers had a profound effect on the development of thermometry and, in popular opinion, they are the only “real” thermometers! Liquid-in-glass thermometer sensors were developed in variety to fill nearly every niche in temperature measurement from  $-190^{\circ}\text{C}$  to  $+600^{\circ}\text{C}$ , including the measurement of temperature differences to a millikelvin. In spite of the fragile nature of glass, the popularity of these thermometers continues because of the chemical inertness of the glass, as well as the self-contained nature of the thermometer.

Measurement sensor designers are unlikely to develop their own liquid-in-glass thermometers, but many will use them to check the performance of a new temperature sensor. The emphasis in this chapter section will therefore be on the use of mercury-in-glass thermometers — the most successful liquid-in-glass thermometer — as calibration references. Mercury-in-glass thermometers provide a stable temperature reference to an accuracy of  $0.1^{\circ}\text{C}$ , provided they are chosen and used with care. The extra requirements to achieve higher accuracy are indicated, but are beyond the scope of this section.

The trend is, however, to move away from mercury-in-glass thermometers for specialized uses (in particular, where the risk from glass or mercury contamination is not acceptable; for example, in the food or aviation industries). Other forms of temperature sensors described in this handbook are more suitable.

### General Description

A common form of mercury-in-glass is a solid-stem glass thermometer illustrated in [Figure 32.70](#). The other major form of liquid-in-glass thermometer is the enclosed scale thermometer, for which the general principles discussed will also apply.

There are four main parts to the liquid-in-glass thermometer:

- The bulb is a thin glass container holding the bulk of the [thermometric liquid](#). The glass must be of suitable type and properly annealed. The thinness is essential for good thermal contact with the medium being measured, but it can result in instabilities due to applied stress or sudden shock.

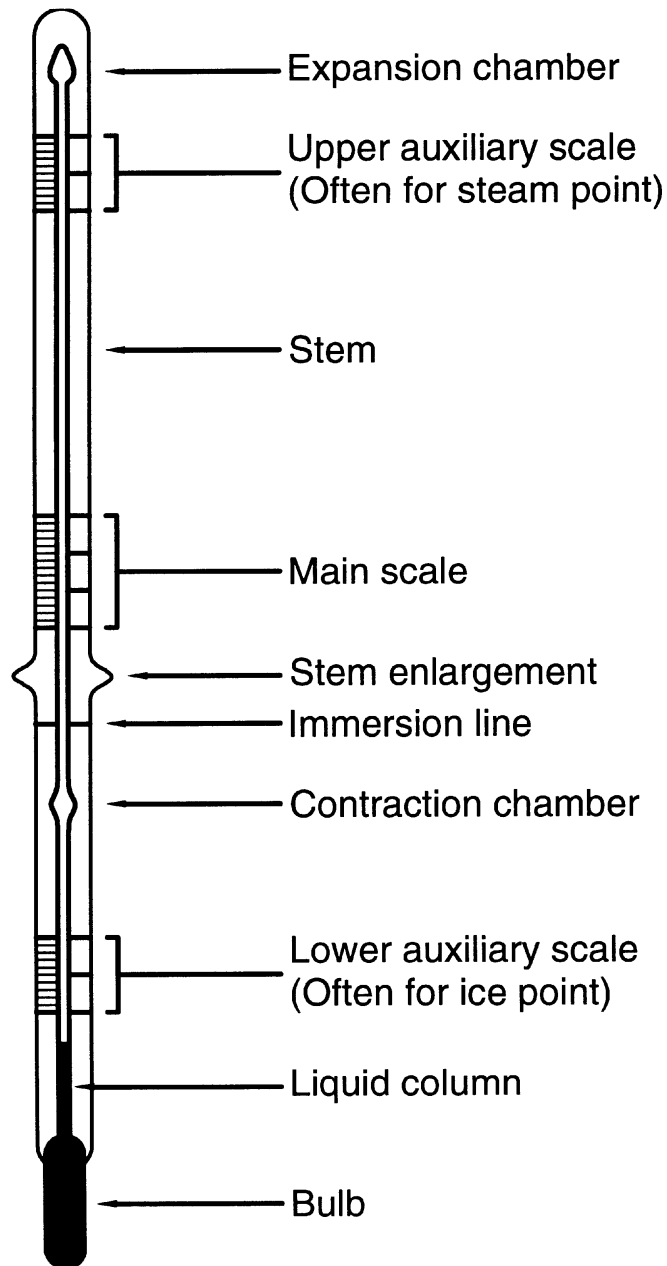


**FIGURE 32.70** The main features of a solid-stem glass thermometer. The thermometer can have an enlargement in the stem or an attachment at the end of the stem to assist in the positioning of the thermometer. Thermometers will display several of these features, but seldom all of them.

Some lower-accuracy, general-purpose thermometers are made with a thicker glass bulb to lower the risk of breakage.

- The stem is a glass capillary. Again, a suitable glass is necessary and may differ from that of the bulb. The bore can be gas-filled or vacuous. The volume of the bore must be somewhat smaller than the volume of the bulb for good sensitivity. In addition, the bore must be smooth, with a uniform cross section.

- The liquid is usually mercury for best precision, or an organic liquid for lower temperature ranges.
- The markings are usually etched or printed onto the stem. The markings include the scale, to allow direct reading of the temperature, as well as other important information.

Figure 32.70 illustrates the main parts of a mercury-in-glass thermometer, along with a nomenclature for other features commonly found. Not all of the features will be found on all thermometers.

The operation of liquid-in-glass thermometers is based on the expansion of the liquid with temperature; that is, the liquid acts as a transducer to convert thermal energy into a mechanical form. As the liquid in the bulb becomes hotter, it expands and the liquid is forced up the capillary stem. The temperature of the bulb is indicated by the position of the top of the mercury column with respect to the marked scale. The flattest part of the liquid meniscus is used as the indicator: for mercury, this is the top of the curve; for organic liquids, the bottom.

The thermometers appear to have a simplicity about them, but this is lost when accurate measurements are required. By accuracy, we mean any reading where the temperature needs to be known to within 1°C or better. The chief cause of inaccuracy is that not all of the liquid is at the required temperature due to its necessary presence in the stem. Thus, the thermometer is also sensitive to the stem temperature. The main advantage of a liquid-in-glass thermometer is that it is self-contained; but this means that the thermometer stem has to be seen to read the scale. Even in a well-designed apparatus, a good part of the stem will not be at the temperature of the bulb. For example, with a bulb immersed in boiling water and the entire stem outside, an error of 1°C results from the cooler stem. Correction for this error can be incorporated in the scale of a partial immersion thermometer, or the error can be corrected with a chart of stem corrections.

The next most significant cause of error comes from the glass, a substance with complex mechanical properties. Like mercury, it expands rapidly on heating but does not contract immediately on cooling. This produces a hysteresis which, for a good glass, is about 0.1% of the temperature change. A good, well-annealed thermometer glass will relax back over a period of days. An ordinary glass might never recover its shape. Besides this hysteresis, the glass bulb undergoes a secular contraction over time; that is, the thermometer reading increases with age, but fortunately the effect is slow and calibration checks at the [ice point](#), 0°C, can correct for it.

A bewildering number of types of liquid-in-glass thermometers are available, with many of the variations being designed with different dimensions and temperature ranges to suit specific applications.

For best performance, solid-stem mercury-in-glass thermometers should be restricted to operation over the maximum range –38 °C to 250°C. The purchase should be guided by a specification as published by a recognized standards body. Such bodies include the International Standards Organisation (ISO) [1]; the American Society for Testing and Materials (ASTM) [2]; the British Standards Institute (BS) [3]; or the Institute for Petroleum (IP). Be aware that some type numbers are the same, yet may refer to different thermometers, such as in the IP and ASTM ranges. Make sure the specification body is referred to; for example, an order for a 16C thermometer could result in either an ASTM 10C, the equivalent of an IP 16C, or an IP 61C, the equivalent of ASTM 16C.

One's choice of thermometer will most probably be a compromise between the best range, scale division, and length for the purpose. If good precision is required, then the thermometer range will be constrained to avoid extremely long and unwieldy thermometers. [Table 32.20](#) gives the specification for precision thermometers based on the compromise as seen by the ASTM [2]. The cost of these thermometers depends on the range and varies from \$50 to \$180 at 1996 prices. The best precision for the ASTM liquid-in-glass thermometers is around 0.1°C, with the thermometers supplied being accurate to one scale division. Consult the references at the end of this chapter section if higher-resolution thermometers are required. As a rule, choose thermometers subdivided to the accuracy desired, and do not rely on visual interpolation to increase the accuracy. If relying heavily on interpolation, then a better choice of thermometer should be made.

[Table 32.20](#) has thermometers with an ice point either in the main scale or as an auxiliary scale. The ice point is a very convenient way to check on the on-going performance of a thermometer, and without it, more expensive time-consuming procedures may be needed.

**TABLE 32.20** Summary of Requirements for ASTM Precision Thermometers

ASTM Thermometer Number	Range (°C)	Maximum length (mm)	Graduation at each (°C)	Maximum error (°C)
62C	-38 to +2	384	0.1	0.1
63C	-8 to +32	384	0.1	0.1
64C	-0.5 to +0.5 and 25 to 55	384	0.1	0.1
65C	-0.5 to +0.5 and 50 to 80	384	0.1	0.1
66C	-0.5 to +0.5 and 75 to 105	384	0.1	0.1
67C	-0.5 to +0.5 and 95 to 155	384	0.2	0.2
68C	-0.5 to +0.5 and 145 to 205	384	0.2	0.2
69C	-0.5 to +0.5 and 195 to 305	384	0.5	0.5
70C	-0.5 to +0.5 and 295 to 405	384	0.5	0.5

**TABLE 32.21** Working Range of Some Thermometric Liquids and Their Apparent Thermal Expansion Coefficient in Thermometer Glasses Around Room Temperature

Liquid	Typical apparent expansion coefficient (°C <sup>-1</sup> )	Possible temperature range (°C)
Mercury	0.00016	-35 to 510
Ethanol	0.00104	-80 to 60
Pentane	0.00145	-200 to 30
Toluene	0.00103	-80 to 100

## Liquid Expansion

The equation that best describes the expansion of the mercury volume is:

$$V = V_0(1 + \alpha t + \beta t^2) \quad (32.131)$$

where  $V_0$  = Volume of mercury at 0°C

$\alpha$  and  $\beta$  = Coefficients of thermal expansion of mercury, with

$$\alpha = 1.8 \times 10^{-4} \text{°C}^{-1}$$

$$\beta = 5 \times 10^{-8} \text{°C}^{-2}$$

See [Table 32.21](#) for the expansion coefficients of other liquids and their range of use.

Equation 32.131 is the ideal equation for a mercury-in-glass thermometer. In practice, several factors modify the ideal behavior because of the way in which the thermometers are constructed.

Because the glass of a mercury-in-glass thermometer also expands, it is the apparent expansion coefficient due to the differential expansion of the mercury with respect to the glass that is of interest. Glass used in a typical thermometer has a value of  $\alpha = 2 \times 10^{-5} \text{°C}^{-1}$ , about 10% that of mercury. Hence, both the glass and the mercury act as temperature transducers and thus justify the description “mercury-in-glass.”

The mercury also serves as the temperature indicator in the stem and consequently might not be at the same temperature as the mercury in the bulb. While this effect is small for mercury, where the bulb volume is 6250 times the volume of the mercury in a 1°C length of the capillary stem, thermometers used in partial immersion often need correcting.

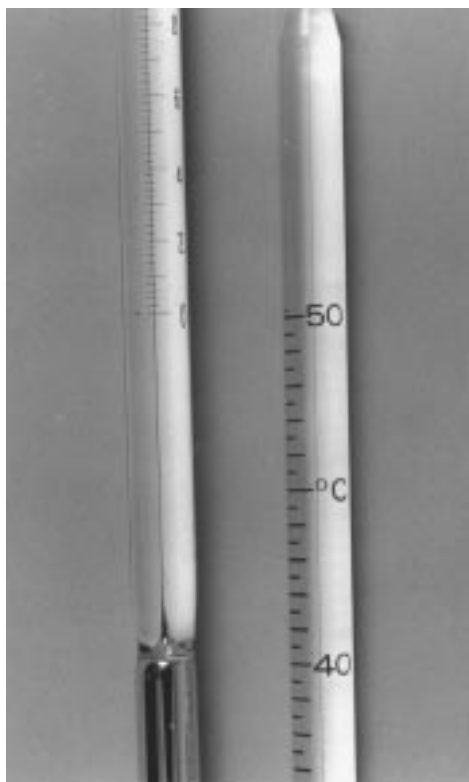


**FIGURE 32.71** Calibration marks are usually scratched on at both ends of a thermometer's scale to locate the ruling of the scale. Left: A good quality thermometer. The calibration mark is immediately alongside the 0°C mark. Right: A general-purpose thermometer. Here, the calibration mark is about  $\frac{1}{4}$  scale division above the 50°C mark. Since it is a cheaper thermometer, the manufacturer is content to locate the scale within the  $\frac{1}{4}$  scale division, and this would vary from thermometer to thermometer in the same batch. Readings could be expected to be accurate to about one scale division, 0.5°C in this instance.

The bore in the stem needs to be smooth and uniform. An allowed departure from uniformity is a contraction chamber that, by taking up a volume of the expanding mercury, allows the overall length of the thermometer to be kept a reasonable size. The chamber shape must be very smooth to prevent bubbles of gas being trapped. An auxiliary scale is usually added for the ice point if a contraction chamber is used.

The marked scale allows the user to read the column length as a temperature. For a well-made thermometer, the change in length is proportional to the change in volume and hence to the temperature, as per Equation 32.131. In order to make the scale, the manufacturer first places “calibration” marks on the thermometer stem, as shown in Figure 32.71. Depending on the range and accuracy, more than two calibration marks can be used and, thus, the thermometer stem is divided into segments. A ruling engine is then used to rule a scale between each pair of marks, with careful alignments between the adjacent segments if they occur. The scale rulings will be spaced to approximate Equation 32.131 to the accuracy expected for the thermometer type. A good indicator of the quality of a thermometer is how close these calibration scratches are to the scale markings.

Because of the segmented ruling, it pays to check that the scale markings are uniform in appearance with no obvious glitches. Quite marked discontinuities in the scale are sometimes found. The markings are individual to each thermometer and the total scale length can vary from thermometer to thermometer. This can be an inconvenience if a thermometer has to be replaced; but fortunately, most quality thermometer specifications restrict the amount of variation permissible.

**TABLE 32.22** Time Constants for a Mercury-In-Glass Thermometer with a 5-mm Diameter Bulb

Medium	Still (s)	0.5 m s <sup>-1</sup> flow (s)	Infinite flow velocity (s)
Water	10	2.4	2.2
Oil	40	4.8	2.2
Air	190	71	2.2

## Time-Constant Effects

The time constant is determined almost entirely by the diameter of the bulb because heat must be conducted from the outside to the center of the bulb. A typical bulb of diameter 5 mm has a relatively short time constant. The length of the bulb is then determined by the sensitivity required of the thermometer, given that there is a minimum useful diameter for the capillary bore.

The choice of bore diameter is a compromise involving several error effects. A large-diameter bore requires a larger volume bulb to achieve a given resolution, thus increasing the thermal capacity. A small-diameter bore not only becomes difficult to read but also suffers from stiction — the mercury moving in fits and starts due to the surface tension between the mercury and the bore wall. Stiction should be kept less than 1/5 of a scale division.

Table 32.22 gives the  $1/e$  time constants in various media for a 5-mm diameter bulb. Time constants for other diameters can be estimated by scaling the time in proportion to the diameter. The table clearly indicates that the thermometer is best used with flowing (or stirred) fluids.

## Thermal Capacity Effects

Glass thermometers are bulky and have considerable mass, especially high-precision thermometers that have a long bulb. The high thermal mass or heat capacity can upset temperature measurements, making high precision difficult. Inappropriate use of liquid-in-glass thermometers occurs when the thermometer is too massive to achieve the precision required. Preheating the thermometer can alleviate the worst of the problem. For higher precision and low mass, choose a platinum resistance thermometer or thermistor instead.

Simple estimates of the heat requirements are made by measuring the volume of thermometer immersed, and assuming that 2 J are required to raise 1 cm<sup>3</sup> of the thermometer volume (glass or mercury) by 1°C.

## Separated Columns

A common problem is for a part of the thermometric liquid in the stem to become separated from the main volume. While this will show as an ice point shift, it is still important to make a simple visual check when using the thermometer.

With organic liquids, the problem might be more difficult to identify because liquid adheres to the surface of the capillary and may not be visible. Spirit thermometers need to be held vertically to allow the thermometric liquid to drain down. Warm the top of the thermometer to prevent condensation of any vapor. Allow time for drainage of the liquid in the thermometer if the temperature is lowered quickly (approximately 3 min per centimeter). Cool the bulb first in order to keep the viscosity of the liquid in the stem low for better drainage.

For mercury, the separation is usually visible. Two causes can be identified: boil-off and mechanical separation (Figure 32.72).

To help retard the boil-off of mercury vapor at high temperatures (e.g., above 150°C), the capillary tube is filled with an inert gas when manufactured. Usually, dry nitrogen is used under pressure to prevent

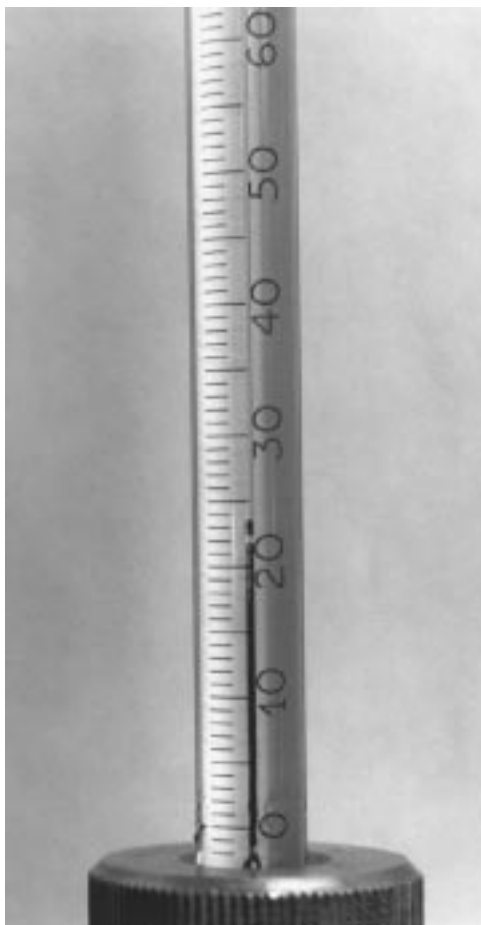


**FIGURE 32.72** A typical break in the mercury column of a thermometer.

oxidation of the mercury. The expansion chamber must be kept cooler than the bulb to prevent a high pressure build-up. The high pressure can permanently distort the bulb even if rupture does not occur.

Mechanical separation of the liquid column is, unfortunately, a common occurrence, particularly after shipment. A gas fill will help prevent this separation but, conversely, the gas makes it more difficult to rejoin. There is also a risk of trapped gas bubbles in the bulb or expansion chambers and careful inspection is needed to locate them. A vacuum in the capillary tube will give rise to more breaks, but they are easily rejoined.

With care, it is often possible to rejoin the column and still have a viable thermometer. However, it must be realized that attempts to join a broken column could also result in the thermometer being discarded if the procedure is not successful. Column breaks that occur only when the thermometer is heated often require that the thermometer be discarded.

Various procedures for joining a broken mercury column can be tried. The procedures below are given in order of preference.

- Lightly tap the thermometer while holding it vertically. This may work for a vacuum thermometer.
- Apply centrifugal force, but avoid a flicking action, and be careful to avoid striking anything. This can be best done by holding the bulb alongside the thumb, protecting it with the fingers, and with the stem along the arm. Raise the arm above the head and bring it down quickly to alongside the leg.
- If both the above are unsuccessful, a cooling method can be attempted. This method relies on sufficient cooling of the bulb for all the mercury to contract into the bulb, leaving none in the

stem. The column should be rejoined when it has warmed to room temperature. Carry out the warming slowly so that all the mercury is at the same temperature. More than one attempt might be needed. The first two methods might also need to be applied to assist movement of the mercury.

Three cooling mediums readily available are:

1. Salt, ice, and water (to  $-18^{\circ}\text{C}$ )
2. Dry ice, i.e., solid  $\text{CO}_2$  ( $-78^{\circ}\text{C}$ )
3. Liquid nitrogen ( $-196^{\circ}\text{C}$ )

The last two refrigerants require more care as they could freeze the mercury. An excessive cooling rate could stress the glass. **Cold burns to the user could also occur.**

If the broken column has been successfully rejoined, then an ice point (or other reference point) check should be made. If the reading is the same as obtained previously, then the join can be considered completely successful and the thermometer ready for use. (It is essential to keep written records here.) However, a significant ice-point shift indicates that the join was not successful and that the thermometer should be discarded. If the ice-point shift is within that specified for the thermometer type, then treat the thermometer with suspicion until there is evidence of long-term stability, i.e., no significant ice-point changes after use.

## Immersion Errors

It was previously mentioned that problems are expected if not all the liquid in a liquid-in-glass thermometer is at the same temperature as the bulb. Because the scale must be read visually, liquid-in-glass thermometers are used at various immersion depths, which results in different parts of the thermometric liquid being at different temperatures. In addition, the clutter around an apparatus often necessitates the thermometer being placed in a nonideal position.

Three distinct immersion conditions are recognized for a liquid-in-glass thermometer, and each requires a different error treatment. [Figure 32.73](#) illustrates the three conditions.

- *Complete immersion:* By definition, if the complete bulb and stem are immersed at the same temperature, the thermometer is completely immersed. This condition is not common, except at room temperature, and should be avoided at higher temperatures. High pressure build-up in the thermometer can cause it to rupture, spreading deadly mercury vapor throughout the laboratory. Laboratories where there is a danger of mercury exposure to high temperatures should be kept well ventilated. In other words, DO NOT put a mercury thermometer completely inside an oven to measure the temperature. Specialized applications that use complete immersion, take into account pressure effects on the thermometers.
- *Total immersion:* Total immersion applies to the situation where all the thermometric liquid, i.e., all the mercury in the bulb, the contraction chamber, and the stem, is at the temperature of interest. The remaining portion of the stem will have a temperature gradient to room temperature (approximately). Especially at high temperatures, the expansion chamber should be maintained close to room temperature to avoid pressure build-up. A very small part of the mercury column can be outside the region of interest, to allow visual readings to be made. The error introduced by this can be estimated by the procedures given below for partial-immersion thermometers. Obviously, the thermometer will have to be moved to allow a range of temperatures to be measured. Total-immersion thermometers are generally calibrated at total immersion and therefore do not need additional corrections.
- *Partial immersion:* One way around the problem of scale visibility and the need to move the thermometer is to immerse the thermometer to some fixed depth so that most, but not all, of the mercury is at the temperature of interest. The part of the mercury column not immersed is referred to as the **emergent column**. Corrections will be needed to compensate for the error arising from the emergent column not being at the same temperature as the bulb. Many thermometers are

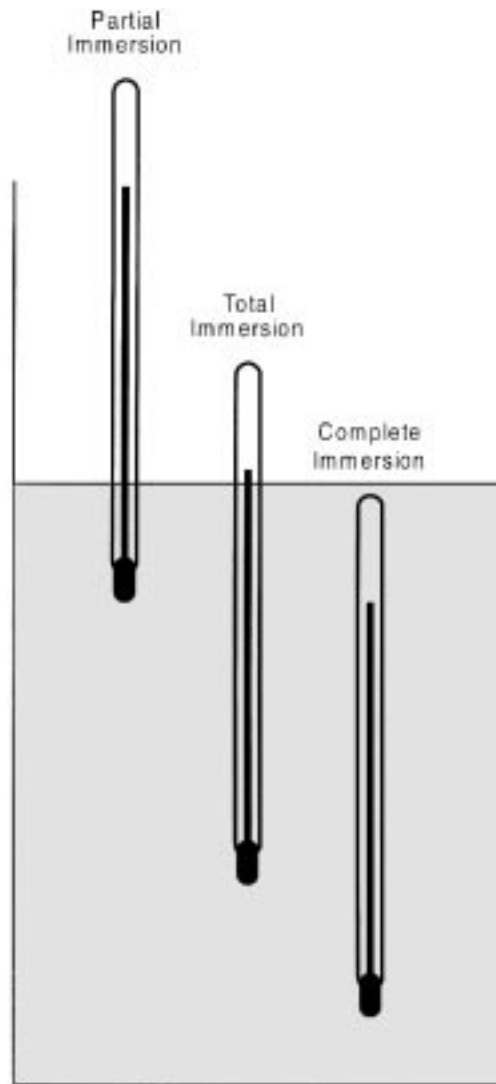


**FIGURE 32.73** Three types of immersion conditions used for liquid-in-glass thermometers. The preferred immersion condition is usually marked as a line or distance on the stem for partial-immersion thermometers or is given by the thermometer specification.

designed and calibrated for partial immersion and are marked accordingly on the stem with an immersion depth or an immersion line (see Figure 32.70).

A partial-immersion thermometer is properly defined when the temperature profile of the emergent column is also specified. Usually, an average stem temperature is quoted to represent the temperature profile of the emergent column. Thermometer specifications can define the expected stem temperature for a set of test temperatures, but they do not usually define stem temperatures for all possible readings.

A measure of the stem temperature is required if the accuracy of the thermometer reading is to be assessed. The traditional way to measure the stem temperature is with a Faden thermometer. These are mercury-in-glass thermometers with a very long bulb, and various bulb lengths available. The bulb is mounted alongside the part of the stem containing the emergent column with the bottom of the bulb in the fluid. An average stem temperature is obtained as indicated by the Faden thermometer. Other ways of measuring the temperature profile are to use thermocouples along the length of the thermometer, or

even several small mercury-in-glass thermometers. The stem temperature can be calculated as a simple average; but strictly speaking, it should be a length-weighted average.

Because the measured stem temperature might not be the same as that given on the calibration certificate, it is necessary to make corrections for the difference. For partial immersion thermometers, the true temperature reading  $t$  is given by:

$$t = t_i + N \times (t_2 - t_1) \times k \quad (32.132)$$

where  $t_i$  = Indicated temperature

$N$  = Length of emergent column expressed in degrees, as determined by the thermometer scale

$t_2$  = Mean temperature of the emergent column when calibrated (i.e., the stem temperature on a certificate for partial immersion or the thermometer reading for a total-immersion certificate)

$t_1$  = Mean temperature of the emergent column in use

$k$  = Coefficient of apparent expansion of the thermometric liquid used in the glass of which the thermometer stem is made

See [Table 32.21](#) for suitable values to use for normal temperature ranges.

The use of Equation 32.132 with typical  $k$  values from [Table 32.21](#) is estimated to give a 10% accuracy for the correction. Consequently, the correction is a major source of uncertainty for large temperature differences.

[Figure 32.74](#) gives a chart derived from Equation 32.132 for mercury thermometers that enables the stem correction to be determined graphically. One should become familiar enough with it to make quick estimates in order to determine whether the immersion condition error is significant and therefore needs correction.

Thermometers are usually calibrated at their stated immersion conditions and the actual stem temperatures during calibration are measured and quoted on the certificate. In many applications, a thermometer is used for a standard test method (such as specified by the ASTM or IP). For these instances, the expected stem temperature is specified and there is no requirement for the stem temperature to be measured. The user will, however, need to adjust the certificate correction terms to the immersion conditions of the specification in order to see that the thermometer corrections meet the appropriate quality criteria.

The chart of [Figure 32.74](#) is useful, either to find corrections or to show faults with a particular measurement method. For example, consider the case of measuring boiling water in a beaker with a total-immersion thermometer. The thermometer is too long to immerse and the water level is around the 20°C mark. The emergent column is therefore 80°C long and one assumes that the stem is close to room temperature of 20°C, resulting in an 80°C temperature difference from calibration conditions. On the chart, one finds that the intersection of the 80°C emergent line and the 80°C difference line gives a correction value of just over 1°C. If this value is unacceptable, then clearly a redesign of the measurement method is warranted. More detailed examples can be found in the text of Nicholas and White [5].

## Organic Liquids

Thermometers with organic liquids have three possible uses:

- To measure temperatures below –38°C
- In situations where mercury is to be avoided
- For inexpensive thermometers

The utility of spirit thermometers is limited because of the lower achievable accuracy, the high nonlinearities, and the volatile nature of the liquids. Organic-liquid thermometers are also difficult to read because of the very clear liquid and concave meniscus. However, the use of a suitable dye and wide bore

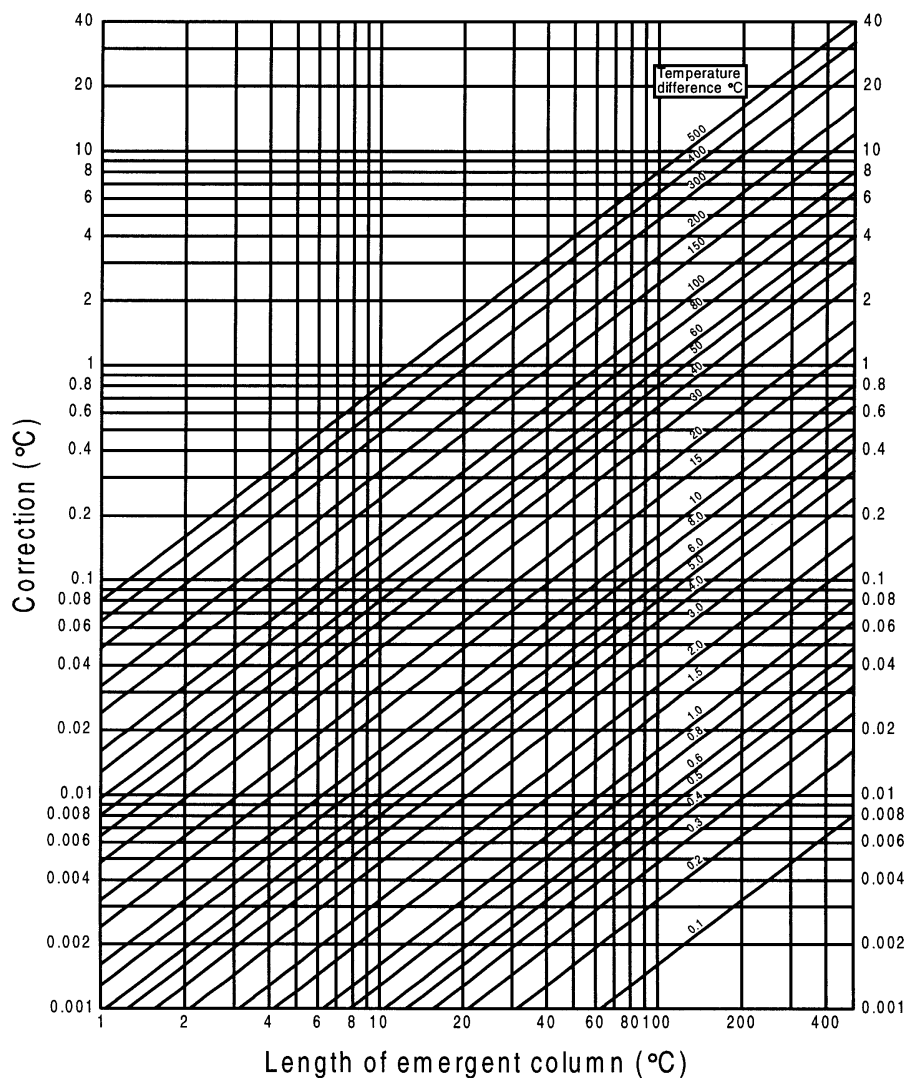


FIGURE 32.74 Chart of stem exposure corrections for mercury-in-glass thermometers with  $k = 0.00016^{\circ}\text{C}^{-1}$ .

can give them as good a readability as mercury. Follow the recommendations of the section on Separated Columns and the section on Storage to get the best result from organic-liquid thermometers.

### Storage

Most mercury-in-glass thermometers can be stored horizontally on trays in cabinets, care being taken to avoid any weight or pressure on the bulbs (one reason for the horizontal position). Avoid vibration. Corrugated cardboard, or similar material, can be used as a liner for a tray to prevent the thermometers from rolling.

Thermometers whose main range is below  $0^{\circ}\text{C}$  are better stored vertically, bulb down, in a cool place, but do not rest the thermometer on its bulb. This particularly applies to organic-liquid thermometers, which also should be shielded from light sources, as ultraviolet radiation can often degrade the liquid. If the top of the bore of a spirit thermometer is kept at a slightly higher temperature than the rest of the thermometer, then the volatile liquid will not condense in the expansion chamber.

## High Accuracy

If a higher accuracy than 0.1°C is sought, the user will need to not only consult the references [4, 5], but also consult their calibration laboratory. Not all authorities give the same advice on how to achieve higher accuracy. It is important to apply very consistent procedures in line with the calibration. Below are the more important factors that will need further consideration.

Control of the *hysteresis effect* is important. The thermometers should not be used for 3 days after being exposed to elevated temperatures. Residual effects may be detectable for many weeks. That is, temperature measurements must always be made under rising temperature conditions. Three days is needed for the glass to relax, and in some cases, prolonged conditioning at a fixed temperature is required.

Avoidance of *parallax reading errors* is important because interpolation of the finer scale is essential. Optical aids are used, but they increase the parallax error. Good mechanical alignment is therefore required to keep parallax to a minimum.

The *pressure on the bulb* due to the length of mercury in the stem becomes important. Thermometers will give different readings in the horizontal and vertical positions. *External pressure variations* should also be considered.

In general, total immersion use of the thermometer is required to achieve the higher accuracy.

## Defining Terms

See Figure 32.70 for an illustration of the terms used to describe the parts of a liquid-in-glass thermometer.

**Emergent column:** The length of thermometric fluid in the capillary that is not at the temperature of interest.

**Ice point:** The equilibrium between melting ice and air-saturated water.

**Thermometric liquid:** The liquid used to fill the thermometer.

## References

1. ISO issue documentary standards related to the liquid-in-glass thermometer:
  - ISO 386-1977 *Liquid-in-glass laboratory thermometer — Principles of design, construction and use.*
  - ISO 651-1975 *Solid-stem calorimeter thermometers.*
  - ISO 653-1980 *Long solid-stem thermometers for precision use.*
  - ISO 654-1980 *Short solid-stem thermometers for precision use.*
  - ISO 1770-1981 *Solid-stem general purpose thermometer.*
2. ASTM in their standards on Temperature Measurement, Vol. 14.03 include two standards related to liquid-in-glass thermometers:
  - E1-95 *Specification for ASTM Thermometers.*
  - E77-92 *Test Method for Inspection and Verification of Liquid-in-glass Thermometers.*
3. BSI publish a series of documentary specifications for thermometers, including:
  - BS 593:1989 *Laboratory Thermometers.*
  - BS 791:1990 *Thermometers for Bomb Calorimeters.*
  - BS 1704:1985 *General Thermometers.*
  - BS 1900:1976 *Secondary Reference Thermometers.*
4. J. A. Wise, *Liquid-in-glass Thermometer Calibration Service*, Natl. Inst. Stand. Technol. Spec. Publ., 250-23, 1988. A good treatment of calibration practice for liquid-in-glass thermometers, with a wider coverage than given here.
5. J. V. Nicholas and D. R. White, *Traceable Temperatures*, Chichester: John Wiley & Sons, 1990. The present chapter section was extracted and adapted from this text. The text explains how to make traceable calibrations of various temperature sensors to meet international requirements.

## 32.9 Manometric Thermometers

---

*Franco Pavese*

Manometric thermometers are defined in this Handbook as those thermometers that make use of the pressure of a *gaseous* medium as the physical quantity to obtain temperature. Very seldom are they available from commercial sources; for example, the temperature control of a home freezer is often of this kind. Consequently, instead of simply buying one, every user must build his own if this kind of thermometer is needed. They can be a quite useful choice since, in the era of electronic devices and sensors, it is still possible to make a totally nonelectronic thermometer, which in addition keeps its calibration indefinitely, as long as the quantity of substance sealed in it remains unchanged. The range of temperatures that can be covered by this kind of thermometer depends on the principle and on the substance used. When the thermodynamic equilibrium between the *condensed* phase of a substance (either liquid or solid) and its vapor is used, one has a “vapor-pressure thermometer” and the temperature range spanned by each substance is generally narrow. In addition, only substances that are gaseous at room temperature (i.e., condensed at temperatures lower than 0°C) are normally used, confining the working range to below room temperature; however, some substances that are liquid at room temperature and have a high vapor pressure (i.e., which easily evaporate) have been used, but do not result in a sizable extension of the working range much above room temperature. A special case of vapor pressure being used at high temperature is the device called a “heat pipe,” which is not used as a thermometer, but instead as an accurate thermostat [1]; using sodium, the working range is pushed up to ~1100°C. When a pure substance is used only in its gaseous state, one has a “gas thermometer,” whose temperature range can be very wide, especially for moderate accuracy, depending mainly on the manometer; on the other hand, its fabrication is somewhat more complex and its use less straightforward.

Both thermometers can be built to satisfy the state-of-the-art accuracy of national standards (uncertainty better than  $\pm 0.001$  K) or for lower accuracies, down to an uncertainty of  $\pm 1\%$  or higher. Both thermometers require the measurement of pressure, in the range from less than 1 Pa up to 100 bar. Directions about the choice of the manometer can be found in Chapter 5.1 of this Handbook. A complete and specialized treatment on both vapor-pressure and gas thermometers up to room temperature and on pressure measurement instruments and techniques for gaseous media can be found in [2]. Gas thermometry above room temperature is treated in [3, 4].

In consideration of the fact that these kinds of thermometers typically must be built by the users, the following will concentrate on the basic guidelines for their design and fabrication.

### Vapor Pressure

Figures 32.75 and 32.76 show the pressure values and the sensitivities in the temperature range allowed for each of the most common gaseous substances, considering also, in addition to the liquid phase, the use of the solid phase (where vapor pressure is lower) below the triple point. The lower end of the range is determined by the manometer uncertainty (for a given accuracy), the upper end by the full-scale pressure of the manometer (or by the full evaporation of the condensed phase).

Table 32.23 reports “certified” vapor pressure equations, linking the measured pressure  $p$  to the unknown temperature  $T$ . The reader might prefer them to the plethora of equations found in the literature, since they have been checked by official bodies and  $T$  is expressed in the ITS-90, the International Temperature Scale [5, text in 2]. More checked equations can be found in [6].

Figure 32.77 shows the general layout of a vapor-pressure thermometer. The fabrication of a vapor-pressure thermometer is not exceedingly difficult if a few guidelines are followed. Table 32.24 summarizes the most critical ones — design criteria and filling information — in a compact form [2]. Much more constructional details can be found in [1, 3]. In most cases, the manometer is located at room temperature, and the bulb is connected to it via a small-bore tube (the “capillary tube”) without critical drawbacks. The accuracy of these thermometers ranges from  $\pm 0.0001$  K using very pure substances in calorimeters and precision mercury manometers, to  $\approx \pm 1\%$  using dial manometers.

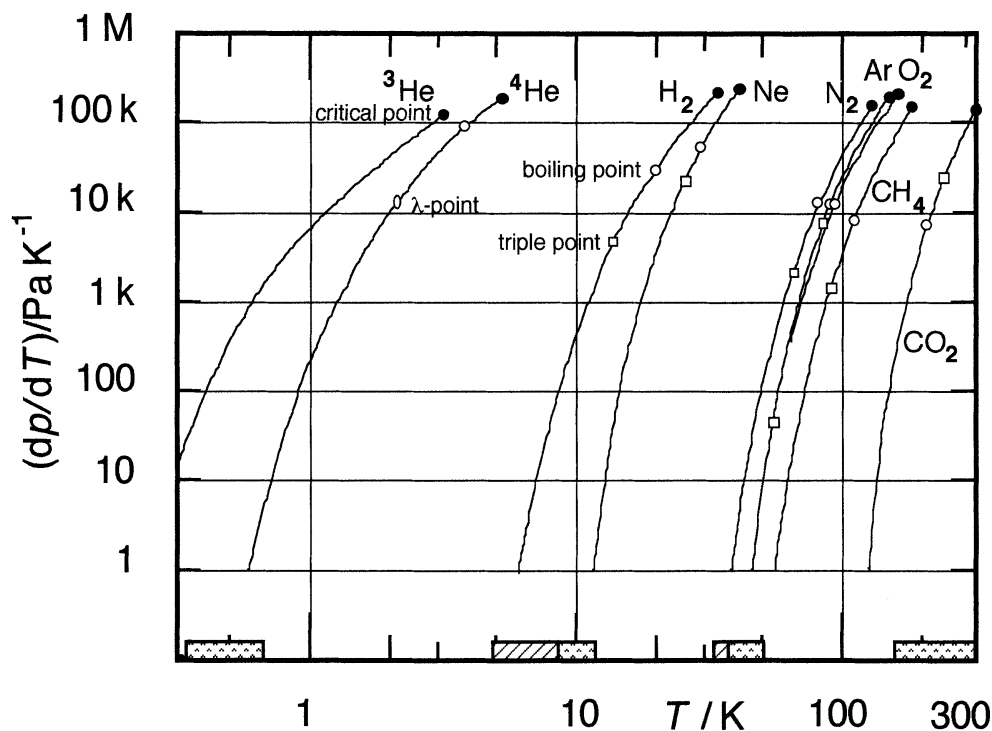
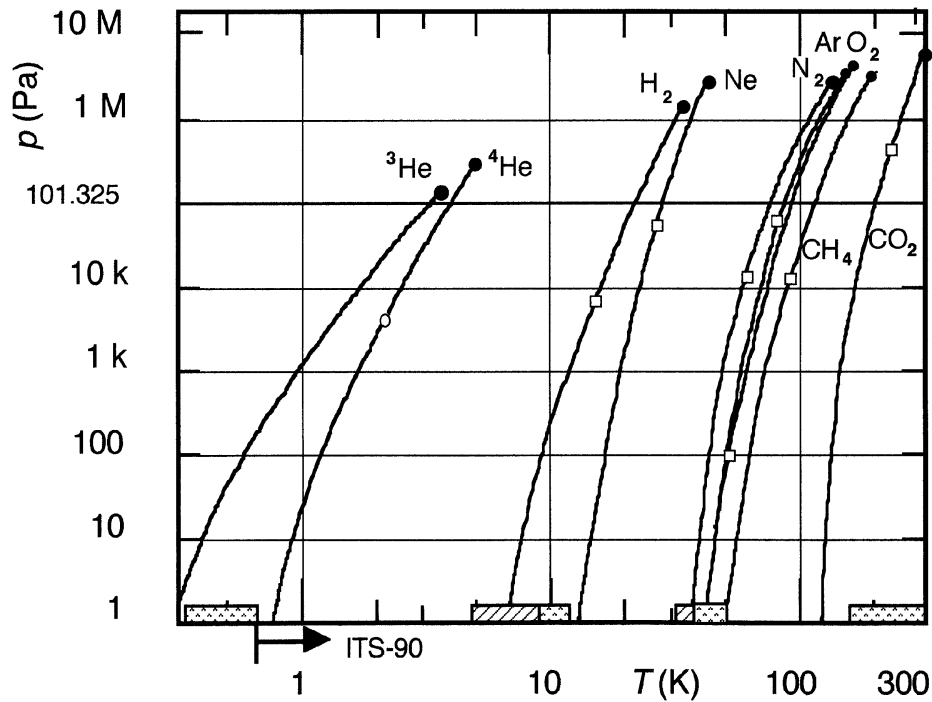


FIGURE 32.75 Range for vapor-pressure thermometry of various gases. The shaded parts indicate regions where it is less common or less accurate. , not available; , lower accuracy; ●, critical point; ○, triple point; ◊, lambda-point.

### Gas Thermometry

The layout of Figure 32.77 also applies to the design of a *constant-volume* gas thermometer (more common than the constant-pressure type), with the differences indicated in the relevant caption. The lower temperature end of the working range of a gas thermometer is stated, well before condensation of the substance takes place, by the increase of the uncertainty due to the increase in the nonideality of the gas — i.e., deviation from linearity of the relationship  $p(T)$  — which takes place when approaching the condensed state or for increasing gas densities, or due to excessive absorption of gas on the bulb surface, thereby changing the quantity of the thermometric substance. All these conditions act at the lower end of the range. The upper end is stated by technological reasons or by the manometer full-scale capability. The best substances are, as listed, helium (either isotopes), hydrogen, and nitrogen.

From a design point of view, Table 32.25 summarizes the most critical issues. The major problem, apart from gas purity and ideality, is meeting the constant-volume requirement. Being that the manometer is generally at room temperature, the fraction of gas filling the connecting “capillary” tube is subtracted from the total amount of thermometric substance amount filling the system, and since this fraction is not constant, but depends on temperature and on technical conditions, it tends to increase the measurement uncertainty, which is contrary to the case of the vapor-pressure thermometer; this error is called the *dead-volume error*. Also, the bulb volume itself changes with temperature, due to thermal expansion and, to a much smaller extent, to the change in internal pressure. Design and fabrication criteria and measuring procedures are given in great detail in [2]. The case where the gas thermometer is *calibrated* at a number of fixed points is also described, with a discussion of the simplification in the use of the gas thermometer introduced with this instrument (called the *interpolating gas thermometer*, defined in the ITS-90 for use between 3 K and 26 K).



**FIGURE 32.76** Sensitivity  $dp/dT$  of vapor-pressure thermometry for selected gases. The shaded parts indicate regions where it is less common or less accurate. , not available; , lower accuracy; ●, critical point; ○, triple point; ◊, lambda-point.

**TABLE 32.23** Vapor Pressure Equations

Equilibrium state	$T_{90}$ (K)	Uncertainty $\pm \delta T$ (mK)	Purity of material <sup>1</sup> (vol%)
Liquid-vapor phases of helium-4	1.25–2.1768	0.1	99.9999
$T_{90}/K = A_0 + \sum_{i=1}^9 A_i \left[ \frac{\ln(p/\text{Pa}) - B}{C} \right]^i$			
	$A_0 = 1.392408$	$A_1 = 0.527153$	$A_2 = 0.166756$
	$A_3 = 0.050988$	$A_4 = 0.026514$	$A_5 = 0.001975$
	$A_6 = -0.017976$	$A_7 = 0.005409$	$A_8 = 0.013259$
	$B = 5.6$	$C = 2.9$	
	2.1768–5.0	0.1	99.9999
	$A_0 = 3.146631$	$A_1 = 1.357655$	$A_2 = 0.413923$
	$A_3 = 0.091159$	$A_4 = 0.016349$	$A_5 = 0.001826$
	$A_6 = -0.004325$	$A_7 = -0.004973$	$B = 10.3$
	$C = 1.9$		
Liquid-vapor phases of equilibrium hydrogen	13.8–20.3	1 <sup>b</sup>	99.99
$p/\text{Pa} = (p_0/\text{Pa}) \exp \left[ A + \frac{B}{T_{90}/K} + C T_{90}/K \right] + \sum_{i=0}^5 b_i (T_{90}/K)^i$			
	$A = 4.037592968$	$B = -101.2775246$	
	$C = 0.0478333313$		
	$b_0 = 1902.885683$	$b_1 = -331.2282212$	$b_2 = 32.25341774$
	$b_3 = -2.106674684$	$b_4 = 0.060293573$	$b_5 = -0.000645154$

**TABLE 32.23 (continued)** Vapor Pressure Equations

Equilibrium state	$T_{90}$ (K)	Uncertainty $\pm \delta T$ (mK)	Purity of material <sup>1</sup> (vol%)
Liquid-vapor phases of natural neon <sup>c</sup>	24.6–40	2	99.99
	$\log\left(\frac{p}{p_0}\right) = A + \frac{B}{T_{90}/K} + C(T_{90}/K) + D(T_{90}/K)^2$		
	$A = 4.61948943$	$B = -106.478268$	
	$C = -0.0369937132$	$D = 0.00004256101$	
Solid-vapor phases of nitrogen	56.0–63.1	2	99.999
	$\log\left(\frac{p}{p_0}\right) = A + \frac{B}{T_{90}/K} + C(T_{90}/K)$		
	$A = 12.07856655$	$B = -858.0046109$	$C = -0.009224098$
Liquid-vapor phases of nitrogen	63.2–125	5	99.999
	$\ln\left(\frac{p}{p_c}\right) = \frac{T_c}{T_{90}} \left[ A\tau + B\tau^{0.5} + C\tau^3 + D\tau^6 \right]; \quad \tau = 1 - \frac{T_{90}}{T_c}$		
	$A = -6.10273365$	$B = 1.153844492$	$C = -1.087106903$
	$D = -1.759094154$	$T_c = 126.2124 \text{ K}$	$p_c = 3.39997 \text{ MPa}$
Liquid-vapor phases of oxygen	54–154	2	99.999
	$\ln\left(\frac{p}{p_c}\right) = \frac{T_c}{T_{90}} \left[ A\tau + B\tau^{1.5} + C\tau^3 + D\tau^7 + E\tau^9 \right]$		
	$\tau = 1 - T_{90}/T_c$	$A = -6.044437278$	
	$B = 1.176127337$	$C = -0.994073392$	$D = -3.449554987$
	$E = 3.343141113$	$T_c = 154.5947 \text{ K}$	$p_c = 5.0430 \text{ MPa}$
Liquid-vapor phases of argon	83.8–150	5	99.999
	$\ln\left(\frac{p}{p_c}\right) = \frac{T_c}{T_{90}} \left[ A\tau + B\tau^{1.5} + C\tau^3 + D\tau^6 \right]; \quad \tau = 1 - \frac{T_{90}}{T_c}$		
	$A = -5.906852299$	$B = 1.132416723$	$C = -0.7720072001$
	$D = -1.671235815$	$T_c = 150.7037 \text{ K}$	$p_c = 4.8653 \text{ MPa}$
Liquid-vapor phases of methane	90.7–190	5 <sup>d</sup>	99.99
	$\ln\left(\frac{p}{p_c}\right) = \frac{T_c}{T_{90}} \left[ A\tau + B\tau^{1.5} + C\tau^{2.5} + D\tau^5 \right]; \quad \tau = 1 - \frac{T_{90}}{T_c}$		
	$A = -6.047641425$	$B = 1.346053934$	$C = -0.660194779$
	$D = -1.304583684$	$T_c = 190.568 \text{ K}$	$p_c = 4.595 \text{ MPa}$
Liquid-vapor phases of carbon dioxide	216.6–304	15	99.99
	$\ln\left(\frac{p}{p_c}\right) = A_0 \left( 1 - \frac{T_{90}}{T_c} \right)^{1.935} + \sum_{i=1}^4 A_i \left( \frac{T_c}{T_{90}} - 1 \right)^i$		
	$p_c = 7.3825 \text{ MPa}$	$T_c = 304.2022 \text{ K}$	$A_0 = 11.37453929$
	$A_1 = -6.886475614$	$A_2 = -9.589976746$	$A_3 = 13.6748941$
	$A_4 = -8.601763027$		

Note: For the relevant references and more gases, see [6].  $p_0 = 101325 \text{ Pa}$ , except when otherwise indicated.

<sup>a</sup> Minimum purity of the material to which the listed values of temperature and uncertainty apply.

<sup>b</sup> The summation term in the equation adds to the value of  $p$  a pressure amounting to the equivalent of 1 mK maximum.

<sup>c</sup> These values are for neon with an isotopic composition close to that specified in the ITS-90 definition.

<sup>d</sup> Above 100 K. It increases to 15 mK at 91 K, and to 10 mK near the critical point.

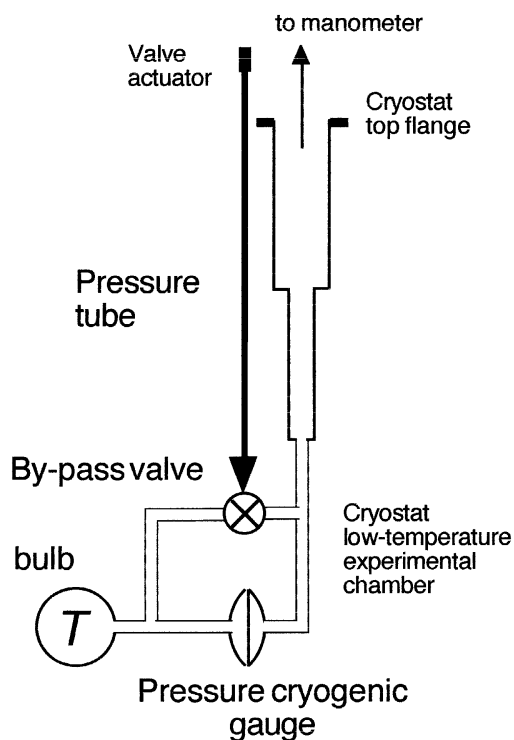


**FIGURE 32.77** The general layout of a manometric thermometer. It is shown with a cryogenic diaphragm pressure transducer; when the transducer is placed instead at room temperature, the bypass valve is also placed at room temperature. *Vapor-pressure thermometer*: the diameter of the pressure tube increases in steps when pressures lower than  $\approx 10$  Pa must be measured, in order to decrease the thermomolecular pressure drop. *Gas thermometer* (constant-volume): the diameter of the pipes connecting the bulb to the cryogenic pressure transducer must be small in order to reduce the so-called “dead-volume.” This requirement is much more stringent when the pressure transducer is moved up to room temperature. In this case, in order to reduce the error due to the “dead-volume,” the bulb volume must be increased significantly.

**TABLE 32.24** Summary of Design Criteria for Vapor-Pressure Thermometers

	Example
1. Choice of working substance:	
• Temperature range: Each substance spans only a narrow temperature interval. $T_{\max}/T_{\min} < 2-3$ (including solid-vapor range), except helium. The limit:	$T_{\max} = p_c$ $T_{\min} = 100 \text{ Pa K}^{-1}$ $T_{\max}/T_{\min} =$
– $T_{\max}$ set by maximum manometer pressure.	$^3\text{He} \approx 10$
– $T_{\min}$ set by manometer sensitivity.	$^4\text{He} \approx 9$
• Accuracy:	$\text{H}_2 \approx 3$
– Manometer: No single manometer spans whole range from $\approx 1$ Pa ( $dp/dT \approx 100 \text{ Pa K}^{-1}$ ) and critical point ( $p_c > 10^6$ Pa, except helium) with high or constant accuracy, or with sufficient sensitivity.	$\text{Ne} \approx 3$
– Substance: Not all substances allow for maximum accuracy, due to purity or to thermal problems related to a low thermal diffusivity value.	$\text{N}_2 \approx 2.5$
	$\text{O}_2 \approx 2.5$
	$\text{Ar} \approx 2.5$
	$\text{CO}_2 \approx 2$
	(solid $\approx 1.5$ )
2. Choice of pressure measuring system:	
Sensitivity and accuracy must be matched to the range of $dp/dT$ and of $p$ , i.e., $T$ , to be measured.	
• Without separating diaphragm: Can be used only for low to medium accuracy, as thermometric gas also fills the entire manometric apparatus, with problems of contamination and increases in vapor volume.	
– Dial manometers: Used only for accuracy $> \pm 1\%$ .	
– Metal diaphragm or bellows (electronic) manometers: Can achieve a $\pm 0.1-0.03\%$ accuracy.	

TABLE 32.24 (continued) Summary of Design Criteria for Vapor-Pressure Thermometers

	Example
<ul style="list-style-type: none"> <li>– Quartz bourdon gages: can approach a <math>\pm 0.01\%</math> accuracy, but helium leaks through quartz.</li> <li>– Cryogenic pressure transducers: None commercially available with accuracy better than <math>\pm 0.1\%</math> (after cryogenic calibration). Eliminate need of the connecting tube in sealed thermometers, but transducer must withstand high room-temperature pressure.</li> <li>• <i>With</i> separation diaphragm: Mandatory for high or top accuracy. Only zero reproducibility and a moderate linearity near zero are important.               <ul style="list-style-type: none"> <li>– Capacitive diaphragms: Several commercial models, when properly used, allow zero sensitivity and reproducibility better than <math>\pm 0.1</math> Pa.</li> <li>– Cryogenic diaphragms: Only laboratory-made diaphragms available, some with high zero reproducibility. Allow to confine thermometric gas at low temperatures, but the tube connecting the diaphragm to room-temperature manometer is still necessary.</li> </ul> </li> </ul> <p>Room-temperature manometers: When a cryogenic diaphragm is used, only manometers allowing helium as manometric gas can be used.</p> <p>3. Choice of sealed vs. “open” thermometer:</p> <ul style="list-style-type: none"> <li>• Sealed: Low-accuracy only (e.g., dial) thermometers.               <ul style="list-style-type: none"> <li>– Medium-accuracy sealed thermometers still very simple when using cryogenic manometer and reducing vapor volume, but room-temperature pressure can be higher than 10 MPa. Therefore, only low-sensitivity manometers can be used and thermometer measures only upper part of vapor-pressure scale.</li> <li>– High-accuracy sealed thermometers can be made, using ballast room-temperature volume and precision room-temperature diaphragm.</li> </ul> </li> <li>• “Open”: Vapor-pressure thermometers using gases are open only since working substance does not stay permanently in working bulb, but (new) samples are condensed in it only during measurements. Requires permanent use of a gas-handling system.</li> </ul> <p>4. Gas purity, isotopic composition and spin equilibrium:</p> <ul style="list-style-type: none"> <li>• Purity: Must be known, and possibly checked, e.g., by performing a triple-point temperature measurement. Dew-boiling point difference measurement must also routinely be performed, before sealing in the case of sealed devices.</li> <li>• Isotopic composition: Some gases show irreproducibility in results due to sample-to-sample changes in isotopic composition. It is impossible to obtain top accuracy with these substances, unless pure isotopes are used.</li> <li>• Spin equilibrium: With some gases, showing different spin species, equilibrium must be ensured with use of a suitable catalyst.</li> </ul> <p>5. Thermometer filling:</p> <ul style="list-style-type: none"> <li>• Amount of substance <math>n_{\max}</math> at <math>T_{\min} \rightarrow V^L \approx V_b</math>:               <math display="block">n_{\max} \leq \frac{p_{\min}}{R T_r} \left[ \frac{2V_c T_r}{T_r + T_{\min}} + V_r \right] + \frac{V_b}{M} \rho_{\min}</math> </li> <li>• Amount of substance <math>n_{\min}</math> at <math>T_{\max} \rightarrow V^L = V_{\epsilon}^L \approx 0</math>:               <math display="block">n_{\min} \geq \frac{V_{\epsilon}^L \rho_{\max}}{M} + \frac{p_{\max}}{R T_r} \left[ \frac{2V_c T_r}{T_r + T_{\min}} + V_r + \frac{T_r}{T_{\max}} (V_{\max} - V_{\epsilon}^L) \right]</math> </li> <li>• Bulb volume <math>V_b</math>:               <math display="block">V_b \left[ \frac{\rho_{\min}}{M} - \frac{p_{\max}}{R T_{\max}} \right] \leq \frac{V_r}{R T_r} [p_{\max} - p_{\min}] + V^L \left[ \frac{\rho_{\max}}{M} - \frac{p_{\max}}{R T_{\max}} \right] + \frac{2V_c}{R} \left[ \frac{p_{\max}}{T_r + T_{\max}} - \frac{p_{\min}}{T_r + V_{\min}} \right]</math> </li> </ul> <p>to a first approximation the terms in <b>bold</b> can be omitted.</p>	<p>Problems only for high accuracy Kr, Xe H<sub>2</sub>, D<sub>2</sub></p> <p><sup>4</sup>He thermometer T<sub>min</sub> = 2.2 K p<sub>min</sub> = 5.263 kPa ρ<sub>min</sub> = 146 kg m<sup>-3</sup> T<sub>max</sub> = 5.2 K p<sub>max</sub> = 227.5 kPa ρ<sub>max</sub> = 67.5 kg m<sup>-3</sup> T<sub>f</sub> = 4.2 K p<sub>f</sub> = 100 kPa T<sub>r</sub> = 300 K p<sub>r</sub> = 200 kPa V<sub>r</sub> = 220 cm<sup>3</sup> V<sub>c</sub> = 16 cm<sup>3</sup> V<sub>T</sub> = 500 cm<sup>3</sup> M = 4 g mol<sup>-1</sup></p> <p>It follows: V<sub>b</sub> ≥ ≈2 cm<sup>3</sup> Taking the minimum volume 0.074 ≥ n n ≥ 0.034</p>

**TABLE 32.24 (continued)** Summary of Design Criteria for Vapor-Pressure Thermometers

	Example
<ul style="list-style-type: none"> <li>Calculation of the amount of substance <math>n</math> to condense in the thermometer: the gas is stored at <math>p_r</math> in the room-temperature reservoir of volume <math>V_r</math>. When the substance is condensed in the thermometer bulb at a temperature <math>T_i</math>, a residual <math>n_o = p_r V_r / R T_i</math> remains in <math>V_r</math>. Therefore, in order to condense a quantity <math>N</math>, one must have in the system:</li> </ul> $n' = \frac{p_r V_r}{R T_i} \left[ 1 - \frac{p_i}{p_r} \right] + (V_b + V_c + V_r)$	<p>In order to seal-in 0.05 mol, the filling system must contain 0.069 mol</p>

*Symbol caption:*  $V^l$  = volume of the liquid phase;  $\rho$  = density;  $p$  = pressure;  $V$  = volume; subscript r = room temperature, c = capillary, b = bulb.

**TABLE 32.25** Summary of Design Criteria for an Absolute Constant-Volume Gas Thermometer (CVGT) in the Low-Temperature Range ( $T < 273.16$  K)

- Choice of temperature range and of span  $T_{\min} \leftrightarrow T_{\max}$ :  
This choice is preliminary to the choice of most of the design parameters.
  - Below 273.16 K,  $^4\text{He}$  gas thermometry is limited down to 2.5 K. With  $^3\text{He}$ , accurate virial corrections available down to 1.5 K.
  - Only CVGTs of special design can be used in full span. Being that  $p \propto T$ , the 2.5 K to 273.16 K range corresponds to  $p_{\max}/p_{\min} > 100$ . For top accuracy,  $\delta p/p < 0.01\%$ , corresponding at  $p_{\min}$  to  $\delta p < 10^{-6} p_{\max}$ , generally not achievable.
  - Being that  $p \propto n/V$ , molar density must generally be changed over the range to optimize accuracy, but  $n/V$  must be limited to avoid third virial correction, especially below  $\approx 2$  K.
  - In general, a CVGT is designed for work only below or only above a temperature between 25 K and 100 K.
- Choice of reference temperature  $T_0$ :
  - Truly absolute thermometer: only one choice possible — 273.16 K.
    - Two-bulb CVGT: Avoids necessity to bring up to  $T_0$  the bulb measuring  $T_{\min} > T < T_{\max}$ . Useful with thermometers designed for use at  $T \ll T_0$ .
    - Single-bulb CVGT: Same bulb spans the entire range up to  $T_0$ .
  - Temperature reference temperature  $T_0^*$  ( $\approx$  from 25 K to 90 K):
    - Single-bulb CVGT commonly used.  $T_0^*$  value assigned by an independent experiment, and, therefore, not exact by definition. However, the additional uncertainty is a minor inconvenience with respect to the advantage of limiting bulb temperature within the span  $T_{\min} \leftrightarrow T_{\max}$ .
- Choice of thermometric gas and filling density:
  - Thermometric gas:
    - Nitrogen: Low-medium accuracy.
    - e-Hydrogen: Not used for over 50 years, but still suitable for low-medium accuracy and temperature range above  $\approx 20$  K.
    - Helium-4: Commonly employed in recent gas thermometers. Use limited to above 2.5 K.
    - Helium-3: Considered more in modern gas thermometry. Use presently limited to above 1.5 K; potential for use down to  $< 1$  K.
  - Filling density:  $p \propto n/V$  and  $dp/dT \propto n/V$  (1 kPa  $\text{K}^{-1} \triangleq 121 \text{ mol m}^{-3}$ ). Always advantageous increasing  $n/V$ , up to an upper boundary set by need of third virial correction. As a rule,  $n/V < 250 \text{ mol m}^{-3}$  above  $\approx 2.5$  K,  $n/V < 160 \text{ mol m}^{-3}$ , down to 1.2 K and  $n/V < 30 \text{ mol m}^{-3}$  at 0.8 K.
- Choice of the pressure measuring system:
  - See Table 32.24.
- CVGT parameter design:
 

A. Room-temperature pressure transducer <ul style="list-style-type: none"> <li>Bulb: Top accuracy, 1 L volume typical; low accuracy, as low as <math>50 \text{ cm}^3</math>.</li> <li>Dead-volume: Top accuracy, <math>&lt; 10 \text{ cm}^3</math>; low accuracy: up to 10% of bulb volume.</li> </ul>	B. Cryogenic pressure transducer No difference with respect to a vapor-pressure thermometer.
--	---
- Bulb design:
  - Volume may not be constant, because of:
    - Compression modulus: Walls must be thick to limit deflection due to pressure, or bulb must be enclosed in a guard chamber kept at bulb pressure. Stress in bulb material must be relieved by annealing after machining.

**TABLE 32.25 (continued)** Summary of Design Criteria for an Absolute Constant-Volume Gas Thermometer (CVGT) in the Low-Temperature Range ( $T < 273.16$  K)

- 
- Thermal expansion: Nothing can be done to suppress this effect, except using glass; must be corrected for. Small effect below  $\approx 30$  K.
  - Amount of “active” gas might not be constant, because of:
    - Gas adsorption: Physicochemical interaction of bulb walls with the gas determines the amount adsorbed. Copper often gold-plated to limit adsorption: this prevents heating the bulb above  $50\text{--}70^\circ\text{C}$ .
    - Impurity molecules on walls and leaks: Clean machining used for metal bulbs, followed by physicochemical cleaning. The bulb sealing gaskets must be stable in shape and leak-proof at working temperatures.
7. Dead-volume design:  
Dead-volume effect comes from combination of geometrical volume, working pressure, and gas density distribution, i.e., from the amount of substance contained in it.
- Room-temperature dead-volume: Consists of all volumes of the gas measuring system at room temperature. Must be kept at uniform temperature (except diaphragm, often thermostated at  $\approx 40^\circ\text{C}$ ), to be measured within  $0.1\text{--}1^\circ\text{C}$ .
  - Low-temperature dead-volume: (Part of) capillary tube between room and bulb temperature. Temperature and density change from one end to the other. Tube diameter is a tradeoff between geometrical volume and thermomolecular pressure effect: typical values between 0.5 mm and 3 mm. Advantageous keeping the parts of tube where temperature variations occur as short as possible. For medium-high accuracy, temperature distribution must be known accurately.
8. Gas handling and measuring system (for non-sealed CVGTs):
- Handling system: Must ensure purity, checked on-line with a mass spectrometer for the highest accuracy, and include gas recovery with cryogenic pumps and clean storage (or purification).
  - Measuring system (case A): Separating diaphragm requires valve system for zero check, including constant-value valves and provisions to avoid (or to restore) thermometric gas losses and contamination from the manometric gas. For this purpose, a second diaphragm separator can be used.
- 

## References

1. R. E. Bedford, G. Bonnier, H. Maas, and F. Pavese, *Techniques for approximating the ITS-90*, Monograph 90/1 of the Bureau International des Poids et Mesures, Sèvres: BIPM, 1990.
2. F. Pavese and G. F. Molinar, *Modern gas-based temperature and pressure measurements*, International Monograph Series on Cryogenic Engineering, New York: Plenum Publishing, 1992, and references therein.
3. J. F. Schooley, *Thermometry*, Boca Raton, FL: CRC Press, 1986.
4. T. J. Quinn, *Temperature*, London: Academic Press, 1983.
5. R. E. Bedford, G. Bonnier, H. Maas, and F. Pavese, Recommended values of temperature on the ITS-90 for a selected set of secondary reference points, *Metrologia*, 33, 133-154, 1996.
6. F. Pavese, Recalculation on ITS-90 of accurate vapour-pressure equations for e- $\text{H}_2$ , Ne,  $\text{N}_2$ ,  $\text{O}_2$ , Ar,  $\text{CH}_4$  and  $\text{CO}_2$ , *J. Chem. Thermodynam.*, 25, 1351-1361, 1993.

## 32.10 Temperature Indicators

---

*Jan Stasiak, Tolestyn Madaj, and Jaroslaw Mikielawicz*

Temperature indicators serve for approximate determination of bodies' temperatures and are used to control a variety of temperature treatment processes. The temperatures are determined based on knowledge of characteristic rated temperatures, which are mean critical temperatures of the indicator. However, it should be stressed that the accuracy of these measurements is satisfactory only if the measurement conditions are similar to the standard conditions for which the temperature indicators were calibrated. Otherwise, the critical temperatures of the indicators can be different from their rated temperatures listed in the standards and the measurements can have considerable errors.

The temperature indicators can be classified into two groups, each group using different physical properties for the determination of the temperature. The indicators belonging to the first group melt at certain temperatures. For some of these indicators, such as pyrometric cones, thermoscope bars and rings, the process of melting manifests itself as a shape/size deformation for which the temperature is

determined by measuring the degree/rate of deformation of the indicator. For others, such as melting pellets, liquids, crayons, and monitors, the melting means turning entirely into a liquid smear. This can also be accompanied by color changing. The second group consists of color-change indicators containing pigments that at different temperatures, show different colors by selectively reflecting incident white light. Among this group are reversible and irreversible paints, color-change crayons, and liquid-crystal indicators.

## Melting and Shape/Size Changing Temperature Indicators

The latest British Standard BS 1041, Part 7, 1988 [1] lists the following temperature indicators: Seger cones, thermoscope bars, and Bullers rings. Some temperature indicators used in the past — such as Watkin cylinders and Holcdorft bars — are no longer used and are of historical value only. In the U.S., melting pellets, crayons, liquids and monitors are available on the market and widely used.

The rated temperature for Seger cones (pyrometric cones) and thermoscope bars is defined by appropriate shape deformation resulting from the transformation of a certain amount of the indicator substance from the solid to liquid state. For chemically pure elements and compounds at a constant pressure, the temperature during the entire process of phase change remains constant. If the pressure changes within the range of changes for atmospheric pressure, then the temperature changes are insignificant and can be neglected even during precise measurements. The pyrometric cones and thermoscope bars are prepared from complex mixes of frits, fluxes, clays, calcium and magnesium compounds, silica, etc. The melting temperatures of the indicators, also referred to as the critical or rated temperatures, vary with the proportions of the above compounds. Therefore, a set of indicators differing in the proportions of the compounds is capable of covering a required range of rated temperatures. The melting temperatures can also change, to a degree, with the proportion of phases. For mixes that constitute pyrometric cones and thermoscope bars, the temperature difference between the beginning and the end of the melting process can be as large as 25 to 40°C. At the rated temperature, one can assume that the temperature is either at the beginning or at the end of the melting process. In practice, an intermediate value is assumed, referring to an expected shape deformation of the temperature indicator.

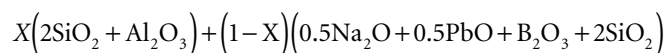
For Bullers rings, the rated temperature is determined by a shape deformation that can be described as a temperature shrinkage. An indication of the required temperature is a proper contraction of the outer diameter of the ring made of special clay (a mix of appropriate materials) that contracts uniformly with the increase in temperature throughout the operating range.

For melting pellets, crayons, liquids, and monitors, the rated temperature is that of the beginning of the melting process when the indicator turns entirely into a liquid smear. Usually, on cooling, the liquid mark solidifies and becomes glossy-transparent or translucent in appearance. The entire process can be accompanied by a change in color — mostly because the color of the workpiece surface or the back of an adhesive label, which enables the contact of the indicator with the surface, will show up from under the transparent mark. However, the moment of melting — not a color change — is the temperature signal.

### Segger Cones

The pyrometric cones are typically slender, truncated, trihedral pyramids, about 25 mm to 60 mm in height. The base of the pyramid is a regular triangle of side 7 mm to 16 mm. One edge of the pyramid is vertical or slightly leaned outward (see [Figure 32.77a](#)). The recommended height of the standard cones is 60 mm; the laboratory cones are 30 mm high.

The pyramids are manufactured by pressing a powder mixture of a number of minerals mixed in different proportions throughout the required range of rated temperatures. The main components are silicon oxide (SiO<sub>2</sub>), aluminium oxide (Al<sub>2</sub>O<sub>3</sub>) with additives in the form of oxides (MgO, K<sub>2</sub>O, Na<sub>2</sub>O, CaO, B<sub>2</sub>O<sub>3</sub>, PbO), and an organic binder. The following equation is an example of chemical constitution of the pyrometric cone for the temperature range of 600°C to 900°C:



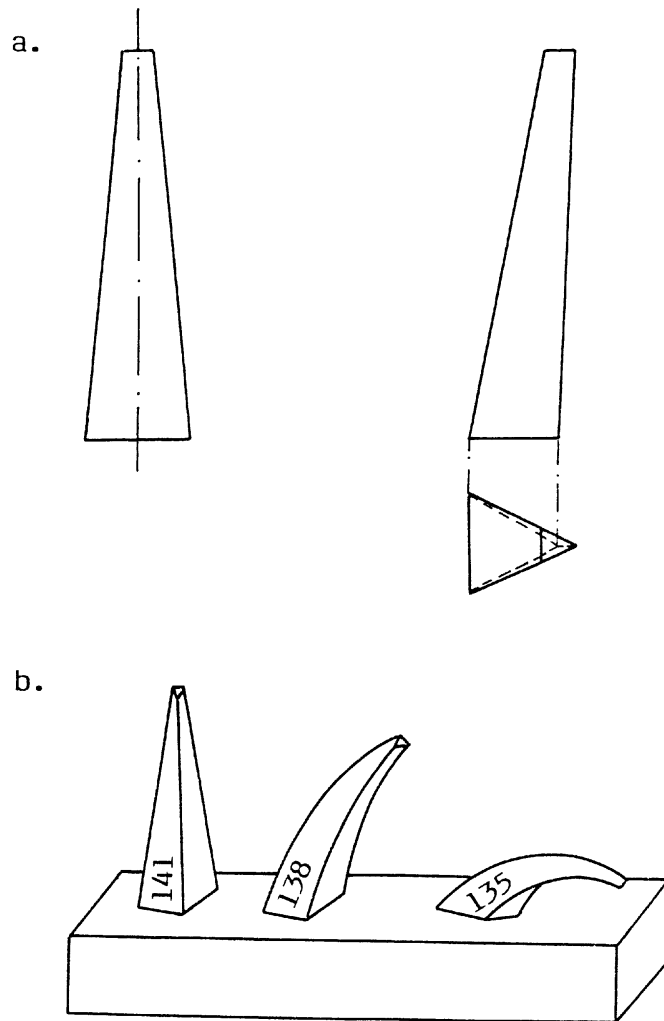


FIGURE 32.77 Pyrometric cones (a) in cross-sections; (b) on a plaque during firing.

where  $X$  is a mass unit. The pyramids designed for higher rated temperatures are prepared based on similar equations.

#### Touch-down Temperatures for Seger Cones.

As the heating progresses, the cone used for the measurement begins to soften and bends until its tip touches down on the surface on which it was placed. The rated temperature referring to this deformation is called the *touch-down temperature*. The touch-down temperatures for the Seger cones are determined in an electric kiln with clean atmospheric air at a heating rate of  $60^{\circ}\text{C h}^{-1}$ .

According to the earlier German standard DIN 51063 [2], the range of touch-down temperatures from  $600^{\circ}\text{C}$  to  $2000^{\circ}\text{C}$  at 10 to  $50^{\circ}\text{C}$  steps is covered by a series of Seger cones denoted traditionally by numbers from 022 to 42 (see Table 32.26a).

According to the latest British Standard BS 1041, Part 7, 1988, the touch-down temperatures within the range of  $600^{\circ}\text{C}$  to  $1535^{\circ}\text{C}$  at temperature intervals of 15 to  $35^{\circ}\text{C}$  are realized by a series of Seger cones numbered from 022 to 20 (see Table 32.26b).

The precision of determination of the touch-down temperatures for the industrial cones should be better than  $\pm 15^{\circ}\text{C}$ ; for the laboratory cones, better than  $\pm 10^{\circ}\text{C}$ . If the heating rate undergoes change

**TABLE 32.26a** Approximate Touch-Down Temperatures of Pyrometric Cones (DIN 51063)

Cone no.	Temperature (°C)						
022	600	07a	960	9	1280	29	1650
021	650	06a	980	10	1300	30	1670
020	670	05a	1000	11	1320	31	1690
019	690	04a	1020	12	1350	32	1710
018	710	03a	1040	13	1380	33	1730
017	730	02a	1060	14	1410	34	1750
016	750	01a	1080	15	1435	35	1770
015a	790	1a	1100	16	1460	36	1790
014a	815	2a	1120	17	1480	37	1825
013a	835	3a	1140	18	1500	38	1850
012a	855	4a	1160	19	1520	39	1880
011a	880	5a	1180	20	1530	40	1920
010a	900	6a	1200	26	1580	41	1960
09a	920	7	1230	27	1610	42	2000
08a	940	8	1250	28	1630		

**TABLE 32.26b** Approximate Touch-Down Temperatures of Pyrometric Cones (BS 1041)

Cone no.	Temperature (°C)						
022	600	011	880	1	1135	11	1310
021	615	010	900	2	1150	12	1330
020	630	09	925	3	1165	13	1350
019	665	08	950	4	1180	14	1380
018	700	07	975	5	1195	15	1410
017	730	06	1000	6	1210	16	1435
016	760	05	1030	7	1230	17	1460
015	790	04	1060	8	1250	18	1485
014	810	03	1085	9	1270	19	1510
013	830	02	1105	10	1290	20	1535
012	860	01	1120				

*Note:* 1. Each temperature given in the table is that at which the tip of a cone will bend sufficiently to touch the base in an electric kiln with a heating rate of 60°C h<sup>-1</sup>. 2. The touch-down temperature depends on the rate of heating; reports on firing behavior should quote the cone number, not the temperature taken from the above table. 3. Intermediate degrees of bending can be referred to the hands of a clock, e.g., 3 o'clock would represent a cone bent halfway to the stand.

within the range of 20 to 150°C h<sup>-1</sup>, then the rated temperatures can change by -40°C for the above lower limiting value of the heating rate up to 60°C for the upper value. A 0.35% content of SO<sub>2</sub> in the atmosphere increases the rated temperatures by about 35°C. Also, the presence of soot in the atmosphere slightly raises the rated temperatures.

#### How to Use the Materials.

While single cones are sometimes used, usually three or four consecutively numbered cones, including a cone whose rated temperature is equal to the required temperature of the heat treatment and two cones of neighboring numbers (one less and one more) are employed for the temperature determination (see [Figure 32.77b](#)). They are installed into specially unfired plaques with tapered holes and protrusions that hold the cones firmly. The plaques are mounted to a workpiece surface to allow observations. A cone can be set up in other ways, such as inserting its base into refractory clay. However, it is necessary to assure a correct angle and firm hold of the cones during the firing cycle. Failure in these respects will

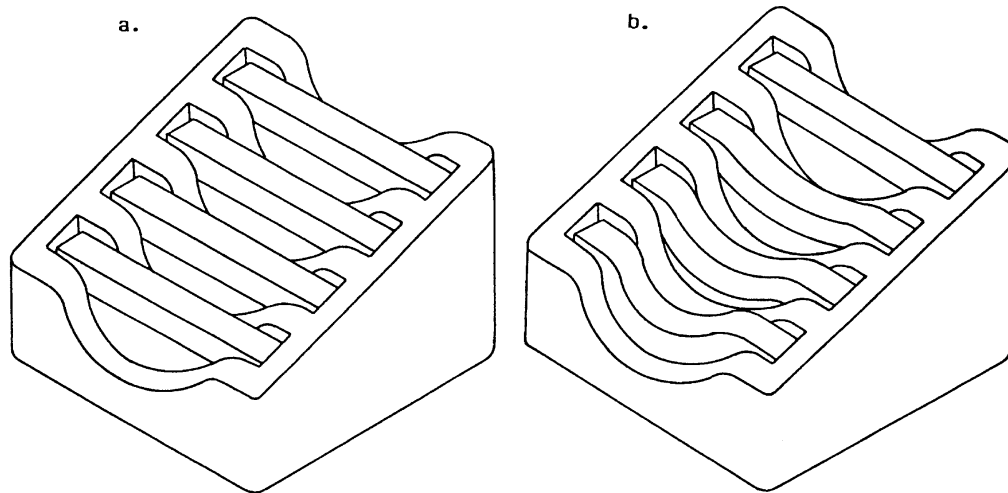


**FIGURE 32.78** Thermoscope bars on a stand before and after firing.

cause the cone to bend unpredictably and give incorrect assessment of the heat treatment. If the process of heating takes place with a standard heating rate, then the rated temperature is reached when the tip of the central cone touches the base of the plaque. With further prolongation of the firing cycle, the cone will melt completely to form a blob on the plaque. The process of reaching the rated temperature is signaled in advance by the cone of one-less number. The cone of one-more number is there to prove that the required temperature value is not exceeded. Placing a series of cones with lower numbers (lower rated temperatures) provides the opportunity to carry out the process of heating at a required rate.

Typical Application.

Seeger cones are used for the control of firing processes in the ceramics industry and artistry.

### Thermoscope Bars

These indicators have the shape of bars of rectangular cross-sections. The typical dimensions of the bars are: length, 57 mm; width, 8 mm; and height, 6 mm. Bars of consecutive numbers (rated temperatures) are placed horizontally on a refractory stand as in [Figure 32.78](#). The set of thermoscope bars is a more convenient and slightly modified form of Holcdorft bars. The bars are made of the same composites (mineral mixes and organic binder) as the pyrometric cones. The mixed powders are pressed and can be hardened by prefiring at relatively low temperatures, below those at which bending should occur.

Bending Temperatures of Thermoscope Bars.

The rated temperatures of thermoscope bars, referred to as the bending temperatures, are found during the calibration in an electric kiln with a heating rate of  $60^{\circ}\text{C h}^{-1}$  when the bars start to exhibit deformation (i.e., begin to bend).

According to the British Standard BS 1041, the range of rated temperatures from  $590^{\circ}\text{C}$  to  $1525^{\circ}\text{C}$  at temperature intervals of 15 to  $35^{\circ}\text{C}$  is covered by 42 thermoscope bars (see [Table 32.27](#)).

The precision of determination of the bending is about  $\pm 15^{\circ}\text{C}$ ; the other properties of the thermoscope bars referring to changes of the standard conditions are the same as for the pyrometric cones.

How to Use the Materials.

Four thermoscope bars of consecutive numbers — the first two having lower bending temperatures, the third one having the bending temperature equal or close to the required temperature, the fourth one having a higher bending temperature — are placed in sequence on a special refractory stand as in [Figure 32.78a](#). The set is mounted to the workpiece surface where observations take place. If the process of heating takes place with a standard heating rate, then the beginning of deformation (bending) of the

**TABLE 32.27** Approximate Bending Temperatures of Thermoscope Bars (BS 1041)

Bar no.	Temperature (°C)	Cone no.	Temperature (°C)	Cone no.	Temperature (°C)	Cone no.	Temperature (°C)
1	590	12	870	23	1130	33	1300
2	610	13	890	24	1145	34	1320
3	625	14	915	25	1160	35	1340
4	650	15	940	26	1175	36	1365
5	685	16	965	27	1190	37	1395
6	715	17	990	28	1205	38	1425
7	745	18	1015	29	1220	39	1450
8	775	19	1045	30	1240	40	1475
9	800	20	1075	31	1260	41	1500
10	820	21	1095	32	1280	42	1525
11	845	22	1115				

*Note:* 1. Each temperature given in the table is that at which the bar starts to bend in an electric kiln with a heating rate of 60°C h<sup>-1</sup>. 2. The bending temperature depends on the rate of heating; reports on firing behavior should quote the bar number, not the temperature taken from the above table. 3. The bar can be expected to bend sufficiently to touch the stand at a temperature of 10°C to 30°C higher than the values given in the table, depending on the composition of the bar.

third bar indicates that the required temperature is reached. The process of reaching the rated temperature for the third bar is signaled in advance by the deformation of the preceding bars whose behavior allows the evaluation of the heating rate. The unbent fourth bar testifies that the required temperature is not exceeded (see Figure 32.78b).

Typical Application.

The application of the thermoscope bars is identical to that of the Seger cones.

### Bullers Rings

These temperature indicators in the form of rings have the following dimensions: outer diameter, 63 mm; inner diameter, 22 mm; and width, 8 mm. The appropriate measuring unit consists of a Bullers ring and a specially prescaled device for measurement of the temperature shrinkage of the ring. This contraction gage measures the outer diameter of the heated ring, based on which the heating work is assessed. The full measuring range of rated temperatures from 960°C to 1440°C is covered by four types of rings manufactured by pressing powders of ceramics mixes, with a binder, and without prefiring.

1. Rings denoted as 55 of brown color, suitable for temperatures from 960°C to 1100°C are used in the firing of glost ware and common building bricks where the finishing temperatures are relatively low.
2. Rings numbered 27/84, colored green, suitable for temperatures from 960°C to 1250°C are used for firing earthenware at the medium finishing temperatures, as well as tiles and bricks refractory with respect to low temperatures.
3. Rings numbered 75/84, colored natural, recommended for firing temperatures from 960°C to 1320°C, allow for higher finishing temperatures and are used for firing electrical porcelain, china, grinding wheels, and bricks refractory with respect to higher temperatures.
4. Rings numbered 73, colored yellow, recommended for temperatures from 1280°C to 1440°C for slow firing conditions as used in the manufacture of high-temperature ceramics and heavy refractories.

Approximate rated temperatures for the Bullers rings and corresponding readings of the contraction gage according to the British Standard BS 1041 are presented in [Table 32.28](#).

How to Use the Materials.

One or more rings of the same type are placed vertically in a prefired stand and mounted to a workpiece surface. To determine the temperature as the firing progresses, the heated rings are withdrawn from their

**TABLE 32.28** Approximate Rated Temperatures for Bullers Rings

Temperature (°C)	Gage readings			
	Ring no. 55	Ring no. 27/84	Ring no. 75/84	Ring no. 73
960	3	0	0	
970	7	1	1	
980	11	2.5	2	
990	15	4	3	
1000	18	5.5	4	
1010	21	7	5	
1020	24	8.5	6	
1030	27	10	7	
1040	30	11.5	8.5	
1050	32	13	10	
1060	34	14	11	
1070	36	15.5	12.5	
1080	37	17	14	
1090	38	18.5	15.5	
1100	39	20	17	
1110		21.5	18	
1120		23	20	
1130		24.5	21	
1140		26	22	
1150		27	23	
1160		28.5	24.5	
1170		30	26	
1180		31.5	27	
1190		33	28	
1200		34.5	29	
1210		36	30	
1220		37.5	31	
1230		38.5	32	
1240		40	33	
1250		41.5	34.5	
1260			36.5	
1270			38.5	
1280			40	29.5
1290			42	30
1300			44	31
1320			46	34
1340				37
1360				40.5
1380				44
1400				48
1420				51
1440				54

*Note:* These values should be used with caution because they are dependent on the firing cycle to which the rings are subjected.

stands, cooled to the ambient temperature, and then measured for contraction. This measurement is carried out on a gage consisting of a brass base plate on which a radial arm with a pointer moving over a scale and two steel dowel pins, against which the ring is pressed by the movable arm, are mounted (see [Figure 32.79](#)). A contraction of the ring gives rise to an amplified movement of the pointer over the scale. The divisions on the scale are numbered from -5 to 60. More heavily fired rings contract more and give higher readings on the gage. The divisions below 0 indicate expansion of the ring; above 0 indicates contraction. Rings should be measured across several diameters by turning them around in the gage so as to find the mean value to which the temperature can be assigned with the help of Table 32.28. Placing several rings in the stand in a manner that allows their easy withdrawal gives the possibility of measuring

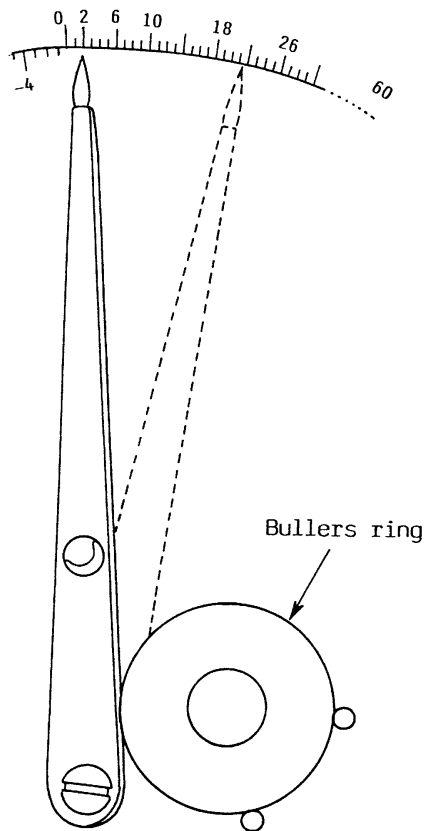


FIGURE 32.79 Contraction gage.

the heating rate. In a similar way, distribution of a number of rings throughout the furnace enables the determination of the temperature field in the furnace.

Usually, one or more test pieces from a series of rings are picked out for the sake of calibration so as to compare the obtained readings with the standard values enclosed in Table 32.28. Intermediate measurements are also carried out to evaluate the effect of the heating rate on the temperature shrinkage of the rings. The accuracy of the temperature determination for the standard heating conditions is  $\pm 0.5$  of a single division of the scale.

#### Typical Application.

The application of the Bullers rings is similar to the Seger cones and thermoscope bars. An inconvenience is the fact that the Bullers rings require gage measurements and the temperature cannot be solely determined based on naked-eye observations.

### Temperature-Indicating Pellets, Liquids, Crayons, and Monitors

#### Temperature-Indicating Pellets.

Temperature-indicating pellets are manufactured by pressing powders of mineral mixes of certain melting temperatures and an indifferent binder. Melting pellets are recommended as standard tablets  $\phi 7/16 \times 1/8$  and miniature tablets  $\phi 1/8 \times 1/8$  (see Figure 32.80). There are 112 different pellets which cover the temperature range from  $40^\circ\text{C}$  ( $100^\circ\text{F}$ ) to  $1650^\circ\text{C}$  ( $3000^\circ\text{F}$ ); see Table 32.29. The accuracy of the temperature determination is  $\pm 1\%$  of the rated temperature. There are also available pellets for temperature control in strongly reducing atmospheres.

#### How to Use the Materials.

A pellet of the rated temperature equal to the required temperature of heat treatment is placed on the investigated surface before the heating starts. When the heating progresses, the beginning of melting

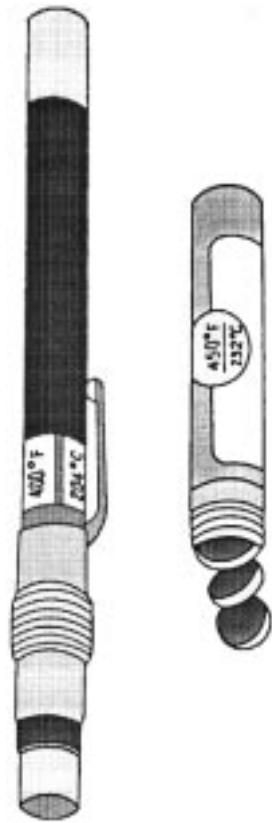


FIGURE 32.80 Temperature indicating crayon and pellets.

signals that the rated temperature is reached. Placing more pellets with the rated temperatures lower and higher than the required temperature enables more precise control of the heating process.

*Typical Application.*

Typical applications are checking furnace temperatures, control of heat treating of large units, as well as other applications involving long-duration heating.

Temperature-Indicating Liquids.

Temperature-indicating liquids are solutions of powdered mineral mixes in indifferent highly volatile solvents. They are available for use by brushing or spraying. There are over 100 different liquids with the rated temperatures from 40°C (100°F) to 1371°C (2500°F); see Table 32.29. The accuracy of the temperature determination is  $\pm 1\%$  of the rated temperature.

*How to Use the Materials.*

A thin coating of the liquid is put on the clean and dry surface by brushing or spraying before the heating starts. It dries almost instantly to a dull opaque mark. When the required temperature is reached, this mark liquefies. The melted coating does not revert to its original opaque appearance but remains glossy-transparent on cooling. It should be noted that color changes do not signal the required temperature. The melting, not the color change, is the temperature signal.

*Typical Application.*

They are recommended for temperature control on fabrics, rubber, plastics, on smooth surfaces such as glass or polished metals, as well as for monitoring critical temperatures in electronic fields.

**TABLE 32.29** Rated Temperatures for Temperature-Indicating Pellets, Liquids, and Crayons

°F	°C	°F	°C	°F	°C
100	38	325	163	1200 <sup>a</sup>	649
103	39	331	166	1250 <sup>a</sup>	677
106	41	338	170	1300 <sup>a</sup>	704
109	43	344	173	1350 <sup>a</sup>	732
113	45	350	177	1400 <sup>a</sup>	760
119	48	363	184	1425	774
125	52	375	191	1450 <sup>a</sup>	788
131	55	388	198	1480	804
138	59	400	204	1500 <sup>a</sup>	816
144	62	413	212	1550	843
150	66	425	218	1600	871
156	69	438	226	1650	899
163	73	450	232	1700	927
169	76	463	239	1750 <sup>a</sup>	954
175	79	475	246	1800	982
182	83	488	253	1850	1010
188	87	500	260	1900 <sup>a</sup>	1032
194	90	525	274	1950	1066
200	93	550	288	2000	1093
206	97	575	302	2050	1121
213	101	600	316	2100	1149
219	104	625	329	2150 <sup>a</sup>	1177
225	107	650 <sup>a</sup>	343	2200 <sup>a</sup>	1204
231	111	675	357	2250 <sup>a</sup>	1232
238	114	700	371	2300 <sup>a</sup>	1260
244	118	725	385	2350 <sup>a</sup>	1288
250	121	750 <sup>a</sup>	399	2400	1316
256	124	800 <sup>a</sup>	427	2450	1343
263	128	850 <sup>a</sup>	454	2500 <sup>a</sup>	1371
269	132	900	482	2550 <sup>b</sup>	1390
275	135	932	500	2600 <sup>b</sup>	1427
282	139	950	510	2650 <sup>b</sup>	1454
288	142	977	525	2700 <sup>b</sup>	1482
294	146	1000	538	2800 <sup>b</sup>	1538
300	149	1022	550	2900 <sup>b</sup>	1593
306	152	1050 <sup>a</sup>	566	3000 <sup>b</sup>	1649
313	156	1100	593		
319	159	1150	621		

<sup>a</sup> Series “R” pellets for use in strongly reducing atmospheres.

<sup>b</sup> Available in pellets only.

#### Temperature-Indicating Crayons.

Temperature-indicating crayons are sticks manufactured from powders of mineral mixes of certain melting temperatures and an indifferent binder. The crayons are put in specially adjustable metal holders with labels saying their rated temperatures; see Figure 32.80. Similar to the temperature-indicating liquids, there are over 100 different crayons that cover the temperature range from 40°C (100°F) to 1371°C (2500°F); see Table 32.29. The accuracy of the temperature determination is also  $\pm 1\%$  of the rated temperature.

#### *How to Use the Materials.*

During heating, the workpiece should be struck repeatedly by the crayon. Below its rated temperature, the crayon leaves a dry opaque mark. When the rated temperature is reached, the crayon leaves a liquid

smear. On cooling, the liquid mark will solidify with a transparent or translucent appearance. For temperatures below 700°F, the mark can be put on the workpiece surface before the heating process. The mark will liquefy when the rated temperature is reached. It should be remembered that the moment of melting, not any change in color, is the temperature signal.

*Typical Application.*

The crayons can be applied in welding, forging, heat treating and fabrication of metals, molding of rubber and plastics, wherever the workpiece is accessible during the heating process. Very smooth surfaces are excluded.

Temperature Monitors (Labels).

These temperature indicators are adhesive-backed labels with one or more heat-sensitive indicators under transparent circular windows. The indicators turn black (show black paper backing) when the rated temperature is reached. The rated temperatures are from 40°C (100°F) to 320°C (600°F). They are available as single temperature or multi-temperature indicators with 10°, 25°, or 50° steps. The tolerance of the temperature determination is ±1°C (±1.8°F) below 100°C, and ±1% of the rated temperature above 100°C. Exemplary rated temperatures for a series of 4-temperature (4-dot) indicators are presented in Table 32.30. A 4-dot temperature monitor is displayed in Figure 32.81.

**TABLE 32.30** Rated Temperatures for 4-Temperature (4-dot) Labels

Model no.	°F	°C	°F	°C	°F	°C	°F	°C
4A-100	100	38	110	43	120	49	130	54
4A-110	110	43	120	49	130	54	140	60
4A-120	120	49	130	54	140	60	150	66
4A-130	130	54	140	60	150	66	160	71
4A-140	140	60	150	66	160	71	170	77
4A-150	150	66	160	71	170	77	180	82
4A-160	160	71	170	77	180	82	190	88
4A-170	170	77	180	82	190	88	200	93
4A-180	180	82	190	88	200	93	210	99
4A-190	190	88	200	93	210	99	220	104
4A-200	200	93	210	99	220	104	230	110
4A-210	210	99	220	104	230	110	240	116
4A-220	220	104	230	110	240	116	250	121
4A-230	230	110	240	116	250	121	260	127
4A-240	240	116	250	121	260	127	270	132
4A-250	250	121	260	127	270	132	280	138
4A-260	260	127	270	132	280	138	290	143
4A-270	270	132	280	138	290	143	300	149

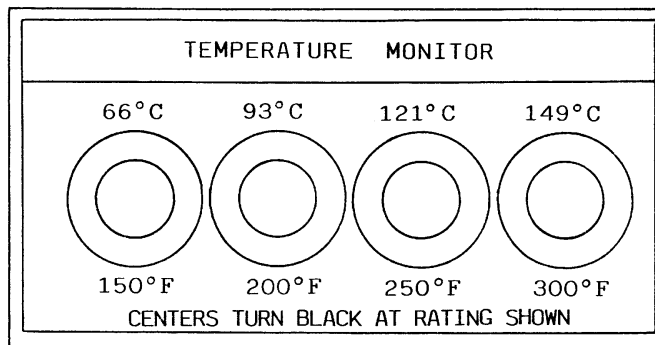


**FIGURE 32.81** Four-dot label.

#### *How to Use the Materials.*

After removing the backing, the label is pressed firmly to the dry and clean workpiece surface. A change in color to black is the temperature signal. Application of multitemperature-indicating labels allows more precise temperature determination.

#### *Typical Application.*

They are especially applied for monitoring the safe operating temperature of equipment and processes, safeguarding temperature-sensitive materials during storage and transport.

The melting temperature indicators are described in the catalogs of their manufacturers [3, 4]. As the melting indicators are widely used in the U.S., temperatures in Fahrenheit are also given.

## **Color-Change Temperature Indicators**

Color-change indicators comprise temperature-indicating paints, crayons, as well as liquid crystal indicators.

### **Temperature-Indicating Paints and Crayons**

Temperature-indicating paints are basically acrylic lacquers containing finely dispersed temperature-sensitive inorganic pigments. The principle of operation of these indicators draws on the change in color of incident light reflected from the surface of the paint due to chemical reactions which the dispersed pigments undergo and creation of new compounds at specific transition temperatures. The color-change temperatures are also determined by the heating time. According to the British Standard, it is assumed that the rated temperatures of the paints correspond to the change in color at a heating interval of 10 min. To make the characteristics of temperature-indicating paints complete, the manufacturers also provide, together with the paints, graphs of trigger temperature vs. heating time relationships.

Temperature-indicating paints and crayons can be divided into two groups:

- Irreversible indicators: where the change of color becomes permanent
- Reversible indicators: after cooling and some time, they revert to previous colors.

Irreversible color-change indicators are complex compounds containing various metals, including cobalt, chromium, molybdenum, nickel, copper, vanadium, or uranium. However, they are lead- and sulphur-free. They are available on the market in the form of paints and crayons.

#### *Irreversible Color-Change Paints.*

The irreversible paints can change color once or several times during the heating process. Thus, another division can be made on single-change and multichange paints. The range of rated temperatures is from 40°C to 1350°C at 10 to 200°C steps. At the standard conditions, the tolerance of measurements is  $\pm 5^\circ\text{C}$  for lower temperature values and  $\pm 1\%$  for higher temperatures. Exemplary single-change paints with two critical temperatures — the initial trigger temperature for which the paint changes color after 10 min heating, and the cut-off temperature being the lowest temperature for which the color change is achieved for long-duration heating — are collected in [Table 32.31](#). Color changes and critical temperatures for some multichange paints (changing color 2, 3, 3 or 6 times throughout the heating cycle) are presented in [Table 32.32](#).

#### *How to Use the Materials.*

A thin layer of the paint is applied to a workpiece surface by brushing or spraying like an ordinary paint and allowed to dry before the heating starts. During the heating, when a point of the surface reaches or exceeds the critical temperature, a color change will take place. To determine the distribution of temperature, a multichange paint can be applied. With a nonuniform temperature rise, a number of colored bands separated by isothermal lines will appear on the workpiece surface, allowing the thermal record to be made of the temperature gradient across the surface.

#### *Typical Application.*

The temperature-indicating paints are widely used in industrial applications for observing heat patterns, detecting high and low temperature points on surfaces of heat engines, pipelines, and refrigeration fins.

**TABLE 32.31** Single-Change Paints

Original color	Signal color	Initial trigger temperature <sup>a</sup> (°C)	Cut-off temperature (°C)
Pink	Blue	48	30
Pink	Blue	135	110
Mauve pink	Blue	148	120
Blue	Dark green	155	46
Yellow	Red	235	180
Blue	Fawn	275	150
Mauve red	Grey	350	220
Mauve	White	386	290
Green	Salmon pink	447	312
Green	White	458	312
Orange	Yellow	555	482
Red	White	630	450

<sup>a</sup> Color-change temperature for 10-min heating.

**TABLE 32.32** Multichange Paints

Original color	Signal color	Initial trigger temperature <sup>a</sup> °C	Cut-off temperature °C
Light tan	Bronze green	160	150
Bronze green	Pale indian red	230	210
Reddish orange	Dark gray	242	193
Dark gray	Medium gray	255	211
Medium gray	Dirty white	338	228
Purple	Pink	395	355
Pink	Fawn	500	386
Fawn	Blue	580	408
Red	Dusty gray	420	310
Dusty gray	Yellow	555	328
Yellow	Orange	610	450
Orange	Green	690	535
Green	Brown	820	621
Brown	Green/gray	1050	945

<sup>a</sup> Color-change temperature for 10-min heating.

They can be also used for controlling temperatures of powered elements and surfaces that are inaccessible or revolve at high speeds.

#### Color-Change Crayons.

Color-change crayons, available in more than 10 distinct colors, similar in shape to regular crayons for drawing, cover the temperature range from 65°C to 670°C at 10 to 100°C temperature intervals. Exemplary single-change crayons are presented in [Table 32.33](#). The accuracy of the temperature determination is the same as for the temperature-sensitive paints. They can be used for evaluating the temperature on already heated surfaces. They change color 2 min after reaching the rated temperature. Easy to use and inexpensive, they are invaluable for occasional temperature control in auto repairs, soldering, welding, electrical wiring, enameling, and for any operation involving boiling, baking, and other forms of heating.

**TABLE 32.33** Single-Change Crayons

Original color	Signal color	Initial trigger temperature (°C)
Ivory	Light green	65
Yellow & green	Light green	75
Light pink	Blue	100
Gray & white	Light blue	120
Light ivory	Pink	150
Light blue	Black	200
Green	Black	280
Light green	Gray & brown	300
Blue	White	320
Brown	Red orange	350
White	Yellow	410
Light pink	Black	450
Ochre	Black	500
Blue	White	600
Green	White	670

#### Reversible Color-Change Indicators.

Reversible color-change indicators are available on the market as paints and in label form. The thermal pigments of these temperature indicators are mercury-based complexes. Therefore, they cannot be applied directly to metal surfaces as this causes decomposition. They also tend to decompose after long exposure to heat, but the decomposition can be retarded by using a clear over-lacquer. The pigments find their most successful application when encapsulated into labels.

The rated temperatures for the reversible color-change paints do not exceed 170°C. For temperatures up to 70°C under standard conditions, the tolerance of measurements is  $\pm 1^\circ\text{C}$ ; for 70 to 150°C,  $\pm 2^\circ\text{C}$ ; and for 150 to 170°C,  $\pm 3^\circ\text{C}$ .

#### *How to Use the Materials.*

A thin layer of a reversible paint is applied to a workpiece surface by brushing or spraying, or a label is pressed to the surface. During the heating, a color change will take place when the temperature of the surface reaches or exceeds the critical temperature.

#### *Typical Application.*

The reversible color-change paints are widely used in the electrical industry, especially on busbars, live conductors, and connectors in high-current switches and in electronic fault-finding. They also find application as warning and indicating devices of domestic appliances. They are invaluable for controlling lower temperatures when it is necessary to detect undesirable temperature excursions, correct faults, and revert to normal conditions.

### **Thermochromic Liquid Crystals**

Liquid crystals constitute a class of matter unique in exhibiting mechanical properties of liquids (fluidity and surface tension) and optical properties of solids (anisotropy to light, birefringence). Certain liquid crystals are thermochromic and react to changes in temperature by changing color. They can be painted on a surface or suspended in a fluid and used to make the distribution of temperature visible. Normally clear, or slightly milky in appearance, liquid crystals change in appearance over a narrow range of temperatures called the color-play bandwidth (the temperature interval between first red and last blue), centered around the nominal event temperature (midgreen temperature). The displayed color is red at the low temperature margin of the color-play interval and blue at the high end. Within the color-play interval, the colors range smoothly from red to blue as a function of temperature; see [Figure 32.82](#). Liquid

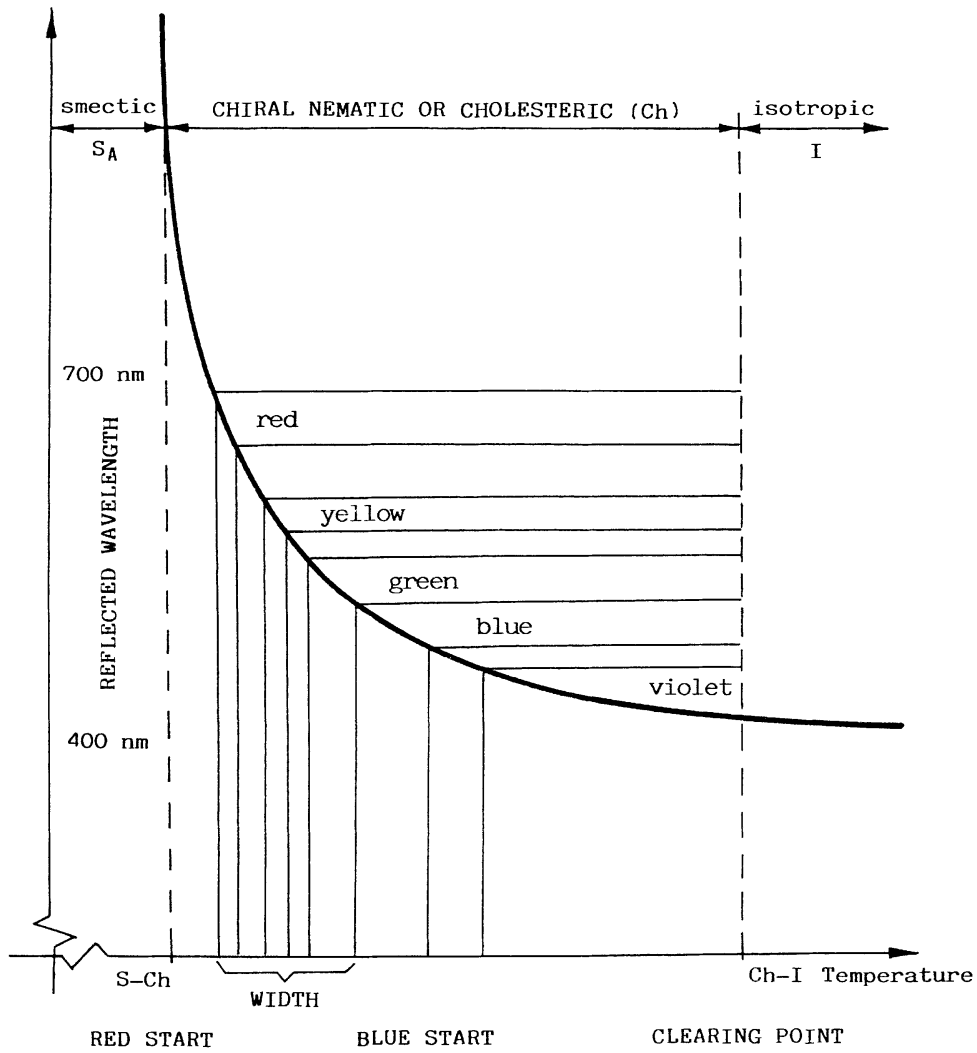


FIGURE 32.82 Typical pitch vs. temperature response of thermochromic liquid crystals.

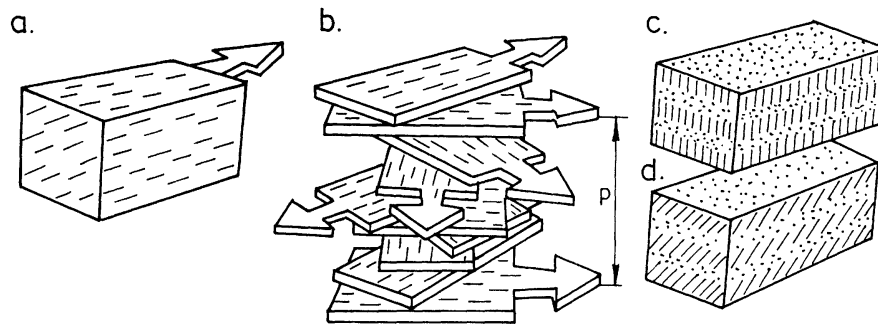


FIGURE 32.83 Structures of liquid crystals (a) nematic; (b) cholesteric; (c) smectic A; (d) smectic B.

crystals or mesophases have been classified as smectic, chiral nematic, cholesteric, and blue. The structure of liquid crystals is shown schematically in [Figure 32.83](#).

#### Temperature-Sensitive and Shear-Sensitive Formulations.

Temperature-sensitive liquid crystals show colors by selectively reflecting incident white light. Conventional temperature-sensitive mixtures turn from colorless (or black against a black background) to red at a given temperature and, as the temperature is increased, pass smoothly through the other colors of the visible spectrum in sequence (orange, yellow, green, blue, violet) before turning colorless (or black) again in the ultraviolet at a higher temperature. The color changes are reversible and on cooling the color change sequence is reversed.

Temperature-insensitive (sometimes called shear-sensitive) formulations can also be made. These mixtures show just a single color below a given transition temperature (called the clearing point) and change to colorless (black) above it. The working temperature range is thus below the clearing point. Both reversible and hysteretic (memory) formulations can be made. All liquid crystal mixtures should be viewed against nonreflecting backgrounds (ideally black, totally absorbing) for best visualization of the colors.

#### Color-Play Properties and Resolution.

Temperature-sensitive thermochromic mixtures have a characteristic red start or midgreen temperature and color-play bandwidth. The bandwidth is defined as the blue start temperature minus the red start temperature. The color play is defined by specifying either the red start or midgreen temperature and the bandwidth. For example, R35C1W describes a liquid crystal with a red start at 35°C and a bandwidth of 1°C, i.e., a blue start 1°C higher, at 36°C; G100F2W describes a liquid crystal with a midgreen temperature at 100°F and a bandwidth of 2°F.

Both the color-play bandwidth and the event temperature of a liquid crystal can be selected by its proper chemical composition. The event temperatures of liquid crystals range from -30°C to 115°C with color-play bands from 0.5°C to 20°C, although not all combinations of event temperature and color-play bandwidth are available. Liquid crystals with color-play bandwidths of 1°C or less are called narrow-band materials, while those whose bandwidth exceeds 5°C are referred to as wide-band. The type of material to be specified for temperature indicating should depend very much on the type of available image interpretation technique — human observers, intensity-based image processing, or true-color image processing systems (see [7]). The uncertainty associated with direct visual inspection is about 1/3 the color-play bandwidth, given an observer with normal color vision — about ±0.2°C to 0.5°C. The uncertainty of true-color image processing interpreters using wide-band liquid crystals is of the same order as the uncertainty assigned to human observers using narrow-band materials, and depends on the pixel-to-pixel uniformity of the applied paint and the size of the area averaged by the interpreter (about ±0.05°C can be achieved). Using a multiply filtered, intensity-based system, the resolution is better than ±0.1°C.

#### How to Use the Materials.

Liquid-crystal indicators can be used in a number of different forms: as unsealed liquids (also in solutions), in the microencapsulated form (as aqueous slurries or coating formulations), and as coated (printed) sheets. The different forms of the materials have selective advantages and suit different temperatures and flow visualization applications. Individual products are described in more detail in relevant booklets issued by the manufacturers of liquid crystals [5, 6].

#### Typical Application.

Liquid-crystal indicators are ideal for monitoring temperatures of electronic parts, transformers, relays, and motors. They are invaluable for a fast visual indication of temperatures.

## References

1. BS 1041: Part 7. Temperature Measurement.
2. DIN 51063: Part 1. Testing of Ceramic Raw and Finished Materials, Pyrometric cone of Seger. Part 2. Testing of Ceramic Materials.
3. OMEGA International Corp. P.O. Box 2721, Stanford, CT 06906 (The Temperature Handbook).
4. TEMPIL Division, Big Three Industries, Inc. South Plainfield, NJ 07080 (Catalog GC-75).
5. HALLCREST Products Inc. 1820 Pickwick Lane, Glenview, IL 60025.
6. MERC Industrial Chemicals, Merc House, Poole Dorset, BH15 1TD, U.K.
7. Moffat, R.J., Experimental heat transfer, *Proc. 9th Int. Heat Transfer Conf.*, Jerusalem, Israel, 1990.

## 32.11 Fiber-Optic Thermometers

---

*Brian Culshaw*

Optical fiber sensing is a remarkably versatile approach to measurement. A fiber sensor guides light to and from a measurement zone where the light is modulated by the measurand of interest and returned along the same or a different optical fiber to a detector at which the optical signal is interpreted. The measurement zone can be intrinsic within the fiber that transports the optical signal, or can be extrinsic to the optical waveguide. The versatility of the fiber sensing medium arises in part because of the range of optical parameters that can be modulated and in part because of the diversity of physical phenomena that involve environmentally sensitive interactions with light.

For example, highly coherent light from a laser source can be introduced into a fiber and its phase modulated by a parameter of interest. The resulting phase changes can then be detected interferometrically. The phase change is simply a modification to the optical path length within the fiber, and can be modulated by shifts in temperature, strain, external pressure field or inertial rotation. A well-designed interferometer can detect  $10^{-7}$  radians — equivalent to  $10^{-14}$  m!

The laser light could also be Doppler shifted through reflection from a moving object. Its state of polarization can be changed. Its throughput intensity can be modified or the light can be used to stimulate some secondary emissions, which in turn can be monitored to produce the relevant optical signal. If the light is incoherent, then its wavelength distribution (color) can be modified, in addition, of course, to the possibilities for polarization changes and intensity changes.

The physical phenomena capable of imposing this modulation are again many and varied. They include, for example, periodically bending an optical fiber to introduce a localized loss that depends on the sharpness of the bend (usually referred to as microbend loss); changing the relative refractive indices of the core and the cladding of the optical fiber and thereby changing the guiding properties and again introducing a loss; modifying an optical phase delay by introducing a change in refractive index or a change in physical length; examining changes in birefringence introduced through modifications to physical stress and/or temperature; using external indicators to color modulate a broadband source and relate the color distribution to temperature, chemical activity, etc. These are all linear effects where the input optical frequency is the same as the output optical frequency (regarding Doppler shift as a rate of change of phase of an optical carrier) and where, for a given system setting, the output at all frequencies is directly proportional to the input.

Nonlinear effects are also widely exploited. Of these, the most important are fluorescence, observed usually in fluorophores external to the optical fiber, and Raman and Brillouin scattering, usually observed within the fiber itself. In all these phenomena, the light is absorbed within a material and re-emitted as a different optical wavelength from the one that was observed. The difference in optical wavelengths depends on the material and usually on strain and temperature fields to which the material is subjected. These major features of optical fiber sensors are encapsulated in [Figure 32.84](#).

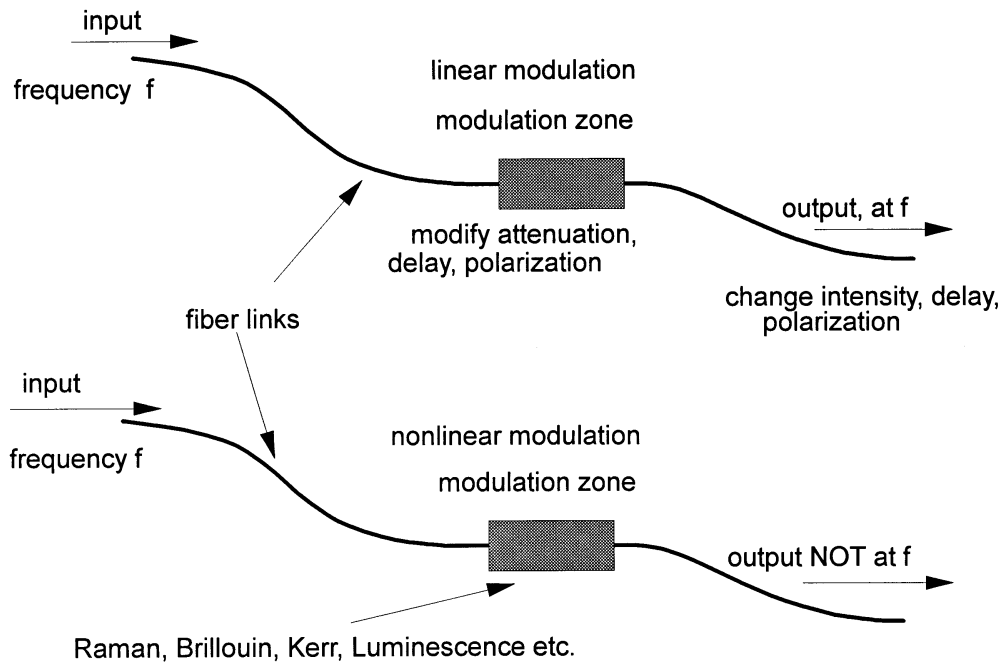


FIGURE 32.84 Linear and nonlinear optical processes for measurement using optical fiber sensors.

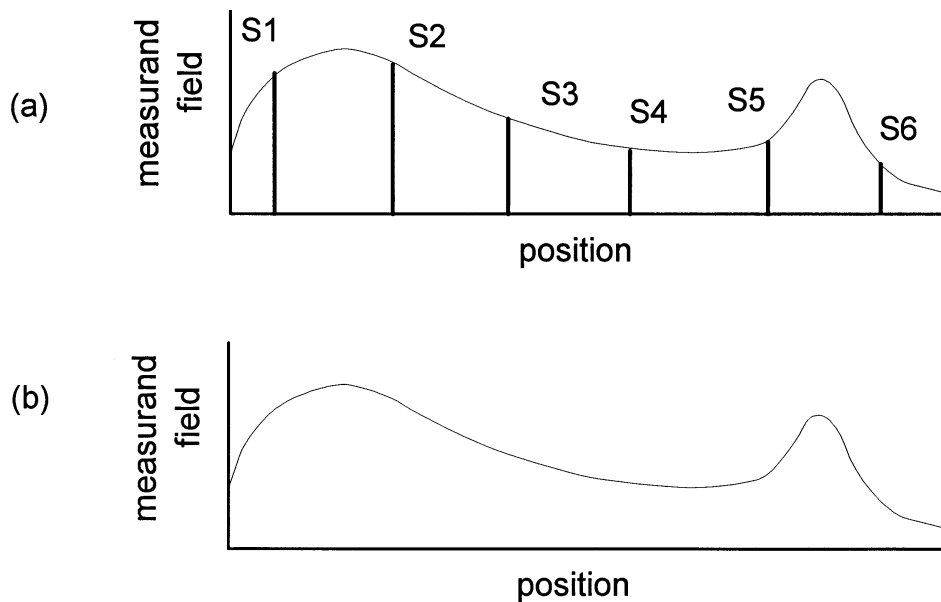


FIGURE 32.85 Sensor system outputs for (a) point array and (b) distributed sensor systems.

Optical fiber sensors have an additional feature that is unique to the medium — namely, the abilities for intrinsic networking in either distributed, quasi-distributed/multiplexed, or discrete (point) configurations. The essential features of these architectures are sketched in Figure 32.85. For intrinsic sensors, the fiber responds to the measurand throughout its length, and the output in transmission is an integral

of this linear response. However, using an interrogation scheme in reflection that incorporates a delay proportional to distance along the fiber enables the system to retrieve the measurand as a function of position. These are distributed sensors. The quasi-distributed architecture examines separately identified individual (usually adjacent) lengths of fiber and extracts the integral of the measurand along each of these individual lengths. Distributed and quasi-distributed sensors effectively convolve the measurand field along the interrogation fiber with a window determined by either the time resolution of the interrogating electronics (distributed architectures) or the defined lengths of the individual fiber sections (quasi-distributed systems).

Point and multiplexed systems address the measurement as essentially a point sample located at a specific distance along the interrogating fiber. All these architectures can be realized in all optical fiber form and have been demonstrated to address a very wide range of measurements, often within a single network. The availability of distributed sensing is unique to optical fiber technology, as indeed are optical fiber-addressed passive arrays.

In summary, the optical fiber approach to measurement has the demonstrated capability to address a wide range of physical, chemical, and biological parameters. It must take its place along side other competing technologies against which its merits must be assessed. The principal benefits of using fiber optics include:

- Immunity to electromagnetic interference within the sensor system and within the optical feed and return leads
- The capacity for intrinsic distributed measurements
- Chemical passivity within the sensor system itself and inherent immunity to corrosion
- Small size, providing a physically, chemically, and electrically noninvasive measurement system
- Mechanical ruggedness and flexibility: optical fibers are exceptionally strong and elastic — they can withstand strains of several percent
- High temperature capability — silica melts at over 1500°C

There remain cost and user acceptability deterrents within the exploitation of optical fiber sensor technology. Consequently, the majority of field experience in optical fiber sensors is targeted at addressing the specialized problems where these aforementioned benefits are paramount. Many of these lie in the area of temperature measurement.

## **Fiber Optic Temperature Sensors**

The important phenomena that have been exploited in the optical techniques for temperature measurement include:

- Collection and detection of blackbody radiation
- Changes in refractive index of external media with temperature
- Changes in fluorescence spectra and/or fluorescence rise times with temperature
- Changes in Raman or Brillouin scatter with temperature
- Phase transitions in carefully selected materials imposing mechanical modulation on optical fiber transmission properties
- Changes within an optical path length with temperature, either within the fiber or an external interferometer element

Within these phenomena, Brillouin and Raman scatter and mechanical phase transitions have been primarily used in distributed measurement systems. Some distributed measurement/quasi distributed measurement systems based on modulated phase delay have also been evaluated, although they have yet to reach commercial reality. The remaining phenomena are almost exclusively used in point sensor systems.

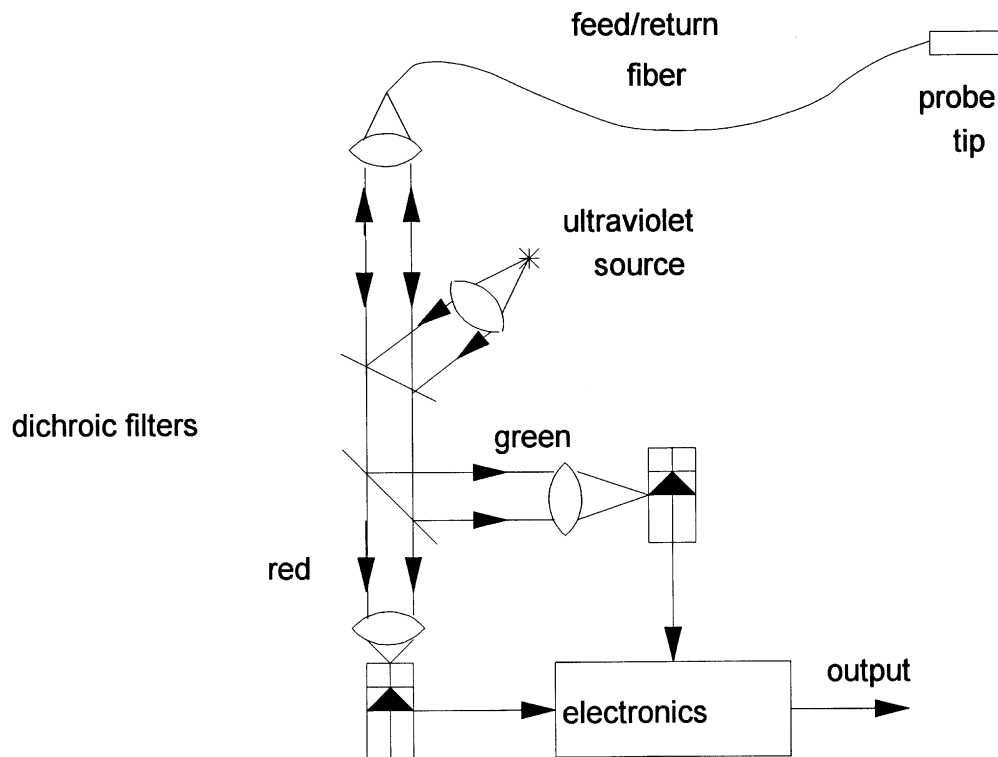


FIGURE 32.86 Optical fiber fluorescent thermometer.

### Fiber Optic Point Temperature Measurement Systems

One of the first commercial optical fiber sensors was a fluorescence-based temperature probe introduced in the early 1980s by the Luxtron Corporation of Mountain View, CA. Successors to these early sensors are still commercially available and are a very effective, but expensive, approach to solving specific measurement problems. These include monitoring temperature profiles in both domestic and industrial microwave ovens, examining temperatures in power transformer oils, motor/generator windings, and similar areas where (primarily) the issue is the operation of a reasonably precise temperature probe within very high electromagnetic fields. In such circumstances, a metallic probe either distorts the electromagnetic field significantly (e.g., in microwave ovens) or is subjected to very high levels of interference, producing spurious readings. Other applications sectors exploit the small size or chemical passivity of the device, including operation within corrosive solvents or examination of extremely localized phenomena such as laser heating or in determining the selectivity of radiation and diathermy treatments.

The principles of the probe are quite simple and are shown in Figure 32.86. The rare earth phosphor is excited by an ultraviolet light source (which limits the length of the silica-based feed fiber to a few tens of meters) and the return spectrum is divided into “red” and “green” components, the intensity ratios of which are a simple single-valued function of phosphor temperature. For precision measurement, the detectors and feed fiber require calibration and, especially for the detectors, the calibration is a function of ambient temperature. However, this can be resolved through curve fitting and interrogation of a thermal reference. The instrument, which has now gone through several generations to improve upon the basic concept, is capable of accuracies of about  $\pm 0.1^\circ\text{C}$  within subsecond integration times over a temperature range extending from approximately  $-50^\circ\text{C}$  to  $\pm 200^\circ\text{C}$ . Since its introduction, this particular

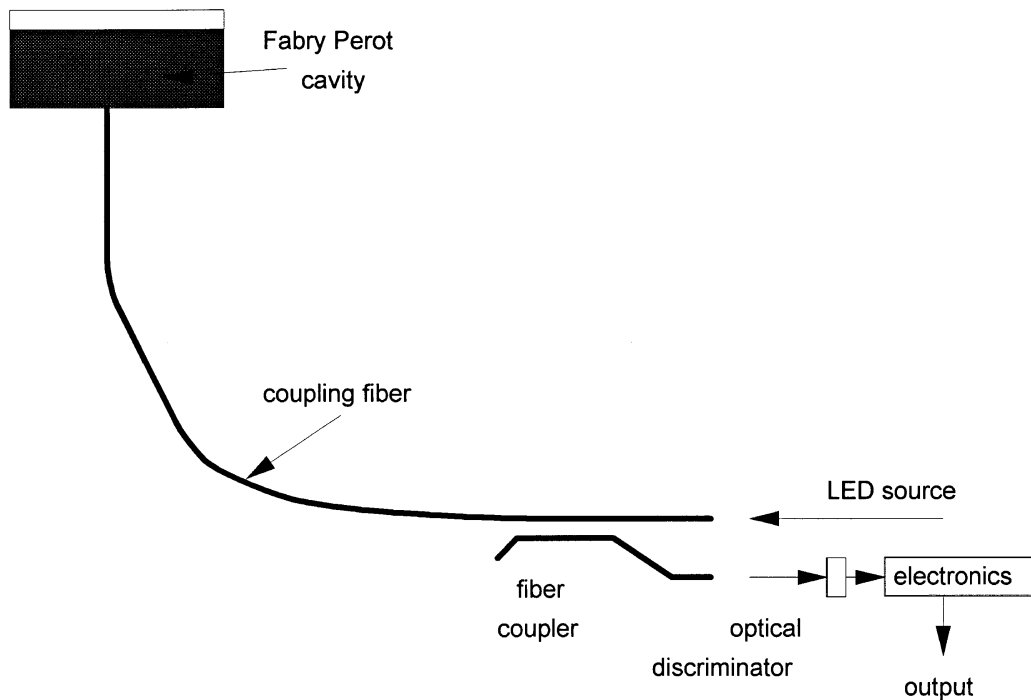


FIGURE 32.87 Optical fiber thermometry using short temperature-sensitive Fabry Perot cavity.

probe has accumulated extensive field experience in a wide variety of applications and remains among the most widely exploited fiber optic sensor concepts.

A number of temperature probes based on fluorescence decay time measurements have also been demonstrated. The level of commercial activity exploiting these concepts has, to date, been very modest, partly because the accurate measurement of decay times can be problematic.

Measuring the temperature response of dyes and other thermally sensitive color-selective materials can afford a very simple approach to temperature measurements. Among the most successful of these has been the temperature probe examining the bandedge of gallium arsenide introduced by ASEA (now ABB), again in the early 1980s and now transferred to Takaoka. The bandedge can either be monitored through examining the spectra of induced fluorescence or through interrogating the absorption characteristics of the material when subjected to a constant spectrum excitation. The accuracy and temperature range of this probe are comparable with those of the Luxtron system, and this particular version of the bandedge probe has the additional benefit of operating primarily in the near-infrared range of the spectrum, thereby accessing the best transmission characteristics of the optical fiber medium. The probe was originally conceived to address ASEA's internal needs in monitoring electrical power system components. Similar bandedge probes have also been demonstrated based on absorption edge detection in materials such as ruby.

Refractometry and interferometry are potential extremely sensitive thermal probes. Several have been demonstrated, some of which achieve microkelvin resolution. Interferometric detection or exploitation of sensitive mode coupling phenomena is the source of this very high sensitivity, although rarely is such high sensitivity required in practice. The relatively simple Fabry Perot probe shown in Figure 32.87 has been introduced commercially with simplified spectral analysis and a semiconductor source, although as yet its market penetration has been relatively modest.

Optical pyrometry is a well-established approach to measuring temperatures in the hundreds to thousands of degrees Centigrade. The disappearing filament pyrometer has been used in this fashion for over half a century. The optical fiber equivalent has also found a few niche applications. The general

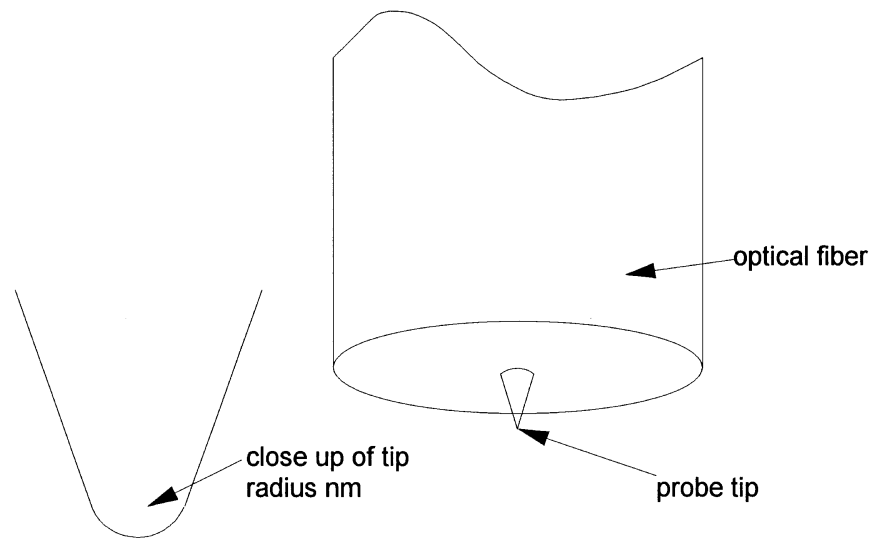


FIGURE 32.88 Probe for photon tunneling microscope and nano optrode.

form of such a sensor is to place the black body at the end of the fiber and place it with the fiber into the hot zone. The consequent radiation within the transmission spectrum of the fiber is then monitored using a semiconductor photodetector that can be based on III-V materials or silicon. The received radiation is then primarily within the red and near-infrared from about 600 nm to, depending on the detector, 1.8  $\mu\text{m}$ . Blackbodies radiate significantly in this range at temperatures in the hundreds of degrees Centigrade and above. The most significant success of this approach has been in the fabrication of the reference standard temperature probe at NIST for temperatures above 1200°C. This uses a sapphire rather than silica collection fiber because of its superior optical and thermal properties within the temperature and the wavelength ranges of interest. It defines these high temperatures with subdegree precision.

Optical fibers also have the capacity to make unique nanoprobes — the opposite end of the scale by orders of ten from the distributed sensors discussed below. These (Figure 32.88) are tapered optical fibers with the end reduced in diameter to tens of nanometers. The tapered region is coated with a metal, often aluminium or silver, to confine the optical field. This produces an intense spot of light at the fiber tip which irradiates an area nanometers in dimensions. The tip can be coated with the dye or the fluorescent thermally sensitive material and used to monitor temperature over extremely small areas. This enables thermal profiles within cellular dimensions to be assessed. In other formats, the same probe can also be used to address chemical activity and chemical composition.

Fiber optic temperature sensing can be realized using a wide variety of techniques primarily, but not exclusively, based on the variation of optical properties of materials with temperature. An example of the exceptions is the optical excited vibrating element probe shown in Figure 32.89. This probe has been primarily used for pressure measurement and is now available commercially for pressure assessment down-hole in oil wells. It can also be configured to exhibit extremely high temperature sensitivity with accuracies and resolutions in the millikelvin region. It uses the beneficial features of mechanical resonators and the consequential frequency read-out in parallel with optomechanical excitation and direct optical interrogation to produce a probe that can be reliably exploited over interrogation lengths of tens of kilometers.

Fiber optic point sensors for temperature measurement are now a relatively mature technology. Most of the devices mentioned above were first introduced and characterized 10 or more years ago and have since been refined to address specific applications sectors. They remain expensive, especially when compared to the ubiquitous thermocouple, but their unique capability for noninvasive electrically passive interference immune measurement give them a very specific market address that cannot be accessed using alternative technologies. Within these market areas, the probes have been extremely successful.

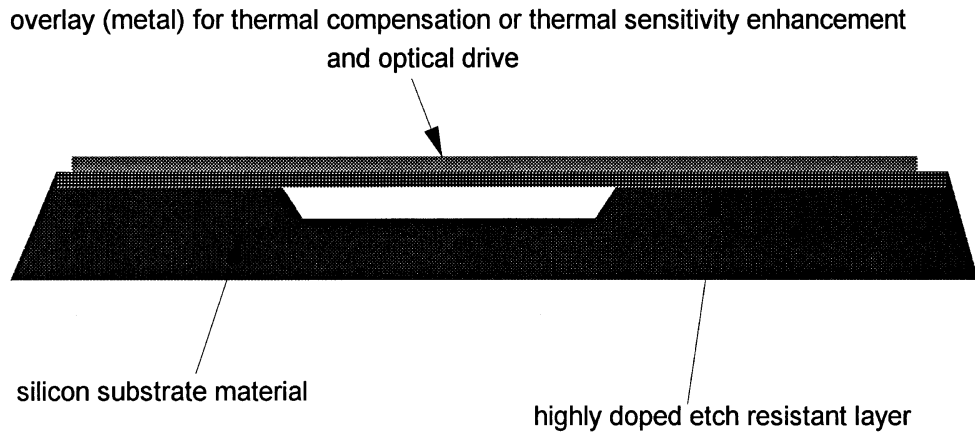


FIGURE 32.89 Longitudinal section of silicon optically excited microresonator.

## Distributed and Quasi-distributed Optical Fiber Temperature Measurement Systems

These systems all exploit the unique capability for optical fibers to measure and resolve environmental parameters as a function of position along the fiber length. This generic technology is unique to optical fiber systems and, while there are a few commercial distributed temperature sensor systems available, the research in this sector continues.

The stimulated Raman scatter (SRS) distributed temperature probe is the most well established of these and, in common with many of the point sensors, was originally introduced commercially in the late 1980s. The principle (Figure 32.90) is quite simple. Within the Raman backscatter process (and also within the spontaneous Brillouin backscatter process), the amplitudes of the Stokes and anti-Stokes lines are related to the energy gap between these lines by a simple  $\exp(-\Delta E/kT)$  relationship. Therefore, measuring this ratio immediately produces the temperature. Furthermore, this ratio is uniquely related to temperature and cannot be interfered with by the influence of other external parameters. The system block diagram is shown in Figure 32.91. The currently available performance from such systems enables resolutions of around 1 K in integration times of the order of 1 min, with resolution lengths of one to a few meters over total interrogation lengths of kilometers. The interrogation can extend to tens of kilometers if either the interrogation times are increased or the temperature and/or spatial resolutions are relaxed. The system is available from both European and Japanese manufacturers. The applications are very specific, as indeed they must be to accommodate an instrument price that is typically in tens of thousands of dollars. The instruments have been used in a variety of highly specific areas, ranging from monitoring temperature profiles in long process ovens to observing the thermal characteristics within large volumes of concrete during the curing process.

Distributed temperature alarms triggering on and locating the presence of either hot or cold spots along the fiber can be realized at significantly lower costs and have been modestly successful as commercial systems. The first of these — and probably the simplest — was originally conceived in the 1970s. This uses a simple step index fiber in which the refractive index of the core material has a different temperature coefficient than that of the cladding material. The temperature coefficient is designed such that at a particular threshold temperature, the two indices become equal and thereafter that of the cladding exceeds that of the core. Within this section, light is no longer guided. Simple intensity transmittance measurement is then very sensitive to the occurrence of this threshold temperature at a particular point along the fiber. If used with an optical time domain reflectometer, the position at which this first event occurs can be located. This system is now in use as a temperature alarm on liquefied natural gas storage tanks. Here, the core and cladding indices for a plastic-clad silica fiber cross at a temperature in the region of

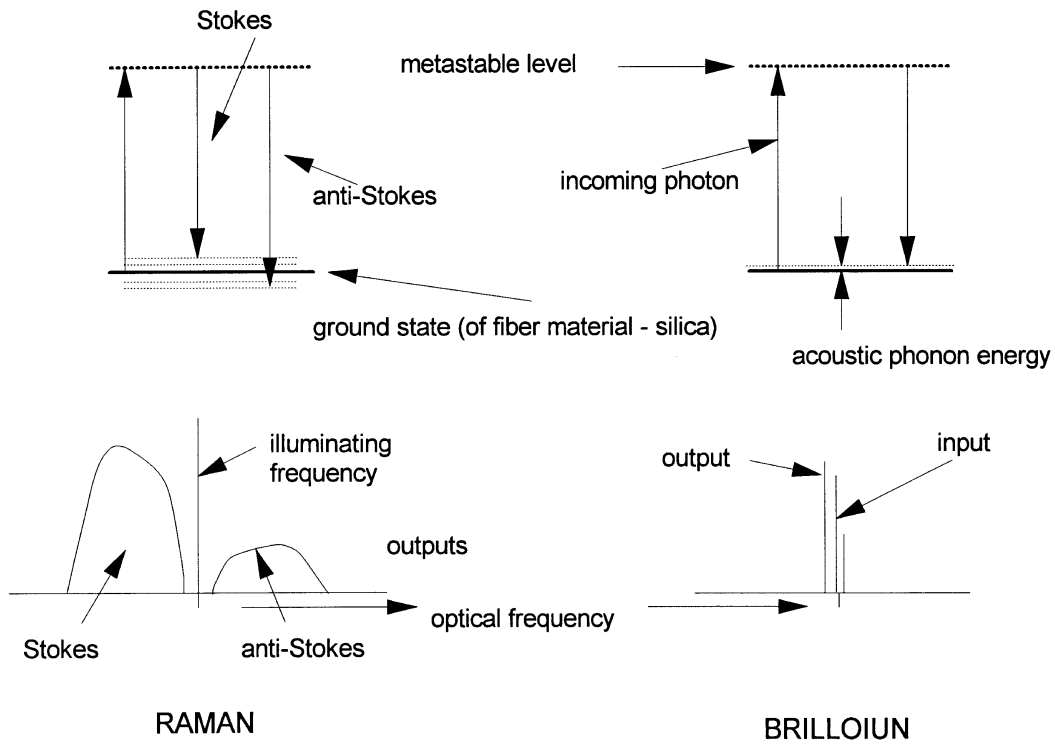


FIGURE 32.90 Thermally sensitive nonlinear scattering processes in optical fibers.

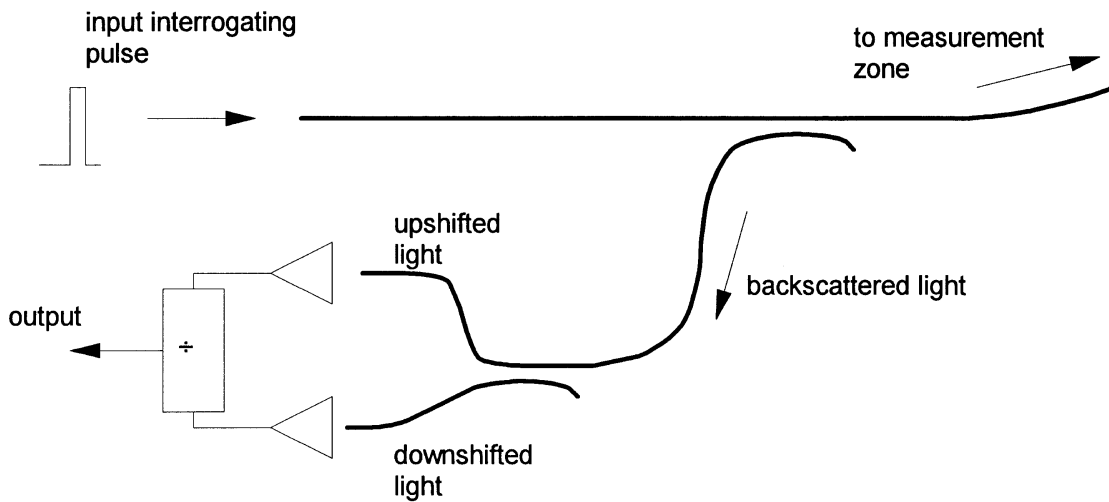


FIGURE 32.91 Raman distributed temperature probe: basic schematic.

50°C. Such temperatures can only be achieved when a leak occurs. Further, the system has the obvious benefit of intrinsic safety and total compatibility with use within potentially explosive atmospheres.

A heat — as opposed to cold — alarm system that has also been introduced commercially is shown in Figure 32.92. In this system, the central tube is filled with a wax that expands by typically 20% when passing through its melting point. This expansion in turn forces the optical fiber against the helical

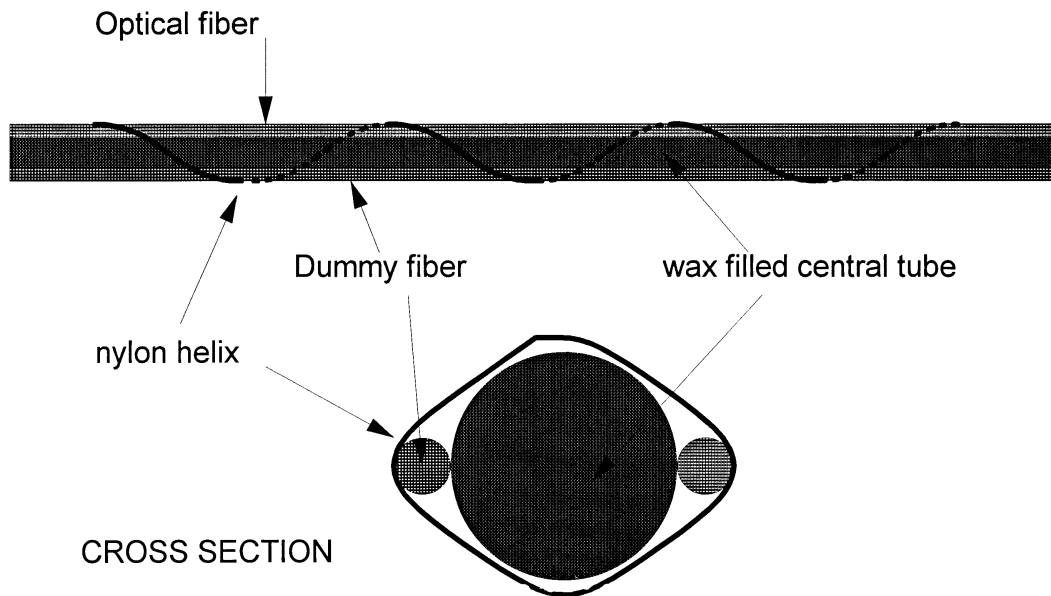


FIGURE 32.92 Fiber optic distributed heat (fire) alarm.

binding, introducing a periodic microbend and thereby increasing the local loss within the fiber. The wax transition temperatures can be defined over a relatively wide range (say 30 to 70°C) and a low-cost OTDR system enables location of the hot spot to within a few meters. This system presents a very cost-effective over-heat or fire alarm when such systems are required and are in intrinsically safe areas or in regions of very high electromagnetic interference. Again, it is the unique properties of the optical fiber sensing medium — especially intrinsic safety and electromagnetic immunity — which provide this system with its market address.

Brillouin scatter is very similar in character to Raman scatter except that in Brillouin scatter the interaction is with an acoustic phonon rather than an optical phonon. The frequency shifts are then correspondingly significantly smaller (typically 10 to 15 GHz). Additionally in Brillouin scatter, the frequency of the scattered light depends on the acoustic velocities in the medium within which the light is scattering. Consequently, the Brillouin scatter spectrum is a function of both temperature (through variations of modulus and density) and strain applied to the optical fiber. Usually this is exploited as a complex but very effective means for measuring strain distributions along an optical fiber. The Brillouin scatter cross-section is much higher than that for Raman scatter so that distributed strain distributions can be measured over distances well in excess of 100 km. This measurement is particularly effective when exploiting stimulated Brillouin scatter that guides the scattered light back toward the source. However, since the apparent value of strain depends on temperature through the variation of acoustic velocity with temperature, temperature correction is required in most practical situations and, in principle, this correction can be implemented by measuring spontaneous Brillouin scatter and specifically the intensity ratio of this in the upper and lower sidebands. This particular correction technique is currently in its infancy, and accuracies in the degree kelvin range are the current state of the art. The difficulty in temperature measurement is that the energy gap between the two sidebands is very small so that the ratio of the amplitudes is close to unity but must be measured very accurately in order to invert the exponential.

The optical Kerr effect manifests itself as an intensity-dependent refractive index. Consequently, this nonlinearity gives rise to either second harmonic generation or sum and difference frequencies. It has been investigated for distributed temperature sensing using pump:probe configurations and birefringent fiber from which the beat length is a function of temperature and strain. This beat length in turn

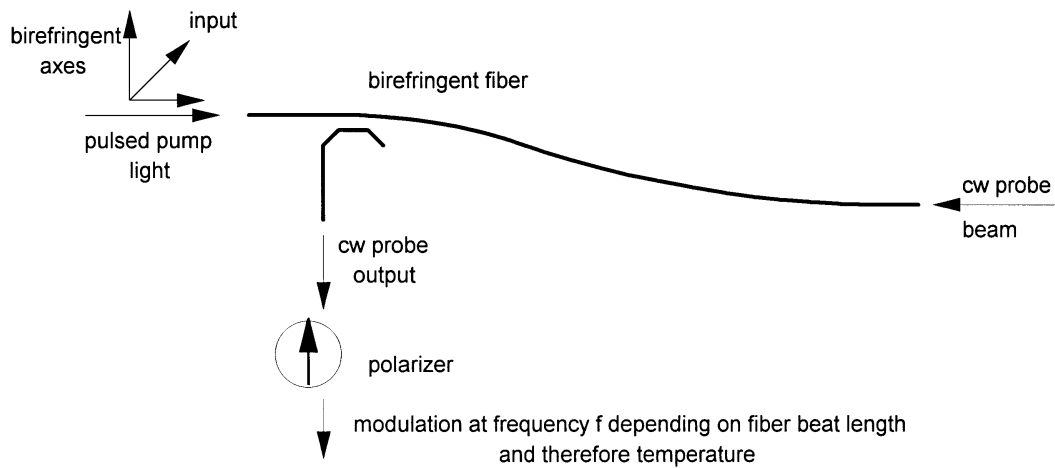


FIGURE 32.93 Distributed Kerr effect probe for temperature or strain field measurements.

determines the frequency offset through phase matching conditions of the mixed pump and probe signal (Figure 32.93). The overall situation is conceptually similar — this offset frequency depends on temperature and strain although in principle, dual measurements and adequate calibration can retrieve both, or alternatively the probe can measure a temperature field in the absence of strain. Again, the actual experimental results that have been achieved remain in the laboratory and the accuracies and resolutions are modest.

In quasi-distributed sensing and point multiplexed systems, temperature probes have, as yet, been but little exploited. There are many variations on the basic theme of a marked optical fiber within which the optical interrogation system measures the optical path length between the marks. These marks can be introduced using partially reflective gratings, mode coupling Bragg gratings, partially reflective splices or connectors, low reflectivity directional couplers, or a multitude of other arrangements. Similarly, the optical delay between the markings can be measured directly as an optical or subcarrier phase or indirectly through monitoring dispersion between adjacent modes typically in low moded or birefringent fibers. Yet again, the different delays depend on both temperature and strain so that for temperature measurement, a strain-free mounting is ideal. The context within which most, if not all, of this class of system has been evaluated is that of smart structures and here the technique does offer some promise as a means for deconvolving strain, mechanical, and thermal effects, and assessing structural integrity. It could also function as a temperature measurement probe, but to date has been minimally addressed in this application.

In multiplexed systems, the current fashion, again primarily for combined strain and temperature measurement, is to incorporate arrays of Bragg gratings used here as wavelength filters rather than as broadband reflectors. In this configuration, the Bragg grating presents a combined temperature/strain field at its location encoded within the reflection wavelength. Multiple addressing schemes can deconvolve temperature and strain sensitivities. There have also been a few demonstrations of discrete temperature-sensitive elements inserted at strategic points along an optical fiber. Of these the use of bandedge shifting in ruby crystals interrogated using a pulsed source observed in reflection has probably been the most successful. In this arrangement, the reflectors are replaced by the crystals and sample the temperature field at these points. The receiver then determines the return to spectrum as a function of time.

## Applications for Optical Fiber Temperature Probes

Instrumentation is a very applications-specific discipline and, in particular for sensors, a particular technology is usually only relevant in a limited number of application sectors. As the technology becomes more and more specialized and expensive, these applications niches become much more tightly defined.

For optical fiber sensors and their use in temperature probes, the more conventional approaches (thermocouples, thermistors, platinum resistance thermometers, etc.) are always easier and simpler. The fiber optic technology must exploit one or more of electromagnetic immunity, small size, noninvasiveness, chemical immunity, or the capacity for distributed measurement.

Point optical sensors are therefore primarily used as measurement probes in regions of very high electromagnetic fields, in zone zero intrinsically safe areas, and as *in vivo* medical probes.

The distributed capability of fiber sensors is especially relevant in structural monitoring and in other specialized areas such as measuring the temperature distribution along underground power lines, tunnels or similar structures or in experimental circumstances such as the measurement of curing processes in large volumes of concrete.

Fiber optics then is exactly similar to all other sensing techniques — it is an inappropriate temperature probe for the majority of applications; but for those for which it is appropriate, it offers a unique and effective solution to frequently otherwise intractable measurement challenges. As a technology evolves and becomes both more widely accepted and readily available, the applications address will no doubt expand.

### **Further Information**

Additional information on optical fiber temperature measurements can be obtained from the following.

B. Culshaw and J. P. Dakin, *Optical Fiber Sensors, Vol. I–IV*, Boston: Artech House, Vol. 1, 1988; Vol. II, 1989; Vols. III and IV, 1997.

B. Culshaw, *Optical Fiber Sensing and Signal Processing*, Stevenage, UK: IEE/Peter Perigrinus, 1983.

*International Conferences on Optical Fiber Sensors (OFS)* are regarded as the principal forum for the dissemination of research results OFS(1), London 1983 to OFS(12) Williamsburg, 1997, various publishers.

Proceedings of series of *Distributed and Multiplexed Optical Fiber Sensors and of Laser and Fiber Sensors Conf.* available from SPIE, Bellingham, Washington.

E. Udd (ed.), *Optical Fiber Sensors*, New York: John Wiley & Sons, 1991.